GEOLOGY OF GREENLAND SURVEY BULLETIN 181 · 1999

Precambrian geology of the Disko Bugt region, West Greenland

Edited by
Feiko Kalsbeek

GEOLOGICAL SURVEY OF DENMARK AND GREENLAND
MINISTRY OF ENVIRONMENT AND ENERGY

Geology of Greenland Survey Bulletin 181

Keywords
Age determinations, Archaean, Disko Bugt, economic geology, geological map, Proterozoic, structural geology, West Greenland.

Cover
Unconformity between Archaean greenstones and Palaeoproterozoic metasedimentary rocks of the Anap nunâ Group on Qapiarfiit, north-east of Disko Bugt. The rocks of the Anap nunâ Group, to the right of the river, are here hardly deformed and at very low metamorphic grade. The lower part consists of a marble conglomerate and is overlain by dark sandstones and siltstones, within which sedimentary structures are well preserved. Photo: A.A. Garde.

Chief editor of this series: Peter R. Dawes
Scientific editor of this volume: Feiko Kalsbeek
Editorial secretaries: Esben W. Glendal and Birgit Eriksen
Critical readers: P.R. Dawes (Denmark), B. Hageskov (Denmark), L.M. Larsen (Denmark), D.C. Rex (UK), H. Sørensen (Denmark), J. van Gool (Denmark), M. Whitehouse (Sweden), as well as intra-project reviewing.
Graphic production and reproduction: Knud Gr@phic Consult, Odense, Denmark
Manuscripts submitted: 29th December, 1997
Final versions approved: 26th March, 1999
Printed: 22nd July, 1999

ISBN 87-7871-063-4
ISSN 1397-1905

Geology of Greenland Survey Bulletin
The series *Geology of Greenland Survey Bulletin* is a continuation of *Bulletin Grønlands Geologiske Undersøgelse* and incorporates *Rapport Grønlands Geologiske Undersøgelse.*

Citation of the name of this series
It is recommended that the name of this series is cited in full, viz. *Geology of Greenland Survey Bulletin*
If abbreviation of this volume is necessary the following form is suggested: *Geology Greenland Surv. Bull.* 181, 179 pp.

Available from
Geological Survey of Denmark and Greenland
Thoravej 8, DK-2400 Copenhagen NV, Denmark
Phone: +45 38 14 20 00, fax: +45 38 14 20 50, e-mail: geus@geus.dk
or
Geografforlaget ApS
Fruerhøjvej 43, DK-5464 Brenderup, Denmark
Phone: +45 63 44 16 83, fax: +45 63 44 16 97, e-mail: go@geografforlaget.dk

Contents

Preface

Between 1988 and 1992 the Geological Survey of Greenland (GGU) launched a number of expeditions to the Disko Bugt region in central West Greenland (Fig. 1), the 'Disko Bugt Project' (Kalsbeek 1989, 1990; Kalsbeek & Christiansen 1992; Christiansen 1993). The aim of this project was threefold. Firstly, it was important to enhance the general geological knowledge of the region, especially the eastern (Precambrian) parts being rather poorly known. Secondly, reconnaissance studies by Kryolitselskabet Øresund A/S in the 1970s and early 1980s and follow up investigations by GGU had revealed mineral showings with Cu, Zn, Au and Ag, which required further investigation. The third major aim of the Project was to obtain more information on the development of the onshore part of the late Phanerozoic West Greenland Basin, which is parti-cularly relevant to the hydrocarbon potential of the basin.

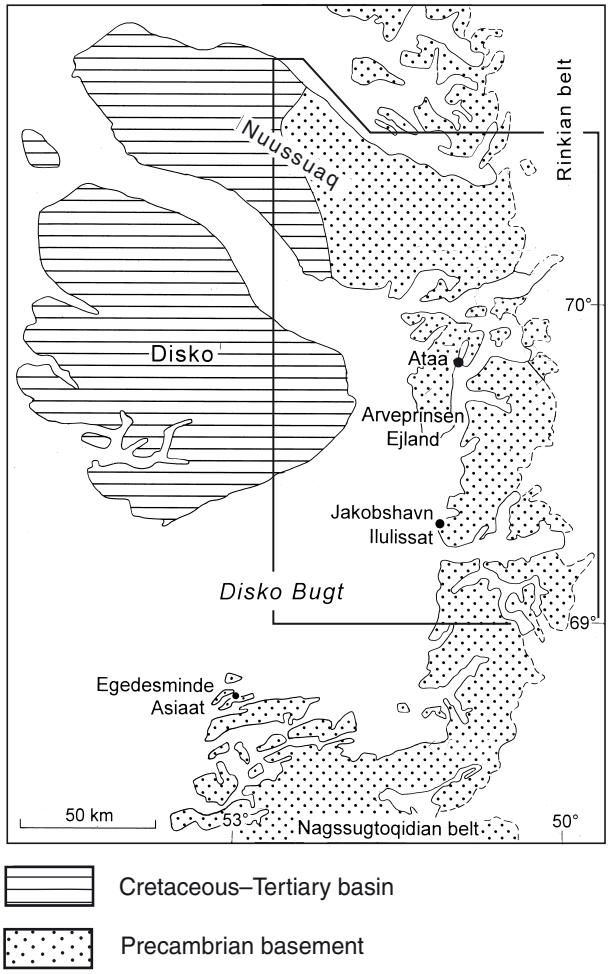

Fig. 1. The Disko Bugt region with the Precambrian basement in the east and the onshore part of the Cretaceous–Tertiary West Greenland Basin in the west. The figure also shows the outline of the 1:250 000 geological map (Garde 1994) enclosed with this volume.

This volume reports on the Precambrian geology of the region. Work was centred on the area around the abandoned settlement Ataa (Fig. 2), where many mineral showings had been recorded within Archaean supracrustal rocks. Although this area was visited by various geologists in the 19th and in the beginning of the 20th century, the first detailed geological map was made by Escher & Burri (1967; this paper also summarises earlier work). These authors, however, were unable to distinguish the Archaean supracrustal rocks from the early Proterozoic metasedimentary sequences which were later shown to occur in the area (Fig. 2), essentially because routine radiometric age determinations were not then available. Moreover, the hypothesis of massive alteration of rocks by 'granitisation' processes was adhered to by many geologists working in Greenland at that time, which heavily influenced the interpretations (and, to some extent, the map) of these authors. Therefore, although the map of Escher & Burri (1967) was useful during the Disko Bugt Project, new field studies were necessary.

The Disko Bugt Project was thus inaugurated and a base camp was erected at Ataa, from which field work in the Precambrian basement was carried out in 1988, 1989 and 1991. The work was carried out in close cooperation with the Geological Institute of the University of Copenhagen; several staff members took part in the mapping, and five students wrote their Danish (cand. scient.) theses on various aspects of the Precambrian geology of the region.

Results of the field investigations have earlier been documented by the 1:250 000 geological map 'Precambrian Geology between Qarajaq Isfjord and Jakobshavn Isfjord, West Greenland' (Garde 1994), and a sheet in the Survey's 1:100 000 series Geological map of Greenland, Ataa 69 V.3 Nord (Escher 1995). The 1:250 000 map sheet is included with this volume.

The present volume contains 14 papers describing various aspects of the Precambrian geology of the Disko Bugt region. The first paper presents a broad overview of the geology of Nuussuaq and the area north-east of Disko Bugt (Fig. 1), and serves as an introduction

Geology of Greenland Survey Bulletin 181, 4–5 (1999)

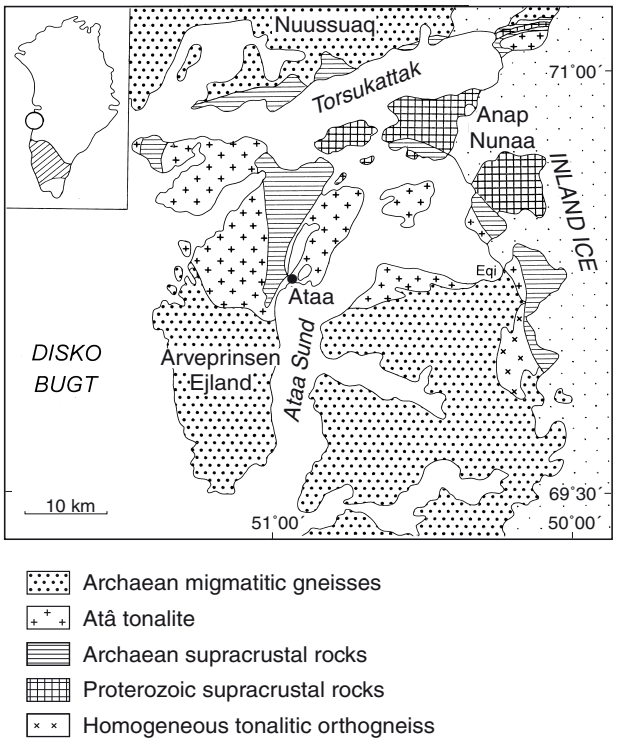

Fig. 2. Geological sketch map of the Ataa area north-east of Disko Bugt.

to the following contributions and as a description of the 1:250 000 map of Garde (1994). This is followed by three papers with geochronological data, dealing with the original formation age of the rocks and with the age(s) of later metamorphism. It is shown that, although most rocks in the Disko Bugt region were formed during the late Archaean, early Proterozoic overprinting has been intense. The next five papers describe lithostratigraphic units in the Ataa area, with emphasis on the Archaean supracrustal rocks. The latter are much better preserved here than is generally the case elsewhere in Greenland, and show many similarities with the greenstone belts which occur, for example, in the Canadian Shield.

Next follow two papers which describe the gold mineralisation locally associated with Archaean supracrustal sequences; interestingly, the setting of the gold mineralisation at the two localities is very different. The final three papers deal with the structural evolution of the region. Although it is often difficult to distinguish between Archaean and early Proterozoic structures, it is evident that early Proterozoic tectonism has had a major impact on the present-day structural grain of large parts of the Disko Bugt region.

For several reasons publication of this volume has been much delayed. Anticipated papers on regional aspects of the mineral potential of the region and on geophysical investigations carried out during the field work have not materialised, but may be published at a later date.

Acknowledgements

I gratefully acknowledge the help of colleagues within and outside GEUS for careful reviews of papers. I thank Stuart Watt for generous help and advise with the technical editing of this volume.

References

Christiansen, F.G. 1993: Disko Bugt Project 1992, West Greenland. Rapport Grønlands Geologiske Undersøgelse **159**, 47–52.

Escher, A. & Burri, M. 1967: Stratigraphy and structural development of the Precambrian rocks in the area north-east of Disko Bugt, West Greenland. Rapport Grønlands Geologiske Undersøgelse **13**, 28 pp.

Escher, J.C. 1995: Geological map of Greenland, 1:100 000, Ataa 69 V.3 Nord. Copenhagen: Geological Survey of Greenland.

Garde, A.A. 1994: Precambrian geology between Qarajaq Isfjord and Jakobshavn Isfjord, West Greenland, 1:250 000. Copenhagen: Geological Survey of Greenland.

Kalsbeek, F. 1989: GGU's expedition in the Disko Bugt area, 1988. Rapport Grønlands Geologiske Undersøgelse **145**, 14–16.

Kalsbeek, F. 1990: Disko Bugt Project, central West Greenland. Rapport Grønlands Geologiske Undersøgelse **148**, 21–24.

Kalsbeek, F. & Christiansen, F.G. 1992: Disko Bugt Project 1991, West Greenland. Rapport Grønlands Geologiske Undersøgelse **155**, 36–41.

Feiko Kalsbeek

Contents:

Precambrian geology of Nuussuaq and the area north-east of Disko Bugt, West Greenland

Adam A. Garde and Agnete Steenfelt

The Precambrian terrain of eastern Nuussuaq and north-east Disko Bugt largely consists of late Archaean (*c.* 2800 Ma) orthogneisses, intercalated with units of strongly deformed Archaean supracrustal rocks. The latter are up to several kilometres wide and comprise both metavolcanic and metasedimentary rocks within which local occurrences of gold have been found. In central Nuussuaq a layered complex of anorthosite, leucogabbro, gabbro and ultramafic rocks is tectonically intercalated with Archaean orthogneisses, and an intrusive complex of Archaean tonalites and trondhjemites, largely unaffected by Archaean and Proterozoic deformation, occurs in the area north-east of Disko Bugt. Here an up to *c.* 3.5 km thick sequence of early Proterozoic shallow marine clastic sediments and minor marble unconformably overlies Archaean rocks. Several suites of basic dykes are present, and dykes and small plugs of ultramafic lamprophyre and lamproite (age *c.* 1750 Ma) are common in the central part of the region.

Most of the region was overprinted by early Proterozoic deformation and metamorphism. Prominent Proterozoic flat-lying ductile shear zones with north- or north-westward movement of the hanging wall are overprinted by open folds.

Geological Survey of Denmark and Greenland, Thoravej 8, DK-2400 Copenhagen NV, Denmark.
E-mail: *aag@geus.dk*.

Keywords: anorthosite, Archaean rocks, Disko Bugt, Nuussuaq, Proterozoic deformation, Proterozoic rocks, West Greenland

This paper describes the Precambrian geological evolution of the Disko Bugt – Nuussuaq region (Fig. 1). It is based on field work by the former Geological Survey of Greenland (GGU) and the Geological Institute, University of Copenhagen, in 1988, 1989 and 1991 during the Disko Bugt Project (Kalsbeek 1989, 1990; Kalsbeek & Christiansen 1992). The account also serves as a description of the geological map at scale 1:250 000 (Garde 1994) enclosed in the present volume, and in the course of the geological description reference is made to the main lithological and structural units on this map.

Precambrian basement is exposed in the eastern part of Nuussuaq and on the mainland north-east of Disko Bugt (Fig. 1). There are both Archaean and Proterozoic rocks, and most of the region has been exposed to both Archaean and Proterozoic phases of deformation. Several geotectonic settings are recognised in the region: an Archaean low-grade granite-greenstone terrain, an active continental margin, and a high-grade gneiss-amphibolite terrain. In addition, a Proterozoic setting with platform sedimentation and basic and lamproitic magmatic activity is present in the central part of the region.

A small number of isotopic age determinations has been carried out (Kalsbeek *et al.* 1988; Kalsbeek & Taylor 1999, Nutman & Kalsbeek 1999 and Rasmussen & Holm 1999, all in this volume), but most of the tentative distinctions made in this account between Archaean and Proterozoic rocks and structures are inferred from field observations. In particular it has been difficult to separate Archaean and Proterozoic deformation events.

The present account is primarily based on information gathered by the authors during reconnaissance mapping, but it also relies heavily on more detailed work in the central part of the region by the other participants in the Project, see the 1:100 000 geological

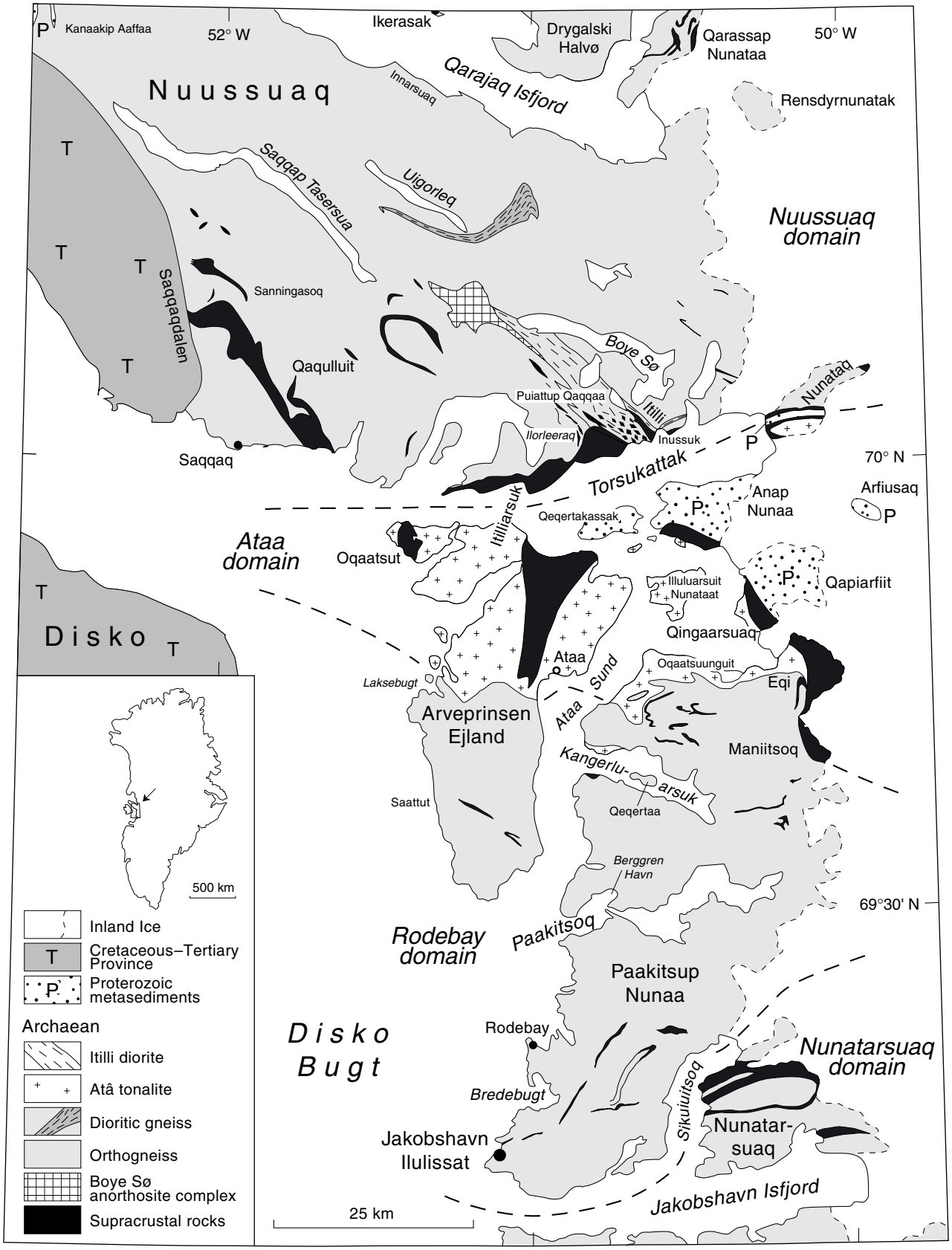

Fig. 1. Principal Archaean and Proterozoic rock units and four structural domains between Qarajaq Isfjord and Jakobshavn Isfjord. Inset map shows location in West Greenland.

map of the Ataa area compiled by Escher (1995), and contributions in this volume. The authors have mainly worked by helicopter from the Survey base camp at the former settlement Ataa 60 km north of Ilulissat, supplemented by short field camps.

Prior to the Disko Bugt Project, the Precambrian geology of the Disko Bugt region was poorly known. The first geological investigation by the Geological Survey of Greenland (GGU; Escher & Burri 1967; Escher & Pulvertaft 1976) consisted of reconnaissance mapping by boat in 1964 between latitudes 69° and 70° along the coasts east and south-east of Disko. The results were shown on a preliminary map at scale 1:250 000 (Escher & Burri 1967, map 1) and as part of the geological map sheet Søndre Strømfjord – Nûgssuaq at scale 1:500 000 (Escher 1971).

Escher & Burri (1967) divided the Precambrian rocks between Jakobshavn Isfjord and Nuussuaq (Fig. 1) into a lower, older gneiss group and an upper, younger group, the 'Anap nunâ Group', in which they included all exposures of supracrustal rocks on both sides of Torsukattak. They also recognised the 'Atâ granite', which they considered was formed largely by granitisation of earlier gneisses and supracrustal rocks. Escher & Burri (1967) thought that all the supracrustal rocks were younger than the gneisses, but it is now known that some of them are Archaean and furthermore older than some of the Archaean plutonic rocks, whereas others are Proterozoic (Kalsbeek *et al*. 1988). The term 'Anap nunâ Group' is now restricted to the Proterozoic part of the supracrustal rocks. Escher & Burri (1967) proposed a simplified model for the structural evolution of the region, according to which the supracrustal rocks form a rim syncline around a large diapiric dome of reactivated gneiss basement; however more recent field work has not supported this interpretation.

The northern coast of Nuussuaq and areas north of Qarajaq Isfjord included in the present map (Garde

Table 1. Archaean and lower Proterozoic lithological units between Jakobshavn Isfjord and Qarajaq Isfjord

Nuussuaq domain	Ataa domain	Rodebay and Nunatarsuaq domains
	ARCHAEAN	
Nuussuaq gneisses	Orthogneisses *c. 2800 Ma*	Orthogneisses
Boye Sø anorthosite complex *(tectonic contacts with other units)*	Anorthosite on Arveprinsen Ejland	
Unconformity (?)		
Saqqaq and Itilliarsuk supracrustal rocks; supracrustal rocks on Nunataq *(unconformably resting on orthogneiss?)*	Arveprinsen–Eqi supracrustal rocks *c. 2800 Ma* *(intruded by Atâ tonalite)*	Nunatarsuaq supracrustal rocks Supracrustal enclaves *(relationships with orthogneisses unknown)*
Itilli diorite (intrudes homogeneous amphibolite)	Atâ tonalite 2800 Ma (intrudes Arveprinsen–Eqi supracrustal rocks)	Rodebay granodiorite
Trondhjemite sill *(intrudes Saqqaq supracrustal rocks)*	Late granitoids *c.* 2750 Ma *(intrude Atâ tonalite)*	Late granitoids *c.* 2750 Ma (?)
	EARLY PROTEROZOIC	
Nuussuaq marble Sedimentary rocks on Nunataq *(probably equivalent to Anap nunâ Group)*	Anap nunâ Group *(partly Archaean provenance)*	
Ilorleeraq dykes Metabasic sills Basic sill on Nunataq	Basic sills	Basic dykes and sills
Dolerite dykes	Dolerite dykes	Dolerite dykes
	Albitised sandstone and siltstone	Albitised rocks

Approximate ages are summarised from Kalsbeek *et al.* (1988), Kalsbeek & Taylor (1999, this volume) and Nutman & Kalsbeek (1999, this volume).

1994, enclosed in pocket) were reconnoitred in 1965 and 1980 by T.C.R. Pulvertaft (personal communication 1988, 1993) during field work for geological map sheets at scale 1:100 000 in the Uummannaq region north of Nuussuaq.

The mining company Kryolitselskabet Øresund A/S carried out a mineral exploration programme north-east of Disko Bugt in the beginning of the 1980s (see Gothenborg 1982). The exploration comprised airborne and ground magnetic and electromagnetic surveys in search of base and precious metal deposits, supplemented by local detailed geological mapping around various prospects. Other companies have later prospected in the same region, primarily for gold.

The area north-east of Disko Bugt was visited again several times in the mid-1980s by geologists from the Geological Survey of Greenland and the University of Copenhagen (Kalsbeek *et al.* 1988; Knudsen *et al.* 1988; Steenfelt 1988). The results obtained from these small expeditions provided the basis for the Disko Bugt Project in 1988–1991.

Descriptions of lithological units on the 1:250 000 scale map

In the following, the main lithological units that occur on the geological map (Garde 1994) are referred to in italics, and their labels on the map quoted in brackets. However, since the different rock units have not been formally defined in a stratigraphical sense, we use informal terms like 'Atâ tonalite' (with lower case t) instead of 'Atâ Tonalite' as employed on the map. A geological overview of the region is shown on Fig. 1, and the main lithological units and their age relationships are presented in Table 1.

Both the orthogneisses and supracrustal rocks of presumed Archaean age and the Proterozoic (meta)-sediments and intrusive rocks are described below according to their occurrence in four different structural domains (see *Structural and metamorphic evolution*, p. 33).

Archaean gneisses north of Torsukattak

Orthogneisses *s.l.* (including the essentially undeformed Atâ tonalite and local granitic rocks) form about 90 per cent of the Precambrian of Nuussuaq and the region north-east of Disko Bugt and comprise the Nuussuaq gneisses north of Torsukattak, the rocks belonging to the Atâ tonalite centred around the northern part of Arveprinsen Ejland, the Rodebay granodiorite towards Jakobshavn Isfjord, and the gneisses on Nunatarsuaq in the south-east. The orthogneisses are all presumed to be late Archaean in age, broadly coeval with the Atâ tonalite dated at *c.* 2800 Ma (Kalsbeek *et al.* 1988; Nutman & Kalsbeek 1999, this volume).

Nuussuaq gneisses

The Nuussuaq gneisses, which form the greater part of Precambrian Nuussuaq, appear to form a basement to the Archaean supracrustal rocks along Torsukattak, because conglomerates which contain boulders of orthogneiss have been found at two localities within these supracrustal rocks (descriptions follow below, p. 14). The most common type of Nuussuaq gneiss is *homogeneous orthogneiss* (gn). This consists of predominantly medium-grained, light grey, biotite-bearing rocks of tonalitic to trondhjemitic composition with weak migmatisation. The gneiss commonly shows a strong flat-lying to subhorizontal foliation, and in the north-western part of the exposed basement towards the Cretaceous – lower Tertiary province in western Nuussuaq it is variably crushed and epidotised. Extensive supracrustal units occur in the southern part of Nuussuaq, but elsewhere the homogeneous orthogneiss is mostly almost devoid of supracrustal enclaves; tectonic slices of an anorthosite-leucogabbro-gabbro suite (see p. 22) are the most prominent marker horizons.

On Nuussuaq, within the rather homogeneous orthogneiss described above, areas with distinctive lithologies were identified during helicopter reconnaissance; however, in most cases their mutual relationships could not be established. In the central and north-western part of the Nuussuaq basement there occurs an about 20 km long and up to 500 m thick, flat-lying unit of dark grey *hornblende-biotite gneiss* (dgn). In the north-eastern part of Nuussuaq ash-grey, sugary plagioclase-rich varieties of orthogneiss (*tonalitic gneiss*, bgn) are spatially associated with layers of anorthosite, leuco- and gabbro; especially in the area south-east of the head of Qarajaq Isfjord and on Rensdyrnunatak this gneiss unit may be very heterogeneous (and commonly strongly deformed), consisting of several phases of orthogneiss mixed with anorthosite, leucogabbro and gabbro (Fig. 2) and possibly also mafic supracrustal rocks (see also colour photograph in Kalsbeek 1990, p. 21). Dark, homogeneous, plagioclase-rich ortho-

Fig. 2. Grey plagioclase-rich orthoneiss with interleaved pale layers of anorthosite-leucogabbro and dark layers of gabbro at the *c.* 1000 m high cliff side Innarsuaq, north coast of Nuussuaq. Note the *c.* 100 m long subhorizontal dark body of irregular shape (lower right), which we interpret as a deformed Proterozoic metabasic sill. The pronounced flat-lying structure is almost certainly of Proterozoic age.

gneiss also occurs north of Qarajaq Isfjord, e.g. on Drygalski Halvø and Qarassap Nunataa. In both of the two latter areas the dark gneiss appears to have tectonic contacts to the underlying biotite gneiss (T.C.R. Pulvertaft, personal communication 1993).

A *c.* 25 km long and up to 1 km thick layer of dark grey tonalitic to dioritic gneiss, banded *hornblende-biotite gneiss* (dgn) occurs in the area south-east of the lake Uigorleq. This gneiss commonly possesses a distinct compositional banding at a scale of centimetres to decimetres, formed by alternating hornblende- and biotite-rich layers (Fig. 3).

Around Saqqaq there is a large area of *augen gneiss* (agn), which lithologically resembles the augen gneiss that forms characteristic marker horizons in the Uummannaq region (Pulvertaft 1986; Henderson & Pulvertaft 1987); however, intense deformation in the boundary area towards the Tertiary volcanic province west of Saqqaqdalen has modified all gneissic textures so strongly that it was not possible to identify the northern boundary of the augen gneiss with certainty.

North and east of Boye Sø pale leucocratic gneisses with evenly distributed, fine-grained biotite predominate. These gneisses are not well known due to the reconnaissance nature of the geological mapping and are not differentiated on the geological map.

The *Itilli diorite* (id) is a large composite NW-trending body south of Boye Sø. It consists of homogeneous,

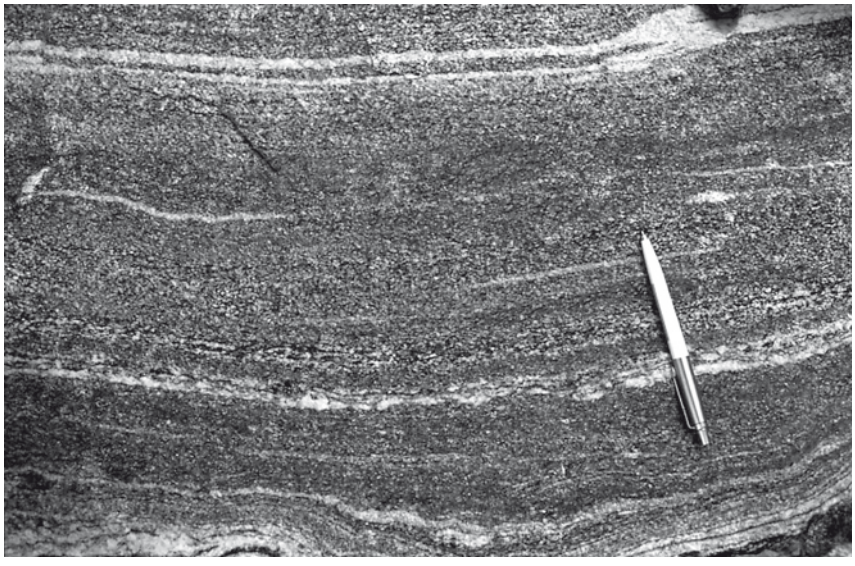

Fig. 3. Dioritic gneiss with compositional banding of alternating centimetre-thick hornblende- and biotite-rich layers and a few millimetres thick streaks of leucosome. Locality 3 km west of the southern end of lake Uigorleq in central Nuussuaq.

Fig. 4. Two vertical sheets and second-order veins of Itilli diorite intruding fine-grained supracrustal amphibolite, *c.* 1 km west of Itilli, south-eastern Nuussuaq.

medium to dark grey, biotite- and hornblende-bearing diorite and differs from other gneisses on Nuussuaq by its more mafic composition. Besides, it is clearly intrusive into a fine-grained supracrustal amphibolite of presumed Archaean age (Fig. 4), which occurs south-west of Itilli (see p. 16). In places, especially along its north-eastern margin, the Itilli diorite is strongly foliated; it is locally cut by younger granitoid rocks. During the reconnaissance mapping it was often difficult to distinguish between the Itilli diorite and gabbroic rocks belonging to the *Boye Sø anorthosite complex* (p. 22); the two groups of lithologies have been tectonically mixed in the area west of Boye Sø by tight to isoclinal folding and shearing, and their primary relationship is unknown.

Along the north coast of Saqqap Tasersua there is a distinct flat-lying, few metres thick *pyrite- and quartz-rich horizon* (P), which can be followed intermittently for 15 km. It is of unknown origin, maybe deposited from fluids along a Proterozoic shear zone.

Gneisses on Nunataq

Nunataq, an isolated area bounded by the head of Torsukattak and two glaciers (Fig. 1; Higgins & Soper 1999, this volume), breaches the gap of no exposure across Torsukattak between the deformed tonalitic orthogneisses on southern Nuussuaq and the Atâ tonalite south of the fjord, which is more leucocratic and only little deformed. The northern part of Nunataq mainly consists of polyphase banded gneiss reminiscent of that in the eastern part of Nuussuaq. Within the predominant banded gneiss in the central part of Nunataq there are small bodies of heterogeneous, pinkish, muscovite-, garnet- and fluorite-bearing miarolitic granite. This granite is younger than the gneisses and was emplaced at a shallow crustal level.

In the southern part of Nunataq are two major folds: an isoclinal syncline of Archaean and Proterozoic supracrustal rocks, and to the south an anticline with a core of homogeneous granitoid rocks that strongly resemble (and are probably related to) the Atâ tonalite.

Archaean supracrustal rocks along the coasts of Torsukattak and in the Ataa domain

The most important occurrences of Archaean supracrustal rocks in the Disko Bugt – Nuussuaq region are found on both sides of Torsukattak (Fig. 1). Those on the northern side of the fjord are likely to be continuous with similar rocks on Nunataq; their relationships to the supracrustal rocks south of the fjord are discussed in a later section (p. 22).

Along the north coast there are several, up to *c.* 25 km long occurrences of metasedimentary and metavolcanic rocks, some or all of which were probably deposited on a basement of Nuussuaq gneiss along an unstable continental margin. The two largest occur-

Fig. 5. Saqqaq supracrustal rocks on NE-facing cliff face 9 km north-north-east of Saqqaq, opposite the mountain Qaqulluit. Ultramafic metavolcanic rocks (partially unexposed) are followed upwards by dark grey mafic metavolcanic rocks and clastic metasedimentary rocks in grey shades. The white irregular layer in the middle part of the *c*. 450 m thick succession is a trondhjemitic sill.

rences are the *Itilliarsuk* and *Saqqaq supracrustal rocks*. Indirect evidence (p. 17) suggests that both are of Archaean age. The sequences are metamorphosed under low to intermediate amphibolite facies conditions and have probably been exposed to both Archaean and Proterozoic deformation.

South of Torsukattak, Archaean rocks of volcanic and sedimentary origin, the *Arveprinsen–Eqi supracrustal rocks*, occur on Oqaatsut, in the northern part of Arveprinsen Ejland, on southern Anap Nunaa, Qingaarsuaq, and from Eqi to Maniitsoq in the east (Fig. 1). The north-eastern part is overlain by Proterozoic platform sediments. The Archaean supracrustal rocks are intruded by the 2800 Ma Atâ tonalite and have been metamorphosed under upper greenschist to low amphibolite facies conditions; the metamorphic grade increases towards the margins of the Atâ tonalite. This part of the Disko Bugt - Nuussuaq region contains characteristic features of a classic granite-greenstone terrain (see p. 35).

Saqqaq supracrustal rocks

A *c*. 25 km long and at least 500 m thick sequence of metavolcanic and metasedimentary rocks, the *Saqqaq supracrustal rocks* (Sms, Sa and Sub), occurs north-east of the settlement Saqqaq on the south coast of Nuussuaq. These rocks and their chemistry are described in some detail by Garde *et al*. (1999, this volume).

The south-eastern end of the sequence forms a large upright, south-east-plunging antiform which apparently refolds an earlier recumbent isocline. The rocks in the central part of the sequence are well exposed in a *c*. 7 km long, north-east facing steep cliff profile opposite the mountain Qaqulluit (Fig. 5), and in this area an internal stratigraphy has been established by means of a few traverses across the lower, accessible part of the sequence, combined with a profile constructed by means of the multi-model geological photogrammetry method (Garde *et al*. 1999, this volume; see Dueholm 1992 and Dueholm *et al*. 1993 for a description of the method). From the lowermost exposures upwards the sequence comprises a thin quartz-, amphibole- and pyrrhotite-rich rusty horizon, which is followed by about 150 m of ultrabasic and subordinate basic metavolcanic rocks (*ultrabasic metavolcanic rocks*, Sub) heavily affected by carbonate alteration. Then follows a second, 3–4 m thick rusty horizon which consists of finely laminated exhalative silica- and iron-rich rocks (with quartz, pyrrhotite, fuchsite, garnet, tourmaline, hornblende, staurolite and kyanite). This horizon contains up to 3 ppm gold over a thickness of *c*. 3 m (Thomassen & Tukiainen 1992). The gold is associated with arsenopyrite and is interpreted as syngenetic. The metavolcanic and associated volcanogenic-exhalative rocks are overlain by minimum *c*. 100 m of muscovite-, biotite- and garnet-bearing quartzo-feldspathic rocks of metasedimentary or volcaniclastic origin, which form the middle part of the supracrustal sequence. A several kilometres long and up to *c*. 100 m thick trond-

Fig. 6. Ultramafic rocks near the base of the supracrustal succession at Itilliarsuk: light brown dunitic rocks intercalated with green diopside-rich rocks.

hjemitic sill with second-order aplitic veins has intruded the metasediments and can be seen as an irregular light-coloured band along the cliffs. The thick upper part of the sequence is inaccessible but probably consists of alternating horizons of metavolcanic amphibolite and metasediment. By analogy with the supracrustal rocks exposed further east (see below) it is thought that the Saqqaq supracrustal rocks lie right way up in the 7 km long cliff where they are best known.

Itilliarsuk supracrustal rocks

Along the southern coast of Nuussuaq there are several continuous exposures of amphibolite facies supracrustal rocks, here referred to as the *Itilliarsuk supracrustal rocks*. The westernmost part has been mapped by Rasmussen & Pedersen (1999, this volume); the remainder has been investigated in variable detail by the present authors and by A.K. Higgins and N.J. Soper (personal communication 1994). Kryolitselskabet Øresund A/S has explored several sulphide occurrences.

Western occurrence, around Itilliarsuk

The supracrustal rocks are thickest (about 2.5 km) and best preserved on both sides of Itilliarsuk (Fig. 1). The sequence strikes *c.* 80° with intermediate southerly dips, and appears to have retained substantial elements of an original stratigraphy in spite of Archaean and Proterozoic deformation events that have produced internal isoclinal folds and thrusts.

The contact between the supracrustal sequence and the underlying gneiss is generally strongly tectonised, and an unequivocal basal unconformity has not been located. The orthogneiss immediately below the contact commonly contains small, strongly foliated slivers of supracrustal rocks, which could be interpreted either as relics of contemporary or older xenoliths, or as fragments of (younger) supracrustal rocks tectonically emplaced in the orthogneisses. The occurrence of conglomerates with orthogneiss boulders and quartz-rich metasediments in the supracrustal sequence, which are described below, makes the second of these two possibilities more likely.

The lowermost rocks that have been recognised as belonging to the supracrustal sequence consist of sheared lenses and semi-continuous layers of *ultrabasic rocks* (lub; Fig. 6) and associated mafic metavolcanic *amphibolites* (la). The mineralogical composition of the ultrabasic rocks varies from olivine-rich to mixtures of olivine, diopside, tremolite and carbonate; locally the rocks are entirely retrograded with serpentine, talc, tremolite and carbonate. Up to 1 m thick layers of impure carbonates are also present. It is possible that carbonates and their metamorphic reaction products such as diopside and tremolite are signs of pre-metamorphic metasomatic processes involving carbonic fluids.

Discontinuous exposures of polymict conglomerate with felsic and mafic clasts occur over a strike length

Fig. 7. Polymict conglomerate with clasts of medium-grained, grey orthogneiss, fine-grained pale grey rocks (probably of acid metavolcanic origin) and dark green calc-silicate-rich rocks. Itilliarsuup Qaqqaa (near Itilliarsuk), *c*. 500 m south of the contact between the orthogneiss and the supracrustal succession.

of about 1.5 km west of Itilliarsuk about 300 m south of the contact to the Nuussuaq orthogneisses (Rasmussen & Pedersen 1999, this volume), and similar conglomerates occur east of Itilliarsuk *c*. 500 m south of the orthogneiss contact (Fig. 7). The former conglomerates directly overlie serpentinitic ultrabasic rocks and contain up to about 1 m long, rounded boulders of weakly foliated orthogneiss set in a dark biotite-, garnet- and staurolite-bearing matrix, which also contains up to *c*. 50 cm thick, broken-up bands of amphibolite and medium-grained hornblendite. The conglomerates are deformed, and the dimensions of the gneiss clasts suggest moderate stretching in a SE-plunging direction. The orthogneiss boulders, which resemble little-deformed varieties of the gneisses north of the supracrustal rocks, suggest that the Itilliarsuk supracrustal rocks rest unconformably on the Nuussuaq gneisses.

The overlying rocks are amphibolites (± garnet), minor *acid metavolcanic rocks* (lc; Fig. 8) and dark variegated biotite-rich rocks with variable proportions of garnet, staurolite and hornblende. The latter rocks

Fig. 8. Acid metavolcanic rock with flattened, up to *c*. 5 cm long lithic fragments. East of Itilliarsuk, *c*. 500 m south of the contact between the orthogneiss and supracrustal rocks.

Fig. 9. Cross-bedded sandstone in the lower part of the Itilliarsuk supracrustal rocks, indicating right way up of the supracrustal succession and provenance from felsic rocks (probably a basement of orthogneisses). Locality *c*. 8 km east of Itilliarsuk, close to Torsukattak. Photo: A.K. Higgins.

may represent sediments derived from a mafic volcanic source. The amphibolites contain local iron sulphides and sporadic chalcopyrite mineralisation with malachite staining. Also muscovite-rich and muscovite-garnet(-kyanite) schists occur, and several centimetres long kyanite crystals have been found in quartz veins.

Close to the coast 8 km east of Itilliarsuk there are several layers of quartz-rich gritty *metasediment* (ls) with locally preserved pebbly bands, cross bedding and graded bedding (Fig. 9; A.K. Higgins, personal communication 1993) which show that the supracrustal sequence at this locality is orientated right way up. The presence of quartz-rich metasediments within the Itilliarsuk supracrustal rocks may furthermore support the suggestion that the sequence rests unconformably on a quartzo-feldspathic basement.

In the lower part of the supracrustal sequence around Itilliarsuk there are several *metagabbros* (lai) which are easy to recognise by their porphyritic texture with scattered centimetre-sized plagioclase crystals. The metagabbros are deformed and form more or less conformable plate-like bodies up to *c*. 100 m thick and more than 1 km long.

The upper part of the Itilliarsuk supracrustal sequence is dominated by *biotite schists* (lms), which east of Itilliarsuk contain a spectacular rusty pyrrhotite-bearing horizon as well as impure iron formation discovered by Kryolitselskabet Øresund A/S during an aeromagnetic survey. The *iron formation* (lbi) consists of finely banded siliceous rocks rich in magnetite, quartz, garnet and amphibole, which occur in a *c*. 200 m thick zone in the southern part of the biotite schists. Also impure calcareous rocks locally occur within the upper, metasedimentary part of the supracrustal sequence.

Several hundred metres of acid metavolcanic rocks terminate the supracrustal sequence towards the point south-east of Itilliarsuk. Both these rocks and the iron formation possess intense stretching lineation fabrics which severely hinder the recognition of primary structures.

Eastern occurrence, Qeqertaarsuk and Inussuk

The relative proportions of volcanic and sedimentary lithologies west of Itilli differ from those at Itilliarsuk, and their structure is different. A *c*. 5 km long, locally very carbonate-rich ultrabasic layer occurs *c*. 2 km west of Itilli; it strikes NW and is up to *c*. 250 m thick. The ultrabasic layer separates a large segment of amphibolite intruded by Itilli diorite in the south-west (see below) from a north-eastern segment dominated by biotite schists with garnet, muscovite, staurolite ± kyanite and subordinate amphibolite. The ultrabasic layer contains several folded and metamorphosed, plagioclase-phyric mafic dykes which are at most *c*. 10 m thick. Similar dykes have also been observed within biotite schists on the south-western side of the agmatitic amphibolite.

The amphibolite in the area west of Itilli is generally very homogeneous and fine grained. Its volume is much greater than found elsewhere among the supracrustal rocks in southern Nuussuaq, and the apparent stratigraphy at Itilli as a whole cannot be matched to the supracrustal rocks in any of the adjacent sequences. The massive character of the amphibolite furthermore brings to mind the greenstones on Arveprinsen Ejland, see p. 19 and Garde & Steenfelt (1999, this volume).

The amphibolite has been intruded (at scales varying from centimetres to tens of metres) by variable proportions of dioritic gneiss, the previously mentioned *Itilli diorite*, which is in places almost undeformed, with clear intrusive contacts to the amphibolite (Fig. 4). Sporadic layers and enclaves of supracrustal amphibo-

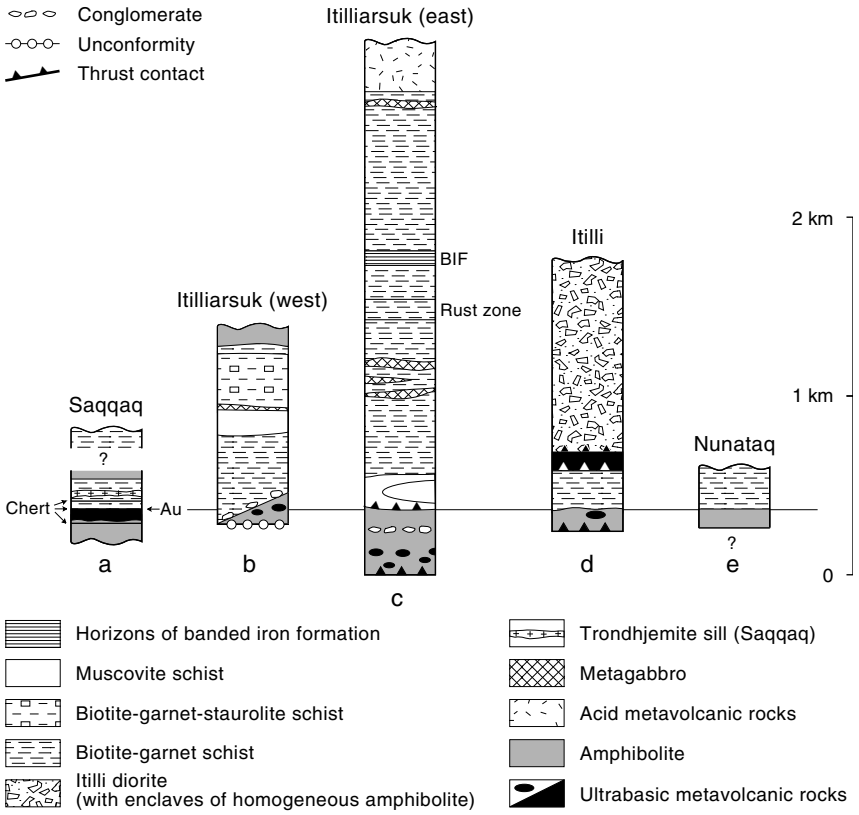

Fig. 10. Simplified stratigraphic columns and correlation of the Archaean Saqqaq (**a**) and Itilliarsuk supracrustal (**b–d**) rocks in southern Nuussuaq, and supracrustal rocks on Nunataq (**e**).

lite and ultrabasic rocks occur in the Itilli diorite as far as 15 km inland towards the north-west. In the Itilli area there are several tectonic enclaves of leucogabbroic and gabbroic rocks, which may belong to the Boye Sø anorthosite complex described in a later section (p. 22).

The amphibolite-diorite agmatite south-west of Itilli contains copper-gold (-cobalt) mineralisation, which has been drilled by Kryolitselskabet Øresund A/S; this company also mapped part of the agmatite (Gothenborg & Morthorst 1981; Gothenborg 1982). The mineralisation is located in epigenetic veins, and the metals may have been remobilised from the supracrustal rocks in the course of the intrusion of the Itilli diorite.

Nunataq

The supracrustal rocks on Nunataq at the head of Torsukattak provide indirect evidence that the extensive amphibolite facies metavolcanic and metasedimentary rocks along the south coast of Nuussuaq (including the Saqqaq and Itilliarsuk supracrustal rocks) are Archaean. In central Nunataq east–west-trending supracrustal rocks occur, repeated by isoclinal folding. The sequence is only a few hundred metres thick, but it consists of two entirely different units: an amphibolite-facies unit of garnet amphibolite and mica-garnet schist with two sets of cleavage, and a pseudo-conformable but less metamorphosed (greenschist facies) unit of cross-bedded and ripple-marked quartzite, tremolite-bearing marble and siltstone with only one cleavage set present (Higgins & Soper 1999, this volume). The former unit is presumably Archaean and may be correlated along strike with the lithologically very similar, east–west-trending supracrustal rocks that are exposed at Itilli. The latter unit closely resembles the basal part of the Proterozoic Anap nunâ Group to the south, and is almost certainly Proterozoic in age.

At the northern tip of Nunataq a minimum *c.* 500 m thick, isoclinally folded sequence of amphibolite-facies mafic metavolcanic rocks and biotite-garnet schists is exposed; these rocks are considered to be Archaean.

Correlation of the Archaean supracrustal rocks north of Torsukattak

The tracts of supracrustal rocks that occur in the southern part of Nuussuaq (Fig. 10) possess a number of similarities in their stratigraphy and structural setting

Fig. 11. Contact between Atâ tonalite and Archaean mafic metavolcanic rocks on southern Oqaatsut (left). In the far distance (right) supracrustal rocks on Arveprinsen Ejland. View towards the east-north-east. The mountain in the centre of the photograph is *c.* 500 m high.

which suggest that they were formerly part of a common, continuous supracrustal group.

Conglomerates and quartz-rich metasediments orientated right way up suggest that the south-dipping supracrustal rocks along the south coast of Nuussuaq were deposited on a basement of Nuussuaq gneisses. Elsewhere the original relationships between the supracrustal rocks and gneisses have been destroyed by deformation. The area west of Itilli is exceptional in that the Itilli diorite has intruded supracrustal amphibolite of unknown setting (see below).

The Saqqaq and Itilliarsuk supracrustal sequences begin with thin units of ultrabasic metavolcanic rocks (which are sometimes tectonically disrupted) and mafic metavolcanics, followed by more voluminous clastic and minor volcaniclastic metasediments. At Itilli the north-eastern part of the supracrustal rocks consists of banded amphibolites and associated ultrabasic rocks overlain by mica schists and aluminous metasediments; these rocks form a continuation on strike of the supracrustal rock sequence at Inussuk and likewise resemble the lower part of the Itilliarsuk supracrustal sequence to the west.

The thick agmatised amphibolite unit in the central part of the Itilli area is bounded by a fault to the south-west and by ultramafic rocks to the north-east. The amphibolite cannot be correlated with units in the neighbouring supracrustal sequences, and we suggest that it is part of a foreign supracrustal sequence dominated by massive amphibolite similar to the one on Arveprinsen Ejland (see next section and Garde & Steenfelt 1999, this volume). The amphibolite may have been emplaced into its present position by thrusting along the ultrabasic layer at the north-eastern amphibolite boundary. The ultrabasic layer itself, on the other hand, is likely to have been locally derived, since similar ultrabasic rocks are known from the lowermost parts of the adjacent supracrustal sequences on southern Nuussuaq.

All the supracrustal rocks in southern Nuussuaq have been exposed to Proterozoic low or intermediate amphibolite facies metamorphism (Rasmussen & Holm 1999, this volume); Archaean metamorphism is presumed to have been of lower grade. Hornblende and plagioclase ± garnet occur in mafic rocks, diopside in impure calcareous rocks, and biotite, muscovite, garnet, kyanite ± staurolite in aluminous to iron-rich metasediments (Rasmussen & Pedersen 1999, this volume).

Arveprinsen-Eqi supracrustal rocks, south of Torsukattak

Most of the *Arveprinsen-Eqi supracrustal rocks* within the Ataa structural domain show only weak Proterozoic deformation and metamorphism and are the best preserved Archaean supracrustal rocks in the Disko Bugt – Nuussuaq region. They are predominantly mafic metavolcanic rocks, but also acid metavolcanics, clastic metasediments and traces of iron formation and chert occur. Three samples of acid metavolcanic rocks have all yielded Sm-Nd model ages of *c.* 2800 Ma (Kalsbeek & Taylor 1999, this volume), suggesting that the Arveprinsen-Eqi supracrustal rocks have broadly the same age as the Atâ tonalite which intrudes them (see p. 24).

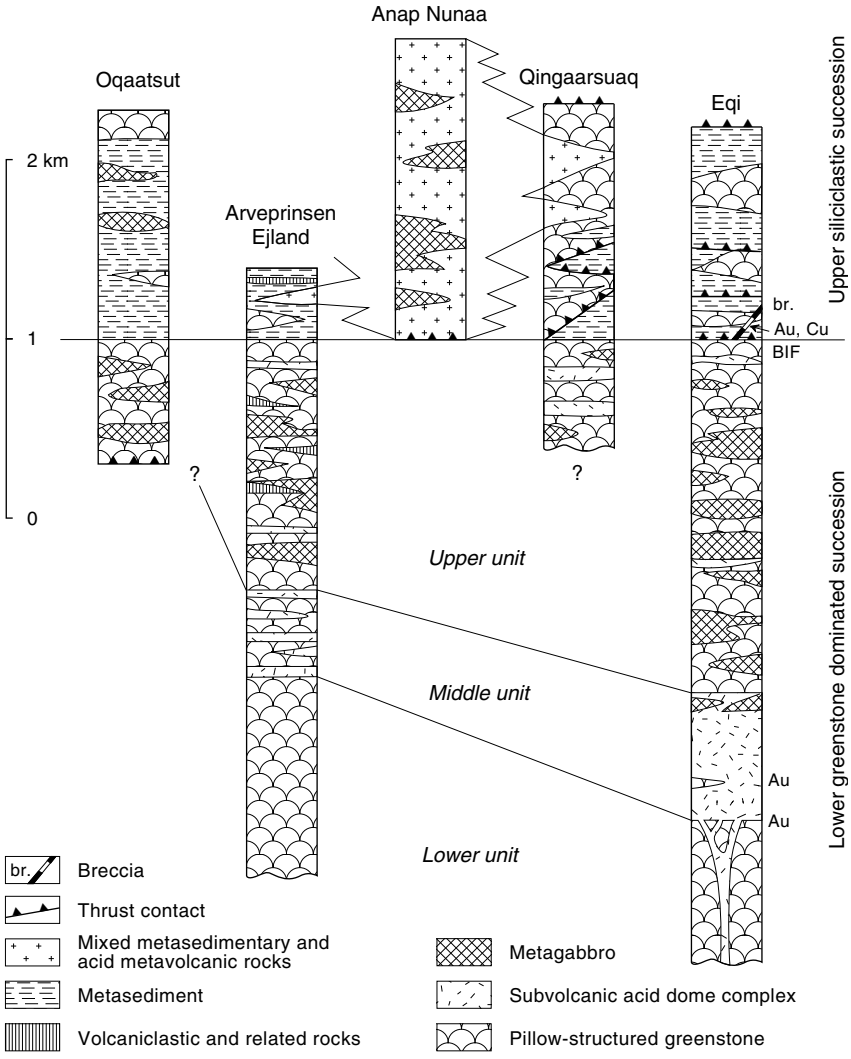

Fig. 12. Simplified stratigraphic columns and correlation of the Archaean Arveprinsen–Eqi supracrustal rocks in the Ataa domain south of Torsukattak. Based on correlation and original hand drawing by M. Marker (personal communication 1992).

Oqaatsut

The supracrustal rocks at Oqaatsut are dominated by metasediments sandwiched between metavolcanic amphibolites which are truncated by tectonic or tectonised intrusive contacts with Atâ plutonic rocks (Fig. 11; Rasmussen & Pedersen 1999, this volume). The metamorphic grade at Oqaatsut is low to middle amphibolite facies with staurolite and kyanite in the metasediments, higher than on Arveprinsen Ejland.

Arveprinsen Ejland

The supracrustal rocks on Arveprinsen Ejland, which have been investigated by Knudsen *et al*. (1988), Nielsen (1992) and Marshall & Schønwandt (1999, this volume), form a *c*. 20 km long and up to *c*. 10 km wide, north–south-trending synclinal keel of greenstones intruded by the Atâ tonalite. The supracrustal sequence is about 3 km thick (with no indications of tectonic repetition), and has been metamorphosed in upper greenschist facies, increasing to lower amphibolite facies as the contact to the Atâ tonalite is approached. Graded bedding is locally preserved in metasediments in the central part of the syncline and shows that the supracrustal sequence is right way up.

The supracrustal sequence has tentatively been divided into a *c*. 3 km thick, predominantly volcanic lower succession and a much thinner, mainly volcaniclastic-sedimentary upper succession (Fig. 12). The most common supracrustal rocks in the lower succession are fine-grained mafic metavolcanic rocks, *greenstone and amphibolite* (Aa). There are also gabbroic intrusive rocks and at least one ultrabasic lens up to *c*. 500 m long with secondary carbonates (*ultrabasic rocks*, Aub).

Fig. 13. Only slightly deformed pillowed lavas *c*. 7 km east of Eqi. Cuspate pillow bases indicate that the sequence is inverted. Pillows about 40 cm in diameter.

Subordinate, up to about 100 m thick layers of acid metavolcanic, volcaniclastic and clastic rocks (*acid metavolcanic rocks*, Ac; *pelitic and psammitic metasediments*, Ams) occur towards the top. Local thin cherts and sulphide-rich horizons also occur (Nielsen 1992). In the southern part of the syncline the greenstones of the lower succession commonly possess calc-silicate and carbonate banding at a scale of centimetres, and in the northern part there are locally well-preserved pillowed lavas. The north-eastern part of the island is dominated by a voluminous hypabyssal *gabbroic sill complex* (Aai) within the metavolcanics (Marshall & Schønwandt 1999, this volume), in which there are also coarse-grained gabbroic to anorthositic rocks (Knudsen *et al*. 1988).

Several mining companies have carried out exploration within the greenstones on Arveprinsen Ejland. A small massive pyrrhotite-chalcopyrite body, the so-called 'Anderson showing', which occurs in the northern part of the greenstones, has been investigated by Kryolitselskabet Øresund A/S (Gothenborg 1983) and by Nielsen (1992) and was drilled by Vestgron Mines Ltd. Electromagnetic work by GGU suggests that the mineralisation does not continue at depth (L. Thorning, personal communication 1988).

Anap Nunaa

The southern part of Anap Nunaa consists of sheared, east–west-trending Archaean rocks. The southernmost exposures consist of strongly foliated granitic rocks belonging to the Atâ tonalite. These have sheared (possibly originally intrusive) contacts to a *c*. 1.7 km thick supracrustal sequence of N- and NW-dipping dacitic quartz- and plagioclase-phyric metavolcanic rocks, *acid metavolcanic rocks* (Ac), besides minor volcanogenic and epiclastic quartzo-feldspathic metasediments. A Sm-Nd model age of *c*. 2800 Ma has been obtained from the acid metavolcanic rocks (Kalsbeek & Taylor 1999, this volume). The sequence is intruded by metagabbroic rocks of presumed Archaean age (shown as amphibolite on the map). The central and northern parts of Anap Nunaa consist of Proterozoic sediments, deposited on the acid metavolcanics with a basal unconformity (p. 29).

Qingaarsuaq

The Archaean rocks at Qingaarsuaq are situated immediately south-west of the Proterozoic sediments at Qapiarfiit (Fig. 1; p. 29). Granitoid rocks belonging to the Atâ tonalite underlie the south-western part of Qingaarsuaq and are bounded by a thrust to a NE-dip-

Fig. 14. Acid metavolcanic rock interpreted as representing a submarine breccia (Stendal *et al.* 1999, this volume), *c.* 8 km east of Eqi. The deformed clasts contain euhedral, *c.* 5 mm large quartz and plagioclase crystals.

ping, *c.* 2 km thick pile of Archaean supracrustal rocks. The supracrustal rocks mainly consist of low-grade metamorphic intrusive and extrusive basic greenstones including pillowed lavas, besides layers and wedges of metasediments, up to a few hundred metres thick. The succession at Qingaarsuaq contains several thrusts which appear to have repeated part of the stratigraphy. No significant Archaean mineralisation is known from Anap Nunaa or Qingaarsuaq.

Eqi and Maniitsoq

The best preserved Archaean supracrustal rocks in the Disko Bugt region occur adjacent to the Inland Ice in the Eqi and Maniitsoq areas. At Eqi the supracrustal sequence is about 4 km thick and has a general north–south structural trend with easterly dips (see Stendal *et al.* 1999, this volume). There is no indication of tectonic repetition. Volcanic textures in well-preserved pillowed lavas in the eastern part of the area indicate that the whole sequence has been inverted.

Figure 12 shows a division into a lower and an upper succession. The base of the lower, eastern succession (now at the top of the sequence) is hidden under the Inland Ice; in the Eqi area it cannot be demonstrated whether the Atâ tonalite intruded the supracrustal rocks. The lower and upper parts of the lower succession are dominated by pillowed greenstones, Aa (Fig. 13). An extensive network of felsic hypabyssal rocks (with a Sm-Nd model age of *c.* 2800 Ma, Kalsbeek & Taylor 1999, this volume) in the lower greenstones may have acted as feeders to a large volcanic dome complex of intermediate to acid rocks, which dominates the central part. These felsic metavolcanic rocks commonly contain horizons with deformed, fragmented lithologies (Fig. 14) which may represent submarine crumbled breccias from the margins of the dome complex. Parts of the felsic metavolcanics have been subject to pervasive metasomatic activity by CO_2-rich fluids, resulting in brownish to greenish carbonate-, quartz-, chlorite- and occasionally fuchsite-rich rocks with gold and copper mineralisation (see below). In the upper part of the lower succession there are several thick, metamorphosed mafic sills, *metadolerite* (As), presumably of Archaean age.

Trace element geochemistry of mafic and felsic metavolcanic rocks from the lower succession suggests that the pillowed lavas and other greenstones represent ocean floor or back arc basalts, whereas felsic metavolcanic rocks from the dome complex have geochemical characteristics of volcanic arc rocks (Garde *et al.* 1991; Stendal *et al.* 1999, this volume).

The upper succession consists of interfingering metavolcanic greenstones (*greenstone and amphibolite*, Aa) including pillowed lavas, hyaloclastic breccias, mafic and felsic tuffs, besides fine- to medium-grained clastic rocks, *pelitic and psammitic metasediments* (Ams). There are also several horizons of banded iron formation, each only about a metre thick. Thin layers of chert are located in the transition zone between the lower and upper successions.

Epigenetic gold mineralisation has been encountered in two different settings. Gold occurs in quartz veins

in zones of carbonate alteration within the felsic volcanic complex, and in a pyrite and pyrrhotite mineralised breccia zone within the upper, sedimentary succession. The latter mineralisation has been drilled by Kryolitselskabet Øresund A/S (Stendal *et al.* 1999, this volume, and references cited therein).

Correlation of the Archaean supracrustal rocks south of Torsukattak

The semicircular tract of well-preserved Archaean supracrustal rocks intermittently exposed from Arveprinsen Ejland to Eqi contains stratigraphic similarities from place to place which suggest the correlation shown on Fig. 12. The sequence at Oqaatsut differs from the former ones by its larger proportion of metasedimentary rocks and higher metamorphic grade, and its stratigraphy seems to have more in common with the Saqqaq and Itilliarsuk supracrustal rocks north of Torsukattak. The thrusts in the Qingaarsuaq area and the inversion of the succession at Eqi leave their original relationships uncertain.

The stratigraphy as preserved today is approximately as follows. Mafic ocean floor basalts prevail in a *c.* 3.3 km thick, lower formation and are associated with a sill complex of leucogabbroic and gabbroic rocks on northern Arveprinsen Ejland. A felsic calc-alkaline dome complex at Eqi forms the middle part of the lower formation; smaller volumes of felsic lavas and pyroclastic rocks may represent eruption products from this or similar hidden dome complexes. A *c.* 2 km thick upper formation is dominated by epiclastic rocks and a volcanic centre with felsic calc-alkaline rocks at Anap Nunaa. At the boundary between the lower and upper formations where clastic sediments become more common than volcanic rocks, thin horizons of banded iron formation occur in Eqi, and cherty rocks (locally with iron sulphides) are found in the west.

Comparison between the Archaean supracrustal rocks north and south of Torsukattak

The supracrustal rocks north and south of Torsukattak have certain similarities but differ from each other in several respects. The lower parts of both sequences contain common mafic volcanic rocks, and clastic sediments and felsic volcanic rocks dominate in their upper parts; thin horizons of iron formation and chemical or exhalative sediments occur in middle or upper zones both north and south of the fjord. Gabbroic intrusives of presumed Archaean age are known from both regions. Two important differences are; (a) the much more common presence of ultrabasic, probably mainly metavolcanic rocks in the lower part of the sequence north of Torsukattak, and (b) the much thicker units of clastic metasediments in the upper part of the northern sequence, compared to the region south of the fjord.

Also the relationships between the supracrustal rocks and orthogneisses appear to be different north and south of the fjord. There is probably a gneiss basement with a depositional unconformity in the north whereas in the south the Atâ tonalite has intruded the supracrustal rocks, and also the orthogneisses themselves are different (polyphase, variably migmatised tonalitic gneisses on Nuussuaq versus more leucocratic and more uniform Atâ rocks).

The metamorphic grade is higher north of the fjord, where deformation is also more intense and more complicated than in the south (Garde & Steenfelt 1999, this volume). Little is known about the structure in the region hidden by the fjord; this problem is discussed in a later section (p. 35).

Boye Sø anorthosite complex

The Boye Sø anorthosite complex (Fig. 15) is a large massif of spectacular (metamorphosed) snowball-type anorthosite, leucogabbro, gabbro and ultrabasic rocks (Fig. 16) that form a snow-capped mountain *c.* 7 km west of Boye Sø (shown as *anorthosite and leucogabbro*, Ban, *metagabbro*, Bai and *ultrabasic rocks*, Bub). The complex is *c.* 25 km^2 in outcrop size. It was found by the authors in 1988 during reconnaissance mapping, and a brief account can be found in Garde & Steenfelt (1989). Its structure appears to be a series of thrust slices, with a large synform fold in the north-eastern part (Fig. 15); a protracted tail of anorthosite-gneiss agmatite extends about 4 km towards the north-west.

Analysis of sediment from small streams draining the Boye Sø anorthosite complex confirmed the elevated contents of Cr and Ni known from a regional geochemical study of eastern Nuussuaq (Steenfelt 1988) but did not reveal any PGE-metal anomalies. The fact that the Boye Sø anorthosite complex consists of several relatively thin thrust sheets probably means that a complete magmatic stratigraphy is not preserved.

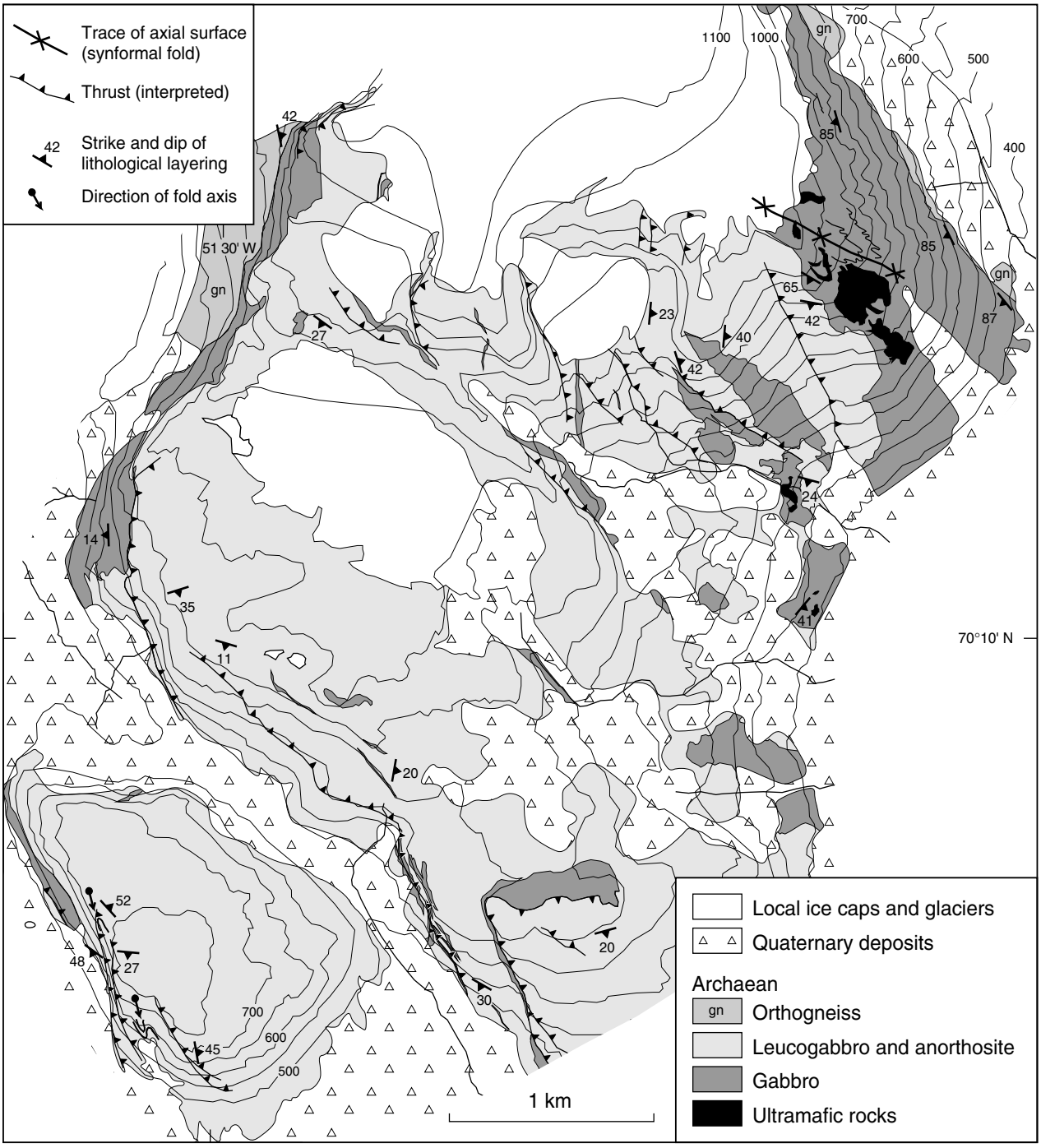

Fig. 15. Outline geological map of the Boye Sø anorthosite complex based on helicopter reconnaissance and interpretation of colour slides, using multi-model photogrammetry at the Technical University of Denmark (the method is described by Dueholm 1992 and Dueholm *et al.* 1993). The photographs, which formed the basis for both the topographic map and geological interpretation, were taken with a hand-held 6 × 6 cm Hasselblad camera from a helicopter.

Fig. 16. Igneous contact between layered gabbro and anorthosite in the upper part of the Boye Sø anorthosite complex, central Nuussuaq.

Other occurrences of anorthosite and related rocks on Nuussuaq

Garde & Steenfelt (1989) outlined other anorthosite-leucogabbro-gabbro occurrences in Nuussuaq (shown as an and ai on the 1:250 000 scale map), which are considered to represent disrupted parts of a common large layered intrusion akin to or originally part of the Boye Sø anorthosite complex. These occurrences are sometimes massive, reaching thicknesses well above 100 m, but commonly just appear as trains of more or less closely packed enclaves in the orthogneiss. They form important marker horizons in the otherwise monotonous basement in north-eastern Nuussuaq (Fig. 2; Garde 1992, figs 2–3; Garde & Steenfelt 1999, this volume).

Archaean rocks south of Torsukattak

Atâ tonalite

The area around Ataa consists of the *Atâ tonalite* (at). This is not a tonalite *sensu strictu* but a plutonic complex of tonalitic, trondhjemitic and subordinate granodioritic rocks, which has largely escaped Proterozoic deformation (Kalsbeek & Skjernaa 1999, this volume). The complex was formerly called the 'Atâ granite' (Escher & Burri 1967); hence the old Greenlandic orthography is retained in its name (Atâ instead of Ataa). On the 1:100 000 scale map of the Ataa area (Escher 1995) the Atâ tonalite is shown as 'Atâ pluton', and Kalsbeek & Skjernaa (1999, this volume) employ the term 'Atâ intrusive complex'.

The southern part of the rocks that have been mapped as Atâ tonalite contains local magmatic layering and numerous undeformed aplite and pegmatite sheets and veins in various directions (Fig. 17). Orbicules and inclusions of volcanic breccias on the island Illuluarsuit Nunataat (Kalsbeek & Skjernaa 1999, this volume) suggest interaction of the Atâ magma with meteoric water and indicate that the top of the intrusion is near the present level of erosion in many localities.

Kalsbeek *et al.* (1988) and Nutman & Kalsbeek (1999, this volume) showed that the age of the Atâ tonalite is *c.* 2800 Ma, using several different methods of isotopic age determination. The tonalite is younger than the Arveprinsen-Eqi supracrustal rocks: on the steep east-facing slopes north of Ataa a granitic sheet belonging to the Atâ complex cuts into overlying supracrustal rocks, and it is likely that the Atâ tonalite has also intruded the supracrustal rocks further east. Deformation has to some extent obscured the original contact relationships to orthogneisses in the boundary areas of the complex. Field observations show that it is younger than the surrounding orthogneisses, and on Arveprinsen Ejland it is cut by *c.* 2740 Ma granitoid rocks.

The Atâ tonalite commonly has a steep internal foliation which is most pronounced towards its margins (Kalsbeek & Skjernaa 1999, this volume). The foliation is cut by the above mentioned undeformed dykes and is thus likely to have formed during emplacement and

Fig. 17. Magmatic layering in Atâ tonalite and cogenetic felsic dykes. Coastal outcrop 3.5 km east of Ataa.

solidification of the Atâ magma. Kalsbeek & Skjernaa (1999, this volume) were able to separate several successive intrusive phases of Atâ tonalite in areas adjacent to the inner part of Ataa Sund, but it has not been possible to trace these phases throughout the intrusion.

The southern boundary of the Atâ tonalite towards other Archaean orthogneisses is difficult to define. Escher & Burri (1967) placed it where deformation becomes obvious, but the situation is complicated by the presence of younger granitoids and flat-lying shear zones in the border area. These shear zones have imposed rapid changes in lithology and intensity of deformation and are difficult to distinguish from the original marginal facies of the complex. On the accompanying map (Garde 1994) a slice of Atâ tonalite has been tentatively shown between two shear zones south of the tonalite massif itself.

Gneisses and supracrustal rocks in the Rodebay domain

The tract of orthogneisses extending between the Atâ tonalite and Jakobshavn Isfjord was originally collectively named the 'Jakobshavn gneiss' by Escher & Burri (1967). During the Disko Bugt Project it has become apparent that the rocks in this area probably belong to two different tectonic domains, the Rodebay and Nunatarsuaq domains (Fig. 1).

The Rodebay domain comprises varieties of grey, migmatised biotite orthogneiss with mafic tonalitic to trondhjemitic compositions (*biotite-rich orthogneiss*, dgn; *orthogneiss*, gn), and a granodioritic unit termed the *Rodebay granodiorite* (Rg) which is described in more detail below. Ion probe U-Pb analysis of zircons from an orthogneiss in the Eqi area predating the Atâ tonalite (field observations by M. Marker, personal communication 1991) gave an age of 2815 Ma (Nutman & Kalsbeek 1999, this volume). The orthogneisses in the areas surrounding Kangerluarsuk and on southern Arveprinsen Ejland commonly resemble the Atâ tonalite in general appearance but mostly lack cross-cutting veins. Ductile shearing is widespread (Escher *et al.* 1999; Grocott & Davies 1999, both in this volume). Supracrustal rocks are subordinate and mainly consist of intensely folded amphibolite bands, but locally there are also horizons of biotite-garnet schist, notably on the coast south of outer Kangerluarsuk. The age relationships between these supracrustal rocks and the surrounding orthogneisses are not known.

Rodebay granodiorite

The *Rodebay granodiorite* (Rg) comprises fairly homogeneous, fine- to medium-grained grey biotite gneiss, typically with up to several centimetres large feldspar crystals. These big feldspars consist of antiperthite cores (presumably originally phenocrysts) with rims of K-feldspar, and may cut foliation surfaces. The foliation is mostly subhorizontal to south or south-east dipping. Pegmatitic segregations (weak migmatisation) at a scale of centimetres are common. Escher & Burri (1967) mapped part of the Rodebay granodiorite as leucocratic siliceous gneisses. The large extent of the Rodebay granodiorite was discovered as a consequence of a systematic rock sampling programme in 1991 (A. Steenfelt, unpublished data). It was recognised that the chemistry of the Rodebay granodiorite is clearly distinguishable from the gneisses to the north, west

Fig. 18. Sheets and irregular blebs of pink granite intruding granitoid gneisses, 9 km south of Laksebugt, west coast of Arveprinsen Ejland. Width of outcrop in the foreground *c*. 5 m.

(Arveprinsen Ejland) and south-east (Nunatarsuaq), and there is good agreement between our field observations of feldspar-phyric granitoid gneisses and the areas with this geochemical signature. The most evolved samples are granitic in composition.

The two areas with Rodebay granodiorite are separated by a *c*. 5 km wide sector of mixed rock units which include banded polyphase tonalitic orthogneiss with basic enclaves (some partly digested), mafic metavolcanics, and granitic gneiss, but individual rock units within this sector have not been mapped in detail. The boundaries with the Rodebay granodiorite appear to be mainly tectonic, although a fairly distinct lithological boundary between the Rodebay granodiorite and neighbouring gneisses was established at one locality *c*. 1.5 km south of Bredebugt. The flat-lying orientation of the Rodebay granodiorite may indicate that it intruded as subhorizontal sheets.

The central part of the Rodebay granodiorite contains two layers (tectonic slices?) of supracrustal rocks dominated by mafic metavolcanics. Their boundaries with the surrounding gneiss are sheared, and the nature of the original contact relationship is unclear. Metre-sized ultramafic bodies occur in the structurally lower section of the sequence. These rocks have a strong S fabric dipping weakly towards SE, as well as south-east-plunging rodding and mineral lineation.

Also the gneisses east of Paakitsoq, shown on the 1:250 000 map with 'orthogneiss' signature, are locally feldspar-phyric. Their chemical composition is reminiscent of the Rodebay granodiorite, and they may be related to it.

Late granitoid rocks

Granitic magma, now in the form of clearly discordant pink microgranite and quartz-feldspar pegmatites (*granitic gneiss*, ggn, and *pegmatite and granite*), has intruded into the gneiss terrain between the Atâ tonalite and the Rodebay granodiorite. The largest occurrences of granite of this type were encountered in southern Arveprinsen Ejland (Fig. 18) and have given a Rb-Sr whole-rock isochron age of 2825 ± 50 Ma (Kalsbeek & Taylor 1999, this volume). Fairly voluminous granitic sheets have also intruded the supracrustal sequences in the mixed sector that separates the two areas of Rodebay granodiorite.

Nunatarsuaq domain

The *orthogneiss* (gn) at Nunatarsuaq comprises fine-grained, commonly banded, light to dark grey biotite-bearing rocks of tonalitic-trondhjemitic composition. Migmatitic appearance and pegmatitic schlieren are common. The gneisses have been folded together with large units of supracrustal rocks described in the following. Although late granite-pegmatite phases of the gneisses can sometimes be seen to intrude supracrustal enclaves it is uncertain whether the bulk of the gneisses are younger than the supracrustal rocks.

Nunatarsuaq supracrustal rocks

The largest occurrences of supracrustal rocks outside the area around Torsukattak occur on the peninsula Nunatarsuaq north of Jakobshavn Isfjord, and are dominated by metasediment. These supracrustal rocks have amphibolite facies mineral parageneses, and outline a

Fig. 19. Alternating layers of light muscovite schist and dark grey biotite (-hornblende) schist of volcanic or sedimentary origin. The rocks are strongly deformed. Northern Nunatarsuaq.

series of approximately east–west-trending refolded folds. The largest sequence in the northern part of Nunatarsuaq has an apparent present thickness of about 4 km and forms an asymmetric, north-vergent composite antiform fold with a *c.* 8 km wide northern flank (Fig. 1). This large fold refolds earlier folds, and the northern flank is probably structurally repeated by two other, earlier isoclinal folds. The true thickness of the supracrustal rocks in their deformed state is probably no more than *c.* 1 km. The supracrustal rocks along the southern flank are only about 300 m thick, strongly sheared, and apparently strongly attenuated by deformation.

No primary structures which could show the direction of younging have been found, and the boundaries to the surrounding gneisses are strongly deformed and do not provide definite clues to age relationships. The gneisses along the well-exposed southern amphibolite-gneiss contact of the northern fold flank contain frequent supracrustal inclusions which range in size from decimetres to metres; this might suggest that the orthogneisses intruded the supracrustal rocks.

Very dark, fine-grained *amphibolite* (Na), commonly garnet-bearing and sometimes with scattered centimetre-sized hornblende crystals, is found mainly in the centre and along the margins of the northern flank; the dark amphibolites may be one and the same refolded unit. Locally the amphibolites are intruded by pre- or synkinematic pegmatite veins. Fine-grained variegated *biotite-garnet schist*, *muscovite schist and semipelite* (Nms) occur adjacent to the amphibolites; grey biotite (-garnet) schists predominate but are intercalated with darker, biotite-rich and lighter, muscovite-garnet-rich schists, which sometimes possess indistinct colour banding (Fig. 19). Coarse-grained quartzo-feldspathic schlieren in the metasediments locally contain garnets up to *c.* 3 cm in diameter. The mica schists commonly contain rusty pyrrhotite-bearing zones (see below), which are up to a few metres thick. In some areas layers of garnet amphibolite, commonly only a few centimetres thick and therefore probably of pyroclastic origin, alternate with the biotite schists.

Disseminated pyrite and pyrrhotite are common in the supracrustal rocks, and also small quartz-feldspar lenses and quartz veins. The regional stream sediment sampling programme by the Survey has indicated a couple of small gold anomalies within the supracrustal rocks at Nunatarsuaq (Steenfelt 1992), but no other exploration has been carried out in the area.

Two *c.* 30 m thick and about 5 km long horizons of impure marble, locally with tremolite and scapolite, are exposed on north-facing cliffs in the northernmost part of the large fold (Fig. 20). Loose blocks of similar marble have been found scattered all over Nunatarsuaq, indicating that *in situ* marble also exists to the east under the Inland Ice.

The central part of the supracrustal rocks contains several semi-concordant bodies of intrusive pinkish *microgranite* (no acronym on the 1:250 000 scale map) which are up to several kilometres long and 200 m thick. These granites are much finer grained than the orthogneisses outside the supracrustal rocks and appear to be less deformed. Their location close to inter-

Fig. 20. North-facing cliff face above the ice margin in northern Nunatarsuaq, showing a variegated series of supracrustal rocks. The two white layers consist of tremolite-bearing marble. The cliff is about 200 m high.

nal hinge zones may suggest that they were intruded during a phase of folding that predated the 8 km antiform structure.

In south-eastern Nunatarsuaq there are several, up to about 1 km wide, exposures of supracrustal rocks, mainly schist and garnet-bearing paragneiss but also agmatised amphibolite. The paragneiss exposures are associated with numerous small bodies and veins of white garnet-bearing granitoid rocks that appear to be partial melt products of the paragneiss.

In summary, the supracrustal rocks in the Nunatarsuaq domain differ from those north and south of Torsukattak in several ways. The succession is dominated by intermediate biotite-rich quartzo-feldspathic rocks, and also contains two *c.* 30 m thick horizons of impure marble. Mafic metavolcanic rocks are subordinate and ultrabasic rocks absent. The concentration of arsenic in stream sediment is low (Steenfelt 1992), and no signs of major volcanic exhalative activity have been observed. The general character of the Nunatarsuaq supracrustal rocks may suggest a platform or intracratonic basin type of setting.

Fig. 21. Basal unconformity and the Proterozoic Anap nunâ Group in south-eastern Anap Nunaa, looking east. Right, with person: Archaean acid metavolcanic rocks. Valley bottom: rubble of basal quartzite and pink marble of the Anap nunâ Group, obscuring the basal unconformity. Lower slope: impure marble succeeded by ultramafic lamprophyric extrusive rocks (including the white bed). The white bed is 1–3 m thick. Upper slope: sandstones and siltstones. Far distance: pink albitised sediments.

Fig. 22. Sheared unconformity (along the river) between Archaean greenstone (left) and Proterozoic marble conglomerate (centre right) overlain by dark sandstones and siltstones of the Anap nunâ Group on Qapiarfiit. Width of outcrop at middle distance *c*. 200 m.

Proterozoic platform sediments and intrusive rocks

Anap nunâ Group

Proterozoic tidal flat and mostly shallow water, presumably marine sediments form an arcuate belt south of Torsukattak on Qeqertakassak, Anap Nunaa and Qapiarfiit. Outcrops also occur on Nunataq and Arfiusaq east and south-east of the head of Torsukattak. At Qapiarfiit the sediments strike NW and dip 25–40° NE. On the island Qeqertakassak and at Anap Nunaa they have a general east–west trend and are folded into a series of upright, open to tight folds; the intensity of deformation increases towards the north and west. The sediments are collectively known as the Anap nunâ Group (Escher & Burri 1967). The Anap nunâ Group originally also comprised the Archaean supracrustal rocks around Torsukattak, since Escher & Burri (1967) were not able to distinguish the two age groups from each other. The sediments of the Anap nunâ Group are partially recrystallised, but unmetamorphosed or only weakly metamorphosed. The lower part has been subject to pervasive albitisation, which was studied on Qeqertakassak by Kalsbeek (1992; see p. 32).

The Anap nunâ Group was deposited on Archaean supracrustal rocks, and the basal unconformity is exposed on Anap Nunaa (Fig. 21), Qapiarfiit and Nunataq. In all three areas thick sequences of silt- and sandstones form the bulk of the sediments; the total thickness of the Anap nunâ Group is at least about 3600 m, but possibly considerably more if the deposits on Arfiusaq form a direct continuation of those on Qapiarfiit. On Anap Nunaa a less than 30 m thick basal quartzite rests on sheared acid metavolcanic rocks and metabasic rocks; on Qapiarfiit a polymict conglomerate with marble clasts rests on Archaean greenstones (Fig. 22).

At Anap Nunaa the Proterozoic sediments have a minimum thickness of 2500 m; they were described by Andersen (1991). The degree of deformation varies considerably, but exposure is generally good and the lower 530 m of the succession show a large lateral continuity of the sedimentary units. A basal shallow marine, clastic quartzitic unit is overlain by 50 m of cream to pink coloured marble (*marble*, m), interpreted as sub- to supratidal deposits in a normal to hypersaline environment (Andersen 1991). The interpretation is based on the presence of oolites, teepee-structures and algal laminae as well as chicken-wire structures indicating the precipitation of nodular anhydrite. The marble is succeeded by *c*. 350 m of mainly clastic, heterolithic sediments characterised by wave-ripples and desiccation cracks interpreted as tidal deposits (Fig. 23). These shallow water deposits are abruptly overlain by deeper water clastic sediments. According to Andersen (1991), siltstones and fine-grained sandstones (*siltstone and sandstone*, fs and ms) with a total thickness of *c*. 2000 m constitute an overall shallowing succession of turbidites, terminated by inner-shelf storm-deposits characterised by hummocky cross-stratification (*sandstone*, s).

The sediments at Arfiusaq, which may represent the uppermost preserved part of the Anap nunâ Group, consist of cross-bedded sandstone with local intrafor-

Fig. 23. Siltstone of the Anap nunâ Group with ripple marks and desiccation cracks, indicating intertidal or shallow water environment. Central Qeqertakassak west of Anap Nunaa.

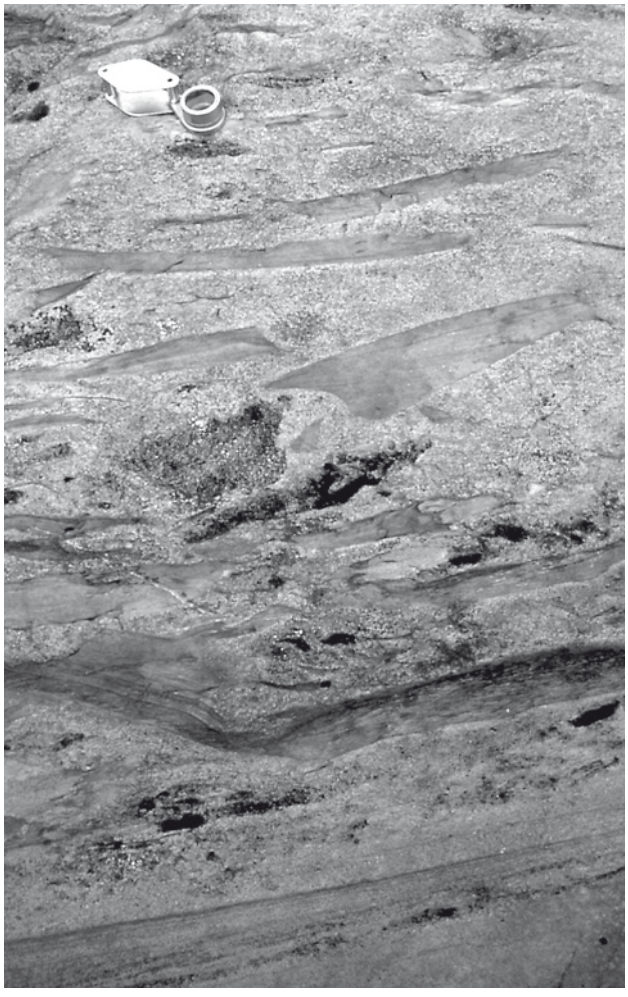

Fig. 24. Sandstone and intraformational conglomerate with angular clasts of siltstone. Anap nunâ Group, Arfiusaq nunatak.

mational conglomerate beds containing angular siltstone fragments of local origin (Fig. 24).

On Nunataq sedimentary rocks of presumed Proterozoic age form a thin, isoclinally folded greenschist facies sequence of *quartzite* (q), *marble* (m) and *metapelite* (mp) (Fig. 25). They overlie Archaean supracrustal rocks (Higgins & Soper 1999, this volume) and are considered by these and the present authors to belong to the lowest part of the Anap nunâ Group.

Proterozoic marble on northern Nuussuaq

An up to *c.* 350 m thick, isoclinally folded marble body (*marble*, m) with two showings of sphalerite mineralisation and a very complex internal structure occurs at Kanaakip Aaffaa in northern Nuussuaq within Archaean orthogneisses (Fig. 26). A couple of thinner marble horizons with local mineralisation lie in the gneisses between Kanaakip Aaffaa and the north coast of Nuussuaq. The marble at Kanaakip Aaffaa is shown on the geological map at scale 1:500 000 (Escher & Burri 1967; Escher 1971), but no descriptions from that time have been published. Economic and structural aspects of the marble have been discussed in unpublished company reports (King 1983; Della Valle & Denton 1991) and by Garde & Thomassen (1990). The marble has several characteristics which closely resemble the Proterozoic Mârmorilik Formation in the Uummannaq district (Garde 1978): it consists of both tremolite-bearing dolomite marble and calcite marble, contains

Fig. 25. Steeply inclined overturned Proterozoic marble (light, middle distance) in contact with Archaean mica schist and amphibolite (far distance) on Nunataq. Width of outcrop at middle distance *c*. 100 m.

quartzitic and semipelitic horizons, and hosts sphalerite mineralisation. Furthermore, its structural setting as an isoclinally folded body tectonically interleaved with Archaean gneisses is also similar (Pulvertaft 1986; Henderson & Pulvertaft 1987). It is therefore believed that the marble occurrences in northern Nuussuaq are Proterozoic and belong to the Mârmorilik Formation.

Basic dykes and sills

Basic dykes and sills (μ) occur around Paakitsoq (Escher *et al*. 1999, this volume), on Nunatarsuaq, and particularly in the south-western and north-eastern parts of the Nuussuaq basement (*dolerite dykes and sills*, δ); flat-lying to inclined sills are most common. The sills can be quite thick, up to 200 m, and the thicker ones are commonly differentiated with olivine-rich ultrabasic bases. Sills on Nuussuaq locally have variable and steeper dips, but it is not always clear if this is a primary feature or due to folding. At least some of them have been sheared and folded, and examples from the north coast of Nuussuaq can be seen on Fig. 2 and in Garde (1992, figs 2–3). Also the sills in the south-western part of Nuussuaq are variably folded and sheared; a sill at Sanningasoq is affected by open folding and

Fig. 26. Isoclinally folded marble (subhorizontal fold axis plunging SE) of presumed Proterozoic age, bounded by Archaean orthogneiss. Locality 15 km north-west of Saqqap Tasersua in northern Nuussuaq. View towards north-west from helicopter. Height of cliffs about 500 m.

has strongly sheared margins, but the centre is almost undeformed with its igneous texture preserved. Another, *c*. 50 m thick sill in that area (see Garde & Steenfelt 1999, fig. 9, this volume) appears from a distance to form a recumbent isoclinal fold, but the supposed hinge zone was not inspected at close hand. The differentiated sills and their geological setting resemble the descriptions by Schiøtte (1988) of deformed Archaean or early Proterozoic metabasites in the Uummannaq district which predate the main event of Rinkian recumbent folding.

North-east of the embayment Ilorleeraq at the south coast of Nuussuaq there is a group of NW-trending dolerite dykes, for which we propose the name Ilorleeraq dykes. The dykes, which are not sufficiently numerous to form a real swarm, are very thin, normally less than 10 m thick. Some of the dykes are variably deformed and metamorphosed (see below), but others are undeformed, have sharp contacts to the orthogneisses that host them, and 10–20 cm thick chilled margins. The Ilorleeraq dykes have therefore intruded cold and stable crust, and are presumably Proterozoic in age. The Ilorleeraq dykes are described in more detail by Garde & Steenfelt (1999, this volume).

Medium- to coarse-grained gabbroic sills, which are undeformed and undifferentiated, have intruded the Anap nunâ Group on Anap Nunaa, Nunataq, Qapiarfiit and at the western end of Qeqertakassak. The sills are generally subparallel to bedding, dipping 20–40°.

Undeformed *dolerite dykes* (δ) of proven or presumed Proterozoic age also occur in the region. The most prominent one is a 400 km long, NNW–SSE-trending, 1645 Ma old dolerite dyke described by Kalsbeek & Taylor (1986), which cuts the eastern part of Nuussuaq and the gneisses east of Disko Bugt. NW-trending dykes are common in the area north-east of Ilulissat.

Albitisation

Both on Qeqertakassak, Anap Nunaa and Qapiarfiit the clastic quartzo-feldspathic rocks in the lower part of the Anap nunâ Group have been partially or completely altered to massive, very fine-grained, pinkish yellow albitites, which are locally cut by narrow vertical carbonate veins. They are shown on the map as *albitised sandstone and siltstone* (αs). Kalsbeek (1992) studied the chemistry of the albitised rocks on Qeqertakassak in detail and showed that their composition has been substantially altered. All primary sedimentary structures have been obliterated in the albitised rocks, which frequently contain scattered, few millimetres large dolomite and pyrite crystals that leave characteristic vugs on weathered surfaces. The albitisation is transgressive with respect to the east–west-trending folds on Qeqertakassak and Anap Nunaa and has affected an undeformed mafic dyke (Kalsbeek 1992; a colour photograph of the altered dyke was shown by Kalsbeek & Christiansen 1992). This shows that the albitisation postdates the regional Proterozoic deformation, which is also supported by isotopic age data reported by Kalsbeek & Taylor (1999, this volume). Nevertheless, the large lateral extent of the alteration and its confinement to the lower part of the sedimentary sequence indicate that the alteration process has exploited the physical properties of the sediments.

Albitisation has also affected Archaean orthogneisses north of Paakitsoq (Ryan & Escher 1999, this volume). In some cases the albitisation follows late north-west-trending faults.

Lamprophyres and lamproites

The area south of Torsukattak contains at least two age groups of Proterozoic lamprophyres and lamproites; field evidence and age determinations by Larsen & Rex (1992) and Rasmussen & Holm (1999, this volume) indicate that the younger group is around 1750 Ma old. The known occurrences were all discovered during the Disko Bugt Project, and it seems likely that more could be found by a systematic effort.

The younger group, which essentially post-dates Proterozoic deformation, comprises a lamproite stock dated at 1743 ± 70 and 1764 ± 24 Ma (phlogopite K-Ar ages, Larsen & Rex 1992; Rasmussen & Holm 1999, this volume) and several ultramafic lamprophyric dykes (1782 ± 70 Ma, Larsen & Rex 1992). The 1750 Ma lamproite was described by Skjernaa (1992). It forms a *c*. 40 × 65 m large stock with ellipsoidal phlogopite nodules, and occurs at Oqaatsunnguit near Ataa Sund; a nearby satellite exposure measures 15 × 25 m. Marker & Knudsen (1989) described an east–west-trending swarm of decimetre- to metre-thick ultramafic lamprophyre dykes south and west of Eqi. Subsequent field work in 1989 and 1991 revealed that such dykes are also common on the mainland further west and in the central part of Arveprinsen Ejland, mostly trending east–west but also with other directions; some are flat-lying and exploit existing shear zones. In the southern part of Arveprinsen Ejland Grocott & Davies (1999, this volume) lo-

Fig. 27. Nodular ultramafic lamprophyre with large corroded crystals of magnesium-rich orthopyroxene. Central part of the island Qeqertaa in Kangerluarsuk.

cated a *c*. 1 km long, north-north-east-trending ultramafic lamprophyre. On the small island Qeqertaa in Kangerluarsuk the authors found an up to 5 m thick dyke with jumbled olivine nodules and large corroded orthopyroxene crystals (Fig. 27) which are probably of mantle origin (L.M. Larsen, personal communication 1989).

The older group occurs on southern Anap Nunaa. Thomsen (1991) described an occurrence of ultramafic lamprophyre with olivine and magnetite nodules, which forms a more or less conformable band along the marble in the basal part of the Anap nunâ Group (Fig. 21). A possible discordance to the Proterozoic deposits occurs in a cliff *c*. 1.5 km north-west of the main, apparently conformable lamprophyre exposure, which might indicate that the lamprophyre in the north-western exposure is a sill. However, thrusting along the lamprophyre horizon has obscured the contact relationships, and the apparent discordance may not be real. The lamprophyre locally contains textures and stratification reminiscent of pyroclastic rocks, and the interpretation is favoured that the ultramafic lamprophyre in both localities is a volcanic surface deposit. The stratified lamprophyre has been cut by a *c*. 80 cm thick carbonate-rich lamprophyre dykelet.

Thomsen (1991) also found two lozenge-shaped plugs of ultramafic lamprophyre with similar olivine and magnetite nodules which have intruded the Archaean acid metavolcanic rocks south of the Anap nunâ Group.

Structural and metamorphic evolution

The following outline of the Precambrian structural and metamorphic history between Qarajaq Isfjord and Jakobshavn Isfjord is mainly based on: (1) geological reconnaissance on Nuussuaq and in the area south of Paakitsoq by the authors, and in the Ataa area by Knudsen *et al*. (1988), (2) studies of the Atâ tonalite complex and the Nunataq area (Higgins & Soper 1999; Kalsbeek & Skjernaa 1999, both in this volume), (3) geological mapping at scale 1:100 000 south of the Atâ tonalite (Escher *et al*. 1999, this volume), and (4) a detailed structural investigation of the southern part of Arveprinsen Ejland by Grocott & Davies (1999, this volume). In addition, hornblende K-Ar ages from samples collected in the whole region (Rasmussen & Holm 1999, this volume) have provided information about the timing of thermal events.

The region between Qarajaq Isfjord and Jakobshavn Isfjord is located in the boundary zone between the previously established Rinkian and Nagssugtoqidian orogenic belts to the north and south (e.g. Grocott & Pulvertaft 1990; Kalsbeek *et al*. 1987). Substantial evidence is now available that at least the northern part of the region has been affected by strong Proterozoic structural and thermal reworking (Garde & Steenfelt 1999; Higgins & Soper 1999, both in this volume). However, field criteria which might serve to separate Archaean and Proterozoic tectonic events are scarce, and apart from the above mentioned hornblende K-Ar study no isotopic ages have so far been obtained from Nuussuaq. At any rate it is difficult to establish the age of a tectonic event *per se* with currently available iso-

topic methods. The conclusions presented in the following may therefore have to be revised in the future.

Based on variations in the structural and metamorphic history in different parts of the region we have distinguished four tectono-metamorphic domains, the Nuussuaq, Ataa, Rodebay and Nunatarsuaq domains (Fig. 1; index map in Garde 1994), which are described below.

Nuussuaq domain

Garde & Steenfelt (1999, this volume) present evidence that the Nuussuaq domain has been subjected to substantial Proterozoic reworking and discuss its boundary relationships along the fjord Torsukattak (Fig. 1) to the Ataa domain which was much less affected by Proterozoic deformation. In the following we highlight the evidence that a major part of the present structure of Nuussuaq was acquired during the early Proterozoic.

As described earlier in this paper, the Nuussuaq domain consists of Archaean amphibolite facies orthogneisses, sequences of Archaean continental margin supracrustal rocks (probably deposited on a basement of Nuussuaq gneisses), inclusions of variable size of amphibolite and metasediments, and kilometre-scale tectonic slices and smaller enclaves of a layered anorthosite-gabbro complex. Repeated and intense deformation, which we presume is Proterozoic, resulted in general flat-lying structures in northern Nuussuaq (Garde 1992), a series of kilometre-scale, NW–SE-trending upright folds, and several shear zones. The upright NW–SE-trending folds and the likewise NW–SE-trending Puiattup Qaqqaa shear zone were formed during crustal shortening, and were succeeded by development of the ENE–WSW-trending Torsukattak shear zone during an episode of crustal extension. The flat-lying structure and major thrusts in the northern part of the Nuussuaq domain have much in common with the structural style of the Uummannaq district to the north. Extensive resetting of hornblende K-Ar isotope systematics (Rasmussen & Holm 1999, this volume) shows that the Nuussuaq basement reached amphibolite facies metamorphism in the early Proterozoic.

Evidence for Proterozoic deformation in Nuussuaq and on Nunataq

Calcite and dolomite marble with zinc mineralisation, and adjacent semipelitic metasediments form a major recumbent fold embedded in orthogneisses north-west of Saqqap Tasersua in central Nuussuaq (Fig. 26). Several other tectonic slices of marble associated with clastic sediments occur farther north. These rocks are considered to belong to the early Proterozoic Mârmorilik Formation (Garde & Thomassen 1990) and show that major thrusting and isoclinal folding of Proterozoic age took place in the north-western part of the Nuussuaq basement, involving both orthogneisses and cover rocks. Local development of calc-silicate minerals like tremolite and diopside in the marble support the evidence from hornblende K-Ar isotope systematics that lower amphibolite facies metamorphic conditions were reached in central Nuussuaq during the early Proterozoic.

Also Nunataq at the south-eastern end of the Nuussuaq basement provides evidence of Proterozoic deformation (see also Higgins & Soper 1999, this volume). Nunataq contains isoclinally folded Proterozoic metasedimentary rocks which are part of the Anap nunâ Group. Proterozoic marker horizons such as metasediment similar to the Mârmorilik Formation or Anap nunâ Group have so far not been found in other parts of Nuussuaq. However, east or south-east-trending tight to isoclinal fold systems overprinting earlier fold structures, as well as late flat-lying shear zones and thrusts, can be recognised in most parts of Nuussuaq.

Both the Ilorleeraq dykes west of Boye Sø and a group of basic sills in central Nuussuaq were emplaced into stabilised Archaean crust and subsequently deformed, and the Ilorleeraq dykes are also metamorphosed with new growth of hornblende. The sills have generally preserved magmatic textures in their interior parts but have developed new cleavage at their margins, and the orthogneiss hosts adjacent to the sills are commonly strongly sheared. Some of these sills appear to have been folded. An isoclinally folded basic sill was observed at the north coast of Nuussuaq (Garde 1992), and similar, isoclinally folded metabasic sills were described by Schiøtte (1988) from the southern part of the Uummannaq district; the latter sills cut the Archaean orthogneiss but predate the main episode of Proterozoic isoclinal folding. We consider that the basic sills in Nuussuaq (and also those in the central part of the Rodebay domain, p. 36) are likely to be of early Proterozoic age.

Shear zones in southern Nuussuaq and the boundary between the Nuussuaq and Ataa domains

The Puiattup Qaqqaa shear zone (Garde & Steenfelt 1999, this volume) is a prominent NW–SE-trending synformal zone of highly strained rocks in the south-eastern part of Nuussuaq, which comprises a tectonic mélange of Archaean supracrustal and infracrustal rocks. The shear zone is probably Proterozoic and contemporaneous with the system of NW–SE-trending folds in Nuussuaq. In the south-eastern end of the shear zone its two margins diverge in opposite directions towards Torsukattak like an inverted Y until they have a common ENE–WSW trend along the fjord (Garde & Steenfelt 1999, fig. 2, this volume), and an intense SE-plunging stretching lineation is developed. These structures are interpreted in terms of later deformation in a second ductile shear zone located along Torsukattak, in which the main sense of displacement was parallel to the extension lineation with oblique south-east downthrow of the southern side (see Garde & Steenfelt 1999, fig. 10, this volume). This interpretation is supported by structural evidence from Nunataq and the northernmost part of the Ataa domain, and also provides an explanation of the contrast in metamorphic grade observed across Torsukattak.

Ataa domain

The Ataa domain in the central part of the Disko Bugt – Nuussuaq region (Fig. 1) consists of a little to moderately deformed Archaean granite-greenstone terrain, namely the Arveprinsen–Eqi supracrustal rocks (forming a large synclinal cusp in the west and an inverted sequence in the east) and the Atâ tonalite that intrudes them. The Archaean rocks are overlain by an unconformable, about 10 km wide belt of Proterozoic epicontinental sedimentary rocks. Part of the Ataa domain has been subject to weak Proterozoic structural and metamorphic reworking which increases towards the north, but the local retention of Archaean K-Ar and Ar-Ar hornblende ages (Rasmussen & Holm 1999, this volume) shows that the Ataa domain to a large extent has escaped the Proterozoic metamorphic (and structural) overprinting that affected the other parts of the region.

The Proterozoic sedimentary rocks contain open upright folds, sometimes associated with internal thrusts. However, much of the Archaean basement south of the Anap nunâ Group hardly appears to have been affected by Proterozoic metamorphism or deformation, or indeed Archaean deformation post-dating the intrusion of the Atâ tonalite (Kalsbeek *et al.* 1988).

This fact formed the basis for the original identification of the 'Atâ granite' by Escher & Burri (1967). It has already been mentioned that a distinct foliation can commonly be observed along the margins of the Atâ tonalite parallel to the greenstone contacts; the foliation is thought to have developed during late stages of the emplacement of the complex (Kalsbeek & Skjernaa 1999, this volume). We have tentatively placed the southern margin of the Ataa domain at the southern boundary of the Atâ tonalite, which occurs in the central part of Arveprinsen Ejland and north of Kangerluarsuk where the granitoid rocks begin to contain flat-lying shear zones. The arbitrary nature of this domain boundary was discussed previously in the section describing the Atâ tonalite.

The supracrustal rocks on Qapiarfiit and Eqi contain several roughly north–south-trending, east-dipping thrusts. One of these appears to be truncated by the Proterozoic unconformity on Qapiarfiit (Fig. 22), and can be followed about 10 km southwards from Eqi into the orthogneisses. This thrust (and perhaps also others with similar orientations in the same area) is therefore most likely of Archaean age.

Proterozoic deformation in the Ataa domain

Both on Anap Nunaa and Qapiarfiit some shearing has occurred along the basal unconformity of the Anap nunâ Group, and the sedimentary sequences have been tilted *c.* 30° towards the NNE and NE respectively in the two areas. On Anap Nunaa and Qeqertakassak a series of approximately E–W-trending, open, non-cylindrical, upright to overturned folds with local thrusts along axial surfaces were formed (Andersen 1991; Kalsbeek 1992; Higgins & Soper 1999, this volume). The sediments on Qapiarfiit are not folded.

There is an apparent structural gap between the steep north-east-trending Archaean greenstones on Arveprinsen Ejland and the east–west-trending, variably dipping Proterozoic sediments on Qeqertakassak. This gap may constitute a Proterozoic shear zone, continuing eastwards along strongly sheared Archaean rocks along the peninsula Saattut on southern Anap Nunaa and perhaps even further south-east to the sheared unconformity on Qapiarfiit.

Fig. 28. Low-angle Proterozoic ductile shear zones in Archaean orthogneisses in a 250 m high, south-facing cliff north of Paakitsoq.

As already mentioned, Proterozoic deformation in the northern part of the Ataa domain generally increases towards Torsukattak. In northern Anap Nunaa delicate sedimentary structures (which are common elsewhere on the peninsula) have been destroyed, and close to the north coast a new north- to north-east-dipping axial plane cleavage was formed. Along the north coast of Oqaatsut and Arveprinsen Ejland a steep east–west cleavage and local small-folds with E–W-trending axes have been observed (Knudsen *et al.* 1988; H. Rasmussen, personal communication 1992) which could also be Proterozoic in age. These features are considered to provide supporting evidence for the proposed ductile shear zone along Torsukattak (Garde & Steenfelt 1999, this volume).

Rodebay domain

The Rodebay domain, which extends from south of the Atâ tonalite to Jakobshavn Isfjord, consists of Archaean orthogneisses with scattered layers and enclaves of supracrustal rocks (mainly banded amphibolite) that might be equivalents of the greenstones in the Ataa domain. Its northern part has been mapped by Escher *et al.* (1999, this volume). Contrary to the Ataa domain the Rodebay domain appears to have suffered moderate to strong deformation in the Archaean and presumably also in the early Proterozoic, when amphibolite facies metamorphic conditions were reached (Rasmussen & Holm 1999, this volume).

On Arveprinsen Ejland a series of low-angle ductile shear zones, which structurally underlie the Atâ tonalite, dip north and south in the central and southern parts of the island, respectively, and have been folded by a large open WNW-trending antiform (Grocott & Davies 1999, this volume). Upright folding with NE-trending axial surfaces followed in the southern part of the island, and right-lateral ductile displacements occurred along narrow near-vertical zones. The latest recognised phase of folding has E–W axial surfaces, was contemporaneous with injection of ultramafic lamprophyres (Grocott & Davies 1999, this volume), and was perhaps restricted to their immediate surroundings.

On the mainland between 69°30′ and 69°45N′ layers and enclaves of amphibolite delineate early (apparently Archaean) tight to isoclinal folds at scales of one to two kilometres. A fold of similar aspect in south-eastern Arveprinsen Ejland may likewise be Archaean. These folds are superimposed by south-vergent folds with east-plunging axial surfaces. The relationship between the folds and the Archaean shear zone that extends southwards into the orthogneisses from the supracrustal rocks at Eqi is not known with certainty.

Like Arveprinsen Ejland, the mainland also contains a number of flat-lying ductile shear zones with variable, generally easterly strike directions (Escher *et al.* 1999, this volume). Whereas there is at present no clear evidence regarding the age of flat-lying shear zones on Arveprinsen Ejland, at least some of those on the mainland are likely to be Proterozoic because they affect the basaltic to picritic sills in the vicinity of Paakitsoq (described above). Both these sills and those in central Nuussuaq are thought to be of Proterozoic age, like similar sills in the Uummannaq district (Schiøtte 1988). Some of the contact zones between the sills and their host gneisses are strongly sheared and the sills themselves are sometimes boudinaged along the

Fig. 29. Stretched, cigar-shaped ultramafic enclaves with south-easterly plunge in granitoid rocks with strong *LS* fabric. Locality east of Paakitsoq.

shear zones as can be seen on a 250 m high cliff face about 2.5 km north-east of Berggren Havn (Fig. 28; see also Escher *et al.* 1999, this volume). At least one episode of ductile shearing thus took place after the intrusion of the basic sills, probably in the early Proterozoic. Also towards the south-eastern boundary of the Rodebay domain there are several flat-lying shear zones, in which σ- and δ-shaped feldspar porphyroclasts indicate transport of the hanging wall in northerly directions.

A prominent late, vertical, ESE–WNW-trending ductile shear zone with shallow easterly-plunging stretching lineation occurs along Paakitsoq (Fig. 29; see also Knudsen *et al.* 1988, and Escher *et al.* 1999, this volume). It is superimposed by brittle faulting. The Paakitsoq shear zone was previously designated by Escher & Pulvertaft (1976) as the boundary between the Rinkian and Nagssugtoqidian mobile belts. Several faults in the southern part of Paakitsup Nunaa follow approximately the same direction as the Paakitsoq shear zone, and a couple of NE-trending, SE-dipping shear zones occur along the south-eastern margin of the Rodebay domain.

Nunatarsuaq domain

The reason for the designation of the Nunatarsuaq peninsula to a separate domain is the fact that neither large structures nor supracrustal and orthogneiss lithologies on Nunatarsuaq can be correlated across the fjord Sikuiuitsoq to the Rodebay domain. Nunatarsuaq with its common mica schists, orthogneisses of intermediate composition and large isoclinal folds (see below) seems to have more in common with the poorly known area south of Jakobshavn Isfjord than with the Rodebay domain. It is therefore likely that a significant structural boundary occurs in the fjord Sikuiuitsoq, which contains a north-east-trending zone of strongly sheared rocks along its western coast.

The most prominent structure in Nunatarsuaq is the large, multiply folded isocline outlined by steeply dipping, ENE-trending mica-garnet schists and amphibolites in the northern part of the peninsula. Measured fold axes and mineral lineations plunge 15–60° in directions around *c.* 80°. Another, east–west-trending isoclinal fold of smaller dimensions with a north-dipping axial surface occurs in the south-eastern part of the area.

Concluding remarks

The investigation of the region between Qarajaq Isfjord and Jakobshavn Isfjord during the Disko Bugt Project has produced several important geological results.

The existence of two different supracrustal groups in the central part of the region suggested by Kalsbeek *et al.* (1988) was firmly established: the Archaean Saqqaq, Itilliarsuk and Arveprinsen–Eqi supracrustal sequences (Garde *et al.* 1999; Rasmussen & Pedersen 1999; Marshall & Schønwandt 1999; Stendal *et al.* 1999, all in this volume), and the early Proterozoic Anap

nunâ Group. Substantial knowledge was attained about the lithologies, depositional environments, structure and economic potential of both groups. Two new types of Archaean gold mineralisation were discovered, one associated with alteration processes in a felsic dome complex east of Eqi (Stendal *et al.* 1999, this volume), the other in a more than 3 km long volcanogenic-exhalative horizon near Saqqaq (Garde *et al.* 1999, this volume).

Helicopter reconnaissance in the interior parts of eastern Nuussuaq, which were virtually unknown prior to the Project, led to the discovery of the large Boye Sø anorthosite complex and the establishment of two major units of orthogneiss in northern Nuussuaq. Besides, new information was gathered about major Proterozoic deformation in Nuussuaq and on Nunataq, and about a flat-lying Proterozoic structure along Qarajaq Isfjord. Furthermore, the importance of Proterozoic ductile thrusting south of the Atâ tonalite was documented by Escher *et al.* (1999) and Grocott & Davies (1999, both in this volume).

New information about geochemistry, structure and isotopic ages was obtained from the Archaean orthogneisses in the remainder of the region; in particular, the Atâ tonalite around Ataa Sund was investigated in detail (Kalsbeek & Skjernaa 1999, this volume).

Widespread but previously unknown Proterozoic albitisation was studied in the lower part of the Anap nunâ Group (Kalsbeek 1992) and around Paakitsoq (Ryan & Escher 1999, this volume), and a new province of lamprophyric and lamproitic rocks with an age of *c.* 1750 Ma was discovered (Marker & Knudsen 1989), including a spectacular ultramafic flow with magnetite nodules (Thomsen 1991), the Oqaatsunnguit lamproite stock with rounded phlogopite aggregates (Skjernaa 1992), and lamproitic dykes with olivine-rich nodules of presumed mantle origin.

Acknowledgements

Many participants in the Disko Bugt Project have helped us during the field work and contributed with knowledge and comments during preparation of this paper. In particular we wish to thank F. Kalsbeek (Geological Survey of Denmark and Greenland), for numerous discussions, many of which took place on key localities in the region. We also thank N.J. Soper (Barnsley, UK) for a constructive review, and G.K. Pedersen (Geological Institute, University of Copenhagen), for help with the section on Proterozoic sediments.

References

Andersen, J. 1991: Tidlig proterozoisk rift-relateret sedimentation og post-sedimentær deformation. Anap Nunâ, Diskobugten, Vestgrønland, 73 pp. Unpublished cand. scient. thesis, Københavns Universitet, Danmark.

Della Valle, G. & Denton, P. 1991: Geological report on the 1990 zinc and lead exploration programme in central Nûgssuaq peninsula, Maarmorilik Formation, West Greenland, 17 pp. Unpublished report, Intergeo-Exploration (in archives of Geological Survey of Denmark and Greenland).

Dueholm, K.S. 1992: Geologic photogrammetry using standard small-frame cameras. In: Dueholm, K.S. & Pedersen, A.K. (eds): Geological analysis and mapping using multi-model photogrammetry. Rapport Grønlands Geologiske Undersøgelse **156**, 7–17.

Dueholm, K.S., Garde, A.A. & Pedersen, A.K. 1993: Preparation of accurate geological and structural maps, cross-sections or block diagrams from colour slides, using multi-model photogrammetry. Journal of Structural Geology **15**, 933–937.

Escher, A. 1971: Geological map of Greenland, 1:500 000, Søndre Strømfjord – Nûgssuaq, sheet 3. Copenhagen: Geological Survey of Greenland.

Escher, A. & Burri, M. 1967: Stratigraphy and structural development of the Precambrian rocks in the area north-east of Disko Bugt, West Greenland. Rapport Grønlands Geologiske Undersøgelse **13**, 28 pp.

Escher, A. & Pulvertaft, T.C.R. 1976: Rinkian mobile belt of West Greenland. In: Escher, A. & Watt, W.S. (eds): Geology of Greenland, 104–119. Copenhagen: Geological Survey of Greenland.

Escher, J.C. 1995: Geological map of Greenland, 1:100 000, Ataa 69 V.3 Nord. Copenhagen: Geological Survey of Greenland.

Escher, J.C., Ryan, M.J. & Marker, M. 1999: Early Proterozoic thrust tectonics east of Ataa Sund, north-east Disko Bugt, West Greenland. In: Kalsbeek, F. (ed.): Precambrian geology of the Disko Bugt region, West Greenland. Geology of Greenland Survey Bulletin **181**, 171–179 (this volume).

Garde, A.A. 1978: The Lower Proterozoic Marmorilik Formation, east of Mârmorilik, West Greenland. Meddelelser om Grønland **200**(3), 71 pp.

Garde, A.A. 1992: Interpretation of flat-lying Precambrian structure by geological photogrammetry along a 65 km coastal profile in Nuussuaq, West Greenland. In: Dueholm, K.S. & Pedersen, A.K. (eds): Geological analysis and mapping using multi-model photogrammetry. Rapport Grønlands Geologiske Undersøgelse **156**, 35–40.

Garde, A.A. 1994: Precambrian geology between Qarajaq Isfjord and Jakobshavn Isfjord, West Greenland,1:250 000. Copenhagen: Geological Survey of Greenland.

Garde, A.A. & Steenfelt, A. 1989: A new anorthosite/gabbro complex at Nûgssuaq, central West Greenland. Rapport Grønlands Geologiske Undersøgelse **145**, 16–20.

Garde A.A. & Steenfelt, A. 1999: Proterozoic tectonic overprinting of Archaean gneisses in Nuussuaq, West Greenland. In: Kalsbeek, F. (ed.): Precambrian geology of the Disko Bugt

region, West Greenland. Geology of Greenland Survey Bulletin **181**, 141–154 (this volume).

Garde, A.A. & Thomassen, B. 1990: Structural and economic aspects of the Proterozoic marble on Nûgssuaq, West Greenland. Open File Series Grønlands Geologiske Undersøgelse **90/6**, 14 pp.

Garde, A.A., Kalsbeek, F., Marker, M. & Schønwandt, H.K. 1991: Archaean supracrustal rocks at different crustal levels in West Greenland, and their metallogeny. Terra Abstracts **3**, 194 only.

Garde, A.A., Thomassen, B., Tukiainen, T. & Steenfelt, A. 1999: A gold-bearing volcanogenic-exhalative horizon in the Archaean(?) Saqqaq supracrustal rocks, Nuussuaq, West Greenland. In: Kalsbeek, F. (ed.): Precambrian geology of the Disko Bugt region, West Greenland. Geology of Greenland Survey Bulletin **181**, 119–128 (this volume).

Gothenborg, J. 1983: Report on the ore exploration in the Ata area, Jakobshavn 1982, 49 pp. Unpublished report, Kryolitselskabet Øresund A/S (in archives of Geological Survey of Denmark and Greenland).

Gothenborg, J. & Morthorst, J. 1981: Report on the ore exploration in the Ata area, Jakobshavn 1981, 88 pp. Unpublished report, Kryolitselskabet Øresund A/S (in archives of Geological Survey of Denmark and Greenland).

Grocott, J. & Davies, S.C. 1999: Deformation at the southern boundary of the late Archaean Atâ tonalite and the extent of Proterozoic reworking of the Disko terrane, West Greenland. In: Kalsbeek, F. (ed.): Precambrian geology of the Disko Bugt region, West Greenland. Geology of Greenland Survey Bulletin **181**, 155–169 (this volume).

Grocott, J. & Pulvertaft, T.C.R. 1990: The Early Proterozoic Rinkian belt of central West Greenland. In: Lewry, J.F. & Stauffer, M.R. (eds): The Early Proterozoic Trans-Hudson Orogen of North America. Special Paper Geological Association of Canada **37**, 443–463.

Henderson, G. & Pulvertaft, T.C.R. 1987: The lithostratigraphy and structure of a Lower Proterozoic dome and nappe complex. Geological map of Greenland, 1:100 000, Mârmorilik 71 V.2 Syd, Nûgâtsiaq 71 V.2 Nord and Pangnertôq 72 V.2 Syd. Descriptive text, 72 pp., 3 maps. Copenhagen: Geological Survey of Greenland.

Higgins, A.K. & Soper, N.J. 1999: The Precambrian supracrustal rocks of Nunataq, north-east Disko Bugt, West Greenland. In: Kalsbeek, F. (ed.): Precambrian geology of the Disko Bugt region, West Greenland. Geology of Greenland Survey Bulletin **181**, 79–86 (this volume).

Kalsbeek, F. 1989: GGU's expedition in the Disko Bugt area, 1988. Rapport Grønlands Geologiske Undersøgelse **145**, 14–16.

Kalsbeek, F. 1990: Disko Bugt Project, central West Greenland. Rapport Grønlands Geologiske Undersøgelse **148**, 21–24.

Kalsbeek, F. 1992: Large-scale albitisation of siltstones on Qeqertakavsak island, northeast Disko Bugt, West Greenland. Chemical Geology **95**, 213–233.

Kalsbeek, F. & Christiansen, F.G. 1992: Disko Bugt Project 1991, West Greenland. Rapport Grønlands Geologiske Undersøgelse **155**, 36–41.

Kalsbeek, F. & Skjernaa, L. 1999: The Archaean Atâ intrusive complex (Atâ tonalite), north-east Disko Bugt, West Greenland. In: Kalsbeek, F. (ed.): Precambrian geology of the Disko Bugt region, West Greenland. Geology of Greenland Survey Bulletin **181**, 103–112 (this volume).

Kalsbeek, F. & Taylor, P.N. 1986: Chemical and isotopic homogeneity of a 400 km long basic dyke in central West Greenland. Contributions to Mineralogy and Petrology **93**, 439–448.

Kalsbeek, F. & Taylor, P.N. 1999: Review of isotope data for Precambrian rocks from the Disko Bugt region, West Greenland. In: Kalsbeek, F. (ed.): Precambrian geology of the Disko Bugt region, West Greenland. Geology of Greenland Survey Bulletin **181**, 41–47 (this volume).

Kalsbeek, F., Pidgeon, R.T. & Taylor, P.N. 1987: Nagssugtoqidian mobile belt of West Greenland: a cryptic 1850 Ma suture between two Archaean continents – chemical and isotopic evidence. Earth and Planetary Science Letters **85**, 365–385.

Kalsbeek, F., Taylor, P.N. & Pidgeon, R.T. 1988: Unreworked Archaean basement and Proterozoic supracrustal rocks from northeastern Disko Bugt, West Greenland: implications for the nature of Proterozoic mobile belts in Greenland. Canadian Journal of Earth Sciences **25**, 773–782.

King, A.R. 1983: Report on prospecting and correlating programme in the Maarmorilik Formation, West Greenland 1982, 21 pp. Unpublished report, Greenex A/S (in archives of Geological Survey of Denmark and Greenland).

Knudsen, K., Appel, P.W.U., Hageskov, B. & Skjernaa, L. 1988: Geological reconnaissance in the Precambrian basement of the Atâ area, central West Greenland. Rapport Grønlands Geologiske Undersøgelse **140**, 9–17.

Larsen, L.M. & Rex, D.C. 1992: A review of the 2500 Ma span of alkaline-ultramafic, potassic and carbonatitic magmatism in West Greenland. Lithos **28**, 367–402.

Marker, M. & Knudsen, C. 1989: Middle Proterozoic ultramafic lamprophyre dykes in the Archaean of the Atâ area, central West Greenland. Rapport Grønlands Geologiske Undersøgelse **145**, 23–28.

Marshall, B. & Schønwandt, H.K. 1999: An Archaean sill complex and associated supracrustal rocks, Arveprinsen Ejland, north-east Disko Bugt, West Greenland. In: Kalsbeek, F. (ed.): Precambrian geology of the Disko Bugt region, West Greenland. Geology of Greenland Survey Bulletin **181**, 87–102 (this volume).

Nielsen, A.T. 1992: Geologi, geokemi og tektonisk setting for Andersens mineraliseringen: En vulkansk massiv sulfidforekomst i det arkæiske supracrustalbelte, Arveprinsen Ejland, Vestgrønland, 98 pp. Unpublished cand. scient. thesis, Københavns Universitet, Danmark.

Nutman, A.P. & Kalsbeek, F. 1999: SHRIMP U-Pb zircon ages for Archaean granitoid rocks, Ataa area, north-east Disko Bugt, West Greenland. In: Kalsbeek, F. (ed.): Precambrian geology of the Disko Bugt region, West Greenland. Geology of Greenland Survey Bulletin **181**, 49–54 (this volume).

Pulvertaft, T.C.R. 1986: The development of thin thrust sheets and basement-cover sandwiches in the southern part of the Rinkian belt, Umanak district, West Greenland. Rapport Grønlands Geologiske Undersøgelse **128**, 75–87.

Rasmussen, H. & Holm, P.M. 1999: Proterozoic thermal activ-

ity in the Archaean basement of the Disko Bugt region and eastern Nuussuaq, West Greenland: evidence from K-Ar and $^{40}Ar/^{39}Ar$ mineral age investigations. In: Kalsbeek, F. (ed.): Precambrian geology of the Disko Bugt region, West Greenland. Geology of Greenland Survey Bulletin **181**, 55–64 (this volume).

Rasmussen, H. & Pedersen, L.F. 1999: Stratigraphy, structure and geochemistry of Archaean supracrustal rocks from Oqaatsut and Naajaat Qaqqaat, north-east Disko Bugt, West Greenland. In: Kalsbeek, F. (ed.): Precambrian geology of the Disko Bugt region, West Greenland. Geology of Greenland Survey Bulletin **181**, 65–78 (this volume).

Ryan, M.J. & Escher, J.C. 1999: Albitised gneisses in the area between Paakitsoq and Kangerluarsuk, north-east Disko Bugt, West Greenland. In: Kalsbeek, F. (ed.): Precambrian geology of the Disko Bugt region, West Greenland. Geology of Greenland Survey Bulletin **181**, 113–117 (this volume).

Schiøtte, L. 1988: Field occurrence and petrology of deformed metabasite bodies in the Rinkian mobile belt, Umanak district, West Greenland. Rapport Grønlands Geologiske Undersøgelse **141**, 36 pp.

Skjernaa, L. 1992: A lamproite stock with ellipsoidal phlogopite nodules at Oqaatsunnguit, Disko Bugt, central West Greenland. Rapport Grønlands Geologiske Undersøgelse **154**, 33–47.

Steenfelt, A. 1988: Progress in geochemical mapping of West Greenland. Rapport Grønlands Geologiske Undersøgelse **140**, 17–24.

Steenfelt, A. 1992: Gold, arsenic and antimony in stream sediment related to supracrustal units between Arfersiorfik and Qarajaq Isfjord (68°N to 70°30′N), West Greenland. Open File Series Grønlands Geologiske Undersøgelse **92/4**, 11 pp.

Stendal, H., Knudsen, C., Marker, M. & Thomassen, B. 1999: Gold mineralisation at Eqi, north-east Disko Bugt, West Greenland. In: Kalsbeek, F. (ed.): Precambrian geology of the Disko Bugt region, West Greenland. Geology of Greenland Survey Bulletin **181**, 129–140 (this volume).

Thomassen, B. & Tukiainen, T. 1992: Gold mineralisation in Precambrian supracrustal rocks on southern Nuussuaq, central West Greenland: 1991 results. Open File Series Grønlands Geologiske Undersøgelse **92/3**, 31 pp.

Thomsen, H.S. 1991: Contrasting types of metasomatic alteration in the low-metamorphic Precambrian Anap Nunâ area, West Greenland, 99 pp. Unpublished cand. scient. thesis, University of Copenhagen, Denmark.

Review of isotope data for Precambrian rocks from the Disko Bugt region, West Greenland

Feiko Kalsbeek and Paul N. Taylor

Pb-Pb and Rb-Sr isotope data yield whole-rock isochron ages of *c.* 2800 Ma for two localities of granitoid rocks in the Disko Bugt region, with little evidence of strong later disturbance. Rb-Sr isotope data on Archaean metasediments from two localities, however, were strongly disturbed during the early Proterozoic. Sm-Nd whole-rock data for acid metavolcanic rocks within Archaean supracrustal sequences yield model ages of *c.* 2800 Ma. The early Proterozoic age of a younger sequence of supracrustal rocks (the Anap nunâ Group) is confirmed by Sm-Nd data, and Rb-Sr whole-rock data for albitised siltstones show that albitisation took place hundreds of millions of years after the peak of early Proterozoic orogenic activity.

F.K., *Geological Survey of Denmark and Greenland, Thoravej 8, DK-2400 Copenhagen NV, Denmark.* E-mail: *fk@geus.dk.*
P.N.T., *Department of Earth Sciences, University of Oxford, Oxford OX1 3PR, UK.*

Keywords: Archaean, Disko Bugt, Pb-Pb ages, Proterozoic, Rb-Sr ages, Sm-Nd ages, West Greenland

The Precambrian terrain of the Disko Bugt region (Fig. 1) consists mainly of grey migmatitic gneisses with units of supracrustal rocks (Henderson 1969; Garde & Steenfelt 1999, this volume). Most rocks in the region are of Archaean age, variably reworked during early Proterozoic orogenic activity (Kalsbeek 1981, 1994). In north-eastern Disko Bugt a sequence of low grade early Proterozoic metasediments, the Anap nunâ Group, unconformably overlies Archaean rocks.

Among the Archaean rocks the well-preserved Atâ intrusive complex (Atâ Tonalite on the 1:250 000 scale map of Garde 1994) in north-eastern Disko Bugt (Fig. 1; Kalsbeek & Skjernaa 1999, this volume) represents an important time marker because it has been emplaced into older gneisses and supracrustal rocks and is itself cut by younger granites. It has been dated at *c.* 2800 Ma (Kalsbeek *et al.* 1988; Nutman & Kalsbeek 1999, this volume), and one of the younger granites has yielded a date of *c.* 2760 Ma (Nutman & Kalsbeek 1999, this volume). Supracrustal rocks in the north-eastern Disko Bugt region cut by Atâ granitoids (Fig. 1) consist mainly of basic metavolcanic rocks (in part pillow lavas) with minor proportions of metasediments; acid metavolcanic rocks are also present.

The Proterozoic sedimentary sequence north-east of Arveprinsen Ejland (Fig. 1) consists mainly of sand- and siltstones (Garde & Steenfelt 1999, this volume) with local sheets and dykes of basic igneous rocks. Large parts of this sequence have been strongly albitised (Kalsbeek 1992).

A few well-preserved basic dykes, up to 100 m wide, cut Archaean and Proterozoic rocks in the easternmost part of the region. One of these has been dated at 1645 ± 35 Ma (Rb-Sr whole rock isochron; Kalsbeek & Taylor 1986).

The Disko Bugt region lies between two early Proterozoic orogenic belts: the Nagssugtoqidian belt to the south and the Rinkian belt to the north (Fig. 1). In both belts the rocks have been affected by high-grade metamorphism and deformation about 1850 Ma ago (Kalsbeek *et al.* 1984; Taylor & Kalsbeek 1990) which strongly disturbed Archaean Rb-Sr and Pb-Pb whole rock isotope systems (e.g. Kalsbeek *et al.* 1987). Rocks in the Disko Bugt region appear to have been less

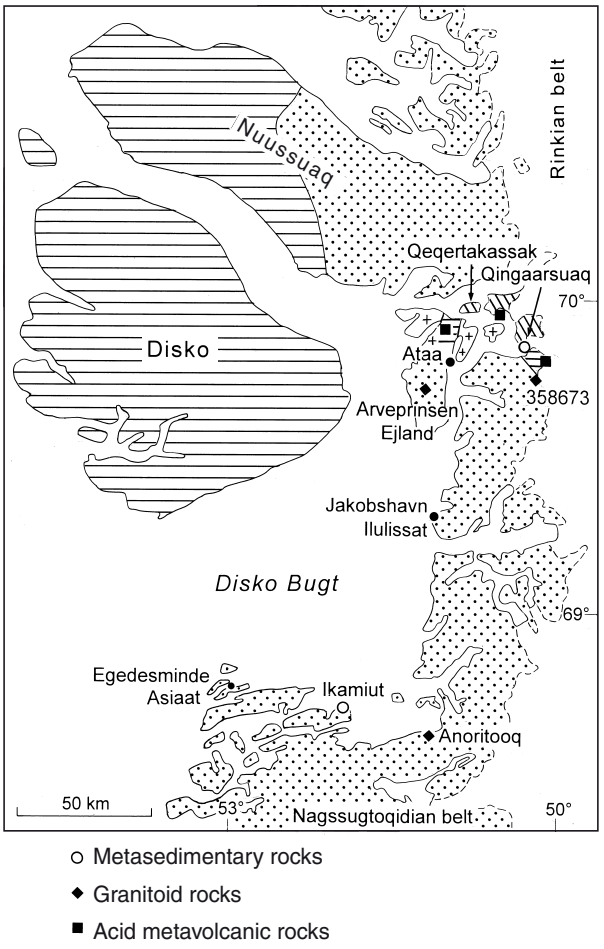

Fig. 1. Geological sketch map of the Disko Bugt region (from Kalsbeek 1991) with sample localities. Stipple: mainly Archaean gneisses. Wide horizontal ruling: mainly Tertiary basalts. In the Ataa area in north-eastern Disko Bugt Archaean gneisses and metavolcanic rocks (horizontal ruling) are intruded by the Atâ intrusive complex (Atâ tonalite, crosses), and unconformably overlain by an early Proterozoic sequence of sand- and siltstones, the Anap nunâ Group (oblique ruling; for a more detailed map of this area see, for example, Nutman & Kalsbeek 1999, this volume).

strongly affected by this orogenic event (Kalsbeek *et al.* 1988); nevertheless, K-Ar isotope data on biotite (Larsen & Møller 1968) and K-Ar and ^{40}Ar-^{39}Ar data on hornblende from different rock types (Rasmussen & Holm 1999, this volume) yield evidence of significant heating during the early Proterozoic.

In this paper we present Pb-Pb, Rb-Sr and Sm-Nd data on various rock units in the Disko Bugt region. Most are from the area around Ataa, recently investigated by the former Geological Survey of Greenland, see geological maps at 1:250 000 (enclosed in this volume) and 1:100 000; Garde 1994 and Escher 1995, respectively. For descriptions of the various rock units see Garde & Steenfelt (1999) and other papers in this volume. Also included are data for rocks from the southern part of Disko Bugt, mapped and described by Henderson (1969). No data are yet available from Nuussuaq.

Gneisses and granitoid rocks

Pb-Pb data for Archaean gneisses at Anoritooq, SE Disko Bugt

Pb-isotope data have been obtained from the regional grey gneisses at Anoritooq on the south-eastern coast of Disko Bugt (Fig. 1). Outcrops here consist of light grey biotite gneisses with variable proportions of pink K-feldspar augen and local remnants of anorthosite

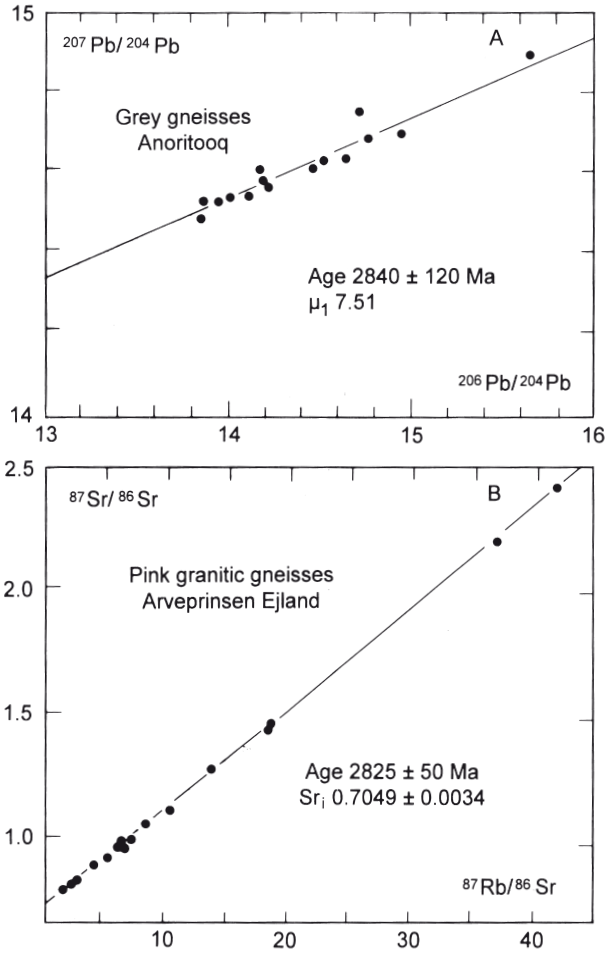

Fig. 2. **A**: Pb-Pb isochron diagram for grey gneisses from Anoritooq, south-east coast of Disko Bugt. **B**: Rb-Sr isochron diagram for pink granitic gneisses, Arveprinsen Ejland.

Table 1. Pb-isotope data for Archaean gneisses at Anoritooq, south-east coast of Disko Bugt

GGU sample no	$^{206}Pb/^{204}Pb$	$^{207}Pb/^{204}Pb$	$^{208}Pb/^{204}Pb$
298731	14.946	14.696	36.502
298732	14.645	14.633	35.261
298733	14.201	14.575	34.639
298734	13.874	14.526	38.166
298735	14.019	14.538	36.824
298736	14.530	14.627	37.699
298737	14.712	14.747	35.287
298738	14.769	14.682	37.068
298739	14.116	14.543	35.892
298740	14.216	14.563	35.388
298741	13.850	14.482	36.816
298742	14.464	14.611	36.638
298743	14.182	14.606	34.896
298745	15.652	14.891	45.333
298746	13.960	14.524	36.596

Analytical data from the Age and Isotope Laboratory, University of Oxford, UK. Pb-isotope ratios have been corrected for mass fractionation and have a precision of *c.* 0.1% (1σ).

and leucogabbro. Fifteen samples were analysed (Table 1); 14 of these define an isochron with age 2840 ± 120 Ma (2σ), μ_1 (first stage $^{238}U/^{204}Pb$) 7.51, and MSWD 2.38 (Fig. 2A). The poor age resolution of the isochron is due to the limited range of Pb-isotope compositions. The reasonably good fit on the isochron, compared to Pb-isotope data from Archaean gneisses in the Nagssugtoqidian belt south of Disko Bugt (Kalsbeek *et al.* 1987), suggests that the rocks at Anoritooq have been less strongly affected by Proterozoic isotopic disturbance than in the Nagssugtoqidian belt.

Rb-Sr data for a pink granitic gneiss from central Arveprinsen Ejland

Rb-Sr data have been acquired for 16 samples of a *c.* 300 m wide granite sheet in central Arveprinsen Ejland (granitic gneiss ggn on the geological map of Garde 1994; see also Garde & Steenfelt 1999, this volume). This body consists of foliated, K-rich granite *sensu stricto*, and has gradational contacts with the surrounding grey gneisses. Field evidence shows that the granite is younger than the gneisses, of which it contains half-digested inclusions. The granite may have formed by anatexis of Archaean gneisses or metasedimentary rocks at depth.

Table 2. Rb-Sr isotope data on Archaean and Proterozoic rocks from the Disko Bugt region

GGU sample no	Rb (ppm)	Sr (ppm)	$^{87}Rb/^{86}Sr$	$^{87}Sr/^{86}Sr$
(1) Pink granitic gneisses, Arveprinsen Ejland				
355163	125	76	5.53	0.92731
355164	142	17	18.16	1.45469
355165	121	63	6.35	0.96379
355166	128	50	8.61	1.05562
355167	154	13	41.62	2.42642
355168	139	45	10.40	1.12208
355169	107	55	6.46	0.97310
355170	166	16	36.87	2.21249
355171	125	57	7.20	0.99634
355172	140	70	6.58	0.96433
355173	132	32	13.81	1.28883
355174	142	26	18.28	1.46445
355175	62	103	1.95	0.78746
355176	101	114	2.91	0.82086
355177	88	65	4.39	0.88884
355178	93	111	2.76	0.81659
(2) Archaean metasediments, Qingaarsuaq				
355133	51	217	0.687	0.73323
355134	36	235	0.442	0.72661
355135	55	187	0.860	0.73842
355136	39	239	0.566	0.73094
355137	28	235	0.347	0.72476
355138	34	161	0.606	0.73367
(3) Archaean metasediments, Ikamiut				
298713	69	249	0.802	0.73246
298714	93	253	1.067	0.74241
298715	67	265	0.736	0.73056
298716	85	272	0.908	0.73689
298717	89	253	1.021	0.73982
298718	92	349	0.764	0.73441
298719	81	344	0.679	0.72966
298720	82	281	0.849	0.73517
298721	72	235	0.891	0.73782
298722	97	256	1.105	0.74285
298723	181	256	2.058	0.76591
298724	219	275	2.323	0.77585
(4) Proterozoic albite-rich rocks, Qeqertakassak				
355034	2.3	19	0.304	0.71979
355038	1.7	23	0.213	0.72090
355119	20	10	5.230	0.81012
355123	7.4	14	1.371	0.73072
355125	20	20	2.822	0.76804
355127	26	12	6.001	0.84060
355130	0.8	31	0.108	0.71454
355144	2.5	31	0.206	0.72089

Sr-isotope ratios were acquired at the Danish Centre for Isotope Geology at the Institute of Geology, University of Copenhagen (1) and at the Age and Isotope Laboratory, University of Oxford, UK (2–4). Precisions *c.* 0.005% and 0.01% (1σ), respectively. At the Danish Centre for Isotope Geology a mean $^{87}Sr/^{86}Sr$ ratio of 0.710262 ± 16 (*n* = 12) was obtained on the NBS 987 Sr standard (accepted value 0.710248). Rb/Sr ratios were measured by X-ray fluorescence spectrometry at the Institute of Geology, University of Copenhagen. Rb and Sr ± *c.* 10%, for the Proterozoic albite-rich rocks ± *c.* 2%, but not better than *c.* 0.5 ppm; $^{87}Rb/^{86}Sr$ ± *c.* 1% (1σ).

The analysed samples have a wide range of $^{87}Rb/^{86}Sr$ ratios (1.95 to 41.6; Table 2-1), mainly due to very variable Sr: 13–114 ppm; Rb shows less variation: 62–166 ppm. In the $^{87}Sr/^{86}Sr$ *v.* $^{87}Rb/^{86}Sr$ diagram (Fig. 2B) the data fall in a well-defined linear array, but do not fit an isochron within analytical precision (MSWD 4.59). The errorchron yields an age of 2825 ± 50 Ma (2σ) with an initial $^{87}Sr/^{86}Sr$ ratio of 0.7049 ± 0.0034. Again, the reasonable fit of the data points on the isochron line compared to that observed for granitic rocks in the central Nagssugtoqidian belt (Kalsbeek *et al.* 1987) shows that disturbance of the Rb-Sr isotope systems was here less severe.

Sm-Nd model age for a homogeneous gneiss SE of Eqi

A Sm-Nd model age (T_{DM}; DePaolo 1981) of 2930 Ma (Table 3) has been obtained for GGU 358673 (for locality see Fig. 1), collected from a mappable unit of relatively homogeneous non-migmatitic gneiss east of Ataa (see Escher *et al.* 1999, this volume). This is significantly older than the Atâ intrusive complex, in agreement with field evidence that the Atâ complex locally has intruded into older gneisses. However, U-Pb data on single zircons from this sample did not yield ages older than *c.* 2835 Ma (Nutman & Kalsbeek 1999, this volume). The Sm-Nd data thus suggest that the rock in question may have incorporated older crustal material, which is not recorded by the zircons.

Archaean supracrustal rocks

Sm-Nd data on acid metavolcanic rocks

Three samples of acid metavolcanic rocks (Ac, Garde 1994; for localities see Fig. 1), associated with Archaean meta-pillow lavas, yielded T_{DM} values of 2770, 2780, and 2810 Ma (Table 3). With estimated precisions of the order of 40 Ma (2σ) these values are not significantly different from that obtained for a sample from the Atâ intrusive complex (2800 Ma, Kalsbeek *et al.* 1988). Field evidence suggests that the Atâ complex intruded at relatively high crustal levels (Kalsbeek & Skjernaa 1999, this volume) and it seems plausible that the acid volcanic rocks are the surface expression of emplacement of the complex into Archaean supracrustal rocks.

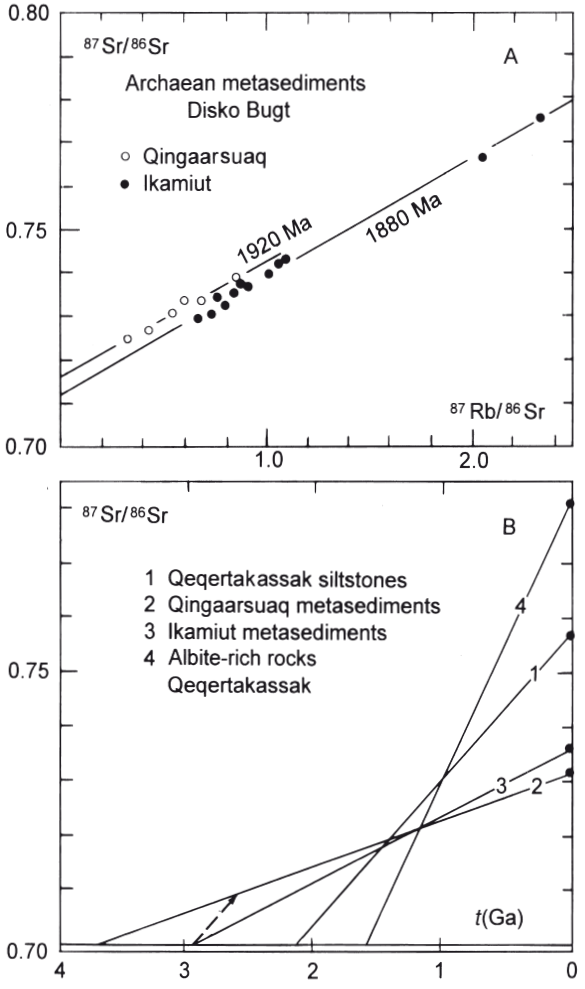

Fig. 3. **A**: Rb-Sr isochron diagram for samples of Archaean metasediments. **B**: Sr-evolution diagram based on measured mean $^{87}Sr/^{86}Sr$ ratios (t = 0, heavy dots) extrapolated backward in time with the help of corresponding mean $^{87}Rb/^{86}Sr$ ratios, see text. The dashed line shows that the Qingaarsuaq metasediments could be *c.* 2800 Ma old if their mean Rb/Sr ratio was significantly reduced during Archaean metamorphism.

Rb-Sr data for Archaean metasediments from Qingaarsuaq

Rb-Sr isotope data have been obtained for six samples of metasediments from within the Archaean supracrustal sequence on Qingaarsuaq east of Ataa (Fig. 1; for description see Garde & Steenfelt 1999, this volume). The analysed rocks are dark grey, fine-grained, biotite-rich gneisses, without aluminosilicate minerals. With 28–55 ppm Rb and 160–240 ppm Sr (Table 2-2) $^{87}Rb/^{86}Sr$ ratios are relatively low for metasediments. The rocks probably represent metagreywackes rather than metapelites.

Table 3. Sm-Nd isotope data and model age calculations for rocks from the Ataa area, north-east Disko Bugt

GGU sample no	Sm (ppm)	Nd (ppm)	$^{147}Sm/^{144}Nd$	$^{143}Nd/^{144}Nd$	T_{DM} (Ma)
Archaean gneiss					
358673	2.726	13.313	0.1237	0.511321	2930
Archaean acid metavolcanic rocks					
355006	2.122	12.201	0.1051	0.511045	2810
355055	1.667	9.669	0.1042	0.511053	2770
355056	2.905	17.481	0.1004	0.510977	2780
Proterozoic metasediments					
298790	5.722	30.754	0.1125	0.511411	2450
355053*	3.572	18.038	0.1197	0.511528	2460

Isotope data from the Age and Isotope Laboratory, University of Oxford, UK. Analytical uncertainties estimated at *c.* 0.1% for Sm and Nd concentrations, 0.2% for $^{147}Sm/^{144}Nd$, and 0.000010 for $^{143}Nd/^{144}Nd$ ratios (1σ).

* sample 355053 is a strongly albitised siltstone.

T_{DM} values represent model ages calculated according to the depleted mantle model of DePaolo (1981); they have a precision of *c.* 40 Ma (2σ).

In an isochron diagram the Rb-Sr data plot in a poorly defined linear array (Fig. 3A). A line of best fit corresponds to an age of *c.* 1920 Ma with Sr_i *c.* 0.715. It is apparent that partial Sr-isotopic homogenisation has taken place during the early Proterozoic, and the *c.* 1920 Ma age is probably a coarse approximation of the time of high-grade metamorphism.

Backward extrapolation of the mean $^{87}Sr/^{86}Sr$ ratio of the analysed samples in the Sr-isotopic evolution diagram (Fig. 3B) shows that, with the present mean $^{87}Rb/^{86}Sr$ ratio, the metasediments from Qingaarsuaq could have existed as far back as *c.* 3.5 Ga. However, reduction of Rb/Sr ratios during Archaean or early Proterozoic metamorphism (cf. Fig. 3B) would reduce this maximum age (for a more detailed discussion, see Kalsbeek 1993). For comparison the Sr-isotopic evolution of early Proterozoic siltstones from Qeqertakassak (Kalsbeek *et al.* 1988) is also shown. With their much higher $^{87}Rb/^{86}Sr$ ratios these sediments cannot have been deposited much earlier than 2 Ga ago. Fig. 3B illustrates the distinctly different Sr-isotopic evolution of the two metasedimentary units.

Rb-Sr data for metasediments from Ikamiut, south Disko Bugt

Kilometre-wide units of supracrustal rocks dominated by mica schists and pelitic gneisses are prominent along the coasts of south-eastern Disko Bugt (for description see Henderson 1969). Similar rocks east of Ilulissat/Jakobshavn (Fig. 1) are shown on the 1:250 000 geological map (Nms, Garde 1994) and have been described by Garde & Steenfelt (1999, this volume). Twelve samples have been analysed from a locality near Ikamiut on the south shore of Disko Bugt (Fig. 1; Table 2-3). In the isochron diagram they scatter about a line of best fit with a slope corresponding to an age of *c.* 1880 Ma and Sr_i *c.* 0.712 (Fig. 3A). Backward extrapolation in the Sr-evolution diagram (Fig. 3B) shows that, with their present $^{87}Rb/^{86}Sr$ ratios, these rocks may have existed for about 2.8 Ga, and it appears likely they represent sediments deposited during the late Archaean and isotopically strongly reset during early Proterozoic metamorphism.

Sm-Nd and Rb-Sr data for Proterozoic rocks and their alteration products

Sm-Nd data for siltstones from the Anap nunâ Group

The Proterozoic sedimentary sequence on the island Qeqertakassak (Fig. 1) consists mainly of dark siltstones which in part have been very strongly altered into albite-quartz-carbonate rocks (Kalsbeek 1992). Locally sheets

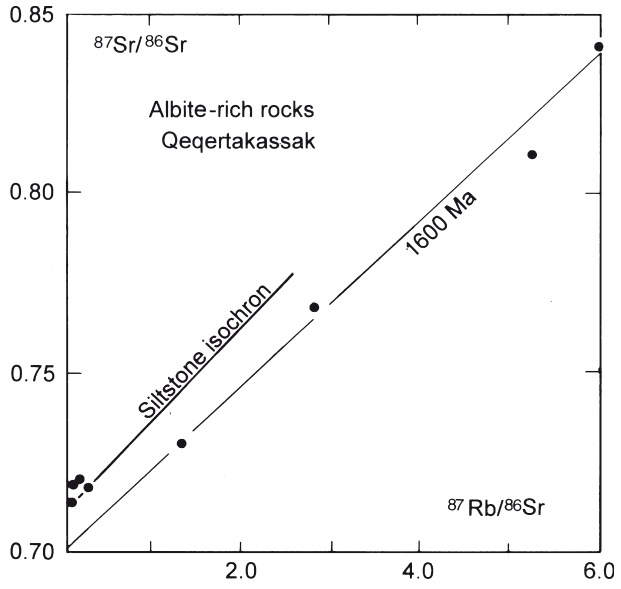

Fig. 4. Rb-Sr isochron diagram for albitised siltstones from Qeqertakassak, compared with the isochron obtained for non-albitised siltstones by Kalsbeek *et al.* (1988).

of metadolerite occur, and these may also be strongly albitised (Kalsbeek 1991). The Proterozoic age of these rocks was based on indirect evidence (Kalsbeek *et al.* 1988), and although later field evidence has revealed the presence of an unconformity towards the underlying Archaean rocks, a few Sm-Nd analyses were acquired to test their age.

Sm-Nd data for GGU 298790 (Table 3), a dark siltstone from Qeqertakassak, give a T_{DM} value of 2.45 Ga. This is much lower than T_{DM} values obtained from Archaean rocks in the area, and it is thus clear that Archaean rocks cannot have been the only source of clastic material for the sediments. If detrital material of Archaean origin is present at all (from the regional geology of the region this would appear to be very likely), then the sediments must also have contained a significant proportion of material that was derived from the mantle during the Proterozoic, later than 2.45 Ga ago. The Sm-Nd data thus strongly support a Proterozoic origin of the sediments.

GGU 355053 (Table 3) is an albitised siltstone. It yielded a T_{DM} value of 2.46 Ga, not significantly different from the non-albitised siltstone 298790. Apart from confirming the Proterozoic age of the rock this result illustrates the robustness of Sm-Nd isotope systems during alteration.

Age of albitisation

The age of the pervasive albitisation of the sediments on Qeqertakassak is not well constrained from field evidence. It may have started shortly after deposition, because albite-rich rocks commonly form conformable layers within less altered sediment, but there is also a clear relationship with late fracture zones (Kalsbeek 1992). There is ample evidence of mobility of Rb and Sr during albitisation, and, since the alteration must have been caused by massive percolation of fluids, it was thought that Sr-isotopic homogenisation might have taken place during the process, and that Rb-Sr isotope data therefore could give an indication of the age of albitisation. This is only partly the case.

The albite-rich rocks have a wide range of $^{87}Rb/^{86}Sr$ ratios (Fig. 4; Table 2–4) because variable proportions of Rb and Sr were leached from the siltstones during albitisation (Kalsbeek 1992). However, the samples do not yield an isochron. Of four samples with low $^{87}Rb/^{86}Sr$ (< 0.4) two plot close to the best-fit isochron line obtained for the Qeqertakassak siltstones, and two fall significantly above this line. Four samples with $^{87}Rb/^{86}Sr$ ratios > 1 plot very significantly below the Qeqertakassak siltstone isochron. Model age calculations for these samples (cf. Fig. 3B) indicate they must have acquired their present Rb/Sr ratios several hundred million years after deposition of the sediments, and much later than the peak of orogenic activity in the Nagssugtoqidian and Rinkian mobile belts (*c.* 1850 Ma, Kalsbeek *et al.* 1984, 1987; Taylor & Kalsbeek 1990). Even with a $^{87}Sr/^{86}Sr$ ratio as low as 0.7000 at the time of albitisation these samples cannot have existed much longer than *c.* 1600 Ma, unless significant later disturbance of the isotope systems has taken place. It is possible that the igneous event registered by the 1645 Ma basic dykes in the eastern part of the region triggered the hydrothermal activity that gave rise to a late phase of albitisation. The dykes themselves, however, appear to be totally unaffected.

Conclusions

1. Pb-Pb and Rb-Sr isotope data confirm that most of the Precambrian basement in the Disko Bugt region is of Archaean origin.

2. Pb-Pb and Rb-Sr systematics in granitoid rocks have been less strongly disturbed by early Proterozoic metamorphism than in the Nagssugtoqidian belt to the south.

3. Rb-Sr data for Archaean metasediments yield evidence of strong disturbance during early Proterozoic metamorphism.

4. Sm-Nd data for acid metavolcanic rocks yield model ages (T_{DM}) of *c*. 2800 Ma, similar to that of a sample from the Atâ intrusive complex.

5. Sm-Nd data confirm earlier considerations that the low-grade supracrustal rocks of the Anap nunâ Group are of early Proterozoic age.

6. Rb-Sr data show that massive albitisation of Anap nunâ Group metasediments took place hundreds of million years after deposition, and much later than high-grade metamorphism in the Nagssugtoqidian and Rinkian mobile belts.

Acknowledgements

We thank Professor Stephen Moorbath for permission to use the facilities at the Age and Isotope Laboratory in Oxford for this study, and Roy Goodwin and Caroline Fry for much of the analytical work. The laboratories in Copenhagen involved in this project are supported by the Danish Natural Science Research Council.

References

DePaolo, D.J. 1981: Neodymium isotopes in the Colorado Front Range and crust-mantle evolution in the Proterozoic. Nature (London) **291**, 193–196.

Escher, J.C. 1995: Geological map of Greenland, 1:100 000, Ataa 69 V.3 Nord. Copenhagen: Geological Survey of Greenland.

Escher, J.C., Ryan, M.J. & Marker, M. 1999: Early Proterozoic thrust tectonics east of Ataa Sund, north-east Disko Bugt, West Greenland. In: Kalsbeek, F. (ed.): Precambrian geology of the Disko Bugt region, West Greenland. Geology of Greenland Survey Bulletin **181**, 171–179 (this volume).

Garde, A.A. 1994: Precambrian geology between Qarajaq Isfjord and Jakobshavn Isfjord, West Greenland, 1:250 000. Copenhagen: Geological Survey of Greenland.

Garde, A.A. & Steenfelt, A. 1999: Precambrian geology of Nuussuaq and the area north-east of Disko Bugt, West Greenland. In: Kalsbeek, F. (ed.): Precambrian geology of the Disko Bugt region, West Greenland. Geology of Greenland Survey Bulletin **181**, 6–40 (this volume).

Henderson, G. 1969: The Precambrian rocks of the Egedesminde–Christianshåb area, West Greenland. Rapport Grønlands Geologiske Undersøgelse **23**, 37 pp.

Kalsbeek, F. 1981: The northward extent of the Archaean basement of Greenland – a review of Rb-Sr whole-rock ages. Precambrian Research **14**, 203–219.

Kalsbeek, F. 1991: Metasomatic alteration of dolerite in the Proterozoic sediments of north-east Disko Bugt. Rapport Grønlands Geologiske Undersøgelse **150**, 33–35.

Kalsbeek, F. 1992: Large-scale albitisation of siltstones on Qeqertakavsak island, north-east Disko Bugt, West Greenland. Chemical Geology **95**, 213–233.

Kalsbeek, F. 1993: Use of Rb-Sr isotope data to constrain the time of deposition of Precambrian metasediments: an example from Hamborgerland, West Greenland. Rapport Grønlands Geologiske Undersøgelse **159**, 95–100.

Kalsbeek, F. 1994: Archaean and Proterozoic basement provinces in Greenland. Rapport Grønlands Geologiske Undersøgelse **160**, 37–40.

Kalsbeek, F. & Skjernaa, L. 1999: The Archaean Atâ intrusive complex (Atâ tonalite), north-east Disko Bugt, West Greenland. In: Kalsbeek, F. (ed.): Precambrian geology of the Disko Bugt region, West Greenland. Geology of Greenland Survey Bulletin **181**, 103–112 (this volume).

Kalsbeek, F. & Taylor, P.N. 1986: Chemical and isotopic homogeneity of a 400 km long basic dyke in central West Greenland. Contributions to Mineralogy and Petrology **93**, 439–448.

Kalsbeek, F., Taylor, P.N. & Henriksen, N. 1984: Age of rocks, structures, and metamorphism in the Nagssugtoqidian mobile belt, West Greenland – field and Pb-isotopic evidence. Canadian Journal of Earth Sciences **21**, 1126–1131.

Kalsbeek, F., Pidgeon, R.T. & Taylor, P.N. 1987: Nagssugtoqidian mobile belt of West Greenland: a cryptic 1850 Ma suture between two Archaean continents – chemical and isotopic evidence. Earth and Planetary Science Letters **85**, 365–385.

Kalsbeek, F., Taylor, P.N. & Pidgeon, R.T. 1988: Unreworked Archaean basement and Proterozoic supracrustal rocks from northeastern Disko Bugt, West Greenland: implications for the nature of Proterozoic mobile belts in Greenland. Canadian Journal of Earth Sciences **25**, 773–782.

Larsen, O. & Møller, J. 1968: Potassium-argon age studies in West Greenland. Canadian Journal of Earth Sciences **5**, 683–691.

Nutman, A.P. & Kalsbeek, F. 1999: SHRIMP U-Pb zircon ages for Archaean granitoid rocks, Ataa area, north-east Disko Bugt, West Greenland. In: Kalsbeek, F. (ed.): Precambrian geology of the Disko Bugt region, West Greenland. Geology of Greenland Survey Bulletin **181**, 49–54 (this volume).

Rasmussen, H. & Holm, P.M. 1999: Proterozoic thermal activity in the Archaean basement of the Disko Bugt region and eastern Nuussuaq, West Greenland: evidence from K-Ar and ^{40}Ar-^{39}Ar mineral age investigations. Geology of Greenland Survey Bulletin **181**, 55–64 (this volume).

Taylor, P.N. & Kalsbeek, F. 1990: Dating the metamorphism of Precambrian marbles: examples from Proterozoic mobile belts in Greenland. Chemical Geology (Isotope Geoscience Section) **86**, 21–28.

SHRIMP U-Pb zircon ages for Archaean granitoid rocks, Ataa area, north-east Disko Bugt, West Greenland

Allen P. Nutman and Feiko Kalsbeek

Zircons from four samples of granitoid rocks from the Ataa area have been studied by SHRIMP ion microprobe. A trondhjemite from the Atâ intrusive complex (Atâ tonalite) yielded an age of 2803 ± 4 Ma, in agreement with earlier age determinations. A sample from the regional migmatitic biotite gneisses gave 2815 ± 4 Ma. A homogeneous granitoid rock, from field observations believed to be younger than the regional gneisses, has two main zircon populations, 2835 ± 4 Ma and *c.* 2800 Ma, respectively, and a granite that intrudes the Atâ complex yielded an age of 2758 ± 2 Ma.

A.P.N., *Research School of Earth Sciences, Australian National University, Canberra, A.C.T. 0200, Australia*. E-mail: *Allen.Nutman@anu.edu.au*.
F.K., *Geological Survey of Denmark and Greenland, Thoravej 8, DK-2400 Copenhagen NV, Denmark*.

Keywords: Archaean rocks, Disko Bugt, SHRIMP, U-Pb ages, zircon ages, West Greenland

Most of the area north-east of Disko Bugt is made up of different generations of quartzofeldspathic plutonic rocks, variably deformed and migmatised to form a regional gneiss complex (Garde & Steenfelt 1999, this volume). Rocks of the 2800 Ma Atâ intrusive complex (Atâ Tonalite on the 1:250 000 geological map of Garde 1994, enclosed in this volume; Fig. 1; Escher & Burri 1967; Kalsbeek *et al.* 1988; Garde & Steenfelt 1999, this volume; Kalsbeek & Skjernaa 1999, this volume) are better preserved than most other granitoid rocks, and locally display clear intrusive relationships with older migmatitic gneisses. However, the Atâ complex itself is intruded by younger granitoid rocks which in turn may also be deformed and gneissified. The purpose of the present study is to obtain an impression of the age range of Precambrian rocks in the Ataa area, north-east Disko Bugt (see the geological map Ataa 69 V.3 Nord, Escher 1995), using SHRIMP zircon U-Pb age determinations.

Four samples (Fig. 1) were investigated: (1) a representative specimen of the regional migmatitic grey biotite gneisses south of the Atâ complex (GGU 358675); (2) a non-migmatitic, homogeneous tonalitic orthogneiss (GGU 358673), which, from field evidence, is believed to be younger than the regional migmatitic gneisses. This sample has yielded a Sm-Nd model age (T_{DM}, DePaolo 1981) of 2.93 Ga (Kalsbeek & Taylor 1999, this volume; see p. 53); (3) a trondhjemitic sample of the Atâ complex (GGU 269310) with T_{DM} 2.80 Ga (Kalsbeek *et al.* 1988); and (4) a late granite intruding rocks belonging to the Atâ complex near its southern margin on Arveprinsen Ejland (GGU 348683).

Analytical method and calculation of ages

U-Th-Pb isotope ratios and concentrations were determined using the SHRIMP 1 ion microprobe (SHRIMP = Sensitive High Resolution Ion MicroProbe) at the Australian National University in Canberra. They were calibrated against the standard Sri Lanka zircon SL 13 ($^{206}Pb/^{238}U$ = 0.0928; age 572 Ma). Details of analytical procedures and data assessment are given by Compston *et al.* (1984) and Williams *et al.* (1996).

In polyphase gneiss areas the interpretation of zircon U-Pb isotope data in terms of rock ages is not always straightforward. First, the analysed zircons may

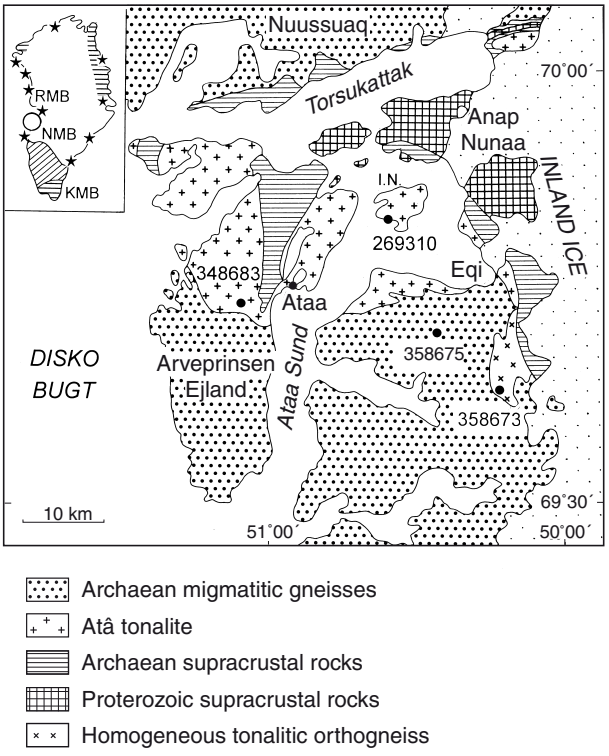

Fig. 1. Geological sketch map of the Ataa area with locations of the investigated samples. I.N. denotes the island Illuluarsuit Nunataat. The inset map shows the main structural elements within the Precambrian shield of Greenland with the location of the Ataa area in West Greenland between the Nagssugtoqidian and Rinkian mobile belts (NMB and RMB, respectively). The Archaean craton of southern Greenland is indicated by oblique ruling. Stars indicate the presence of dated Archaean rocks outside the Archaean craton. Horizontal ruling shows outcrop areas of new-formed early Proterozoic rocks. KMB is the Ketilidian mobile belt of South Greenland. Slightly modified from Garde (1994).

have suffered loss of Pb during later high-grade metamorphism. If metamorphism takes place shortly after emplacement of the igneous precursor of the analysed sample, the analytical data may show a scatter in the concordia diagram towards lower $^{207}Pb/^{206}Pb$ ages without causing detectable discordance. The strategy for calculating a reliable $^{207}Pb/^{206}Pb$ age is then to successively reject analyses which yield the lowest $^{207}Pb/^{206}Pb$ dates, until the remaining ones are undistinguishable from their weighted mean. Second, more than one zircon population may be present, of which the one with the highest $^{207}Pb/^{206}Pb$ ages may be inherited from the parent material which was reworked to form the rock under consideration.

Results

GGU 358675, migmatitic grey biotite gneiss. This is a representative sample of the regional migmatitic orthogneiss complex (Escher *et al.* 1999, this volume), and was collected from the mainland east of Ataa Sund at 69°42.3′ N, 50°23.6′ W (Fig. 1).

Zircons are prismatic, euhedral to subhedral and yellow to dark brown in colour. They display pronounced micron scale euhedral zoning, parallel to the exteriors of the grains. They are interpreted as a homogeneous magmatic population. The centres of a few grains consist of homogeneous structureless zircon whose outline mimics that of the grain exterior, and hence there is no reason to suppose it represents much older inherited material.

Seventeen spots were analysed on 15 zircon crystals (Fig. 2A; Table 1). U and Th contents range from 118–630 ppm and 4–102 ppm, respectively, with relatively low Th/U ratios (0.02–0.24). Most $^{207}Pb/^{206}Pb$ ages lie between 2800 and 2830 Ma. One zircon yielded an age of 2868 Ma and may represent an inherited grain. A few grains have lower $^{207}Pb/^{206}Pb$ ages and may have suffered ancient lead loss. Nine of the remaining analyses yield a mean $^{207}Pb/^{206}Pb$ age of 2815 ± 4 Ma (ages quoted at 2σ), which we interpret to date the time of emplacement of the igneous precursor of the gneiss.

GGU 358673, homogeneous tonalitic orthogneiss. This sample was collected at 69°37.1′ N, 50°13.6′ W (Fig. 1) from a mappable unit of non-migmatitic orthogneisses which is discordant to the regional structure of the migmatitic grey biotite gneisses, and may be younger than the latter (Escher *et al.* 1999, this volume). Zircons are prismatic euhedral crystals, sometimes with rounded terminations. Most crystals are yellow to light brown with distinct euhedral zoning, a few are dark brown and metamict. Some grains are composite with dark brown cores surrounded by lighter coloured zircon.

Eleven grains were analysed (Fig. 2B; Table 1). U and Th contents are highly variable, 73–3887 ppm and 17–267 ppm respectively. Th/U ratios vary from 0.01 to 0.73. The zircons fall into two age groups with $^{207}Pb/^{206}Pb$ ages 2800–2810 Ma (four grains) and 2820–2850 Ma (six grains), respectively. One grain with very high U (3887 ppm) yielded a younger $^{207}Pb/^{206}Pb$ age of 2775 Ma which may be the result of moderate lead loss. The older zircon population yields a common age of 2835 ± 4 Ma; the younger group gives an age just over 2800 Ma. Two interpretations are consistent

Table 1. SHRIMP zircon U-Pb data for granitoid rocks from the Ataa area, north-east Disko Bugt

Site	U (ppm)	Th (ppm)	Th/U	^{204}Pb (ppb)	Comm. ^{206}Pb(%)	^{206}Pb/^{238}U	^{207}Pb/^{235}U	^{207}Pb/^{206}Pb	Age* (Ma)	disc.
GGU 358675 – *migmatitic grey biotite gneiss*										
1-1	212	18	0.09	15	0.20	0.550±10	15.14±0.31	0.1997± 9	2824± 7	0
2-1	575	83	0.14	20	0.11	0.512±10	13.99±0.28	0.1981± 5	2811± 4	–5
3-1	504	99	0.20	26	0.15	0.530±10	14.98±0.30	0.2052± 6	2868± 4	–4
4-1	168	7	0.04	12	0.20	0.562±11	15.36±0.31	0.1982± 9	2811± 7	2
5-1	118	4	0.04	18	0.42	0.571±11	15.63±0.34	0.1986±13	2815±11	3
6-1	126	6	0.05	14	0.31	0.554±11	15.10±0.32	0.1978±13	2808±10	1
7-1	430	102	0.24	10	0.07	0.532±10	14.54±0.29	0.1984± 5	2813± 4	–2
8-1	177	9	0.05	38	0.60	0.549±11	14.77±0.31	0.1952±11	2787± 9	1
9-1	179	24	0.13	9	0.16	0.532±10	14.28±0.29	0.1944± 9	2779± 7	–1
10-1	519	88	0.17	17	0.09	0.539±10	14.71±0.29	0.1980± 5	2810± 4	–1
11-1	630	84	0.13	20	0.10	0.510±10	13.99±0.27	0.1988± 5	2817± 4	–6
12-1	416	63	0.15	7	0.05	0.534±10	14.53±0.29	0.1974± 5	2805± 4	–2
13-1	142	6	0.04	50	0.95	0.575±11	15.81±0.34	0.1996±14	2823±12	4
13-2	209	4	0.02	11	0.15	0.550±11	14.94±0.31	0.1970± 8	2801± 7	1
14-1	164	5	0.03	10	0.17	0.566±11	15.19±0.31	0.1947± 8	2783± 7	4
15-1	254	18	0.07	22	0.25	0.544±11	14.97±0.30	0.1995± 8	2822± 7	–1
15-2	287	50	0.17	5	0.05	0.545±11	15.05±0.30	0.2003± 7	2829± 5	–1
GGU 358673 – *homogeneous tonalitic orthogneiss*										
1-1	201	57	0.29	4	0.06	0.525±11	14.32±0.31	0.1977± 9	2807± 7	–3
2-1	3887	53	0.01	5	<0.01	0.519±10	13.87±0.28	0.1938± 2	2775± 2	–3
3-1	73	21	0.28	3	0.12	0.534±11	14.82±0.34	0.2014±13	2829±15	–3
4-1	498	242	0.49	4	0.02	0.531±11	14.72±0.30	0.2009± 5	2834± 4	–3
5-1	440	17	0.04	5	0.04	0.516±10	14.08±0.30	0.1983± 7	2810± 6	–5
6-1	1764	161	0.09	2	<0.01	0.536±11	14.88±0.30	0.2012± 3	2836± 2	–2
7-1	486	205	0.42	2	0.02	0.523±11	14.40±0.30	0.1997± 6	2823± 5	–4
8-1	274	81	0.30	13	0.14	0.541±11	14.71±0.31	0.1972± 8	2803± 6	–1
9-1	333	126	0.38	1	0.01	0.535±11	14.85±0.31	0.2011± 7	2836± 6	–3
10-1	613	267	0.44	2	0.01	0.554±11	15.09±0.31	0.1976± 5	2807± 4	1
11-1	261	190	0.73	5	0.05	0.532±11	14.89±0.32	0.2029± 9	2849± 8	–3
GGU 269310 – *trondhjemite, Atâ intrusive complex*										
1-1	200	15	0.07	3	0.06	0.457± 7	13.31±0.21	0.2110± 9	2913± 7	–17
1-2	263	37	0.14	1	0.01	0.505± 7	13.70±0.21	0.1969± 7	2800± 6	–6
2-1	96	40	0.41	<1	<0.01	0.515± 8	14.09±0.24	0.1984±12	2813±10	–5
3-1	52	30	0.56	5	0.27	0.555± 9	14.73±0.31	0.1925±22	2763±19	3
4-1	194	55	0.28	25	0.47	0.430± 6	11.83±0.20	0.1994±15	2821±12	–18
5-1	400	53	0.13	15	0.11	0.515± 8	13.92±0.21	0.1963± 6	2796± 5	–4
6-1	604	446	0.74	<1	<0.01	0.522± 7	14.25±0.21	0.1982± 5	2811± 4	–4
7-1	314	142	0.45	13	0.12	0.534± 8	14.54±0.22	0.1974± 7	2805± 6	–2
8-1	721	267	0.37	16	0.07	0.486± 7	12.70±0.19	0.1895± 5	2738± 4	–7
9-1	457	90	0.20	11	0.07	0.536± 8	14.47±0.22	0.1957± 6	2790± 5	–1
10-1	622	136	0.22	6	0.03	0.527± 7	14.27±0.21	0.1963± 5	2796± 4	–2
11-1	670	702	1.05	7	0.04	0.495± 7	13.32±0.20	0.1954± 5	2788± 4	–7
12-1	244	35	0.15	20	0.25	0.503± 7	13.24±0.21	0.1910± 9	2751± 8	–7
13-1	938	202	0.21	4	0.01	0.514± 7	13.70±0.20	0.1933± 4	2770± 3	–3
14-1	387	191	0.49	<1	<0.01	0.524± 8	14.26±0.21	0.1975± 6	2805± 5	–3
15-1	903	227	0.25	15	0.05	0.483± 7	12.68±0.18	0.1905± 4	2746± 3	–8
GGU 348683 – *granite cutting Atâ intrusive complex*										
1-1	1504	958	0.64	7	0.02	0.502±11	13.42±0.29	0.1939± 3	2776± 3	–6
2-1	802	515	0.64	6	0.04	0.493±10	13.08±0.28	0.1924± 4	2762± 4	–6
3-1	1159	1105	0.95	12	0.05	0.512±11	13.54±0.29	0.1917± 3	2757± 3	–3
4-1	2257	1696	0.75	5	0.01	0.531±11	14.01±0.30	0.1915± 2	2755± 2	0
5-1	807	733	0.91	7	0.04	0.522±11	13.84±0.30	0.1924± 4	2763± 3	–2
6-1	895	708	0.79	3	0.02	0.489±10	12.89±0.28	0.1912± 4	2753± 3	–7
6-2	870	788	0.91	152	0.78	0.486±10	10.84±0.24	0.1616± 6	2472± 6	3
7-1	320	172	0.54	1	0.01	0.511±11	11.83±0.26	0.1681± 6	2538± 6	5
8-1	153	65	0.51	2	0.06	0.507±11	13.32±0.31	0.1905±10	2747± 9	–4
8-2	194	108	0.56	2	0.06	0.477±10	12.63±0.29	0.1919±13	2758±11	–9
9-1	1087	566	0.52	73	0.30	0.497±10	12.65±0.27	0.1845± 4	2693± 4	–3
10-1	1493	443	0.30	11	0.03	0.480±10	12.72±0.27	0.1923± 3	2762± 3	–9
11-1	667	452	0.68	97	0.66	0.477±10	12.09±0.26	0.1839± 6	2689± 5	–7
12-1	1093	1071	0.98	12	0.05	0.522±11	13.58±0.29	0.1888± 3	2731± 3	–1
13-1	430	292	0.68	1	0.01	0.535±11	14.17±0.31	0.1921± 6	2760± 5	0
14-1	614	391	0.64	<1	<0.01	0.533±11	14.05±0.30	0.1912± 4	2752± 4	0
15-1	411	197	0.48	<1	<0.01	0.549±12	14.35±0.31	0.1896± 5	2739± 5	3
16-1	265	71	0.27	104	1.82	0.465±10	11.73±0.28	0.1832±14	2682±13	–8

* ^{207}Pb/^{206}Pb ages corrected for very small amounts of common lead. Uncertainties given at 1σ level.
'disc.' (discordance in per cent) calculated as 100 (^{206}Pb/^{238}U age)/(^{207}Pb/^{206}Pb age) – 100.

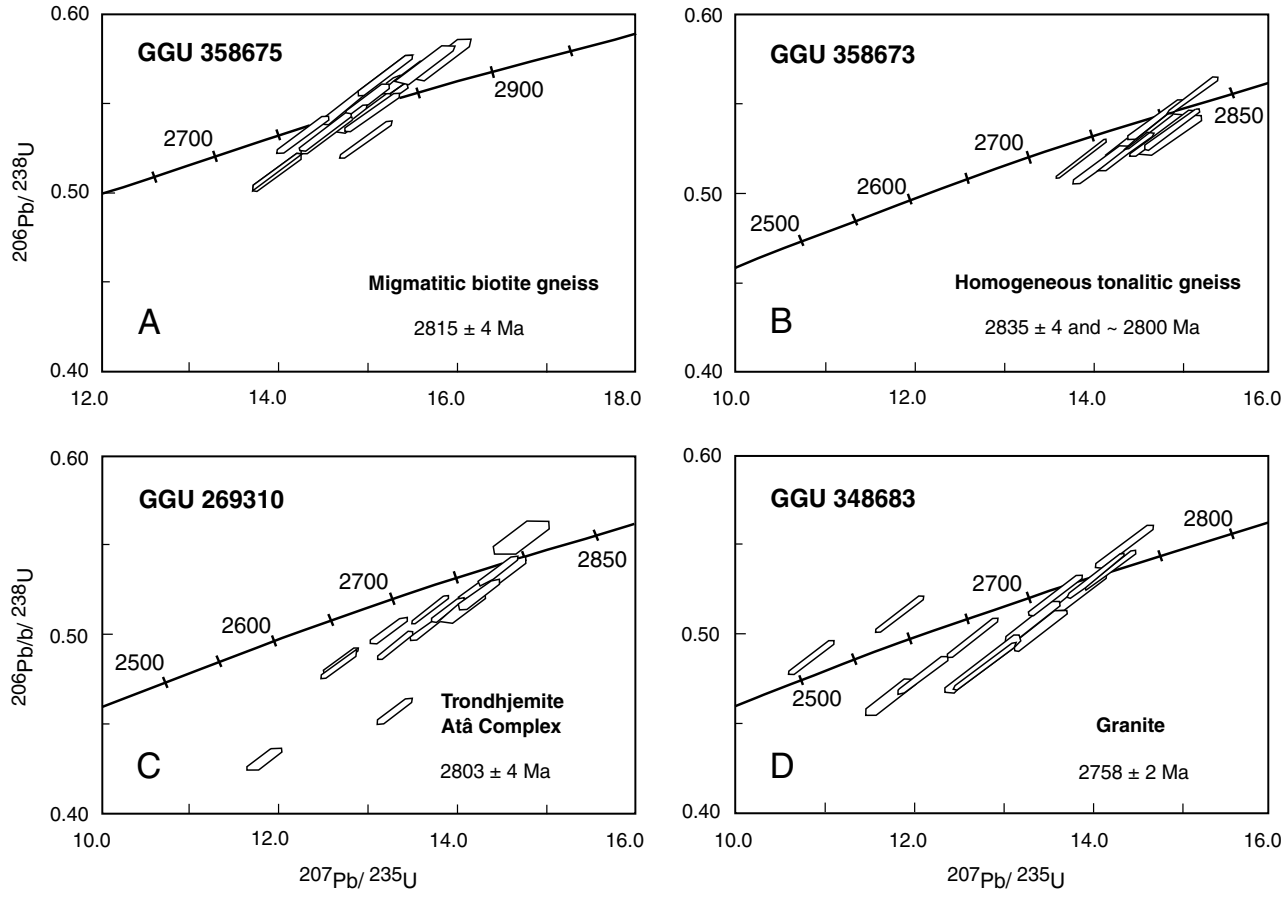

Fig. 2. U-Pb concordia diagrams for zircons from granitoid rocks in the Ataa area, north-east Disko Bugt.

with the data: (1) The older group dates the emplacement of the granitoid rock at *c.* 2835 Ma; the younger $^{207}Pb/^{206}Pb$ ages would then be the result of ancient lead loss. (2) The older group can be regarded as an inherited component within a granitoid rock emplaced *c.* 2800 Ma ago. Neither the analytical data nor the morphology of the zircons permit distinction between the two alternative models.

GGU 269310, trondhjemite from the Atâ intrusive complex. This sample was collected on Illuluarsuit Nunataat (69°50.1′ N, 50°33.8′ W, Fig. 1) from the central part of the eastern Atâ complex (Kalsbeek & Skjernaa 1999, this volume). The rocks are here trondhjemitic in composition and hardly deformed.

Zircons are euhedral prismatic crystals and vary from nearly colourless to dark brown. Euhedral zoning is common, and cores of dark zircon may be present within light brown crystals.

Sixteen analysed spots on 15 zircons show a variation in U and Th from 52 to 938 ppm and from 15 to 702 ppm respectively; Th/U 0.07–1.05 (Table 1). $^{207}Pb/^{206}Pb$ ages range from 2738 to 2913 Ma with a main group around 2800 Ma (Fig. 2C). The two grains with highest $^{207}Pb/^{206}Pb$ ages are highly discordant, and may represent inherited zircon. Successively eliminating analyses with lowest $^{207}Pb/^{206}Pb$ (on the assumption that this is the result of ancient lead loss), a remaining group of 7 grains yields an age of 2803 ± 4 Ma. We interpret this as the age of emplacement of the trondhjemite.

GGU 348683, granite intruding the Atâ complex. The sample was collected on Arveprinsen Ejland at 69°44.8′ N, 51°04.6′ W (Fig. 1) from an undeformed granite which intrudes strongly strained tonalite of the Atâ complex. Most zircons are euhedral prismatic grains up to *c.* 400 µm long, with colours in variable shades of yellow and brown, from water clear to dark brown. A few large brown stubby crystals are also present: one zircon fragment is 550 µm long and 260 µm wide.

Eighteen spots were analysed on 16 zircon grains (Fig. 2D; Table 1). U and Th contents range from 153 to 2257 and from 65 to 1696 ppm respectively, while Th/U shows a moderate range, 0.27–0.98. Thirteen zir-

cons yield $^{207}Pb/^{206}Pb$ ages in the range of 2730–2770 Ma; five analyses gave ages < 2700 Ma, suggesting major lead loss after initial zircon crystallisation. Eliminating a few more analyses on the basis of apparent minor lead loss, 8 remaining grains yield a mean $^{207}Pb/^{206}Pb$ age of 2758 ± 2 Ma, which we interpret to date the time of granite emplacement. Three analyses on stubby brown zircon grains were not significantly different from those on prismatic crystals.

Discussion

The oldest reliable age obtained in this study is 2815 Ma for the grey migmatitic biotite gneiss (GGU 358675). Data for the non-migmatitic tonalitic orthogneiss GGU 358673 do not yield a reliable age. The age obtained for the older group of zircons is 2835 ± 4 Ma. Field evidence (p. 49) has been interpreted to suggest that this rock is younger than the grey migmatitic biotite gneisses. If that is indeed the case the age of emplacement of the tonalitic precursor of GGU 358673 may be around or slightly older than 2800 Ma, equivalent to the age of GGU 269310 from the Atâ intrusive complex. In the field the non-migmatitic tonalitic orthogneisses are reminiscent of rocks from the Atâ intrusive complex, and they occur as a unit along strike of outcrops of the Atâ complex east of Eqi (Fig. 1). However, field relationships in high-grade polyphase gneiss regions are often extremely complex, and heterogeneous strain in an area of plutonic rocks, emplaced as a series of intrusions with age differences of a few million years makes correlations over large distances less reliable. Moreover, the Sm-Nd model age of 2930 Ma obtained for this sample (Kalsbeek & Taylor 1999, this volume) suggests it may contain a component of older crustal material. In summary, the available data do not permit a reliable interpretation of the zircon dates.

The Atâ complex is a composite intrusion with older, more deformed tonalitic phases and younger, largely undeformed trondhjemites and granodiorites (Kalsbeek & Skjernaa 1999, this volume). The sample investigated in this study (GGU 269310) belongs to a young trondhjemitic phase of the complex. The age of 2803 ± 4 Ma is closely similar to the earlier age estimate of *c.* 2800 Ma for the Atâ complex (Kalsbeek *et al.* 1988). These authors report a multigrain U-Pb age of 2794 ± 15 Ma on zircons from an older, deformed tonalite collected near the abandoned village Ataa (Fig. 1). The two ages are the same within error, and the different phases of the complex are probably not very different in age. Kalsbeek *et al.* (1988) report a Sm-Nd (T_{DM}) model age of 2800 ± 40 Ma for GGU 269310, which suggests that it hardly contains significant proportions of older crustal material.

In the southern parts of its outcrop area the Atâ complex is cut by a multitude of thin granitoid dykes. These were interpreted by Kalsbeek *et al.* (1988) as cooling joints filled by late stage melts related to the complex itself. However, subsequent field work during GGU's Disko Bugt Project showed (1) that granitoid dykelets gradually disappear towards the north, and (2) that the Atâ complex is intruded by younger granites at its southern margin. One of these younger granites (GGU 348683), investigated during the present study, has yielded an age of 2758 ± 2 Ma, significantly younger than samples from the Atâ complex. It now seems more likely that the granitoid dykes in the southern parts of the Atâ complex are not related to the complex itself but to the younger intrusions at its southern margin.

Most of the analysed zircons from all four samples are concordant or near concordant. This is consistent with suggestions from other lines of evidence (e.g. the finding of a reasonably well-fitted 2825 ± 50 Ma Rb-Sr isochron for a pink granite from Arveprinsen Ejland; Kalsbeek & Taylor 1999, this volume) that Archaean rocks in the Ataa region did not undergo nearly the same degree of Proterozoic disturbance as in the Nagssugtoqidian and Rinkian mobile belts, respectively to the south and to the north of the Ataa area.

Acknowledgements

We thank Professor W. Compston for permission to use the ion microprobe at the Australian National University, Canberra, for this study, Mogens Marker (at the time with the Danish Lithosphere Centre, Copenhagen) for providing us with samples GGU 358673 and GGU 358675, and Adam A. Garde (Geological Survey of Denmark and Greenland) for constructive comments on the manuscript.

References

Compston, W., Williams, I.S. & Meyer, C. 1984: U-Pb geochronology of zircons from Lunar Breccia 73217 using a sensitive high mass-resolution ion microprobe. Proceedings of the 14th Lunar and Planetary Science Conference, Journal of Geophysical Research Supplement **89**, B525–534.

DePaolo, D.J. 1981: Neodymium isotopes in the Colorado Front Range and crust-mantle evolution in the Proterozoic. Nature (London) **291**, 193–196.

Escher, A. & Burri, M. 1967: Stratigraphy and structural development of the Precambrian rocks in the area north-east of Disko Bugt, West Greenland. Rapport Grønlands Geologiske Undersøgelse **13**, 28 pp.

Escher, J.C. 1995: Geological map of Greenland, 1:100 000, Ataa 69 V.3 Nord. Copenhagen: Geological Survey of Greenland.

Escher, J.C., Ryan, M.J. & Marker, M. 1999: Early Proterozoic thrust tectonics east of Ataa Sund, north-east Disko Bugt, West Greenland. In: Kalsbeek, F. (ed.): Precambrian geology of the Disko Bugt region, West Greenland. Geology of Greenland Survey Bulletin **181**, 171–179 (this volume).

Garde, A.A. 1994: Precambrian geology between Qarajaq Isfjord and Jakobshavn Isfjord, West Greenland, 1:250 000. Copenhagen: Geological Survey of Greenland.

Garde, A.A. & Steenfelt, A. 1999: Precambrian geology of Nuussuaq and the area north-east of Disko Bugt, West Greenland. In: Kalsbeek, F. (ed.): Precambrian geology of the Disko Bugt region, West Greenland. Geology of Greenland Survey Bulletin **181**, 6–40 (this volume).

Kalsbeek, F. & Skjernaa, L. 1999: The Archaean Atâ intrusive complex (Atâ tonalite), north-east Disko Bugt, West Greenland. In: Kalsbeek, F. (ed.): Precambrian geology of the Disko Bugt region, West Greenland. Geology of Greenland Survey Bulletin **181**, 103–112 (this volume).

Kalsbeek, F. & Taylor, P.N. 1999: Review of isotope data for Precambrian rocks from the Disko Bugt region, West Greenland. In: Kalsbeek, F. (ed.): Precambrian geology of the Disko Bugt region, West Greenland. Geology of Greenland Survey Bulletin **181**, 41–47 (this volume).

Kalsbeek, F., Taylor, P.N. & Pidgeon, R.T. 1988: Unreworked Archaean basement and Proterozoic supracrustal rocks from northeastern Disko Bugt, West Greenland: implications for the nature of Proterozoic mobile belts in Greenland. Canadian Journal of Earth Sciences **25**, 773–782.

Williams, I.S., Buick, I.S. & Cartwright, I. 1996: An extended episode of early Mesoproterozoic fluid flow in the Reynolds Range, central Australia. Journal of Metamorphic Geology **14**, 29–47.

Proterozoic thermal activity in the Archaean basement of the Disko Bugt region and eastern Nuussuaq, West Greenland: evidence from K-Ar and ^{40}Ar-^{39}Ar mineral age investigations

Henrik Rasmussen and Paul Martin Holm

K-Ar and ^{40}Ar-^{39}Ar analyses of amphiboles from Archaean amphibolites and gneisses show that Proterozoic tectono-thermal activity has played an important role in the metamorphic and structural development of the Precambrian rocks around north-eastern Disko Bugt and in eastern Nuussuaq. Proterozoic thermal activity lead to resetting of the K-Ar ages of amphiboles in eastern Nuussuaq, resulting in ages of *c.* 1750 to 1925 Ma; in the Disko Bugt area the effects are seen in total or partial resetting with K-Ar ages scattering mostly between 2750 and 1870 Ma. Resetting is caused either by total diffusion of earlier accumulated radiogenic argon or by complete recrystallisation of the amphiboles. Archaean ^{40}Ar-^{39}Ar ages obtained from mafic xenoliths within the Atâ tonalite show that not all parts of the area suffered argon loss during Proterozoic reheating. Incorporation of significant proportions of excess argon in some amphiboles is seen from ^{40}Ar-^{39}Ar mineral age spectra obtained for samples from supracrustal rocks and from mafic xenoliths in the Atâ tonalite.

Phlogopite phenocrysts from a lamproite stock yielded a K-Ar age of 1764 ± 24 Ma, identical to a previously determined K-Ar age of the matrix phlogopite. These ages probably date the emplacement of the lamproite, and mark the time after which no tectono-thermal events affected the area.

H.R.* & P.M.H., *Geological Institute, University of Copenhagen, Øster Voldgade 10, DK-1350 Copenhagen K, Denmark.* *Present address: *Mærsk Olie og Gas AS, Esplanaden 50, DK-1263 Copenhagen K, Denmark.* E-mail: *h_rasmussen@vip.cybercity.dk.*

Keywords: ^{40}Ar-^{39}Ar ages, Archaean rocks, Disko Bugt, K-Ar ages, lamproite, Proterozoic metamorphism, West Greenland

Major parts of West Greenland are underlain by Archaean basement rocks; large parts of this basement have been reworked by later Proterozoic tectono-thermal events (Kalsbeek 1981). K-Ar age determinations on biotite from the gneisses near Jakobshavn/Ilulissat and from a gneiss near Qeqertaq, north-east Disko Bugt (Fig. 1), yielded early Proterozoic dates of *c.* 1.7 Ga (Larsen & Møller 1968), and were interpreted as the time at which the biotites had been reset or were recrystallised. Moreover, Pb-Pb whole-rock isochron dates of *c.* 1.85 Ga on marbles from the Rinkian and Nagssugtoqidian orogens of West Greenland, respectively to the north and south of the present area, give evidence of high-grade metamorphism at that time (Taylor & Kalsbeek 1990). Isotope data for the *c.* 2.8 Ga old Atâ tonalite, together with field evidence, suggested, however, that parts of the north-eastern Disko Bugt area had escaped Proterozoic deformation and metamorphism (Kalsbeek *et al.* 1988).

The objective of the present study is, by means of K-Ar and ^{40}Ar-^{39}Ar isotope analysis, to date amphiboles and phlogopites from gneisses, amphibolites and lamproites from the Disko Bugt region in order to outline areas affected by Proterozoic reheating and to find the extent of the area not significantly affected by these later events. A survey of the regional geology of the region is given by Garde & Steenfelt (1999) in this volume.

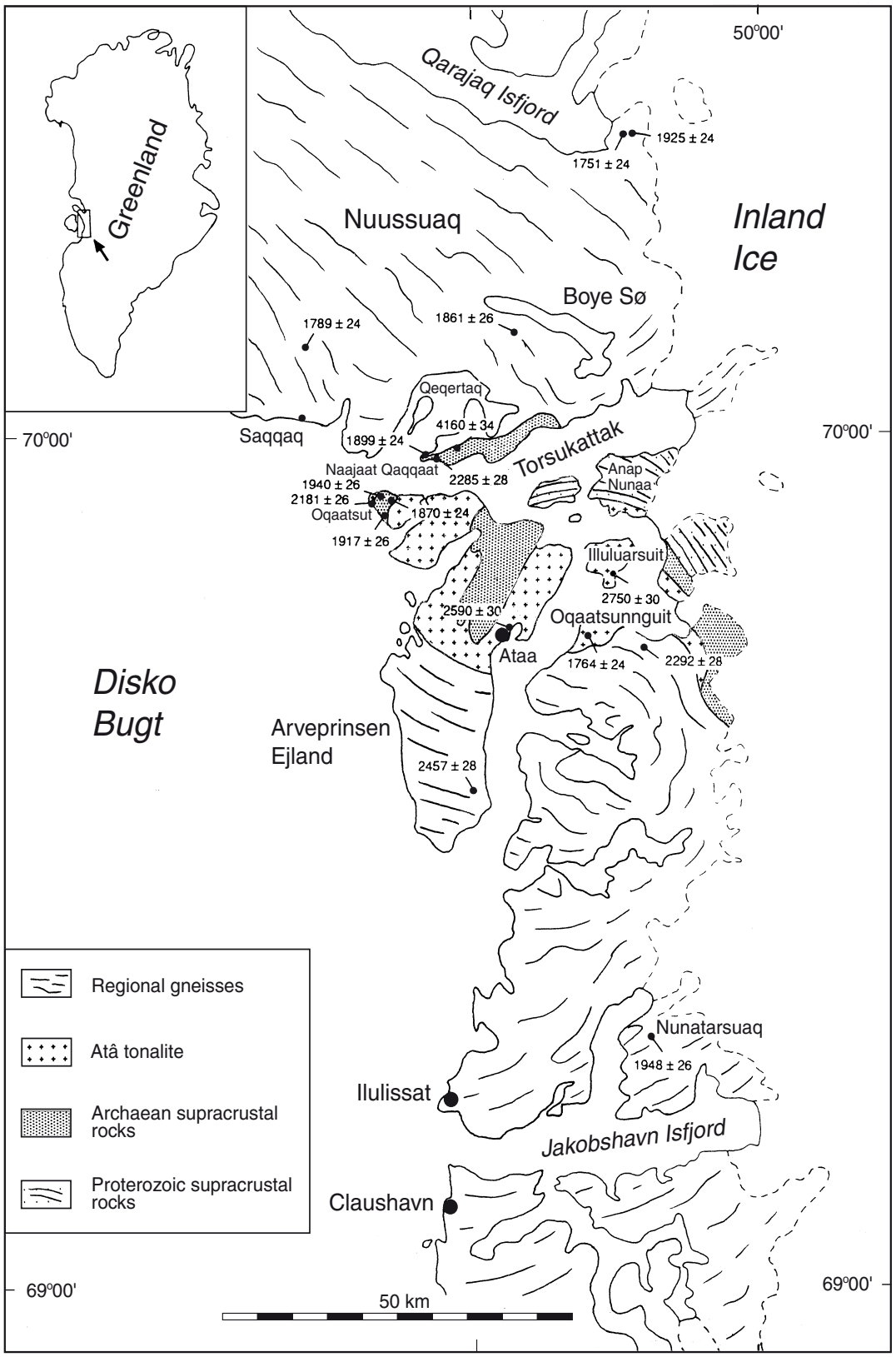

Fig. 1. Map of north-eastern Disko Bugt and eastern Nuussuaq showing the locations of samples collected for the K-Ar and ^{40}Ar-^{39}Ar investigations. Ages in Ma with 2σ errors. Geological units sketched from Garde & Steenfelt (1999, this volume).

Table 1. K-Ar isotope data for amphiboles from north-east Disko Bugt and eastern Nuussuaq

GGU no	mineral†	grain size (μm)	K(%)	$^{40}Ar^*$ ($10^{-5}cm^3/g$)	$\%^{40}Ar^*$	Age‡ (Ma)
Nuussuaq						
269780	ol-gr hbl	75-175	0.180±0.002	2.393, 2.428	96.25, 96.65	1925±24
269782	ol-gr hbl	75-175	0.574±0.004	6.592	96.14	1751±24
266843	bl-gr hbl	75-175	0.800±0.006	9.504, 9.511	99.23, 99.42	1789±24
272696	ol-gr hbl	75-175	0.408±0.002	5.305, 5.034	95.33, 98.30	1861±26
Najaat Qaqqaat and Oqaatsut						
349014	ol-gr hbl	75-175	0.665±0.012	8.607, 8.640	98.60, 98.74	1899±24
349053	pale ol-gr hbl	75-175	0.415±0.003	26.93, 25.65	99.10, 99.15	4160±34
349005	ol-gr hbl	75-175	0.212±0.004	3.861, 3.729	96.62, 98.00	2285±28
354319	bl-gr hbl	75-175	0.562±0.019	7.690, 7.529	98.43, 98.90	1940±26
354346	bl-gr hbl	75-175	0.589±0.004	9.936, 9.473	99.08, 98.18	2181±26
349023	pale bl-gr hbl	75-175	0.272±0.004	3.750, 3.468	96.35, 97.32	1917±26
354328	pale bl-gr hbl	75-175	0.288±0.008	3.655, 3.699	95.12, 97.63	1870±24
Ataa region						
272611	br-gr hbl	75-175	0.875±0.006	17.86, 17.76	99.32, 99.14	2457±28
352239	ol-gr hbl	75-200	0.805±0.003	14.39, 14.55	99.29, 99.21	2292±28
359139	pale ol-gr hbl	75-175	0.404±0.008	9.100, 9.025	97.96, 98.04	2590±30
352234	bl-gr hbl	75-150	0.662±0.002	16.03, 16.66	99.47, 99.51	2750±30
				17.16, 16.90	99.28, 99.24	
343955	phl	250-750	8.513±0.024	98.36, 99.58	99.48, 99.65	1764±24
Eastern Disko Bugt						
355612	pale gr hbl	75-175	0.192±0.004	2.694, 2.534	96.51, 96.95	1948+26

†: ol-gr hbl = olive-green hornblende; bl-gr hbl = blue-green hornblende; br-gr hbl = brown-green hornblende; phl = phlogopite.

‡: Ages are means calculated from different analyses; errors at 2σ.

$^{40}Ar^*$ = radiogenic Ar; the amount of $^{40}Ar^*$ recalculated to standard temperature and pressure.

$\%^{40}Ar^*$ is the percentage of total ^{40}Ar in the sample that is radiogenic.

Analytical techniques

High purity mineral separates of amphiboles were obtained from amphibolites, metagabbros and gneisses. Different sieve fractions used for analysis ranged in size between 75 and 175 μm. Phlogopite from an ellipsoidal nodule found in a lamproite stock at Oqaatsunnguit was taken directly from the nodule by hand. K was analysed by flame photometry on a Perkin Elmer® 5100 Atomic Absorption Spectrometer. K concentrations were checked against the international standard BB-24. Argon analysis for K-Ar and ^{40}Ar-^{39}Ar age determinations was carried out on an on-line AEI MS10C mass spectrometer fitted with a small 1.8 kG permanent magnet at the Danish Centre for Isotope Geology, University of Copenhagen. During the period of analysis, 13 runs on standard biotite LP-6 and 11 runs on standard muscovite P-207 resulted in mean values (in units of 10^{-5} cm^3 g^{-1} at standard T and P) of 4.323 ± 0.066 (1.5% rel.) and 2.830 ± 0.037 (1.3% rel.) for radiogenic ^{40}Ar respectively. Temperature values for the individual steps were not measured. Ages were calculated using the decay constants recommended by the IUGS subcommision on geochronology ($\lambda^{40}K$ = 5.543×10^{-10} a^{-1}; Steiger & Jäger 1977). Analytical techniques and methods are described in detail in Rasmussen (1992) and Holm (1991).

Results of K-Ar and ^{40}Ar-^{39}Ar age determinations

The spatial distribution of the K-Ar amphibole ages from this study is shown in Fig. 1 and the results are listed in Table 1. All uncertainties presented are 2σ errors.

Eastern Nuussuaq

Four K-Ar amphibole ages were obtained from the eastern part of Nuussuaq. In north-eastern Nuussuaq olive-green hornblende from a medium-grained amphibolitic inclusion (GGU 269780) in the gneisses yielded a date of 1925 ± 24 Ma. The amphiboles in this sample are anhedral and contain numerous microcracks.

Fresh and almost inclusion-free olive-green hornblende separated from the adjacent gneisses (GGU

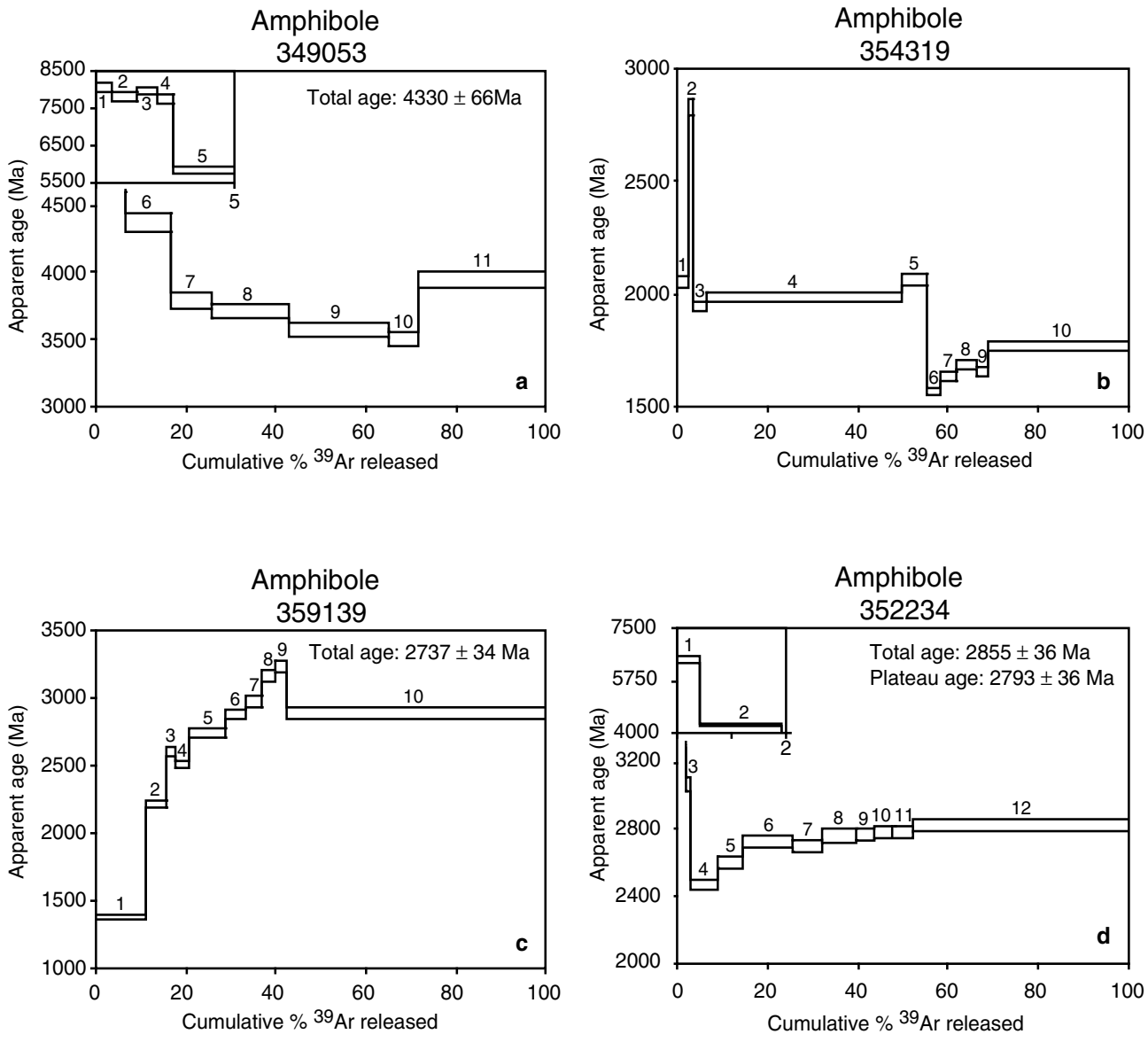

Fig. 2. ^{40}Ar-^{39}Ar age spectrum for hornblende: **a**: GGU 349053, Naajaat Qaqqaat. **b**: GGU 354319, Oqaatsut. **c**: GGU 359139, Ataa area. **d**: GGU 352234, Illuluarsuit Nunataat. Vertical width of the boxes represent 2σ errors.

269782) in this area gave a considerably younger date of 1751 ± 24 Ma.

From the central part of eastern Nuussuaq, about 7 km south of Boye Sø, olive-green hornblende separated from a medium-grained, almost undeformed diorite (GGU 272696) yielded a date of 1861 ± 26 Ma. The hornblende is fairly fresh but contains numerous parallel aligned opaque inclusions.

Further west, in the Sarqaq supracrustal rocks (Garde & Steenfelt 1999, this volume) a blue-green hornblende, obtained from a fine- to medium-grained amphibolite (GGU 266843), yielded a date of 1789 ± 24 Ma.

Comparison of these dates with existing chronological information is not straightforward. Larsen & Møller (1968) reported a K-Ar biotite age of 1732 ± 50 Ma for biotite from a gneiss from east of Saqqaq (age recalculated using the recommended decay constant of Steiger & Jäger 1977). Kalsbeek (1981) obtained a Rb-Sr whole rock isochron age of *c.* 1700 Ma for semipelitic metasediments near the base of the Mârmorilik Formation in the Uummannaq area *c.* 60 km north of the present study area, and Kalsbeek *et al.* (1988) reported a 1760 ± 185 Ma Rb-Sr isochron for siltstones from the early Proterozoic Anap nunâ Group. These ages were interpreted as the time of closure of the K-Ar and Rb-Sr isotope systems after early Proterozoic metamorphism.

An older age for the metamorphism of the Mârmorilik Formation (1911 ± 95 Ma) has been obtained from Pb-Pb isotope data (Kalsbeek *et al.* 1984), and Taylor & Kalsbeek (1990) obtained a Pb-Pb whole-rock isochron age of 1881 ± 20 Ma for marbles of the Mârmorilik Formation.

Two of the new dates from eastern Nuussuaq are of the order of 1750–1800 Ma and may correspond to the time of closure of the K-Ar and Rb-Sr isotope systems in the region during cooling after early Proterozoic metamorphism. The hornblende dates obtained from the slightly deformed diorite collected south of Boye Sø (1861 Ma) and from the amphibolitic inclusion in the gneisses on north-eastern Nuussuaq (1925 Ma) are comparable with the Pb-Pb isochron ages. It is not likely, however, that these dates refer to the peak of early Proterozoic metamorphism since these rocks evidently have undergone the same cooling history as the other samples. More probably, these higher K-Ar ages are due to incorporation of minor amounts of excess argon in the analysed amphiboles.

Naajaat Qaqqaat and Oqaatsut

Three amphibole samples were analysed from Naajaat Qaqqaat. Olive-green hornblende from an amphibolite (GGU 349005) is relatively fresh but contains numerous inclusions of quartz and opaque minerals. This hornblende gave a date of 2285 ± 28 Ma, intermediate between the Archaean age of the Atâ tonalite and the Proterozoic deformation. Similar K-Ar ages which cannot be related to known age information have also been obtained from other parts of the study area.

Hornblende separated from amphibolite sample GGU 349014 is olive green and contains few inclusions. It is relatively fresh although the adjacent plagioclase is almost entirely sericitised and epidotised. The hornblende yielded a Proterozoic date of 1899 ± 24 Ma, which corresponds fairly well with the hornblende and Pb-Pb whole-rock ages obtained from north-eastern Nuussuaq and from the Uummannaq area discussed above.

Pale-green amphibole was obtained from a medium-grained hornblenditic amphibolite (GGU 349053). This sample consists almost entirely of pale-green probably actinolitic hornblende, in a groundmass of biotite and a fine-grained mixture of epidote and chlorite. The amphibole contains few inclusions, mostly of plagioclase, but also minor amounts of biotite are found. The amphibole grains are deformed and often display

Table 2. ^{40}Ar-^{39}Ar analytical data for incremental heating experiments on amphiboles, north-east Disko Bugt and eastern Nuussuaq

Step	$^{40}Ar/^{39}Ar$	$^{36}Ar/^{39}Ar$	$^{37}Ar/^{39}Ar$	$\%^{39}Ar$	$\%^{40}Ar^*$ cumulated	Appar-ent age (Ma ± 1σ)
GGU 349053 (*J* = 0.001765)						
1	5,246.68	0.289	1.638	0.6	98.17	8105±58
2	4,510.02	0.075	1.873	1.5	99.45	7835±57
3	4,916.11	0.161	0.855	2.2	98.94	7989±57
4	4,354.46	0.233	1.042	2.8	98.28	7773±56
5	1,473.81	0.043	1.920	6.4	99.04	5865±46
6	609.72	0.016	4.976	16.4	99.17	4369±33
7	425.87	0.027	5.530	25.7	97.98	3790±27
8	404.92	0.014	5.911	42.7	98.91	3710±27
9	371.50	0.011	5.978	64.9	99.01	3575±25
10	354.66	0.027	5.858	71.4	97.60	3503±25
11	468.17	0.017	5.936	100.0	98.84	3940±29
GGU 354319 (*J* = 0.002452)						
1	90.82	0.095	0.770	2.4	75.97	2055±12
2	161.83	0.133	1.567	3.5	80.11	2825±18
3	83.08	0.061	3.032	6.3	81.94	1948±11
4	86.00	0.005	5.005	49.9	98.19	1989±11
5	91.71	0.015	5.060	55.1	95.25	2067±12
6	59.55	0.042	5.241	58.4	82.60	1574± 8
7	63.09	0.048	6.319	61.9	81.31	1636± 9
8	66.11	0.053	6.953	66.1	80.62	1686± 9
9	64.30	0.073	7.187	68.9	74.41	1656± 9
10	71.40	0.015	6.609	100.00	94.02	1772±10
GGU 359139 (*J* = 0.002479)						
1	48.46	0.067	0.191	11.0	70.53	1378± 7
2	102.35	0.099	0.224	15.7	77.36	2219±13
3	137.15	0.178	1.013	17.7	71.85	2608±16
4	127.82	0.075	4.190	20.8	84.92	2511±15
5	151.18	0.033	8.922	28.7	93.86	2743±17
6	166.92	0.049	9.621	33.3	91.90	2885±19
7	177.83	0.064	11.087	37.0	90.26	2976±20
8	201.89	0.065	12.724	39.7	91.12	3163±21
9	211.37	0.066	13.367	42.3	91.39	3232±22
10	167.39	0.008	10.639	100.0	98.52	2889±19
GGU 352234 (*J* = 0.001765)						
1	2,081.51	0.400	1.085	0.4	94.07	6468±50
2	580.01	0.082	0.624	1.9	95.59	4287±32
3	265.41	0.076	1.168	3.0	91.39	3065±20
4	175.03	0.033	3.169	8.7	94.17	2477±15
5	192.80	0.023	3.359	14.3	96.29	2609±16
6	210.97	0.012	3.512	25.6	98.11	2734±17
7	206.84	0.019	3.507	32.2	97.03	2707±17
8	215.15	0.012	3.841	39.4	98.17	2762±18
9	216.26	0.030	3.451	43.5	95.71	2769±18
10	219.44	0.015	3.333	48.4	97.81	2790±18
11	219.25	0.027	3.327	52.1	96.12	2789±18
12	225.09	0.003	3.268	100.0	99.62	2826±18

Isotopic ratios corrected for the effects of interfering reactions producing Ar during irradiation.

J is a parameter describing the efficiency of the irradiation of the sample; for details see Faure (1986, pp. 93-96).

$\%^{40}Ar^*$ is the percentage of total ^{40}Ar in the sample that is radiogenic.

undulose extinction as well as subgrain formation. Microcracks are common. The amphiboles from this sample yielded a K-Ar date of 4160 ± 34 Ma, which is geologically unrealistic.

In order to investigate this anomalously high K-Ar date, aliquots were irradiated for an ^{40}Ar-^{39}Ar step heating experiment (Fig.2a; Table 2). Very high and geologically unrealistic apparent ages between 8.1 and 5.5 Ga were obtained from the first few steps, representing < 5% of the total ^{39}Ar released (Fig. 2a). The apparent age decreases gradually over the next four steps reaching a minimum of 3503 ± 50 Ma in step 10, followed by an increase in the last step, where a significantly higher age of 3940 ± 58 Ma is obtained. From steps 7 to 10 a weighted mean age of 3644 ± 52 Ma was calculated, which has no geological meaning since it cannot be related to any ages obtained from other parts of the area.

The asymptotic decrease of the apparent age, followed by an increase in the last high temperature step represents a typical saddle-shaped release pattern. This type of pattern is typical for feldspars (e.g. Heizler & Harrison 1988; Harrison 1990; Maluski *et al.* 1990), but has also been described for hornblende (e.g. Lanphere & Dalrymple 1976; Harrison & McDougall 1981; Holm 1991). As demonstrated in this sample, most of the excess Ar component is released at low temperatures, suggesting occupancy of lower activation energy sites within the hornblende (Harrison & McDougall 1981; Maluski *et al.* 1990). Some of the release may, however, come from biotite in the amphibole concentrates, as indicated by the low Ca/K ratios (registered by low $^{37}Ar/^{39}Ar$) in the initial steps (Table 2).

The amphibole from sample 349053 has been subjected to deformation as shown by the strained grains with numerous microcracks. Hornblendes from shear zones commonly take up large quantities of excess argon, and yield discordant spectra (Zeitler 1989). The present sample was collected from a supracrustal amphibolite not far from the strongly sheared contact to the underlying gneissic basement. Furthermore, part of the rock contains substantial amounts of biotite, which could have released Ar at temperatures above *c.* 300°C (the retention temperature of argon in biotite is estimated to be in the range of 280 ± 40°C; Dodson 1973; Harrison & McDougall 1980). Argon released from biotite would have resulted in a significant increase of the partial pressure of Ar within the rock, causing diffusion of this extraneous Ar into microcracks developed in the hornblende during deformation. Furthermore, the Ar pressure in the adjacent gneisses would also have been higher at elevated temperatures during deformation, due to release of Ar from K-rich mineral phases (e.g. biotite and K-feldspar) in the gneisses.

A total gas age of 4330 ± 66 Ma was calculated for all eleven steps in this sample. This age is somewhat higher than the K-Ar age of 4160 ± 34 Ma. This difference is probably caused by sample inhomogeneity.

The four hornblende concentrates from Oqaatsut all come from medium-grained amphibolites located within a mutual distance of about 1 km. Pale blue-green amphiboles separated from samples 349023 and 354328 show clear signs of deformation; they are recrystallised as finer-grained aggregates in a very fine-grained matrix of plagioclase and quartz. These samples yielded dates of 1917 ± 26 Ma and 1870 ± 24 Ma respectively, and demonstrate that Proterozoic metamorphism was accompanied by deformation and shearing, which caused subgrain formation and recrystallisation of the hornblendes.

The amphibole from GGU 354319 is fresh sub- to euhedral, blue-green hornblende with a large number of zircon inclusions. Other mineral phases present are mostly biotite and garnet, indicating an amphibolite facies grade of metamorphism during formation of these amphibolites. The mineral date of 1940 ± 26 Ma obtained from this sample cannot readily be explained as dating the cooling of the hornblende following Proterozoic regional metamorphism, which took place around 1850 Ma (Kalsbeek *et al.* 1984; Taylor & Kalsbeek 1990).

Results of a ^{40}Ar-^{39}Ar age investigation of this sample are listed in Table 2 and the age spectrum obtained is shown in Fig. 2b. The release pattern for this sample is characterised by a first step giving an apparent age of 2055 ± 24 Ma followed by a step yielding a significantly higher date of 2825 ± 36 Ma. Steps 3 to 5 display fairly uniform ages around 1995 Ma. A marked decrease in apparent age to approximately 1700 Ma is observed in the last high temperature steps (6–10).

It is generally agreed to accept as a plateau only adjacent steps (> 3) which represent a large cumulated fraction (> 50%) of the outgassed ^{39}Ar and whose ages differ by no more than a few percent, depending on the analytical uncertainty of each individual age determination. The plateau age is taken as the ^{39}Ar fraction or individual step error weighted average of the individual step ages (Albarede 1982). The age spectrum obtained from this hornblende does not satisfy the criteria referred to above. A weighted mean age of around 1872 Ma for steps 3 to 10 indicates an early Proterozoic age. If this age refers to the crystallisation or total

isotopic resetting of the amphibole, it shows that this part of the Disko Bugt area underwent Proterozoic deformation and metamorphism under amphibolite facies conditions.

Blue-green hornblende separated from the fourth sample from Oqaatsut (GGU 354346) also shows marked signs of deformation and incipient recrystallisation. The groundmass consists of minor quartz and feldspar which sometimes are clearly strained and display undulose extinction. Hornblende in this sample often forms intergrowths with smaller biotite grains, and minor biotite and chlorite also occur in the groundmass. An age of 2181 ± 26 Ma was obtained for GGU 354346, considerably older than the other dates obtained from Oqaatsut. This is probably due to the presence of excess Ar in the hornblende of this sample.

Ataa area

Four samples were studied from the Ataa area; two of these represent metagabbroic xenoliths in the Atâ tonalite which, according to Kalsbeek *et al.* (1988), has largely escaped early Proterozoic deformation. An ^{40}Ar-^{39}Ar study was carried out for hornblende from the latter two samples.

Pale olive-green hornblende from one of the xenoliths (GGU 359139) forms sub- to euhedral prismatic grains with only few inclusions. Minor biotite occurs, partly as intergrowths with hornblende. The hornblende yielded a K-Ar date of 2590 ± 30 Ma.

The ^{40}Ar-^{39}Ar release pattern of this sample (Fig. 2c; Table 2) is characterised by a very low apparent age of 1378 ± 14 Ma in the first low temperature step representing 10% of the released ^{39}Ar. The apparent age increases in the second step to 2219 ± 26 Ma. A steep rise in ages occurs from steps 2 to 9, with a maximum of 3232 ± 44 Ma. This part of the age spectrum makes up *c.* 31% of the total ^{39}Ar released. The last high temperature step (10), with 58% of the total ^{39}Ar release, has an apparent age of 2889 ± 38 Ma. This age is somewhat lower than the ages obtained from steps 8 and 9, but agrees with the ages obtained in steps 6 and 7. There is neither an analytical nor a geological explanation for the differences in apparent ages obtained in steps 6, 7 and 10 and those obtained in steps 8 and 9, but it may be related to the break-down of the crystal structure during heating in the Ar-extraction system or by differential degassing of the lattice sites.

A weighted mean age of 2893 ± 38 Ma has been calculated for steps 6, 7 and 10. This age cannot be separated statistically from the age of 2915 ± 38 Ma calculated for steps 6–10, demonstrating that the high ages of steps 8 and 9 only have a minor effect on the calculated weighted mean age. The 2915 Ma age cannot, however, be regarded as a true plateau age, since the steps used in the calculation fail to display a coherent age pattern within a few percent.

Very low Ca/K ratios (low $^{37}Ar/^{39}Ar$, Table 2) in steps 1 to 4 indicate that part of the argon release could be derived from degassing of small amounts of biotite present as small inclusions within the hornblende (Rasmussen 1992). This suggestion is supported by a recent investigation by Rex *et al.* (1993) which showed that addition of different amounts of biotite (DR16) to hornblende (MMHb-1) yielded age spectra bearing a striking similarity to 'diffusive loss' profiles.

The ^{40}Ar-^{39}Ar data indicate that the hornblende has retained most of its Ar after incorporation of the inclusion in the Atâ tonalite. The age of 2915 ± 38 Ma obtained from the high temperature steps is somewhat higher than the 2800 Ma age of the Atâ tonalite (Kalsbeek *et al.* 1988; Nutman & Kalsbeek 1999, this volume). The cause of this anomaly is not clear.

The other metagabbroic inclusion (GGU 352234) was sampled from a porphyric granitoid rock on Illuluarsuit Nunataat (Fig. 1), regarded as belonging to a younger intrusive phase of the Atâ tonalite (L. Skjernaa, personal communication 1992). Hornblende from this sample is sub- to euhedral, and inclusions of quartz are common; it looks fresh and contains only few microcracks. Small amounts of biotite are present in the rock, sometimes occurring as inclusions in the hornblende. The hornblende yielded a K-Ar date of 2750 ± 30 Ma. It is likely that the K-Ar system was reset during emplacement of the tonalite, and the age is interpreted as representing the time at which the intrusion cooled below the Ar retention temperature of hornblende.

To test the validity of this date and to detect a possible component of excess ^{40}Ar, a step heating ^{40}Ar-^{39}Ar experiment was performed (Table 2). The ^{40}Ar-^{39}Ar age spectrum (Fig. 2d) shows a rather simple release pattern, characterised by yielding unrealistically high apparent ages for the first three steps, representing *c.* 2% of the total ^{39}Ar released. The highest age of 6468 ± 100 Ma, calculated for the first step, gradually decreases to 3065 ± 40 Ma in the third step. High apparent age steps as these can either be produced as a consequence of recoil of ^{39}Ar during the irradiation process, or they can represent excess argon in the mineral. The rest of the ^{40}Ar-^{39}Ar release pattern is typical of a mineral that has suffered partial argon loss by diffusion. This pat-

tern is characterised by a relatively low age of 2477 ± 30 Ma in step 4, followed by a gradual increase in age, reaching an almost constant level at approximately 2800 Ma.

The sample displays a Ca/K distribution (registered by $^{37}Ar/^{39}Ar$, Table 2) that indicates presence of biotite influencing the low temperature steps of the age spectrum (Rasmussen 1992), in accordance with observations by Rex *et al.* (1993).

The total ^{40}Ar-^{39}Ar age of 2855 ± 36 Ma calculated for this sample is 3.8% higher than the date of 2750 ± 30 Ma obtained from the conventional K-Ar age determination. This difference can be explained by some degree of recoil effect of ^{39}Ar in the low activation energy sites within the hornblende, thus producing higher ^{40}Ar-^{39}Ar ratios resulting in high apparent ages without geological significance.

Steps 6 to 12 form a coherent pattern, comprising *c.* 85% of the total cumulated ^{39}Ar released, and satisfy the criteria for defining an age plateau (Albarede 1982). The weighted mean plateau age of 2793 ± 36 Ma conforms within the limits of analytical error with the age of *c.* 2800 Ma obtained for the Atâ tonalite (Kalsbeek *et al.* 1988; Nutman & Kalsbeek 1999, this volume). The hornblende plateau age is therefore interpreted as representing the time at which the intrusion cooled below the Ar retention temperature of the hornblende. Even if the xenolith was very large, it is unlikely that the hornblende could have retained any of its former content of radiogenic argon, since the intrusion temperature of the granite (700–800°C) is significantly higher than the retention temperature of Ar in hornblende (530 ± 40°C; Harrison & McDougall 1980). The ^{40}Ar-^{39}Ar age spectrum further indicates that during later Proterozoic deformation temperatures in this part of the area were not sufficiently high to induce significant diffusive loss of argon from the hornblende, but that the biotite inclusions were affected. This means that the Proterozoic metamorphic grade in this part of the area never reached more than greenschist facies conditions.

Well-preserved brownish-green, anhedral hornblende was separated from a black amphibolite (GGU 272611) occurring within dioritic gneiss in the southern part of Arveprinsen Ejland. It is almost free of inclusions and contains only few microcracks. Plagioclase in this sample is fresh and only displays signs of incipient carbonisation. The hornblende yielded a date of 2457 ± 28 Ma.

A similar intermediate date of 2292 ± 28 Ma was obtained from a basic inclusion (GGU 352239) in a migmatitic gneiss at Oqaatsunnguit. The olive-green hornblende obtained from this rock contains some minor inclusions of quartz and biotite. It contains numerous microcracks. Since these samples have not been investigated using the ^{40}Ar-^{39}Ar method, detailed interpretation of the dates is not possible. Either the K-Ar systems were only partly reset during early Proterozoic tectono-thermal activity, or, if total resetting has taken place, the hornblende contains significant proportions of excess argon.

Eastern Disko Bugt

A pale green hornblende from a medium-grained amphibolite (GGU 355612) in supracrustal rocks at Nunatarsuaq (Fig. 1) yielded a K-Ar date of 1948 ± 26 Ma. The large crystalloblastic amphiboles in this sample form sub- to euhedral, inclusion-free grains. No retrograde mineral assemblages were observed and the associated plagioclase only shows weak signs of sericitisation.

This date is considerably older than the K-Ar biotite age of 1725 ± 30 Ma obtained by Larsen & Møller (1968) from the gneisses near Jakobshavn/Ilulissat. It is also older than the peak of early Proterozoic metamorphism, at *c.* 1850 Ma (Kalsbeek *et al.* 1984; Taylor & Kalsbeek 1990). It is not clear whether the 1948 Ma date refers to Proterozoic metamorphism earlier than 1850 Ma in this part of the area or if the date is related to a component of excess Ar in *c.* 1850 Ma hornblende.

Lamproite at Oqaatsunnguit

A lamproite stock with coarse-grained ellipsoidal phlogopite nodules, *c.* 1 cm in diameter, intruded in rocks of the Atâ tonalite at Oqaatsunnguit (Fig. 1), has been described by Skjernaa (1992). The nodules are monomineralic, dark brown, and consist of phlogopite with a central grain completely surrounded by a concentrically arranged mantle grain, giving the nodules an ellipsoidal appearance. A K-Ar date of 1764 ± 24 Ma was obtained for this phlogopite (GGU 343955), in excellent agreement with the 1743 ± 70 Ma K-Ar age on matrix phlogopite from the same lamproite (Larsen & Rex 1992). The agreement between the K-Ar ages obtained for the coarse-grained phlogopite nodules and the fine-grained matrix phlogopite indicates that the ages represent the crystallisation of the lamproite, and that the K-Ar system has not been significantly affected

since then. The correspondence of the two ages also indicates that the lamproite stock must have been emplaced at a high level in the crust, since significant radiogenic ^{40}Ar loss after crystallisation would be expected (especially from the phlogopite in the matrix because of the smaller grain size) if temperatures had been significantly above the closure temperature of the phlogopite-biotite K-Ar system (*c.* 280°C, e.g. Harrison & McDougall 1980) for a long time after crystallisation.

Summary and conclusions

Regional investigations have shown that the metamorphic grade of the Archaean supracrustal rocks in the Ataa region range from upper greenschist to amphibolite facies (Garde & Steenfelt 1999, this volume). The presence of kyanite, staurolite, garnet, biotite and hornblende at Naujaat Qaqqaat and Oqaatsut makes it possible to estimate metamorphic *P* and *T* levels of at least 5–7 kb and 500–625°C (Winkler 1979; Apted & Liou 1983) for the formation of the dominant mineral assemblages in these two areas.

K-Ar and ^{40}Ar-^{39}Ar age investigations from Naujaat Qaqqaat and Oqaatsut revealed no reliable Archaean hornblende dates. There are two likely explanations of the Proterozoic K-Ar hornblende dates from the two areas. The first explanation is that the temperatures reached during the Proterozoic tectono-thermal event were not sufficiently high, or conditions were too dry, for recrystallisation of the hornblende of an earlier Archaean metamorphic event, but reached temperatures high enough to reset the K-Ar hornblende system. However, amphiboles are usually considered as the most retentive of the minerals used for K-Ar dating, and it has been argued that recrystallisation may be necessary to reset hornblende ages totally (Dallmeyer 1979). The other explanation is that the Proterozoic tectono-thermal reworking reached amphibolite facies grade resulting in either total recrystallisation of the hornblendes or partial modification by dynamic grain-size reduction eventually resulting in crystallisation of fine-grained hornblende aggregates, which has been observed in a number of samples. The consequence of these grain modifications is a total resetting of the K-Ar hornblende clock. The indication of a total resetting by grain-size reduction and recrystallisation is sustained by the rather flat ^{40}Ar-^{39}Ar age spectrum obtained from sample GGU 354319, which yielded Proterozoic ages for over 95% of the total ^{39}Ar released (Fig. 2b). The large spread in K-Ar mineral dates (> 300 Ma) over relatively short distances in the two areas is probably due to incorporation of variable amounts of excess ^{40}Ar in the hornblendes, which has variably raised their bulk ages, as indicated by the ^{40}Ar-^{39}Ar saddle shaped spectrum obtained from GGU 349053 (Fig. 2a). It is therefore clear that Proterozoic deformation and metamorphism have played an important role at Naujaat Qaqqaat and Oqaatsut.

The two age spectra obtained from the inclusions in the Atâ tonalite (GGU 359139 and 352234, Figs 2c, d) demonstrate that in the Ataa area temperatures were not high enough to reset the hornblende ages during Proterozoic reworking. These age spectra also show the influence of biotite contamination in the low temperature steps, in accordance with observations by Rex *et al.* (1993). The calculated average ages for these two samples reflect the time at which the xenoliths together with the surrounding rocks cooled below the retention temperature of the hornblende (*c.* 500–570°C; Harrison 1981).

The date of 1948 ± 26 Ma obtained from the eastern part of the Disko Bugt region suggests that also in this part of the area Proterozoic tectono-thermal reworking provided conditions under which the K-Ar system behaved as an open system.

The dates obtained from north-eastern Nuussuaq (1925 ± 24 Ma and 1751 ± 24 Ma), from central eastern Nuussuaq (1861 ± 26 Ma) and from the Saqqaq area (1789 ± 24 Ma) show that Proterozoic tectono-thermal reworking has taken place in these areas.

The high degree of conformity between the phlogopite mineral ages obtained in this study (1764 ± 24 Ma) and those presented by Larsen & Rex (1992; 1743 ± 70 Ma) indicates that these ages can be interpreted as representing the time of intrusion of the lamproites in the region.

Acknowledgements

Thanks to Feiko Kalsbeek, Agnete Steenfelt, Adam A. Garde and Lilian Skjernaa for providing sample material for this isotopic work. Feiko Kalsbeek is thanked for help with the manuscript, and D.C. Rex for helpful comments on the ^{40}Ar-^{39}Ar age investigations and for reviewing the manuscript.

References

Albarede, F. 1982: The $^{39}Ar/^{40}Ar$ technique of dating. In: Odin, G.S. (ed.): Numerical dating in stratigraphy, 181–197. Chichester, UK: Wiley.

Apted, M.J. & Liou, J.G. 1983: Phase relations among greenschist, epidote-amphibolite and amphibolite in a basaltic system. American Journal of Science **283-A**, 328–354.

Dallmeyer, R.D. 1979: $^{40}Ar/^{39}Ar$ dating: principles, techniques and applications in orogenic terranes. In: Jäger, E. & Hunziker, J.C. (eds): Lectures in isotope geology, 77–104. Berlin: Springer-Verlag.

Dodson, M.H. 1973: Closure temperature in cooling geochronological and petrological systems. Contributions to Mineralogy and Petrology **40**, 259–274.

Faure, G. 1986: Principles of isotope geology, 589 pp. New York: Wiley & Sons.

Garde, A.A. & Steenfelt, A. 1999: Precambrian geology of Nuussuaq and the area north-east of Disko Bugt, West Greenland. In: Kalsbeek, F. (ed.): Precambrian geology of the Disko Bugt region, West Greenland. Geology of Greenland Survey Bulletin **181**, 6–40 (this volume).

Harrison, T.M. 1981: Diffusion of ^{40}Ar in hornblende. Contributions to Mineralogy and Petrology **78**, 324–331.

Harrison, T.M. 1990: Some observations on the interpretation of feldspar $^{40}Ar/^{39}Ar$ results. Chemical Geology (Isotope Geoscience Section) **80**, 219–229.

Harrison, T.M. & McDougall, I. 1980: Investigations of an intrusive contact, north-west Nelson, New Zealand – I. Thermal, chronological and isotopic constraints. Geochimica et Cosmochimica Acta **44**, 1985–2003.

Harrison, T.M. & McDougall, I. 1981: Excess ^{40}Ar in metamorphic rocks from Broken Hill, New South Wales: implications for $^{40}Ar/^{39}$ Ar age spectra and the thermal history of the region. Earth and Planetary Science Letters **55**, 123–149.

Heizler, M.T. & Harrison, T.M. 1988: Multiple trapped argon isotope components revealed by $^{40}Ar/^{39}Ar$ isochron analysis. Geochimica et Cosmochimica Acta **52**, 1295–1303.

Holm, P.M. 1991: Radiometric age determinations in the Kærven area, Kangerdlugssuaq, East Greenland Tertiary igneous Province: $^{40}Ar/^{39}Ar$, K/Ar and Rb/Sr isotope results. Bulletin of the Geological Society of Denmark **38**, 183–201.

Kalsbeek, F. 1981: The northward extent of the Archaean basement of Greenland – a review of Rb-Sr whole-rock ages. Precambrian Research **14**, 203–219.

Kalsbeek, F., Taylor, P.N. & Henriksen, N. 1984: Age of rocks, structures and metamorphism in the Nagssugtoqidian mobile belt, West Greenland – field and Pb-isotope evidence. Canadian Journal of Earth Sciences **21**, 1126–1131.

Kalsbeek, F., Taylor, P.N. & Pidgeon, R.T. 1988: Unreworked Archaean basement and Proterozoic supracrustal rocks from northeastern Disko Bugt, West Greenland: implications for the nature of Proterozoic mobile belts in Greenland. Canadian Journal of Earth Sciences **25**, 773–782.

Lanphere, M.A. & Dalrymple, G.B. 1976: Identification of excess ^{40}Ar by the $^{40}Ar/^{39}Ar$ age spectrum technique. Earth and Planetary Science Letters **32**, 141–148.

Larsen, L.M. & Rex, D.C. 1992: A review of the 2500 Ma span of alkaline-ultramafic, potassic and carbonatitic magmatism in West Greenland. Lithos **28**, 367–402.

Larsen, O. & Møller, J. 1968: Potassium-argon age studies in West Greenland. Canadian Journal of Earth Sciences **5**, 683–691.

Maluski, H., Monie, P., Kienast, J.R. & Rahmani, A. 1990: Location of extraneous argon in granulitic-facies minerals: a paired microprobe-laser probe $^{40}Ar/^{39}Ar$ analysis. Chemical Geology (Isotope Geoscience Section) **80**, 193–217.

Nutman, A.P. & Kalsbeek, F. 1999: SHRIMP U-Pb zircon ages for Archaean granitoid rocks, Ataa area, north-east Disko Bugt. In: Kalsbeek, F. (ed.): Precambrian geology of the Disko Bugt region, West Greenland. Geology of Greenland Survey Bulletin **181**, 49–54 (this volume).

Rasmussen, H. 1992: Petrography, geochemistry and combined K/Ar and $^{40}Ar/^{39}Ar$ mineral age investigations of Archaean amphibolitic, ultramafic and related supracrustal rocks from Naujât qáqât and Oqaitsut, Disko Bugt, West Greenland, 149 pp. Unpublished cand. scient. thesis, University of Copenhagen, Denmark.

Rex, D.C., Guise, P.G. & Wartho, J.-A. 1993: Disturbed ^{40}Ar-^{39}Ar spectra from hornblendes: thermal loss or contamination? Chemical Geology (Isotope Geoscience Section) **103**, 271–281.

Skjernaa, L. 1992: A lamproite stock with ellipsoidal phlogopite nodules at Oqaitsúnguit, Disko Bugt, central West Greenland. Rapport Grønlands Geologiske Undersøgelse **154**, 33–47.

Steiger, R.H. & Jäger, E. 1977: Subcommision on Geochronology: Convention on the use of decay constants in geo- and cosmochronology. Earth and Planetary Science Letters **36**, 369–362.

Taylor, P.N. & Kalsbeek, F. 1990: Dating the metamorphism of Precambrian marbles: examples from Proterozoic mobile belts in Greenland. Chemical Geology (Isotope Geoscience Section) **86**, 21–28.

Winkler, H.G.F. 1979: Petrogenesis of metamorphic rocks, 338 pp. New York: Springer-Verlag.

Zeitler, P.K. 1989: The geochronology of metamorphic processes. In: Daly, J.S., Cliff, R.A. & Yardley, B.W.D. (eds): Evolution of metamorphic belts. Geological Society Special Publication (London) **43**, 131–147.

Stratigraphy, structure and geochemistry of Archaean supracrustal rocks from Oqaatsut and Naajaat Qaqqaat, north-east Disko Bugt, West Greenland

Henrik Rasmussen and Lars Frimodt Pedersen

Two Archaean supracrustal sequences in the area north-east of Disko Bugt, *c.* 1950 and *c.* 800 m in thickness, are dominated by pelitic and semipelitic mica schists, interlayered with basic metavolcanic rocks. A polymict conglomerate occurs locally at the base of one of the sequences.

One of the supracrustal sequences has undergone four phases of deformation; the other three phases. In both sequences an early phase, now represented by isoclinal folds, was followed by north-west-directed thrusting. A penetrative deformation represented by upright to steeply inclined folds is only recognised in one of the sequences. Steep, brittle N–S and NW–SE striking faults transect all rock units including late stage dolerites and lamprophyres.

Investigation of major- and trace-element geochemistry based on discrimination diagrams for tectonic setting suggests that both metasediments and metavolcanic rocks were deposited in an environment similar to a modern back-arc setting.

H.R.* & L.F.P.‡, *Geological Institute, University of Copenhagen, Øster Voldgade 10, DK-1350 Copenhagen K, Denmark.* *Present address: *Mærsk Olie og Gas AS, Esplanaden 50, DK-1263 Copenhagen K, Denmark.* E-mail: *h_rasmussen@vip.cybercity.dk.* ‡Present address: *Falkenberg A/S, Højbrogade 12–14, DK-4800 Nykøbing F, Denmark.*

Keywords: Archaean, Disko Bugt, geochemistry, supracrustal rocks, West Greenland

The Precambrian terrain north-east of Disko Bugt consists of four main rock units: Archaean grey gneisses, Archaean supracrustal rocks, the 2800 Ma Atâ tonalite that intrudes supracrustal rocks and gneisses, and the early Proterozoic Anap nunâ Group (Garde & Steenfelt 1999, this volume).

Archaean supracrustal rocks are dominated by basic metavolcanic rocks and pelitic to semipelitic metasediments, which have been metamorphosed under greenschist to middle amphibolite facies conditions. The rocks are strongly deformed and folded into both tight and open structures as a result of several phases of Archaean and Proterozoic deformation.

This paper deals with the supracrustal rocks of Oqaatsut and Naajaat Qaqqaat, located south and north of the fjord Torsukattak, respectively (Fig. 1). These rocks were briefly investigated during the early regional mapping of the Disko Bugt area (Escher & Burri 1967), but detailed structural and stratigraphical investigations have not been carried out previously, and no geochemical data were available.

Stratigraphy

Oqaatsut

The supracrustal sequence on Oqaatsut is bounded to the west and east by granitoid rocks (Fig. 1). The succession has a general N–S trend and dips moderately to the east. It can be divided into three main units: a lower and an upper amphibolitic greenstone unit, with a metasedimentary unit in between (Fig. 2).

The metasedimentary unit has at present a maximum thickness of *c.* 1150 m in the centre of the island and a minimum thickness of about 850 m in the south. It is dominated by light to dark grey, fine-grained quartzofeldspatic metapelitic schists, often rich in biotite.

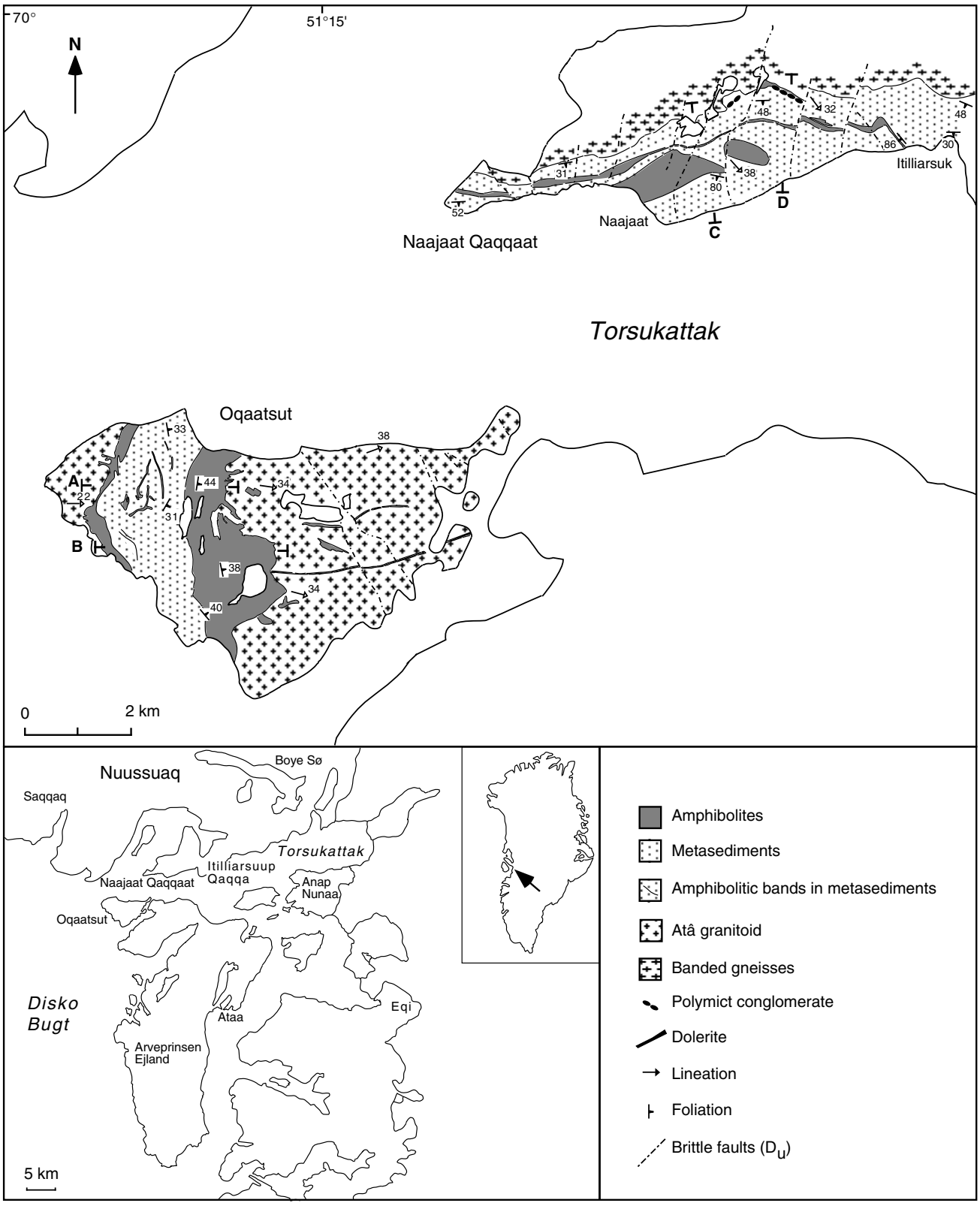

Fig. 1. Geological sketch map of Oqaatsut and Naajaat Qaqqaat, north-east Disko Bugt, West Greenland with location of the profiles A and B (Fig. 2), and C and D (Fig. 3).

Fig. 2. Schematic stratigraphy of supracrustal rocks on Oqaatsut. For location of profiles A and B see Fig. 1.

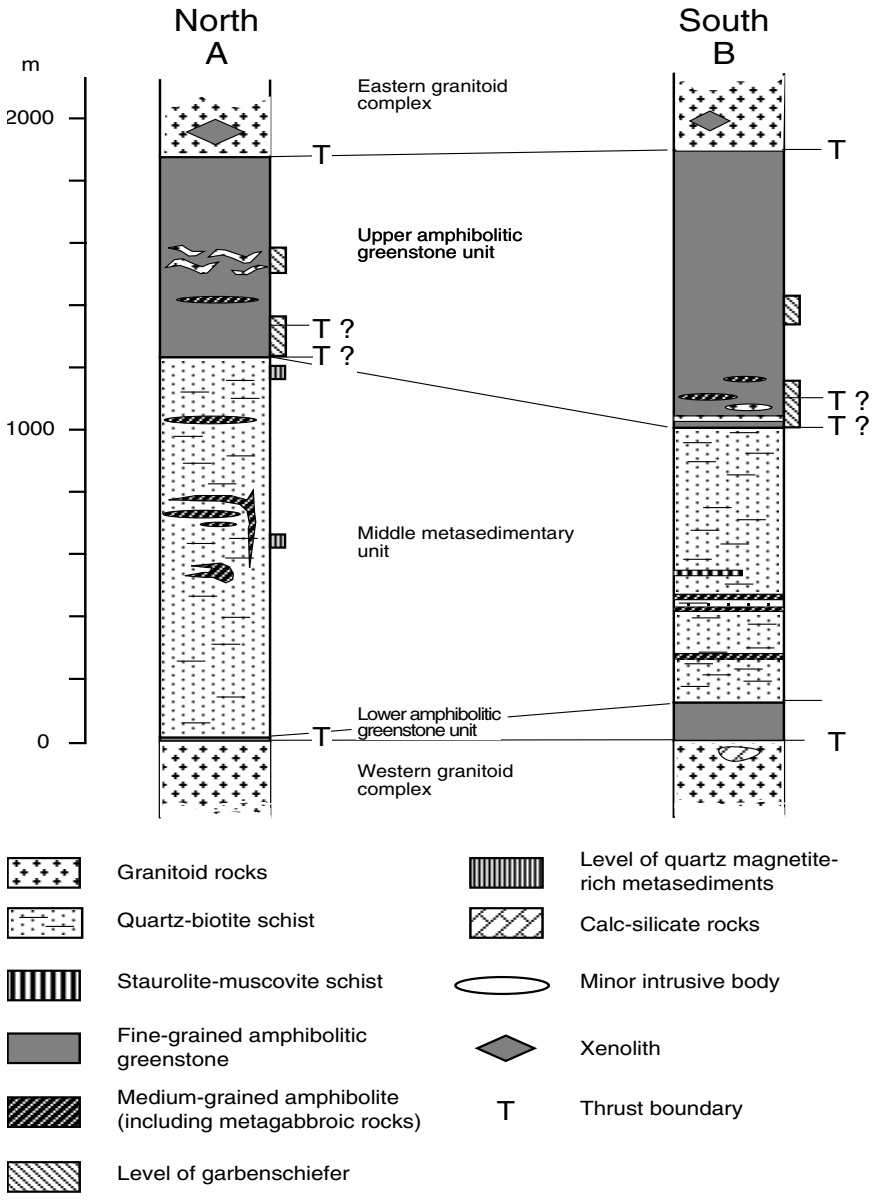

Amphibole is sometimes present and pale blue kyanite was observed at a few localities, sometimes associated with garnet and staurolite. Porphyroblastic garnet is common throughout the entire unit. Minor amphibolitic layers and lenses are common, especially near the contact to the major greenstone units. Amphibolites found within the metasediments are mostly fine grained and occur both as foliation-parallel, sill-like layers and as cross-cutting dykes. The metasediments contain a few, 1–5 m thick, horizons of fine-grained staurolite-muscovite schist with staurolite porphyroblasts (1–3 mm), as well as 1–3 m thick horizons of fuchsite-bearing quartz-muscovite schist. Quartz-magnetite rich rocks were found at two localities as 1–2 m thick layers. They consist of alternating quartz and magnetite laminae a few millimetres to about 1–2 cm wide.

The tectonostratigraphically lower, western amphibolitic greenstone unit is 10–125 m thick. To the west it is disrupted by light grey, medium-grained granioid

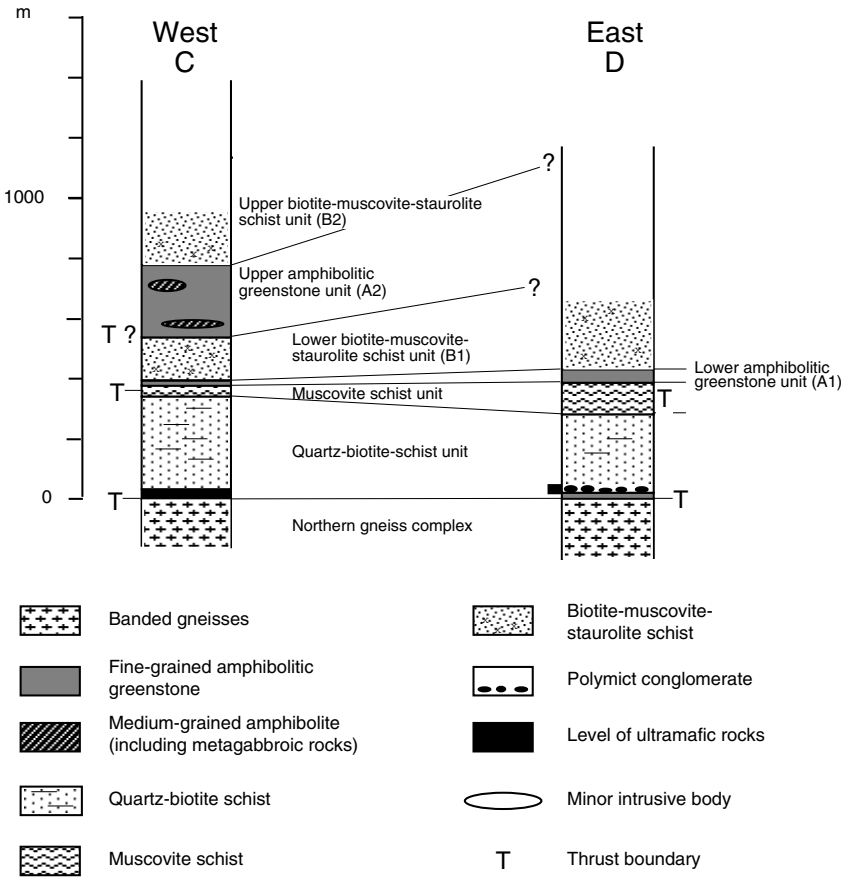

Fig. 3. Schematic stratigraphy of supracrustal rocks on Naajaat Qaqqaat. For location of profile C and D see Fig. 1.

rocks (Fig. 1), and to the east there is a gradual transition to the overlying metasedimentary unit. This lower unit mainly consists of fine-grained amphibolite with a few subordinate bodies of metagabbro. Garnet is found locally. Disseminated sulphides locally give rise to rusty weathering and local malachite staining on joint surfaces. Relationships between the western granitoid complex and the lower amphibolitic unit are not clear because of later shearing and folding at the boundary. The granitoids, however, are believed to be intrusive into the supracrustal rocks.

The upper amphibolitic greenstone unit (Fig. 2) forms a *c.* 900 m thick succession in the central part of the island. It thins both to the south and to the north, where it is *c.* 600 m thick. The amphibolites are mostly fine grained with local layers of garbenschiefer, but minor bodies and lenses of metagabbroic rocks with recognisable igneous textures are also present.

To the east the supracrustal sequence is overlain by granitoid rocks belonging to the 2800 Ma Atâ tonalite (Kalsbeek & Skjernaa 1999, this volume). Granitoid dykes are found in the upper amphibolitic greenstone unit, and xenoliths of amphibolite, up to *c.* 100 m in size, are observed within the granitoids, which clearly suggest they were intruded into the supracrustal sequence. Shear and thrust movements between the two units have resulted in the formation of a mylonitic border zone, within which both units have been strongly deformed.

Lamprophyres (*c.* 1750 Ma; Larsen & Rex 1992; Rasmussen & Holm 1999, this volume) are locally present in up to 1 m thick E–W-trending dykes within the northern and central parts of the eastern granitoids. They are fine grained with a brown to greenish appearance and sometimes show signs of strong internal shearing and deformation; they have not been identified within the supracrustal rocks. Subvertical E–W-trending dolerite dykes, 1 and 4 m thick, also occur in the granitoid rocks. Also these dykes could not be traced into the underlying supracrustal sequences.

Naajaat Qaqqaat

The supracrustal sequence on Naajaat Qaqqaat is dominated by staurolite, muscovite and biotite-rich schists alternating with amphibolitic greenstone units (Fig. 3). It trends E–W with moderate dips towards S and SE,

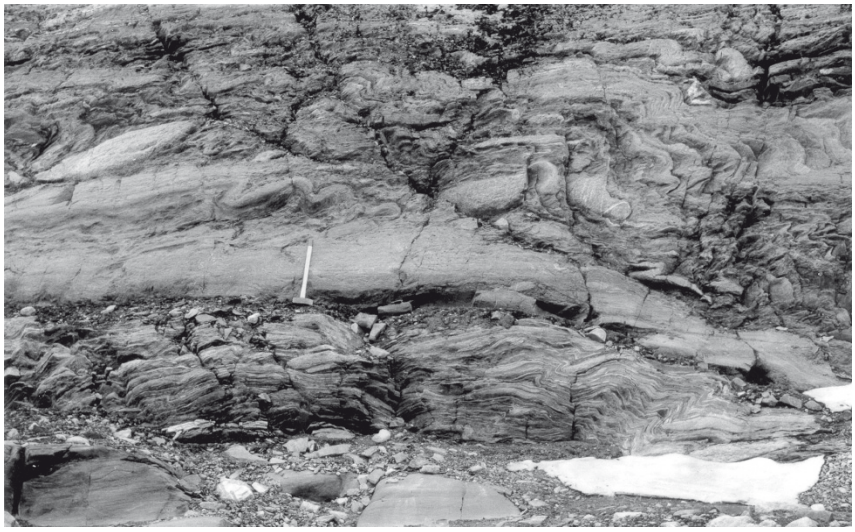

Fig. 4. Folded conglomerate with drag fold near the base of the supracrustal succession at Naajaat Qaqqaat. The drag fold (D_2) in the conglomerate horizon is viewed in a south-easterly direction. The *Z* folds plunge moderately to the SE, subparallel with a mineral liniation.

and rests on a strongly sheared and banded gneiss complex to the north. The contact with the gneisses is strongly sheared; nevertheless the gneiss complex is believed to form the basement of the supracrustal rocks.

The lowermost quartz-biotite schist unit on Naajaat Qaqqaat is between 150 and 350 m thick (Fig. 3). At Itilliarsuk in the easternmost part of the area, however, it reaches a tectonostratigraphical thickness of over 600 m. The dominant rock type is a light-grey schist, rich in quartz, feldspar and biotite. It is sometimes banded at a scale of 1 cm or less. Some horizons are garnetiferous, and hornblende and muscovite are found locally. At a few localities biotite-kyanite-staurolite-rich schists occur.

In the central part of Naajaat Qaqqaat, the base of the quartz-biotite schist unit is marked by a polymict conglomerate (Fig. 4), two exposures of which can be followed 200 m and 500 m along strike. The conglomerate is matrix supported and clasts consist mainly of amphibolite and foliated tonalite. The clasts, which are strongly sheared and folded, range in size from pebbles to cobbles, with a few reaching the size of boulders. A similar exposure of a polymict conglomerate has been reported from Itilliarsuup Qaqqaa (Garde & Steenfelt 1999, this volume). The basal conglomerate and the overlying metasediments indicate a transition from a shallow water environment, adjacent to an exposed area of older crust, towards a deeper water, oceanic environment.

The overlying biotite-muscovite-staurolite schists can be divided into a lower and upper unit (B1 and B2, Fig. 3). The lower unit extends along strike from Naajaat to Itilliarsuk. In this part of Naajaat Qaqqaat it varies in thickness from less than 100 m up to 350–400 m in the east. West of Naajaat it is only exposed in a few outcrops along the coast, and the thickness does not exceed 50 m. The upper unit (B2) has only been found just east of Naajaat along steep coastal cliffs. Because of poor accessibility its thickness is not known, but has been estimated to be at least 220 m. The rocks from the lower and upper units are texturally and mineralogically very similar, and occur in the field as brownish-red, medium- to coarse-grained mica-rich schists. Both biotite and muscovite are present in a matrix dominated by quartz and plagioclase. Garnet, often together with staurolite, is also present. Locally the schists contain kyanite, especially in the lower unit, often together with quartz lenses and veins.

The muscovite schist unit (Fig. 3) is an important marker and can be followed along strike from east to west across the entire area. In the western part this unit is thin, rarely exceeding 3–4 m. In the central part of the area it has a thickness of 50 m and just west of Itilliarsuk it reaches 100 m. It has a well-developed schistosity; in some exposures it is strongly sheared and transformed into a fine-grained banded mylonite. The muscovite schist consists predominantly of fine-grained quartz, feldspar and muscovite and locally contains minor pyrite, garnet and biotite.

Two units of amphibolitic greenstone are present at Naajaat Qaqqaat (Fig. 3, A1 and A2). The lower unit (A1) is continuous; it is approximately 100 m thick in the central eastern part of Naajaat Qaqqaat, but its thickness varies considerably, and at many places it does not exceed 10–20 m. Fine-grained amphibolite dominates this unit. It is foliated and may contain very thin

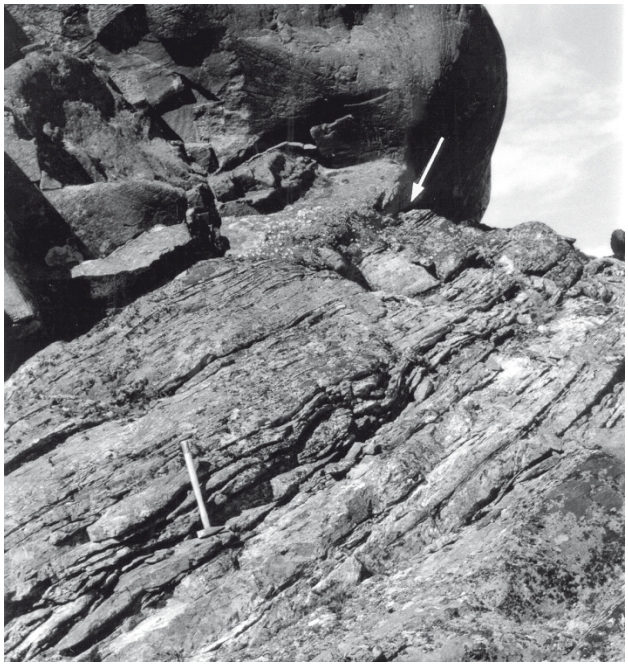

Fig. 5. Moderately SE-dipping sheared contact between the orthogneiss basement and supracrustal (ultramafic) rocks. The sharp contact is one metre above the hammer. Viewed towards west.

layers (up to 5 mm) of felsic material. In a few places more coarse-grained amphibolitic and metagabbroic layers were found. The upper amphibolitic unit is at least 250 m thick in central Naajaat Qaqqaat (Fig. 3), but further west it is only exposed in the coastal areas, where it is only 10–20 m thick. Like the lower greenstone unit, the upper unit is dominated by fine-grained, homogeneous to faintly laminated amphibolites interbedded with thin felsic horizons. Enclaves of medium-grained metagabbroic amphibolite are much more frequent than in the lower unit. Also lenses of hornblende-rich often garnetiferous amphibolite were found. Large (1–2 cm) garnet crystals in these amphibolites are partially altered to chlorite.

Three layers of banded iron formation, less than 1 m thick, could be followed for a few tens of metres along strike in the lower amphibolitic greenstone unit. They are laminated at 1–5 cm scale, with irregular alternating layers of quartz and magnetite; one, however, is regularly banded with a layering of up to 10 cm. Quartz bands comprise about 50% of this rock type.

Ultramafic rocks form irregular, up to *c.* 300 m long lensoid bodies close to the base of the supracrustal succession (Figs 3, 5). The ultramafic rocks are homogeneous to slightly banded. On weathered surfaces they have a typical reddish to brown colour; on fresh surfaces they are generally black to dark grey. They consist predominantly of amphiboles, pyroxenes, chlo-

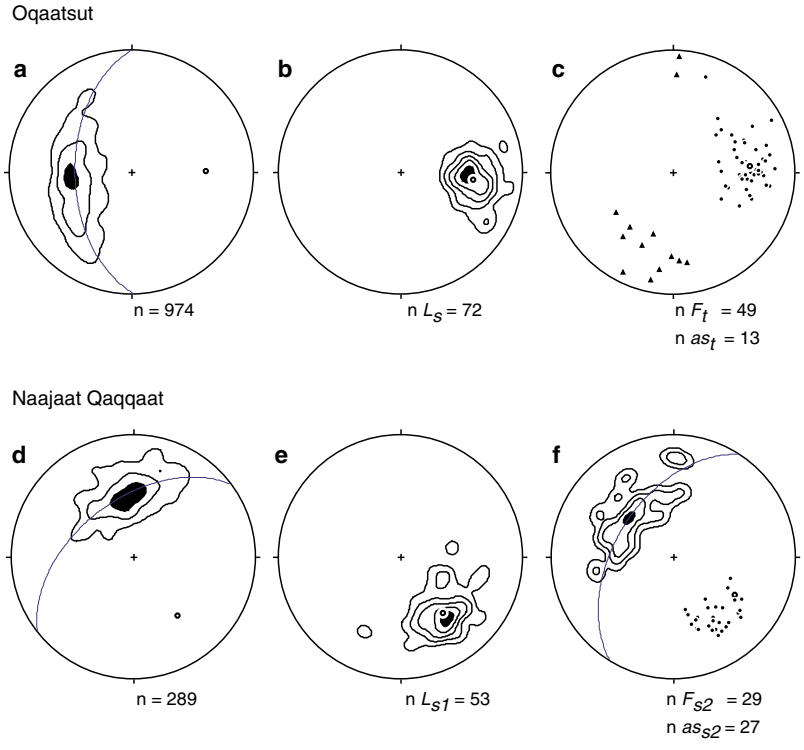

Fig. 6. Lower hemisphere equal-area projections of foliations, lineations and folds, Oqaatsut and Naajaat Qaqqaat. **a**: Poles to foliation, Oqaatsut, contoured at 1, 3 and 6%. The pole to the best fit great circle is 89/39 (open circle). **b**: L_s lineations, reorientated during D_t, Oqaatsut, contoured at 1, 3, 6, 10 and 15%. The mean linear vector is 96/40. **c**: Attitude of F_t folds, Oqaatsut. Black dots: hinge lines, triangles: poles to axial surfaces. The mean linear vector to F_t hinge lines is 87/37. **d**: Poles to foliation, Naajaat Qaqqaat, contoured at 1, 3 and 6%. The pole to the best fit great circle is 142/39. **e**: L_{s1} lineation, Naajaat Qaqqaat, contoured at 1, 3, 6, 10 and 15%. The mean linear vector is 143/41. **f**: Attitude of s_2 drag folds, Naajaat Qaqqaat. Poles to axial surfaces are contoured at 1, 3, 6 and 10%. Black dots: hinge lines to F_{s2} folds. The pole to the best fit great circle to F_{s2} axial surfaces is 122/40. Not shown: the mean linear vector to F_{s2} hinge lines (145/40; Pedersen 1995).

rite and opaque minerals. Amphibole is mostly anthophyllite and cummingtonite, locally tremolite. Strongly metasomatised rocks consisting almost entirely of chlorite and opaque minerals also occur. Ultramafic bodies are often associated and interlayered with amphibolites and amphibole-rich schists, and in some places also with the conglomerate. The amphibolitic rocks are fine to medium grained, and appear as black layers and lenses within the ultramafic bodies.

Structures

Oqaatsut

The supracrustal sequence on Oqaatsut has a moderately steep E-dipping penetrative foliation (Fig. 6a), which is 10–20° steeper at the contact to the eastern granitoids than in the west. A similar increase in the dip of foliation is seen from south to north. Mineral lineations and crenulation lineations follow the general E-dipping structural trend (Fig. 6b).

Four stages of deformation can be distinguished in the supracrustal rocks on Oqaatsut. An early stage of isoclinal folding (D_r) is preserved as local remnants of isolated recumbent folds that plunge down the dip of the foliation plane. Extension of fold limbs caused boudinage of foliation-parallel competent layers (Fig. 7).

Moderately E-dipping as well as moderately to steeply N-dipping shear zones (D_s) occur at the contact between the eastern granitoids and the upper amphibolitic greenstone unit. Mineral lineations and shear sense indicators (rotated plagioclase crystals) show that the hanging wall has moved towards the NW. Two poorly exposed, moderately E-dipping shear zones have been recognised in the upper amphibolitic greenstone unit just above and at the contact to the middle sedimentary unit. In the southern part of the western granitoid complex imbricated quartz boudins in a moderately N-dipping D_s shear zone also indicate movement of the hanging wall towards the NW (Pedersen 1995).

Upright to steeply inclined concentric folds, developed during later penetrative deformation (D_t, Fig. 6c), are prominent within the supracrustal rocks. They have a wavelength of the order of 10–20 m. The fold axis (F_t), constructed from poles to foliation planes, plunges 40°E (Fig. 6a). The contact between the supracrustals and the granitoid rocks was folded into cuspate-lobate folds due to competence contrasts, the granitoids being the most competent. This phase of folding has also affected the E- and NE-dipping D_s shear zones. D_t deformation has also resulted in folding of the boudins mentioned above (see Fig. 7).

The last phase of deformation observed (D_u) is expressed as dextral horizontal displacements along steep NW-striking brittle faults (Fig. 1), which also cut the dolerite and lamprophyre dykes. Displacements were less than 100 m.

Fig. 7. Boudinaged and folded amphibolitic band in the metasediments at the southern coast of Oqaatsut.

Naajaat Qaqqaat

On Naajaat Qaqqaat the foliation dips and the mineral lineation plunges SE (Fig. 6d, e). The dip of the foliation increases from *c*. 30° at the gneiss contact to *c*. 80° near Torssukatak.

Only three of the four deformation phases on Oqaatsut have been recognised in the supracrustal rocks at Naajaat Qaqqaat (D_r, D_s and D_u). D_s has here been subdivided into D_{s1}, D_{s2} and D_{s3} in order to separate structures which appear to be genetically related (Pedersen 1995).

The oldest structures (D_r) are local recumbent isoclinal folds. They plunge S–SE with gently SE-dipping axial surfaces. During subsequent deformation (D_{s1}) a moderately SE-plunging penetrative *L-S* fabric was accompanied by formation of SE-dipping shear zones (Figs 5, 6e-d). Rotated garnet and staurolite crystals suggest movement of the hanging wall towards NE. Close asymmetric *Z* drag folds (F_{s2}) with SE-dipping axial surfaces and moderately S–SE plunging axes represent a late stage of the NE-directed shear movements (Figs 4, 6f). Drag folds (F_{s2}) developed at a high angle to the transport direction as a result of a minor unconformity between the lithologies and the shear plane. In response to progressive strain both axial surfaces and fold axes were re-oriented. Axial surfaces were rotated towards the shear plane and the F_{s2} fold axes were rotated within their axial planes into the transport direction as illustrated by the subparallel orientation of F_{s2} fold axes and the L_{s1} lineations (Fig. 6e–f). Overprinting of D_{s2} drag folds on the isoclinal F_r folds produced local hook-interference patterns (Thiessen & Havland 1986).

F_r and F_{s2} folds were weakly overprinted by gently SE-plunging F_{s3} folds, with upright axial surfaces and a wavelength of *c*. 100 metres. The general increase in dip of the foliation from the gneissic contact towards Torsukattak and an apparent repetition of some of the lithologies indicate imbricated piggyback thrust stacking (Pedersen 1995).

The area was cut by late, steep N–S and NW–SE striking conjugated brittle faults (D_u). Less than 250 m of horizontal sinistral displacement was recorded from the N–S faults; the NW–SE faults had dextral strike slips not exceeding 100 m.

Structural correlation between Oqaatsut and Naajaat Qaqqaat

Naajaat Qaqqaat and Oqaatsut have a common structural chronology: an early stage of folding being followed by ductile shearing and a late stage of brittle faulting. In spite of this, a straightforward structural correlation across Torsukattak cannot be established

Table 1. Major element compositions of quartz-biotite schists from Oqaatsut and Naajaat Qaqqaat

GGU no	354479 Oq	354320 Oq	354335 Oq	354397 NQ	348928 NQ	349122 NQ	349190 NQ	349196 NQ
SiO_2	66.88	67.04	68.54	68.30	65.95	67.07	66.42	64.93
TiO_2	0.39	0.46	0.45	0.43	0.49	0.55	0.56	0.59
Al_2O_3	15.82	16.35	15.60	15.20	16.41	16.08	15.21	15.65
Fe_2O_3	0.70	0.72	0.28	1.12	0.47	1.02	1.07	1.80
FeO	3.57	2.99	3.21	3.63	3.85	3.82	3.37	4.11
MnO	0.07	0.05	0.04	0.07	0.06	0.08	0.07	0.12
MgO	2.53	1.66	2.59	1.38	2.03	1.92	2.34	3.06
CaO	2.28	4.19	3.55	3.09	1.83	2.48	3.98	3.67
Na_2O	3.79	3.75	3.41	3.71	4.89	3.15	3.70	2.81
K_2O	2.37	1.65	0.69	1.77	2.41	2.18	1.74	1.98
P_2O_5	0.11	0.11	0.10	0.11	0.17	0.17	0.14	0.14
LOI	0.87	0.49	1.10	0.51	0.51	0.69	0.81	0.49
Total	99.36	99.46	99.55	99.32	99.07	99.21	99.40	99.34

Oq: Oqaatsut; samples are from the middle metasedimentary unit.

NQ: Naajaat Qaqqaat; all samples from the lower quartz-biotite schist unit.

Major elements (wt%) analysed by XRF on glass discs at the Geological Survey of Denmark and Greenland. Na_2O by AAS.

LOI: loss on ignition (1000°C).

because of marked differences in structural style and orientation (Pedersen 1995). The structures at Oqaatsut dip moderately E whereas at Naajaat Qaqqaat SE dips prevail (Fig. 6). At Naajaat Qaqqaat D_{s2} axial surfaces are closely related to SE-dipping shear planes, whereas on Oqaatsut D_t axial surfaces cut thrusts at a high angle, which led to folding of the D_s shear plane.

Geochemistry

When dealing with the chemistry of metamorphic rocks it is important to consider the issue of secondary mobilisation of elements, and care must be exercised with respect to interpretations based on geochemical data. Alteration and metamorphism most commonly affect concentrations of the following oxides and elements: SiO_2, Al_2O_3, CaO, MgO, K_2O, Na_2O, H_2O, CO_2, Rb, Sr, Ba, Th, U and the Fe^3/Fe^2 ratio, whereas TiO_2, P_2O_5, total Fe, Ni, Cr, V, Zr, Y, Nb, Ce, Ga, Sc and REE (Rare Earth Elements) tend to be less affected, and therefore more useful to evaluate original geochemical characteristics (Winchester & Floyd 1977; Condie 1981; Wilson 1989).

Low loss on ignition for the analysed samples (LOI generally < 2.0 for amphibolites and < 1.0 for metasediments; Tables 1, 2) suggests that secondary hydrothermal alteration may not have been very significant since these values correspond to the range of loss on ignition for fresh unaltered basic volcanic rocks (0.5–2.0%).

Metasediments

Major element analyses of metasedimentary schists from Oqaatsut and Naajaat Qaqqaat (Table 1) show that they probably were derived from (pelitic) greywackes (Rasmussen 1992). In geochemical discrimination diagrams (Fig. 8; Bathia 1983) the rocks plot in or close to the field of 'continental island arc' sediments (which includes greywackes deposited in a deep-sea environment within a back-arc region). Such a tectonic setting would be in agreement with the occurrence of the sediments in a mixed sequence with basic volcanic rocks.

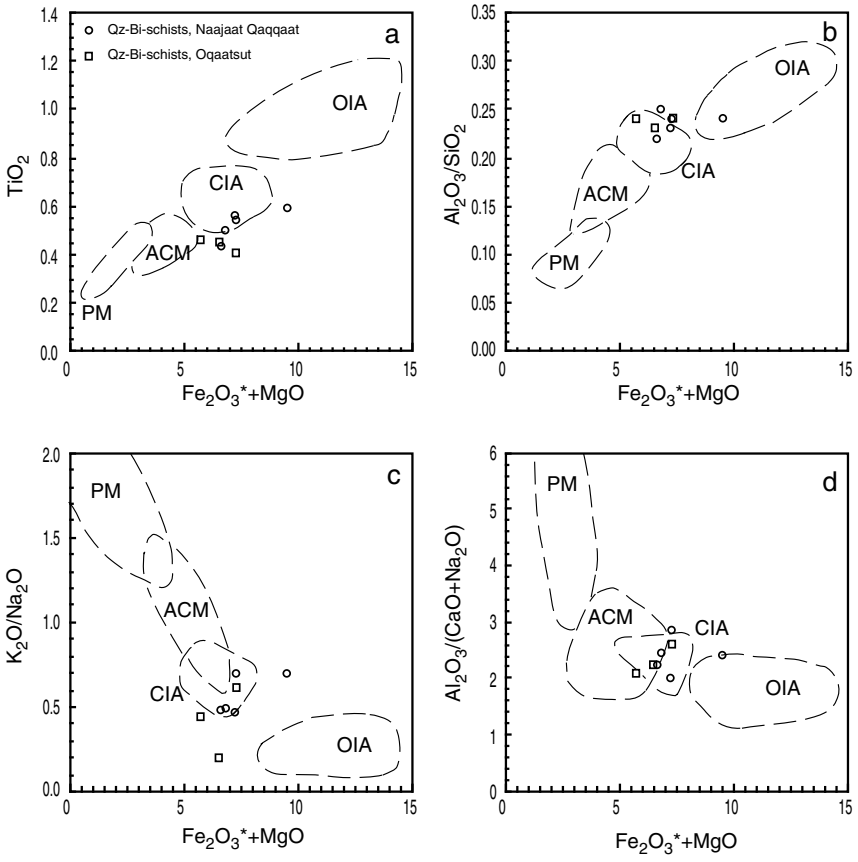

Fig. 8. Major element composition plots of quartz-biotite schists for tectonic setting discrimination (Bhatia 1983). TiO_2, Al_2O_3/SiO_2, K_2O/Na_2O and $Al_2O_3/(CaO+Na_2O)$ versus ($Fe_2O_3^{tot}$ + MgO). Data from Table 1 recalculated to 100% volatile free. Dashed lines mark the major fields of rocks representing various tectonic settings. OIA: oceanic island arc; CIA: continental island arc; ACM: active continental margin; PM: passive margin.

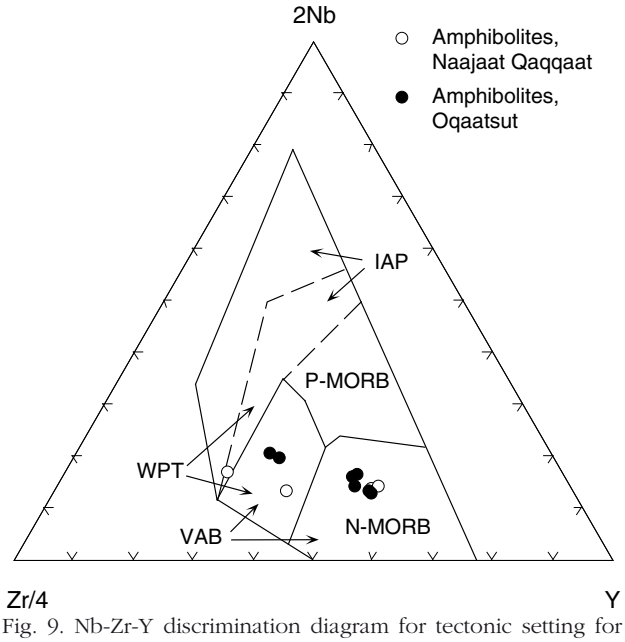

Fig. 9. Nb-Zr-Y discrimination diagram for tectonic setting for basaltic volcanic rocks (Meschede 1986). IAP: within-plate alkali basalts; WPT: within-plate tholeiites; VAB: volcanic arc basalts; P-MORB: plume-type MORB; N-MORB: normal MORB. The majority of samples from the two study areas fall in the N-MORB field, whereas four samples fall close to or within the volcanic arc basalt field.

Amphibolites

Representative major and trace element analyses of amphibolites and metagabbroic rocks from both study areas (Table 2) show that the rocks have compositions typical of Mg- and Fe-rich tholeiites. Discrimination between within-plate, volcanic arc, and N- and P-type MORB basalts can in some cases be accomplished in a Nb-Zr-Y diagram (Meschede 1986). In this diagram most samples plot in the N-MORB field, but four of the samples plot close to or within the volcanic arc basalt field (Fig. 9). In a MORB-normalised multi-element diagram (Fig. 10) the four samples which plot in the volcanic arc field in the Nb-Zr-Y diagram (Fig. 9) show strong LILE (Large Ion Lithophile Elements) enrichment and a distinct positive Ce anomaly (Fig. 10a); this is not seen for the rest of the samples, which show rather flat MORB-normalised patterns (Fig. 10b). It is interesting that some samples show these MORB characteristics, since Archaean ocean floor basalts with geochemical signatures similar to modern N-MORB are very scarce or rarely preserved in the Archaean geological record (Condie 1990, 1994).

The four samples that show strong enrichment in LILE are also characterised by high Th (1–11 ppm), compared to the low LILE (MORB-like) samples which

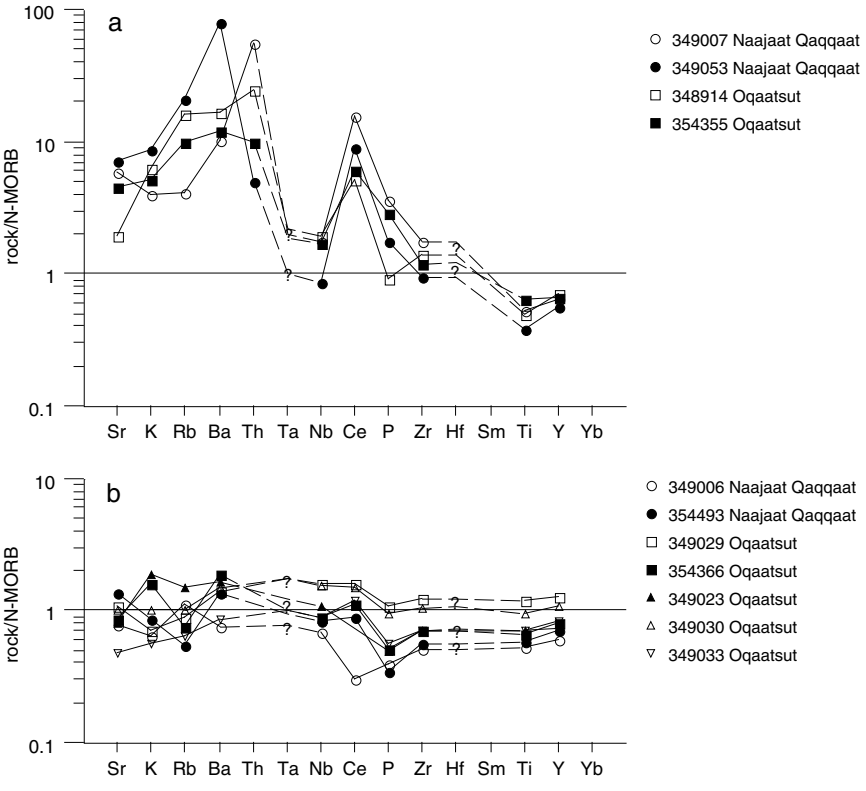

Fig. 10. N-MORB normalised variation diagrams (Pearce 1983) for selected amphibolites from Oqaatsut and Naajaat Qaqqaat. Levels of Ta and Hf (not analysed) are based on their accepted ratios in basaltic rocks with Nb and Zr, respectively (e.g. Jochum *et al.* 1986; Condie 1994). **a**: Samples of amphibolites showing strong LILE enrichment coupled with a strong positive Ce anomaly relative to Nb. **b**: Basic amphibolites showing a flat N-MORB normalised pattern suggesting an oceanic origin.

Table 2. Major and trace element compositions of amphibolites from Naajaat Qaqqaat and Oqaatsut

GGU no	349006	349007	349053	354493	348914	349023	349029	349030	349033	354355	354366
	NQ	NQ	NQ	NQ	Oq	Oq	Oq	Oq	Oq	Oq	Oq
SiO_2	48.51	53.80	42.43	46.99	55.33	48.24	50.45	49.72	48.00	54.26	50.49
TiO_2	0.78	0.78	0.56	0.86	0.74	1.04	1.76	1.40	1.01	0.96	0.98
Al_2O_3	14.95	14.60	18.05	15.19	15.03	15.48	13.49	15.73	14.43	17.57	14.47
Fe_2O_3	1.37	3.01	2.39	1.76	1.39	1.76	2.91	2.24	1.61	2.13	1.69
FeO	10.15	5.75	7.95	10.75	7.58	10.34	12.23	10.21	10.70	5.50	9.69
MnO	0.22	0.15	0.22	0.22	0.13	0.20	0.22	0.19	0.17	0.13	0.19
MgO	8.61	6.25	10.87	8.11	5.38	8.18	5.84	6.17	7.66	4.55	7.17
CaO	10.61	9.84	10.70	10.95	8.26	10.43	9.24	9.74	8.94	7.84	10.60
Na_2O	3.01	2.86	2.49	2.36	3.07	2.33	2.15	2.44	2.03	4.28	2.86
K_2O	0.09	0.58	1.28	0.13	0.94	0.28	0.10	0.15	0.08	0.76	0.23
P_2O_5	0.05	0.42	0.21	0.04	0.11	0.06	0.13	0.11	0.06	0.34	0.06
LOI	1.64	1.66	1.93	1.87	1.20	1.61	1.67	1.80	4.61	1.24	1.47
Total	99.99	99.70	99.08	99.23	99.16	99.95	100.19	99.90	99.30	99.55	99.90
Rb	2.2	8.1	42	1.1	32	3.0	1.8	2.0	1.3	20	1.5
Ba	15	204	1582	27	328	33	28	30	17	238	37
Pb	–	9	21	–	–	2	4	3	–	5	–
Sr	95	698	870	163	235	96	131	121	58	545	103
La	–	76	41	–	27	5	6	4	4	24	3
Ce	3	156	90	9	52	–	16	15	12	61	11
Nd	4	74	46	7	26	6	12	11	5	36	9
Y	18	19	17	21	21	22	38	32	25	20	24
Th	–	11	1	–	5	–	–	–	–	2	–
Zr	46	158	84	50	124	63	110	95	64	108	63
Nb	2.4	6.1	3.0	2.9	6.8	3.8	5.5	5.4	3.1	5.9	3.1
Zn	82	78	90	100	74	108	139	114	86	90	75
Cu	87	9	–	37	46	4	92	72	152	13	34
Co	73	69	81	74	56	76	69	68	64	42	77
Ni	158	263	222	159	89	131	56	94	103	68	70
Sc	47	27	38	47	30	45	56	41	50	21	53
V	241	175	141	280	199	248	407	320	308	117	294
Cr	343	437	488	334	27	605	114	161	337	91	170
Ga	16	18	14	18	18	18	19	19	17	22	19
Zr/Y	2.6	8.3	4.9	2.4	5.9	2.9	2.9	2.9	2.6	5.4	2.6
Ti/Zr	103.1	29.9	41.0	105.6	36.0	100.9	97.3	89.7	99.5	58.8	94.4
Ce/Nb	1.3	25.6	30.0	3.1	7.7		2.9	2.8	3.9	10.4	3.6
Nb/La		0.08	0.07		0.25	0.76	0.92	1.35	0.78	0.25	1.03
Ti/V	19.7	27.0	24.4	18.9	22.5	25.6	26.3	26.6	20.7	54.3	20.3
Zr/Nb	19.2	25.9	28.0	17.2	18.2	16.6	20.0	17.6	20.6	18.3	20.3

NQ: Najaat Qaqqaat.

Oq: Oqaatsut.

Major elements in wt% analysed by XRF on glass discs at the Survey (Na_2O by AAS); trace elements in ppm analysed by XRF on powder tablets at the Geological Institute, University of Copenhagen.

–: not detected.

LOI: loss on ignition (1000°C).

have Th below detection limits. The high LILE samples are also characterised by higher Ce/Nb (7.7–30.0), Zr/Y (5.4–8.3), Zr/Nb (18.3–28.0), Ti/V (22.5–54.3) and lower Nb/La (0.07–0.25), Ti/Zr (29.9–58.8) than the low LILE group, which has lower Ce/Nb (1.3–3.9), Zr/Y (2.4–3.0), Zr/Nb (17.2–20.6) and Ti/V (18.9–26.6) but higher Nb/La (0.8–1.4) and Ti/Zr (89.6–105.6). The significant difference in LILE concentrations and incompatible element ratios cannot plausibly be explained by secondary alteration and metamorphism, and must therefore be related to differences in original magma composition.

The apparent enrichment in LREE (Light REE) and Th relative to Nb for the high LILE group, relative to the low LILE samples, may reflect a subduction-zone component and may be the result either of crustal contamination or of production of magma in a mantle wedge that has been enriched in LILE and LREE during devolatilisation of a possible descending plate (Pearce 1983; Wilson 1989; Condie 1990, 1994). Condie (1990) has shown that more than 90% of the available analyses of Precambrian greenstone basalts are characterised by a subduction-zone component. Exceptions are basalts from Archaean successions where komatiites are an important component; these basalts exhibit rather flat MORB-normalised element distributions from Th to Yb (reflecting a depleted mantle source; Condie 1990) similar to the patterns seen for the present low-LILE samples. Furthermore, when plotted in an AFC-diagram (not shown; see Rasmussen 1992), the four samples showing LILE enrichment follow a trend characteristic of calc-alkaline rocks whereas the other samples follow a tholeiitic trend.

Discussion

The range of lithologies in the Naajaat Qaqqaat and Oqaatsut supracrustal associations – ultrabasic rocks, Mg and Fe-rich tholeiites, together with minor banded iron formation and rocks of detrital sedimentary origin – is typical for Archaean greenstone belts. Geochemical data suggest that parts of the succession were laid down in an ocean floor environment. Some of the metabasic rocks have geochemical signatures similar to modern MORB whereas others, with strong enrichment in LILE and different incompatible element ratios, have an island-arc signature.

Although strong deformation to a certain extent has obscured relationships between the two chemical types, it is certain that they are closely intercalated. Modern ocean floor basalts can be formed both at mid-ocean ridges and in back-arc spreading zones. Major element compositions of basalts from these two environments are very similar; however, volcanic rocks generated in a back-arc environment generally display a more evolved trace element character, due to the influence of a descending lithosphere slab, which is not present in basalts from mid-ocean ridges (Saunders & Tarney 1984; Wilson 1989). Trace element compositions of back-arc basalts are complex, especially in altered and metamorphosed rocks, but both MORB-like and arc-like characteristics have been observed (Wilson 1989). The presence of amphibolites with complex geochemical patterns showing both MORB and arc-like characters suggests to the authors that the amphibolites from the two study areas most likely were deposited in an environment similar to a modern back-arc setting. This suggestion is in agreement with interpretations of the depositional environment of supracrustal rocks on Arveprinsen Ejland (Nielsen 1992; Marshall & Schønwandt 1999, this volume) and in the Eqi area (Stendal *et al.* 1999, this volume; M. Marker, personal communication 1996), and show that the supracrustal rocks around Torsukattak may have been laid down in more or less the same environment as those in areas further south.

The presence of the polymict conglomerate at the base of the Naajaat Qaqqaat sequence suggests that at least in the initial stages of basin formation shallow water depths were predominant. The conglomerate could be related to initial rifting of an older craton and the creation of a continental margin basin. Ultramafic rocks at the base of the sequence at Naajaat Qaqqaat could represent products of initial magmatic activity. The close proximity of Archaean basement, the polymict conglomerate and MORB-like metabasalts may be due to strong telescoping of the sequence during later deformation. The presence of major thrust zones, which have been recognised during mapping (Figs 2, 3) would be consistent with this model.

The available observations do not allow determination with certainty whether these structures are of Proterozoic or Archaean age. However, Proterozoic ductile thrusting with sense of displacent towards W and NW has been described from the area SE of Ataa (Escher *et al.* 1999, this volume), from Nuussuaq (Garde & Steenfelt 1999, this volume) and from the Uummannaq district north of Nuussuaq (Pulvertaft 1986). Shear zones in the supracrustal rocks at Oqaatsut, which post-date emplacement of the Atâ tonalite, have the same sense of displacement and could therefore also be Proterozoic. Sediments of the early Proterozoic Anap nunâ

Group on Anap Nunaa and the island to the west (Fig. 1 inset) show open to tight folds with E–W axial trends (Kalsbeek 1992; Higgins & Soper 1999, this volume), and it is plausible that D_t folds on Oqaatsut with similar trends are also of Proterozoic age. Furthermore, the early Proterozoic lamprophyre dykes on Oqaatsut follow the D_t structural trend, which lends support to this contention.

Garde & Steenfelt (1999, this volume) correlate the supracrustal rocks at Naajaat Qaqqaat with similar occurrences at Saqqaq and Itilliarsuup Qaqqa on the northern side of Torsukattak, and the supracrustals of Oqaatsut with those of Arveprinsen Ejland and Eqi to the south (Fig. 1 inset). Although correlation across Torsukattak is problematic for several reasons (see Garde & Steenfelt 1999, this volume) the similarities in stratigraphy, chemistry and structural style strongly suggest to the authors that the supracrustal sequences at Oqaatsut and Naajaat Qaqqaat are very closely related.

Acknowledgements

We thank Adam Garde and Feiko Kalsbeek for critical reviews of earlier drafts of this manuscript, and our supervisors Paul Martin Holm and Lilian Skjernaa for their support during our studies.

References

Bhatia, M.R. 1983: Plate tectonics and geochemical composition of sandstones. Journal of Geology **91**, 611–627.

Condie, K.C. 1981: Archean greenstone belts, 434 pp. Amsterdam: Elsevier.

Condie, K.C. 1990: Geochemical characteristics of Precambrian basaltic greenstones. In: Hall, R.P. & Hughes, D.J. (eds): Early Precambrian basic magmatism, 40–55. London: Blackie.

Condie, K.C. 1994: Greenstones through time. In: Condie, K.C. (ed.): Archaean crustal evolution, 85–120. Amsterdam: Elsevier.

Escher, A. & Burri, M. 1967: Stratigraphy and structural development of Precambrian rocks in the area north-east of Disko Bugt, West Greenland. Rapport Grønlands Geologiske Undersøgelse **13**, 28 pp.

Escher, J.C., Ryan, M.J. & Marker, M. 1999: Early Proterozoic thrust tectonics east of Ataa Sund, north-east Disko Bugt, West Greenland. In: Kalsbeek, F. (ed.): Precambrian geology of the Disko Bugt region, West Greenland. Geology of Greenland Survey Bulletin **181**, 171–179 (this volume).

Garde, A.A. & Steenfelt, A. 1999: Precambrian geology of Nuussuaq and the area north-east of Disko Bugt, West Greenland. In: Kalsbeek, F. (ed.): Precambrian geology of the Disko Bugt region, West Greenland. Geology of Greenland Survey Bulletin **181**, 6–40 (this volume).

Higgins, A.K. & Soper, N.J. 1999: The Precambrian supracrustal rocks of Nunataq, north-east Disko Bugt, West Greenland. In: Kalsbeek, F. (ed.): Precambrian geology of the Disko Bugt region, West Greenland. Geology of Greenland Survey Bulletin **181**, 79–86 (this volume).

Jochum, K.P., Seufert, H.M., Spettel, B. & Palme, H. 1986: The solar-system abundances of Nb, Ta and Y, and the relative abundance of refractory lithophile elements in differentiated planetary bodies. Geochimica et Cosmochimica Acta **50**, 1173–1183.

Kalsbeek, F. 1992: Large-scale albitisation of siltstones on Qeqertakavsak island, northeast Disko Bugt, West Greenland. Chemical Geology **95**, 213–233.

Kalsbeek, F. & Skjernaa, L. 1999: The Archaean Atâ intrusive complex (Atâ tonalite), north-east Disko Bugt, West Greenland. In: Kalsbeek, F. (ed.): Precambrian geology of the Disko Bugt region, West Greenland. Geology of Greenland Survey Bulletin **181**, 103–112 (this volume).

Larsen, L.M. & Rex, D.C. 1992: A review of the 2500 Ma span of alkaline-ultramafic, potassic and carbonatitic magmatism in West Greenland. Lithos **28**, 367–402.

Marshall, B. & Schønwandt, H.K. 1999: An Archaean sill complex and associated supracrustal rocks on Arveprinsen Ejland, north-east Disko Bugt, West Greenland. In: Kalsbeek, F. (ed.): Precambrian geology of the Disko Bugt region, West Greenland. Geology of Greenland Survey Bulletin **181**, 87–102 (this volume).

Meschede, M. 1986: A method of discriminating between different types of mid-ocean ridge basalts and continental tholeiites with the Nb-Zr-Y diagram. Chemical Geology **56**, 207–218.

Nielsen, A.T. 1992: Geologi, geokemi og tektonisk setting for Andersen mineraliseringen: en vulkansk massiv sulfidforekomst i det arkæiske supracrustalbælte, Arveprinsen Ejland, Vestgrønland, 98 pp. Unpublished cand. scient. thesis, Københavns Universitet, Danmark.

Pearce, J.A. 1983: Role of the sub-continental lithosphere in magma genesis at active continental margins. In: Hawkesworth, C.J. & Norry, M.J. (eds): Continental basalts and mantle xenoliths, 230–250. Nantwich, UK: Shiva Publishing Ltd.

Pedersen, L.F. 1995: Beskrivelse og analyse af deformationsstrukturer på Naajaat Qaqqaat og Oqaatsut, Disko Bugt, Vestgrønland. Indikationer på partitionering af paleostressfeltet i forbindelse med strike-slip bevægelser i Torsukattak fjorden, 158 pp. Unpublished cand. scient. thesis, Københavns Universitet, Danmark.

Pulvertaft, T.C.R. 1986: The development of thin thrust sheets and basement-cover sandwiches in the southern part of the Rinkian belt, Umanak district, West Greenland. Rapport Grønlands Geologiske Undersøgelse **128**, 75–87.

Rasmussen, H. 1992: Petrography, geochemistry and combined K/Ar and $^{40}Ar/^{39}Ar$ mineral age investigations of Archaean amphibolitic, ultramafic and related supracrustal rocks from

Naujât qáqât and Oqaitsut, Disko Bugt, West Greenland, 149 pp. Unpublished cand. scient. thesis, University of Copenhagen, Denmark.

Rasmussen, H. & Holm, P.M. 1999: Proterozoic thermal activity in the Archaean basement of the Disko Bugt region and eastern Nuussuaq, West Greenland: evidence from K-Ar and ^{40}Ar-^{39}Ar mineral age investigations. In: Kalsbeek, F. (ed.): Precambrian geology of the Disko Bugt region, West Greenland. Geology of Greenland Survey Bulletin **181**, 55–64 (this volume).

Saunders, A.D. & Tarney, J. 1984: Geochemical characteristics of basaltic volcanism within back-arc basins. In: Kokelaar, B.P. & Howells, M.F. (eds): Marginal basin geology, volcanic and associated sedimentary and tectonic processes in modern and ancient marginal basins. Geological Society Special Publication (London) **16**, 59–76.

Stendal, H., Knudsen, C., Marker, M. & Thomassen, B. 1999: Gold mineralisation at Eqi, north-east Disko Bugt, West Greenland. In: Kalsbeek, F. (ed.): Precambrian geology of the Disko Bugt region, West Greenland. Geology of Greenland Survey Bulletin **181**, 129–140 (this volume).

Thiessen, R.L. & Havland, T. 1986: A technique for analysis of refold structures. Journal of Structural Geology **8**, 191–200.

Wilson, M. 1989: Igneous petrogenesis, a global tectonic approach. 466 pp. London: Unwin Hyman.

Winchester, J.A. & Floyd, P.A. 1977: Geochemical discrimination of different magma series and their differentiation products using immobile elements. Chemical Geology **20**, 325–343.

The Precambrian supracrustal rocks of Nunataq, north-east Disko Bugt, West Greenland

A.K. Higgins and N.J. Soper

Supracrustal rocks preserved in a major syncline in southern Nunataq comprise an Archaean and a Proterozoic sequence. An angular discordance between the two sequences is preserved locally. The basal development of the younger sequence shows similarities with that of the lower Proterozoic Mârmorilik Formation of the Uummannaq region north of Nuussuaq.

The major syncline–anticline fold pair of southern Nunataq is part of a regional system of E–W-trending Proterozoic folds which also deform the supracrustal rocks of Anap Nunaa, south of Nunataq. Recognition of a major syncline in southern Anap Nunaa, largely obliterated by albitisation, permits a simpler structural interpretation than previously suggested.

A.K.H., *Geological Survey of Denmark and Greenland, Thoravej 8, DK-2400 Copenhagen NV, Denmark.* E-mail: *akh@geus.dk.*
N.J.S., *Department of Earth Sciences, University of Sheffield, Sheffield S3 7HF, UK.*

Keywords: Archaean, Disko Bugt, Proterozoic, structure, supracrustal rocks, West Greenland

The area north-east of Ataa, north-east Disko Bugt (Fig. 1), contains a major Archaean supracrustal belt which is overlain by Proterozoic supracrustal rocks of significantly lower metamorphic grade (Kalsbeek *et al.* 1988; Kalsbeek 1989, 1990). In some areas the contact between the two supracrustal sequences is markedly discordant, but in other areas (as on Nunataq) the sequences are folded together and their contact relationships are not immediately obvious.

Nunataq is a semi-nunatak at the head of the fjord Torsukattak, surrounded on three sides by ice and with a 4 km fjord coast in the south-west (Fig. 1). Supracrustal rocks occur in two areas, a small area in the extreme north-east (not shown in Fig. 1), and a very large area in the southern part of the nunatak (Fig. 2). Between the two is an area of banded gneisses of presumed Archaean age. The obvious structure is an E–W-trending anticline deforming the southern area of supracrustal rocks, and cored by homogeneous granitic gneiss comparable with the Atâ tonalite (2800 Ma; Kalsbeek *et al.* 1988). This structure had been recognised in early photogeological studies by Escher & Burri (1967). Much less obvious is a complementary syncline within the same area of supracrustal rocks, whose existence was deduced by Adam A. Garde during reconnaissance work by helicopter in 1989, from the repetition of a thin unit of marble. The marble and low-grade metasediments occupying the core of the syncline were compared by A.A. Garde (personal communication 1991) to the well-known Proterozoic supracrustal sequences farther north in the Maarmorilik – Karrat Isfjord region (71°05′–71°35′N; Garde 1978; Henderson & Pulvertaft 1987). High-grade metasedimentary rocks surrounding the assumed Proterozoic rocks, and folded by both anticline and syncline, form part of the belt of Archaean supracrustal rocks exposed along Torsukattak, and extending southwards to Ataa and Eqi (Kalsbeek 1989, 1990; Garde & Steenfelt 1999, this volume).

One of the tasks assigned to the writers in the summer of 1991 was the geological mapping and structural interpretation of the supracrustal rocks of Nunataq with a view to testing Garde's hypothesis; Garde's basic interpretation was, in fact, verified. This paper gives a brief description of the rock units encountered dur-

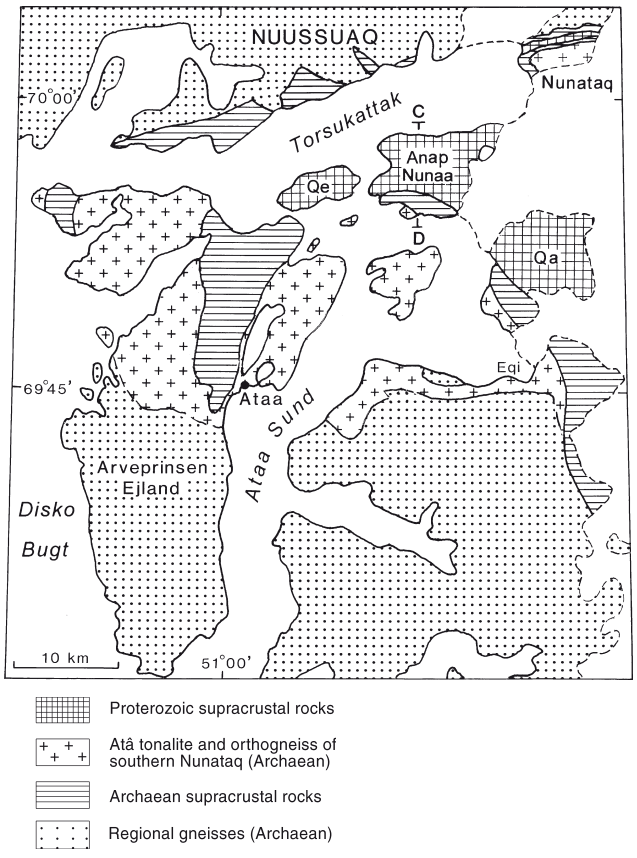

Fig. 1. Geological map of the Precambrian area north-east of Disko Bugt. Qe: Qeqertakassak; Qa: Qapiarfiit; C–D: Section line across Anap Nunaa, see Fig. 5. After Kalsbeek (1990).

ing the mapping, and a discussion of the structural setting.

Archaean gneisses

The gneisses on the north side of the main supracrustal zone are inhomogeneous, in places showing regular banding of light and dark layers with occasional thin amphibolite units. Foliation is generally E–W striking with southerly dips of 30–60°, approximately parallel to the contact with the supracrustal zone. At the contact sheets of aplite and muscovite granite invade both the gneisses and the supracrustal rocks in a zone up to 20 m wide. No basal conglomerate has been observed in the supracrustal rocks adjacent to the gneisses. In places a thin amphibolite is present at the contact. The supracrustal rocks are considered to be younger than the surrounding gneisses, but it is not clear whether the contact is depositional or tectonic.

The gneisses in the core of the major anticline in the southern part of Nunataq (Fig. 2) consist of very homogeneous grey-white orthogneiss. A few conformable leucocratic veins are present, and locally there are late cross-cutting quartz veins. Foliation in the gneiss is parallel to the contact with the supracrustal rocks, and pre-dates the main folding as it is folded by the main anticline; in two traverses across the main structure the turnover of the anticline was located by a narrow zone of shallow foliation orientations. The supracrustal unit next to the orthogneiss is an amphibolite which, as described below, can be traced right round the anticline with no discordance at map scale. The contact is sheeted, with concordant granitic veins present in a zone a few metres wide in the amphibolite. This is taken to indicate an intrusive relationship of the orthogneiss protolith into the Archaean amphibolite.

The orthogneiss of southern Nunataq has a general resemblance to the Atâ tonalite, but lacks the vast number of cross-cutting veins and dykelets so conspicuous around Ataa (Kalsbeek *et al.* 1988). However, north-west of Ataa the tonalite forms agmatites with amphibolitic supracrustal rocks interpreted as an intrusive relationship, as in the case for the orthogneiss of Nunataq. As the Atâ tonalite has yielded an isotopic age of 2800 Ma (Kalsbeek *et al.* 1988), it is likely that the very similar orthogneiss of southern Nunataq is the same age and that the amphibolitic supracrustal rocks veined by the orthogneiss are also Archaean.

The boundary between the inhomogeneous banded gneisses of northern Nunataq and the orthogneiss (tonalite) of southern Nunataq is presumably hidden beneath the major syncline of supracrustal rocks. This boundary may trend ENE–WSW along Torsukattak; tonalites are not recorded north of the fjord (Fig. 1).

Archaean supracrustal rocks

Supracrustal rocks occur in two main strips, respectively north and south of the assumed Proterozoic supracrustals occupying the core of the main syncline (Fig. 2). It is likely that the rock units in the two strips are at least partly equivalent, although one prominent component of the southern sequence (amphibolite) is poorly represented in the northern sequence. In the extreme north-east of Nunataq a small area of amphibolite facies supracrustal rocks, mainly hornblende-rich psammites and semipelites with some amphibolite and locally massive pyrite mineralisation, is probably also Archaean in age.

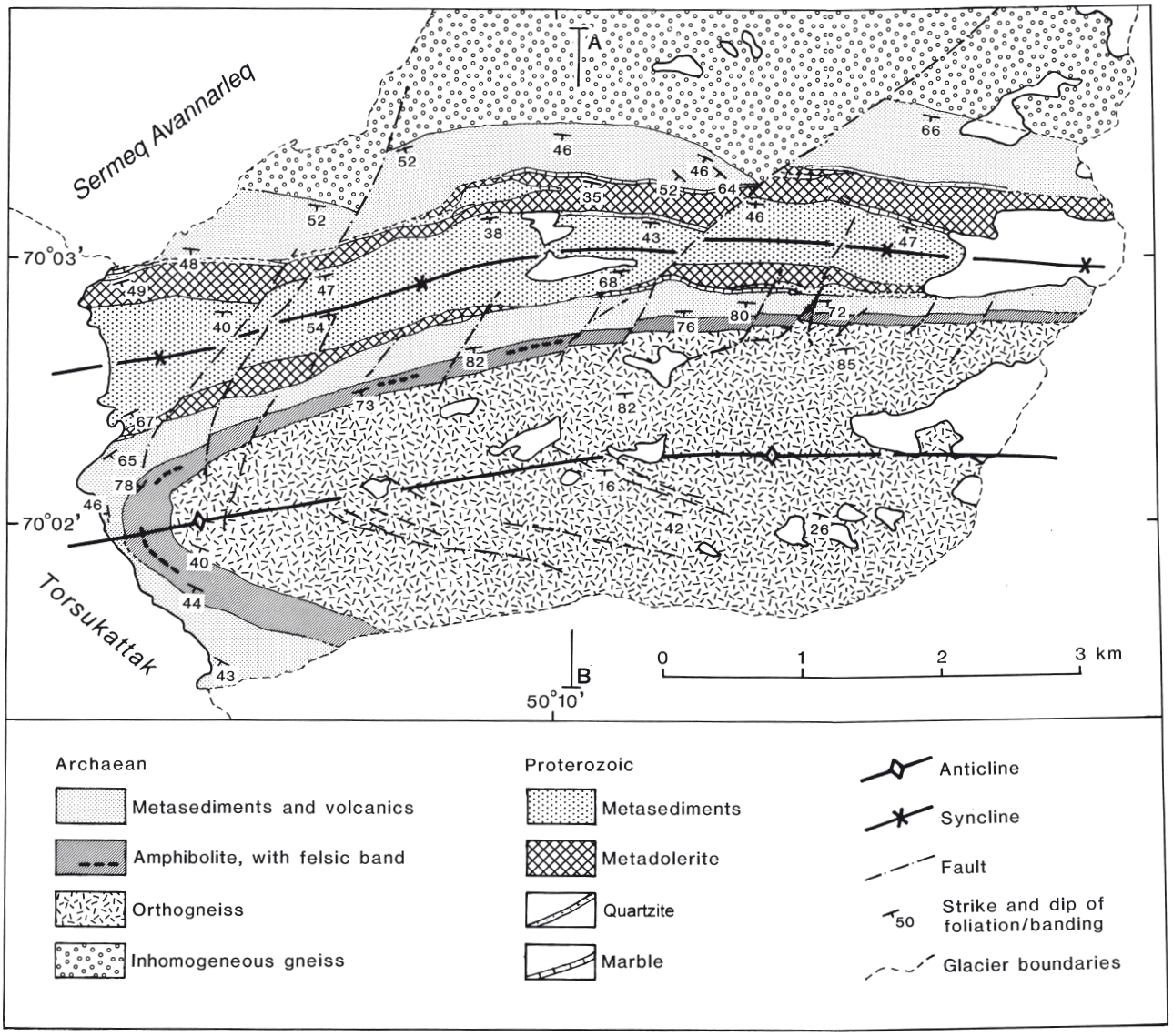

Fig. 2. Geological map of southern Nunataq. A–B: section line, see Fig. 3.

The southern sequence in the main supracrustal outcrop (Fig. 2) comprises two main mappable units, the amphibolite unit which lies next to the orthogneiss, and a structurally higher unit of mixed metasediments and metavolcanics. The two units can be traced for over 10 km along the north limb and around the nose of the main anticline. The amphibolite is strongly foliated, platy to schistose garnet amphibolite. It has a constant thickness of 200–300 m, reaching perhaps 500 m around the nose of the anticline. About 100–150 m from the top of the amphibolite occurs a thin but very persistent light coloured felsic band 1–2 m thick, which may be an acid volcanic rock. It is not known whether the protolith of the amphibolite was intrusive or extrusive, but both basic and acid metavolcanic rocks are reported in the Archaean supracrustal belts in nearby areas.

The overlying unit includes rocks described in the field as brownish weathering garnet-mica schist, greenish biotite psammite and undifferentiated greenstone and metasediments. At several localities, notably near the coast north-west of the main anticline, static recrystallisation of actinolitic amphibole was noted, often selectively developed in layers. It appears to post-date the Archaean foliation, but pre-dates Proterozoic crenulation associated with the main antiform.

The northern sequence, along the north side of the main syncline, is disrupted by two major faults with

marked sinistral displacements of 1–2 km. Amphibolite is limited to a few thin discontinuous bands within this unit, which has been mapped as an undivided sequence of metasedimentary and metavolcanic rocks. Field descriptions of rock types encountered include: platy quartzite, garnetiferous semipelite, garnet-muscovite-chlorite schist, veined greenstone and amphibole-rich schist. Random actinolitic amphibole is sporadically developed on bedding planes.

Proterozoic supracrustal rocks

The presumed Proterozoic supracrustal sequence is found only in the core of the main synclinal fold on Nunataq, and is bounded on both sides by higher grade supracrustal rocks of presumed Archaean age (Fig. 2). The contact between the two sequences on the south flank of the syncline is conformable. However, on the north flank of the syncline there is a marked angular discordance at two localities. The most prominent of these occurs on the west side of the eastern of two major NE–SW-trending faults, where there is a difference in strike of up to 40° between the two sequences. These two faults displace both supracrustal sequences in a sinistral sense, but the principal displacement of 1–2 km seems to affect only the Archaean rocks; reactivation on the faults subsequent to deposition and folding of the Proterozoic supracrustal rocks amounts only to a few hundred metres. These differential displacements are reflected in the present variable outcrop width of the northern Archaean supracrustal sequence.

Four lithological mapping units are recognised within the Proterozoic sequence: marble, quartzite, metadolerite (amphibolite), and an undifferentiated metasedimentary unit dominated by psammitic and semipelitic rocks.

The marble unit forms a conspicuous and persistent marker at the base of the Proterozoic sequence on both sides of the syncline. Even when not exposed its presence is suggested by a vegetation-covered depression. The marble is best exposed on the northern flank of the syncline, where thicknesses of 20–25 m were recorded locally. It varies in colour from grey to creamy white. Minor mineralisation has been noted in siliceous bands within the marble, and at contacts with the massive metadolerite body. The marble unit on the south limb of the syncline is less continuously exposed, and usually (when seen) only 2–5 m thick.

Quartzitic rocks are often associated with the marble, notably the unit on the north flank of the syncline where a conspicuous 3–4 m wide white quartzite bounded by rusty psammites overlies the marble for a distance of several kilometres (sometimes split up by intrusion of the metadolerite). Locally a muscovite-quartz psammite underlies the marble unit, and it is this association which shows resemblance to the lower divisions of the Proterozoic sequence in the Maarmorilik area (71°08′N; Garde 1978; A.A. Garde, personal communication 1991).

A massive unit of amphibolitic metadolerite occurs on both limbs of the synform; its variable thickness and the manner in which it sometimes splits up the marble and quartzite units strongly suggests it was emplaced as a sill. It is very homogeneous, and at the margin grades from very fine to coarse grain size over about 5 m. It is weakly foliated, and notably lacks the platy texture developed in the higher grade Archaean amphibolite.

The main part of the Proterozoic sequence comprises psammitic and semipelitic rock types, which occupy the core of the syncline. A sequence about 390 m thick was measured in the well-exposed western coastal outcrops. This is the only area where way-up criteria (sedimentary structures, bedding-cleavage relationships and vergence of minor folds) are preserved and the main structure can be demonstrated to be a syncline. The dominant rock types are micaceous and non-micaceous pale coloured psammites in beds from a few centimetres to 2.7 m in thickness, interbedded with subordinate dark coloured semipelite and psammite. Lenses and thin layers of spotted calc-silicate rocks are present.

The Proterozoic supracrustal rocks of Nunataq, Anap Nunaa and adjacent areas are ascribed to the Anap nunâ Group (Garde 1994; Garde & Steenfelt 1999, this volume). Low metamorphic siltstones collected on the island of Qeqertakassak (Fig. 1) have yielded a Rb-Sr whole-rock isochron age of 1760 ± 180 Ma, interpreted as the time of closure of the Rb-Sr isotope systems after metamorphism (Kalsbeek *et al.* 1988).

Structure

There is a marked contrast in strain state between the Archaean and Proterozoic supracrustal rock groups preserved in southern Nunataq. Although in many places both appear to contain only one dominant foliation, in clean coastal exposures bedding and cleavage or schistosity can often be distinguished in the

Fig. 3. N–S cross-section of the syncline-anticline fold pair in southern Nunataq; section line is shown on Fig. 2. For key to rock types see Fig. 2.

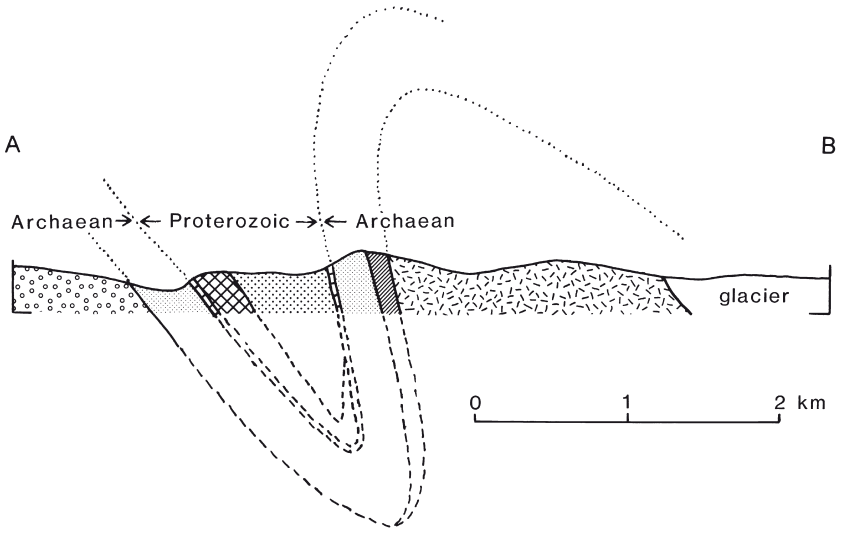

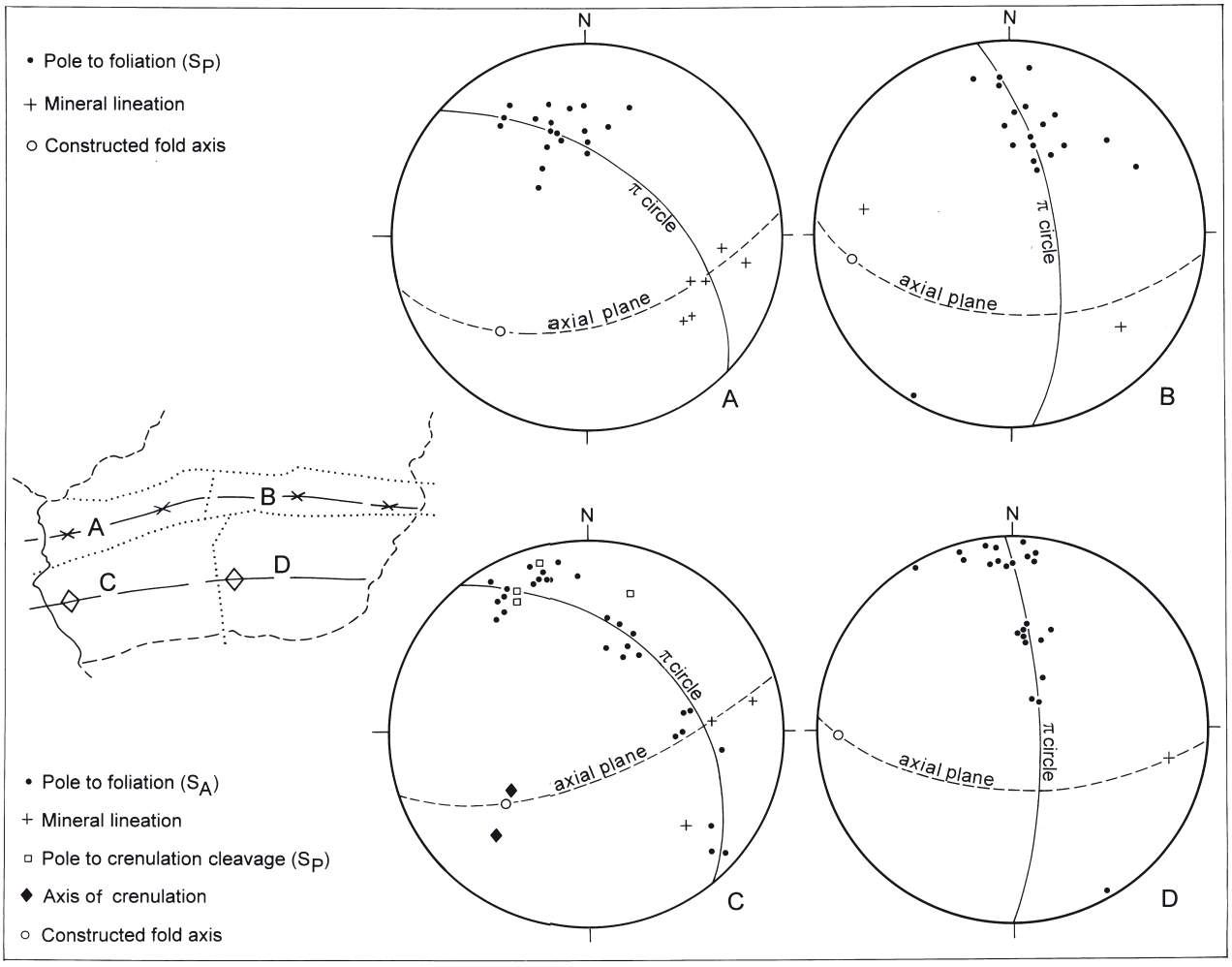

Fig. 4. Lower hemisphere equal area projections of structural data. **A** & **B**: Proterozoic supracrustal areas in syncline. **C** & **D**: Archaean supracrustal and orthogneiss areas in anticline.

Proterozoic metasediments, while the Archaean rocks have a single pervasive foliation which is both a schistosity and compositional layering; the original bedding has evidently been completely transposed. As mentioned above, the contrast in fabric development in the older amphibolites and younger metadolerites is particularly marked. Only in the axial region of the main anticline can a younger, presumably Proterozoic fabric (a crenulation cleavage), be seen to deform the earlier foliation. The latter must be of Archaean age if the correlation of the orthogneiss with the Atâ tonalite is correct, because it affects both the gneiss and its metasedimentary envelope. This foliation is parallel to the contact and is folded around the anticline. We would therefore assign the earlier foliation to the Archaean (S_A), the later to the Proterozoic (S_P).

A difference in metamorphic grade is less obvious in the field, although micaceous lithologies within the older sequence tend to be more coarsely recrystallised, with a greater development of garnet. A phase of static amphibole crystallisation has been recorded locally in the Archaean supracrustals but not in the Proterozoic rocks. It post-dates S_A but is deformed by S_P in the axial region of the main anticline.

The two main folds comprise an anticline-syncline pair and are presumably both of Proterozoic age; the syncline contains upward younging Proterozoic rocks in its core (Fig. 3). The folds trend approximately E–W, and are overturned northwards such that both limbs of the structures dip southwards. The mutual limb of the fold pair dips southwards generally at 70–80°, whereas the northern limb of the syncline dips south at angles for the most part between 30° and 45°; the south limb of the anticline is incompletely exposed, much of it being hidden beneath a glacier.

Planar foliations have been measured throughout the supracrustal area (Fig. 4). In the Proterozoic rocks (Fig. 4 A,B) this foliation is likely to have been a mixture of original bedding and the Proterozoic (S_P) cleavage as, due to the rarity of original sedimentary structures, these two elements could only be distinguished locally in the well-exposed coastal outcrops.

Plots of planar orientations in the Archaean supracrustal rocks (Fig. 4 C,D) show two maxima corresponding to the steep and shallow limbs of the fold pair, but the planar features may be in part Archaean and in part Proterozoic in origin. It is only in the nose region of the anticline that the early Archaean foliation (S_A) can be clearly distinguished from the superimposed Proterozoic crenulation folds and associated cleavage.

Foliation in the orthogneisses forming the core of the anticline is clearly Archaean; it appears to be conformable to the envelope of supracrustal rocks and parallels that boundary as it is deformed in the nose of the anticline. Proterozoic crenulation fabrics are found superimposed on the foliation only rarely.

Mineral lineations in both the Archaean and Proterozoic sediments plunge generally into the SE quadrant at angles of 10–30°, and may be interpreted as cleavage-bedding intersections. Axes of the Proterozoic crenulation folds, congruous with the nose of the main anticline, plunge SW at about 40°. Few minor or mesoscopic Proterozoic folds have been recorded in the core of the syncline. Inland the approximate trace of the axial surface of the main syncline can be determined from the change in dip orientation of the two fold limbs. At the coast the occasional preservation of original way up criteria (cross-bedding) and of bedding-cleavage intersections demonstrate clearly that a major fold is present, although the fold core coincides with an area of non-exposure.

The Archaean supracrustal rocks were displaced by two major faults prior to peneplanation and deposition of the Proterozoic sequence. Subsequent to deformation of the Proterozoic sequence the two faults were reactivated, and together with numerous parallel faults show minor sinistral displacements of tens to a few hundred metres (Fig. 2).

Regional Proterozoic deformation

Proterozoic supracrustal rocks consisting mainly of a very thick sequence of shallow water arenites are well exposed south of the fjord Torsukattak in a broad belt extending from Qeqertakassak through Anap Nunaa to Qapiarfiit (Fig. 1).

There is a general northward increase in the intensity of Proterozoic strain, from Qapiarfiit and the small nunatak east of there where the Proterozoic rocks are in general weakly deformed, through Qeqertakassak (Kalsbeek 1992) and Anap Nunaa (Andersen 1991) where there is upright E–W folding with cleavage, to Nunataq where the folds verge north and there is strong fabric development as described above. There is a zone of albitisation running through Qeqertakassak and Anap Nunaa which when most intense obliterates bedding and cleavage, rendering structural interpretation difficult. The writers visited Anap Nunaa (Fig. 1) in an attempt to clarify the structural interpretation.

On Anap Nunaa it is generally possible to distin-

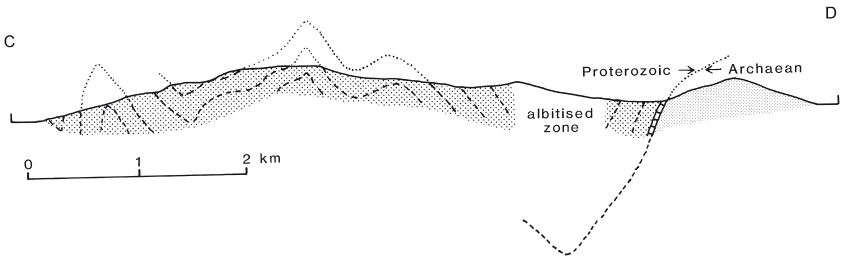

Fig. 5. N–S cross-section through central Anap Nunaa (Fig. 1) showing structure interpretation and position of albitised zone. See Fig. 2 for key to rock types.

guish bedding and cleavage, except where albitisation is pronounced, and their relationships taken in conjunction with a limited number of sedimentary way-up observations enabled a coherent structural interpretation to be made (Fig. 5). A significant element in this interpretation is a major syncline whose presence was inferred from adequate younging evidence on the limbs, although its axial region is obliterated by a zone of intense albitisation; the total lack of foliation in the albitised region suggests the process post-dated deformation. The folds are upright and the cleavage strikes E–W and is subvertical. In the extreme north-east of Anap Nunaa, vertical common limbs of fold pairs are encountered, an indication of the northerly vergence of the Proterozoic folds which is more pronounced on Nunataq (Fig. 3).

The structural interpretation of Figure 5 differs from that of Andersen (1991) in some respects. He recognised additional major folds in areas not visited by the writers, but not the major syncline in the albitised zone of central south Anap Nunaa. As a result, he interpreted a synform in western Anap Nunaa as an overturned nappe-like anticline with a major inverted limb occupying the central part of the area. From a few unambiguous younging observations the writers were able to establish that the synform is in fact a syncline, and to develop the simpler structural interpretation without resource to the multiple deformation phases inferred by Andersen. However, when traversing western Anap Nunaa the writers did encounter a problematic area with divergent foliation orientations in which way-up criteria and cleavage-bedding intersections were ambiguous. On Qeqertakassak, due west of Anap Nunaa, a curious overturned anticline, enveloped by albitised rocks, has been mapped by Kalsbeek (1992).

Two lines of evidence suggest that the Proterozoic deformation involved dextral transpression. In the two areas examined in some detail, north-east Anap Nunaa and coastal exposures of the main syncline on Nunataq, the cleavage strikes a few degrees anticlockwise to bedding on steep overturned fold limbs. This indicates anticlockwise transection of the folds by the cleavage, and if the two are related by a 'flattened buckle' mechanism, that the deformation took place by a dextrally transpressive mechanism (Soper 1986).

The second line of evidence is provided by deformed trough cross-bedding in vertical beds beautifully exposed in glacially smoothed coastal exposures in north-

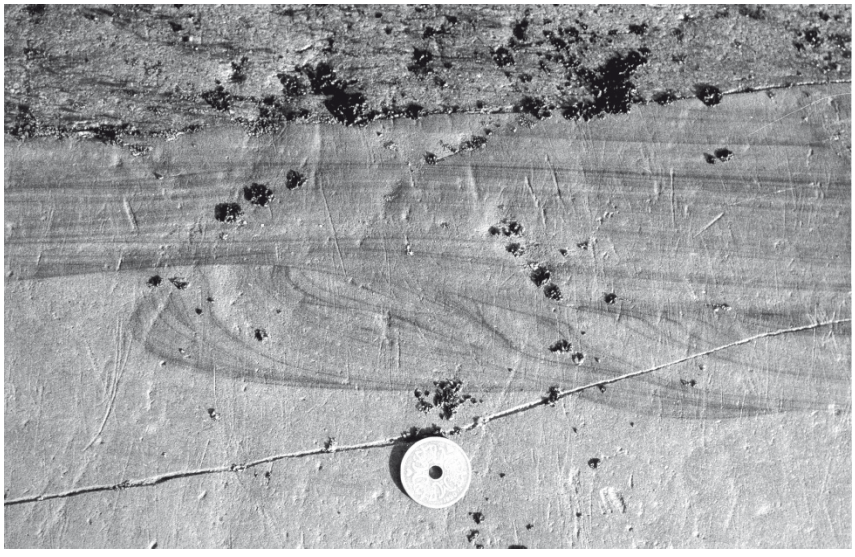

Fig. 6. Deformed trough cross-bedding in north-east Anap Nunaa.

east Anap Nunaa (Fig. 6). The manner in which the troughs are consistently deformed into 'Z' shapes requires a component of top-to-right shear strain, that is, dextral.

Summary of geological events

The following minimum sequence of Precambrian events can be inferred from the evidence on Nunataq and Anap Nunaa:

Archaean

1. Development of the banded gneiss complex
2. Erosion to mid-crustal levels
3. Deposition of sediments and volcanics
4. Emplacement of dolerite sills
5. Emplacement of the orthogneiss protolith (? 2.8 Ga)
6. Metamorphism and deformation to produce the S_A fabric
7. Static metamorphism

Proterozoic

8. Erosion; faulting on lines which now trend NE–SW
9. Subsidence and deposition of the Anap nunâ Group
10. Emplacement of the younger sills
11. Folding and cleavage development (S_P) under dextral transpression
12. Albitisation
13. Faulting, including sinistral reactivation of earlier faults

References

Andersen, J. 1991: Tidlig proterozoisk rift-relateret sedimentation og post-sedimentær deformation. Anap Nunâ, Diskobugten, Vestgrønland. 73 pp. Unpublished cand. scient. thesis, Københavns Universitet, Danmark.

Escher, A. & Burri, M. 1967: Stratigraphy and structural development of the Precambrian rocks in the area north-east of Disko Bugt, West Greenland. Rapport Grønlands Geologiske Undersøgelse **13**, 28 pp.

Garde, A.A. 1978: The Lower Proterozoic Marmorilik Formation, east of Mârmorilik, West Greenland. Meddelelser om Grønland **200**(3), 71 pp.

Garde, A.A. 1994: Precambrian geology between Qarajaq Isfjord and Jakobshavn Isfjord, West Greenland, 1:250 000. Copenhagen: Geological Survey of Greenland.

Garde, A.A. & Steenfelt, A. 1999: Precambrian geology of Nuussuaq and the area north-east of Disko Bugt. In: Kalsbeek, F. (ed.): Precambrian geology of the Disko Bugt region, West Greenland. Geology of Greenland Survey Bulletin **181**, 6–40 (this volume).

Henderson, G. & Pulvertaft, T.C.R. 1987: Lithostratigraphy and structure of a Lower Proterozoic dome and nappe complex. Geological map of Greenland, 1:100 000, Mârmorilik 71 V.2 Syd, Nûgâtsiaq 71 V.2 Nord and Pangnertôq 72 V.2 Syd. Descriptive text, 72 pp. Copenhagen: Geological Survey of Greenland.

Kalsbeek, F. 1989: GGU's expedition in the Disko Bugt area, 1988. Rapport Grønlands Geologiske Undersøgelse **145**, 14–16.

Kalsbeek, F. 1990: Disko Bugt Project, central West Greenland. Rapport Grønlands Geologiske Undersøgelse **148**, 21–24.

Kalsbeek, F. 1992: Large-scale albitisation of siltstones on Qeqertakavsak island, Northeast Disko Bugt, West Greenland. Chemical Geology **95**, 213–233.

Kalsbeek, F., Taylor, P.N. & Pidgeon, R.T. 1988: Unreworked Archaean basement and Proterozoic supracrustal rocks from northeastern Disko Bugt, West Greenland: implications for the nature of Proterozoic mobile belts in Greenland. Canadian Journal of Earth Sciences **25**, 773–782.

Soper, N.J. 1986: Geometry of transecting, anastomosing solution cleavage in transpression zones. Journal of Structural Geology **8**, 937–940.

An Archaean sill complex and associated supracrustal rocks, Arveprinsen Ejland, north-east Disko Bugt, West Greenland

Brian Marshall and Hans Kristian Schønwandt

Archaean supracrustal rocks on Arveprinsen Ejland comprise mafic and felsic volcanic rocks overlain by an epiclastic sedimentary sequence invaded by a mafic to ultramafic sill complex. The latter has a strike-length of 7500 m and a cumulative preserved thickness of 2000–2500 m and amounts to nearly 50% of the exposed thickness of the supracrustal rocks. Chilled and locally peperitic contacts are developed between component sills and the inter-sill metasedimentary septa. The sub-alkalic sill complex and mafic lavas and tuffs are high-magnesium tholeiites and basaltic komatiites whereas the felsic rocks are calc-alkaline rhyolites and dacites. Chondrite- and MORB-normalised spider diagrams affirm the close similarity of the mafic volcanic rocks and the sill complex; they are also consistent with a tholeiitic or komatiitic affinity. Tectonomagmatic discrimination plots suggest an ensialic arc-related setting for the sill complex and the mafic and felsic volcanic rocks.

The sill complex was progressively emplaced, as an upward-younging sequence of component sills, beneath 2 to 2.5 km of seawater and substantially less than 0.5 km of wet sediment. Sills formed when the magmatic pressure exceeded the *effective* overburden pressure of the sediment plus the vertical tensile strength (T_o) of the host materials. Intrusion was probably promoted by the drop in T_o at the interface between contact-lithified and poorly lithified strata. The thickness of the sill complex was accommodated by dilational lifting plus the capacity of an intrusion to create space through expulsion of water from wet sediment.

B.M., *Department of Applied Geology, University of Technology, Sydney, P. O. Box 123 Broadway, N.S.W. 2007, Australia*. E-mail: *Brian.Marshall@uts.edu.au*.
H.K.S., *Geological Survey of Denmark and Greenland, Thoravej 8, DK-2400 Copenhagen NV, Denmark*. Present address: *Government of Greenland, Bureau of Minerals and Petroleum, DK-3900 Nuuk, Greenland*.

Keywords: Archaean, Disko Bugt, geochemistry, sill complex, subvolcanic rocks, supracrustal rocks, West Greenland

The rocks of Arveprinsen Ejland, Disko Bugt, central West Greenland (Fig. 1) were divided by Escher & Burri (1967) into an infrastructure of 'Jacobshavn gneiss' and 'Atâ granite' (Atâ Tonalite on the geological map of Garde 1994), and a suprastructure termed the 'Anap nunâ Group'. Kalsbeek *et al.* (1988) demonstrated that, at least for north-eastern Arveprinsen Ejland, the supracrustal rocks are Archaean and distinct from the Proterozoic supracrustal sequence that occurs east of Arveprinsen Ejland.

The Archaean supracrustal rocks of north-eastern Arveprinsen Ejland (henceforth called the Arveprinsen supracrustals) comprise a metamorphosed sequence of massive to pillowed basaltic flows and mafic tuffs, with subordinate felsic volcanic rocks, overlain by and gradational into an epiclastic sedimentary sequence, also with felsic volcanic rocks. Metamorphosed and deformed mafic sills (herein termed a sill complex) totally dominate the upper portion of the supracrustals. Two distinctly younger sets of mafic dykes cut the entire sequence. The older set is inter-kinematic and the younger is post-kinematic with respect to the

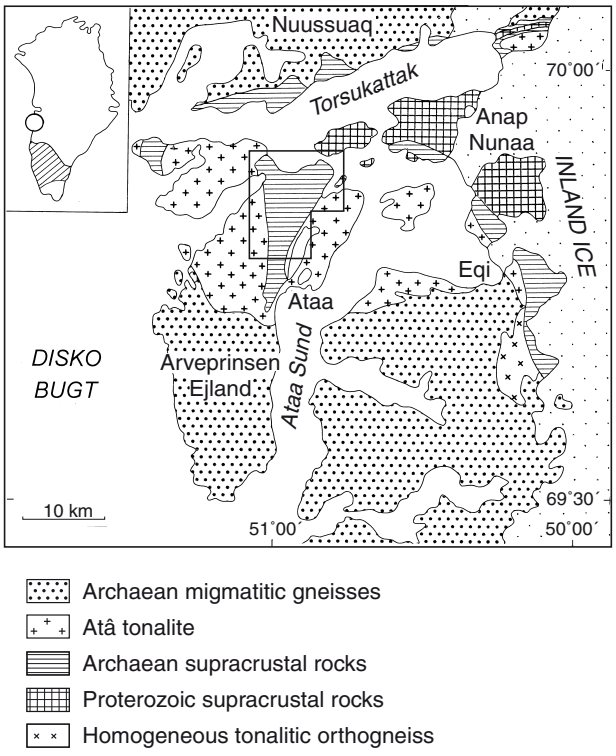

Fig. 1. Simplified geological map of the Ataa Sund region (after Kalsbeek 1990) with the investigated area outlined. The inset shows the location (circled) in central West Greenland, north of the Archaean craton (oblique ruling).

polyphase deformation history, which comprises at least four folding events (Marshall & Schønwandt 1990).

The supracrustal rocks have undergone at least one phase (but probably two phases) of regional metamorphism. The resulting greenschist and amphibolite facies assemblages define a south-closing form within the Atâ granite (Knudsen *et al.* 1988). The metamorphic facies boundary is approximately parallel to primary layering on the west of the structure, but it is discordant on the east side where the contact truncates the layering.

Sill complexes are known from other Archaean metavolcanic-metasedimentary greenstone belts (e.g. Naldrett & Mason 1968; Jaques 1976; Raudsepp & Ayres 1982). They are typically emplaced at a high crustal level, provide samples of magmas which probably were the source of the spatially associated basaltic lavas, and may be termed subvolcanic (Raudsepp & Ayres 1982). Similar associations of mafic plutonic rocks and mafic volcanites exist in the Proterozoic rocks of southern Finland (Härme 1980; Suominen 1988).

The aims of this paper are to present field observations, petrography and chemical data relating to parts of the sill complex on Arveprinsen Ejland, in order to discuss its emplacement mechanism, and its petrogenetic and tectonic significance.

Field observations

The Arveprinsen supracrustals, including the sill complex, occupy a north- to north-east-trending D_1 regional fold, which is flexed about a WNW-trending D_2 structure (Fig. 2). Because the D_1 fold youngs into its core (Fig. 2) and has a moderate to very steep southward plunge, it is a non-cylindrical antiformal syncline (the Arveprinsen antiform). A more substantial account of the regional and detailed structure is given by Marshall & Schønwandt (1990).

Stratigraphy

The metavolcanic-metasedimentary preserved succession (excluding the sill complex) consists of a lower unit comprising 2500–3000 m of mafic flows and tuffs, and an upper unit variously comprising 500–750 m of feldspathic, siliciclastic and pelitic epiclastic metasedimentary rocks, with developments of disseminated and massive base metal sulphide (Fig. 2). The lower contact is against the intrusive Atâ tonalite and the upper limit is the coastline of Arveprinsen Ejland, so the section is incomplete. In feldspathic (volcaniclastic?) units, the younging directions are based on scour-and-fill structures, cross lamination and rare grading. Where the metasedimentary rocks consist of quartz-rich sandstone and siltstone with variable amounts of pelitic material, younging may be obtained from bottom structures, grading and cross lamination that collectively comprise incomplete Bouma units. The sill complex, as delineated (Fig. 2), is essentially restricted to the metasedimentary part of the succession. It effectively swells the total thickness of the supracrustal section to between 5000 and 6000 m, and constitutes nearly 50% of the stratigraphic column (Fig. 2). In addition to the sill complex, a few thin (< 50 m) sills occur within the metavolcanic portion of the succession.

The boundary between the sill complex and the supracrustals (Fig. 2) has a superficially discordant appearance which masks the dilational nature of the sills. This could be due to: (1) an inability to show, at this scale, the true extent of the interfingering of metasedimentary septa (terminology after Raudsepp & Ayres

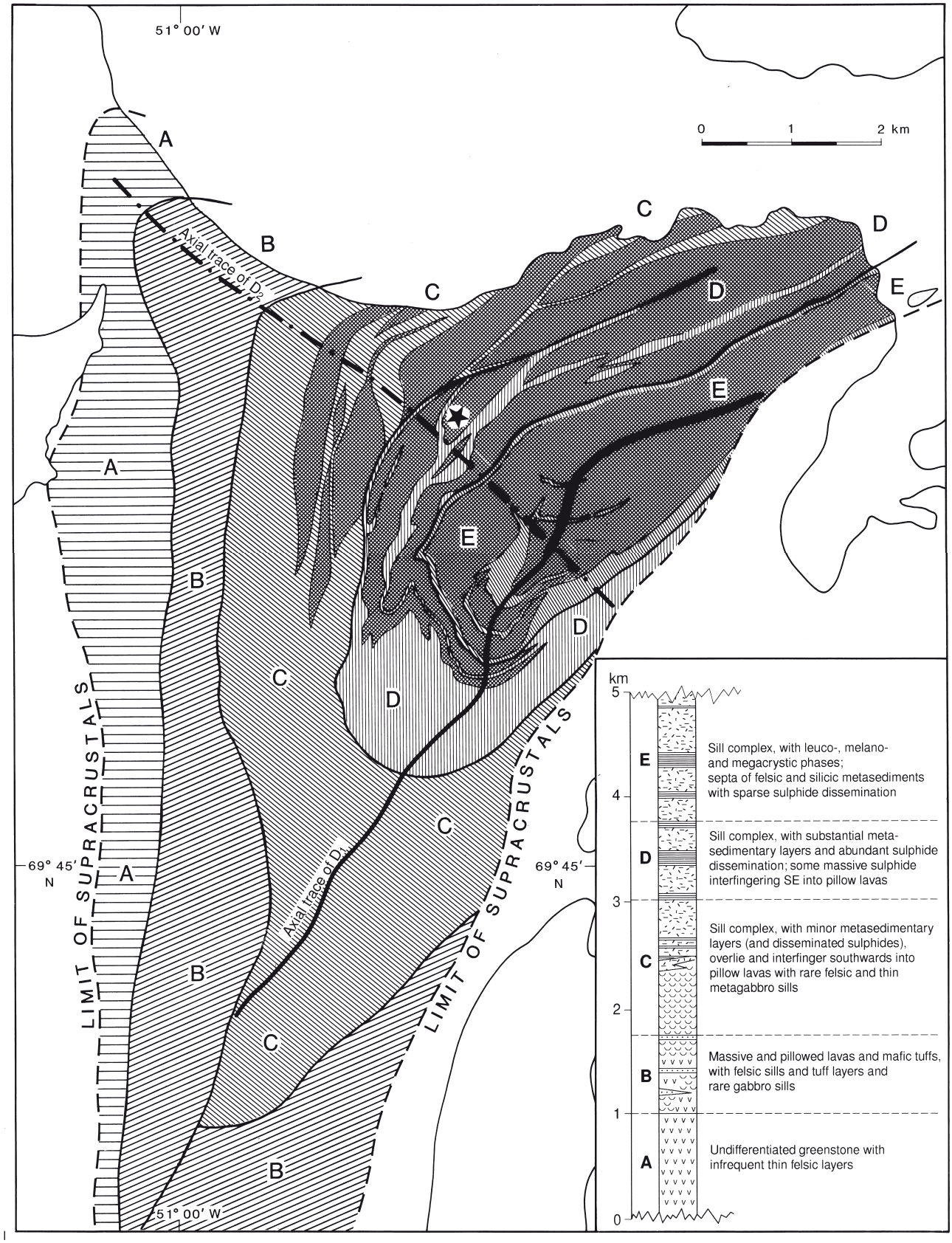

Fig. 2. Interpretative geological map of the sill complex and associated supracrustal rocks, north-eastern Arveprinsen Ejland, with the axial traces of D_1 and D_2 folds (full line and dash-dot line, respectively). The star locates 'Anderson's Prospect'.

1982) and component sills of the sill complex; (2) difficulty experienced in the field in distinguishing between medium- to fine-grained sill rocks and metavolcanics, particularly where the rocks are highly strained and constitute tracts of retrograde greenschist (Knudsen *et al.* 1988); and (3) apparent thickness effects on the western limb of the regional fold caused by dip variation and parasitic folding. The boundary could also result from the sill occupying space created by change of porosity and dissolution accompanying the expulsion of pore-water during contact metamorphism (e.g. Einsele 1980). This and other aspects of sill emplacement are examined in a later section.

Based on reconnaissance mapping, an attempt has been made to indicate component bodies of the sill complex where they are outlined by mappable septa (Fig. 2). The mapping suggests that there are at least eight sills, each differing from the immediately overlying and underlying sills in terms of gross appearance and degree of internal variation. Thus, some of the sills seem to have undergone a degree of post-emplacement differentiation, whereas others show little evidence of significant amounts of crystal-liquid separation following intrusion. In some cases a sill contains cumulate layers of abundant feldspar megacrysts (up to 5 cm across), elsewhere phenocrysts are relatively small (1–3 cm), sparsely distributed, and consistent with *in situ* growth in equilibrium with the melt. Feldspars decrease in size against the inter-sill septa. Lithological and petrographical summaries of the main rock types comprising the sill complex are presented in Table 1.

Contact relationships

The sills have maximum thicknesses (corrected for dip but not strain) ranging very approximately from 200 to 600 m. Their contacts and internal layering are parallel to the bedding in the metasedimentary sequences, consistent with their emplacement as pre-orogenic sills within a flat-lying stratigraphy. Chilled margins were recorded at upper, lower and lateral contacts. They most probably surround each sill, but this could not be proved because the majority of contacts are shear zones marked by retrograde schist development.

Component sills may be in direct contact with each other at their upper and lower contacts, but they are more typically separated by metasedimentary inter-sill septa which, although they range up to 150 m in thickness, are usually < 50 m thick. Towards the interpreted lateral contacts, thinner (< 20 m), discontinuous, more closely spaced septa are encountered. These are either intra-sill, and result from interfingering of magma at the margin, or they separate closely related (in time and composition) magma pulses which combined to build a substantial sill unit. In some cases, thin septa obliquely separate two sills between shared inter-sill septa.

Uncommon features of the contacts include small (< 1 m) cuspate and lobate magmatic incursions, and larger (up to 10 m) irregular and planar discordances where bedding in the septum is obliquely truncated. In one such instance of oblique truncation, younging reversed along the contact but D_1 vergence remained constant. This suggests that soft-sediment folding preceded or was penecontemporaneous with sill emplacement.

From the contacts examined in detail, there is no quantifiable correlation between the type of contact (whether upper, lower or lateral) and the thickness of the chilled border zones, although the better preserved marginal assemblages do seem to be on the lower contacts. In general, 20–50 cm of extremely fine-grained 'flinty-looking' intrusive rock pass into 1 to 5 m of medium-grained rock which, with increasing grain size, passes imperceptably into the main body of the sill. Where the latter is porphyritic, both matrix and phenocryst grain size progressively coarsen; where non-porphyritic, the rock becomes spotty or blotchy due to retrogression of coarse mafic phases, and in some cases is coarsely poikiloblastic.

Sedimentary rocks at the contact have a chert-like aspect and, depending on the degree of hornfelsing and silica metasomatism, may or may not be overprinted by the D_1 foliation and lineation. Particularly at lower contacts, up to 0.5 m of recrystallised and silicified sedimentary rock are fractured and healed by vein quartz. Although generally sharp and planar, the contact may be locally (over a few metres) irregular and ill-defined due to incorporation of soft sediment in the base of the sill, and sill clasts within the sediment. This mutual invasion has resulted in irregularly developed globular, fluidal peperitic zones (Brooks *et al.* 1982; Busby-Spera & White 1987), even though peperites are more typical of higher viscosity andesitic magma (Kokelaar 1982). Other than on the scale of the thin peperitic zones, the sill complex lacks metasedimentary xenoliths or rafts (cf. Knudsen *et al.* 1988).

Table 1. Lithology and petrography of representative rock types from the sill complex

Rock type	Lithology and petrography
Porphyritic metabasite (1, 2)*	Equant and prismatic feldspar phenocrysts (up to 2 cm across) are sparsely distributed (spacing in the order of 1 per 100 cm^2) in a fine- to medium-grained (2 to 4 mm) green-grey metabasite – typically unfoliated and unlineated. The metabasite exhibits remnant poikilitic to ophitic igneous textures. Poikiloblasts of amphibole (up to 6 mm, weakly pleochroic from very pale green to colourless, oblique extinction) enclose laths (up to 0.5 mm) of saussuritized feldspar. The matrix comprises metamorphic feldspar, epidote-group minerals, chlorite, sphene, amphibole needles and minor carbonate.
Megacrystic metabasite	Equant euhedral to near spherical calcic plagioclase megacrysts (up to 5 cm across) are abundantly distributed (3 to 4 per 100 cm^2) in layers up to 2 m thick within a metabasite matrix. The matrix is as above.
Metagabbro and metadolerite (3, 6, 7)*	Speckled rocks comprising dark grey prismatic mafic grains (up to 7.5 mm) in a felsic matrix – approximate proportions 50:50 – weakly foliated to unfoliated, but in some cases well lineated. The texture is metamorphic. The prismatic to ragged amphibole crystals (strongly pleochroic from blue-geen to yellow-green) exhibit linear preferred orientation in a finer grained (up to 2 mm) matrix of plagioclase, chlorite, granular epidote, amphibole, minor sphene and uncommon calcite.
(Meta-)leuco-gabbro and leucodolerite	Speckled rocks similar to metagabbro and metadolerite; but mafic to felsic proportions approximate 40:60, the mafic component is pale to medium grey, and foliation and lineation range from strong to absent. Remnant ophitic igneous texture eucodolerite exists where foliation/lineation are lacking. The pale anhedral amphibole is weakly pleochroic from very pale green to colourless.
(Meta-)melano-gabbro and melanodolerite	Melanocratic rocks comprising a dark grey mafic component and an interstitial felsic matrix in approximate 60:40 proportions. The texture is totally metamorphic. The amphibole (intense pleochroism from blue-green to yellow-green, oblique extinction, up to 6 mm) forms decussate ragged prisms and sheaves associated with plagioclase and minor biotite. Chlorite, epidote, sphene and calcite are absent.
Poikiloblastic metagabbro (9, 10, 11)*	Pale to medium grey medium-grained (up to 5 mm) speckly rock with poikiloblastic patches up to 4 cm across – generally unfoliated and unlineated. The igneous poikilitic texture is pseudomorphed by poikiloblastic amphibole after pyroxene.The amphibole (weakly pleochroic, oblique extinction) encloses plagioclase laths. These and the feldspathic matrix are altered to a saussuritic aggegate of epidote goup minerals, chlorite, sphene, amphibole needles and minor calcite.
Spotted metagabbro (4, 5, 8)*	Pale to medium grey rock with closely spaced (4 to 6 per 9 cm^2) dark grey elliptical blotches (0.5 to 1 cm across) which commonly define the foliation and lineation The blotches are masses of oriented fine-grained (0.5 mm to 1 mm) chlorite and minor zoisite (?). They are separated by a matrix of metamorphic plagioclase, abundant carbonate, epidote group minerals, sphene and amphibole needles.

* Analysis numbers from Table 2.

Table 2. Chemical composition of representative samples from the sill complex and associated mafic and felsic volcanic rocks

	Mafic sill complex													
Analysis	1	2	3	4	5	6	7	8	9	10	11	12	13	14
GGU No	362646	362681	362679	362678	362677	362697	362698	362699	362700	362659	362661	362687	362689	362682
SiO_2	46.28	47.83	47.70	46.07	43.02	50.29	44.32	46.50	44.00	47.43	48.57	49.75	48.58	50.16
TiO_2	1.05	0.96	1.02	0.86	0.76	0.62	0.55	0.37	0.56	0.59	0.76	0.61	0.43	0.58
Al_2O_3	15.34	14.81	15.81	16.12	14.89	16.08	13.57	14.83	14.00	15.48	18.35	14.79	17.02	13.52
Fe_2O_3	1.98	0.33	1.11	0.79	0.89	0.75	0.75	0.86	0.99	1.78	2.15	2.45	2.19	1.31
FeO	9.66	10.53	9.82	9.73	9.52	7.32	9.71	7.40	8.57	7.13	5.57	6.25	4.27	7.12
MnO	0.17	0.16	0.18	0.17	0.17	0.11	0.16	0.13	0.14	0.16	0.14	0.14	0.11	0.16
MgO	7.46	7.24	7.95	8.13	8.16	10.02	16.01	13.87	13.84	8.51	6.35	8.39	7.91	8.76
CaO	8.97	8.84	9.62	10.77	9.40	5.91	7.50	8.97	8.26	12.83	11.76	12.08	13.57	12.96
Na_2O	2.31	3.47	2.13	1.85	1.64	3.75	1.25	1.40	1.06	1.56	2.93	2.46	2.03	2.14
K_2O	0.34	0.33	0.15	0.05	0.11	0.04	0.15	0.14	0.03	0.03	0.09	0.04	0.02	0.04
P_2O_5	0.07	0.07	0.04	0.06	0.04	0.04	0.04	0.03	0.04	0.03	0.09	0.04	0.02	0.03
volatiles	5.43	4.85	4.24	5.13	11.09	4.28	5.67	5.22	7.76	4.11	2.90	2.83	3.34	3.12
Tot.(%)	99.07	99.41	99.78	99.74	99.69	99.22	99.68	99.72	99.25	99.64	99.66	99.82	99.49	99.91
mg´	0.54	0.54	0.57	0.58	0.59	0.69	0.73	0.75	0.72	0.64	0.60	0.65	0.69	0.64
Rb	11	8	4.2	1.3	2.3	<0.5	2.3	3.2	0.5	<0.5	1.6	<0.5	<0.5	0.7
Ba	76	83	59	16	29	18	33	60	6	7	20	12	12	19
Pb	18	10	12	11	10	10	8	6	7	7	7	7	6	8
Sr	107	101	113	98	56	119	72	81	82	88	91	107	101	131
La	3	7	4	3	<1	8	4	3	3	<1	3	3	2	<1
Ce	10	12	7	10	6	17	6	6	7	7	11	8	11	6
Nd	7	8	5	6	4	8	3	2	4	4	8	6	5	4
Y	23	21	20	18	14	15	11	8	11	13	21	13	12	13
Th	<1	<1	<1	<1	<1	2	<1	<1	<1	<1	<1	<1	<1	<1
Zr	55	53	54	46	32	65	34	24	31	23	46	30	28	30
Nb	2.5	2.8	2.8	2.5	2.1	3.1	1.8	1.5	1.6	1.9	2.4	2	1.8	1.9
Zn	373	442	404	141	161	112	152	99	99	104	72	73	71	125
Cu	140	13	13	115	41	105	39	34	90	21	7	56	51	45
Co	53	46	49	59	60	53	85	72	76	56	41	53	52	47
Ni	126	129	145	191	214	233	638	457	559	192	70	87	80	89
Sc	38	39	38	33	26	29	25	13	20	37	43	53	55	54
V	306	281	282	260	223	203	192	112	177	232	229	258	269	252
Cr	312	267	323	286	322	608	1690	381	1090	435	544	423	429	544
Ga	19	18	17	18	15	16	14	10	13	15	18	15	14	14

Major elements analysed by XRF on glass discs at the Survey (Na by AAS); trace elements analysed at the Geological Institute, University of Copenhagen, by XRF on powder tablets.

Table 2 *(continued)*

Associated mafic volcanic rocks							Associated felsic volcanic rocks									
15	16	17	18	19	20	21	22	23	24	25	26	27	28	29	30	Analysis
362694	362695	362663	362652	362684	362685	362686	362601	362602	362657	362656	362664	362709	362732	362743	362745	GGUNo
49.15	47.86	46.32	48.74	47.83	52.51	50.35	68.00	69.80	65.63	73.42	68.97	70.80	71.11	70.04	65.73	SiO_2
1.43	1.46	1.03	0.68	0.59	0.55	0.60	0.30	0.26	0.41	0.28	0.27	0.27	0.24	0.24	0.45	TiO_2
14.62	14.84	12.18	17.10	14.88	14.29	14.96	15.17	14.76	15.04	13.75	15.30	14.20	15.35	15.01	16.57	Al_2O_3
2.06	2.34	0.73	1.36	0.97	0.98	0.39	0.00	0.37	2.10	0.52	0.32	0.28	0.14	0.08	0.37	Fe_2O_3
10.12	10.18	10.84	8.69	9.23	8.12	8.25	2.09	1.48	3.67	1.70	1.26	1.59	1.56	1.39	2.93	FeO
0.20	0.25	0.21	0.16	0.17	0.16	0.17	0.04	0.02	0.03	0.01	0.03	0.04	0.03	0.03	0.04	MnO
7.30	6.41	5.97	9.12	11.55	10.16	7.67	1.16	0.93	2.30	1.35	0.87	1.29	0.79	0.90	1.55	MgO
8.94	10.35	8.96	5.10	6.54	6.22	6.41	3.30	2.09	1.92	1.32	2.40	2.08	2.09	2.29	4.09	CaO
2.14	1.88	1.66	2.08	1.97	1.87	3.66	5.04	6.18	5.21	4.58	4.59	4.73	5.77	5.22	5.05	Na_2O
0.09	0.15	0.04	1.27	0.06	0.04	0.08	1.50	0.98	0.59	1.26	2.15	1.71	1.21	1.86	1.14	K_2O
0.14	0.14	0.07	0.03	0.03	0.03	0.04	0.09	0.08	0.15	0.14	0.07	0.09	0.06	0.06	0.08	P_2O_5
3.79	3.59	11.14	5.55	5.99	4.72	6.71	2.69	2.21	2.38	1.55	2.80	1.93	1.04	1.73	1.46	volatiles
99.98	99.46	99.15	99.88	99.81	99.65	99.29	99.38	99.15	99.43	99.88	99.03	99.01	99.4	98.85	99.46	Tot(%)
0.52	0.48	0.48	0.62	0.67	0.67	0.61	0.50	0.48	0.42	0.53	0.50	0.56	0.46	0.52	0.46	mg´
1.7	2.5	1	44	1.2	0.6	1.5	43	21	14	25	49	42	34	46	38	Rb
17	35	13	297	27	14	39	334	355	130	164	492	687	548	469	270	Ba
10	16	11	18	15	14	71	7	6	7	8	6	6	11	10	7	P
95	117	106	99	117	127	86	231	112	93	104	177	95	385	335	262	Sr
6	5	3	4	5	4	44	14	23	35	23	25	22	14	11	12	La
15	16	13	10	9	13	81	32	39	65	47	42	44	27	22	22	Ce
11	9	6	6	4	6	32	15	18	29	19	17	20	12	10	12	Nd
32	33	24	18	13	12	11	6	4	15	9	4	6	4	4	9	Y
2	2	<1	nd	1	<1	<1	4	6	6	9	7	6	4	4	4	Th
100	100	59	49	45	50	39	89	109	128	116	116	89	96	82	103	Zr
5.2	5.1	3.3	2.6	2.6	2.5	2.2	3.1	2.5	5.1	4.2	2.4	4	1.8	2.2	4	Nb
152	216	194	282	425	296	633	41	32	100	37	32	42	33	38	35	Zn
17	79	75	39	62	52	14	6	7	387	123	6	<2	9	<2	24	Cu
61	59	52	53	54	51	106	55	37	72	37	14	16	35	34	33	Co
124	127	57	213	303	281	309	11	10	38	21	9	15	8	9	19	Ni
40	41	58	30	30	26	28	6	4	11	4	4	6	2	4	10	Sc
322	332	379	218	211	181	185	47	33	77	31	37	42	32	31	76	V
275	273	264	538	817	705	872	27	53	85	19	21	37	15	17	43	Cr
19	19	16	17	16	15	10	17	17	20	16	18	18	17	16	18	Ga

Petrography and chemistry

Significant proportions of the petrography and chemistry pertain to the sill complex. Petrographic notes and chemical data for the massive and pillowed basalts, and for the mafic tuffs and felsic rocks, enable comparison with the sill complex and with data from other areas. However, the mafic tuffs are both heterogeneous, on a scale of 0.5 m, and intensely altered; their results should therefore be treated cautiously.

Petrography

Primary textures were, in some cases, pseudomorphically preserved in sill complex rocks, but they have usually been overprinted by greenschist- to amphibolite-facies metamorphism and penetrative deformations. The texture therefore now comprises variably orientated assemblages of amphibole, chlorite, feldspar, sphene and carbonate. In terms of the field appearance, seven principal rock types (Table 1) make up the sill complex. All of these rock types, which probably represent igneous precursors with primary layering due to differentiation processes, are not present in each component sill. This could be due to compositional differences in the magma pulses which formed the various component sills, although other factors such as thickness and rate of cooling could also be involved. Systematic evaluation of this and other aspects of the layering are precluded by the intensity of metamorphism and deformation.

Petrochemistry

The major- and trace-element data determined for rocks from the sill complex, and from basalts, mafic tuffs and felsic volcanic rocks intruded by the complex, are presented in Table 2.

Of the 14 rocks analysed from the sill complex, samples 362646, 362677, 362678, 362679 and 362681 (Analyses 1–5, Table 2) are from the same component sill immediately overlying 'Anderson's Prospect' (Marshall & Schønwandt 1990). Sample 362681 (mg′ 0.54) is from the basal chilled contact, 362646 and 362679 (mg′ 0.54 and 0.57 respectively) are within 20 m of the contact but beyond the zone of obvious chilling, and 362677 and 362678 (mg′ 0.59 and 0.58 respectively) are from coarser-grained spotted metagabbro (Table 1) more distant from the contact.

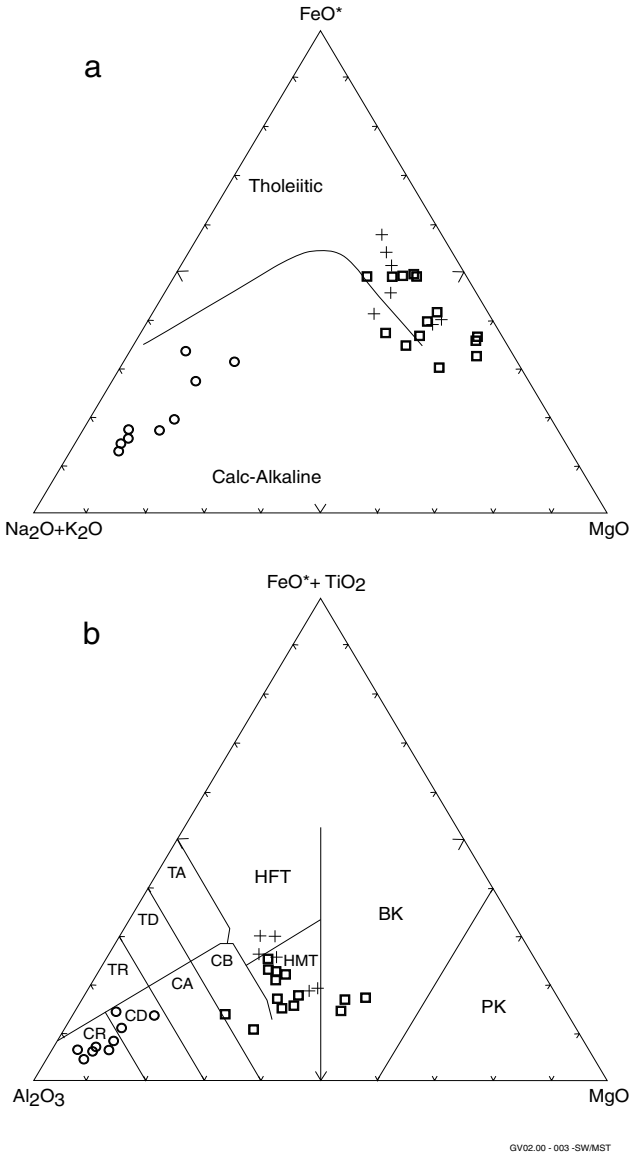

Fig. 3. **a**: AFM diagram for rocks from the sill complex (open squares), mafic volcanics (crosses) and felsic volcanics (open circles). Tholeiite-calc-alkaline division after Irvine & Baragar (1971). **b**: Jensen diagram (Jensen 1976) for rocks from the sill complex, mafic volcanics and felsic volcanics; symbols as for **a**. PK: picritic komatiite; BK: basaltic komatiite; HMT: high magnesium tholeiite; HFT: high-iron tholeiite; CR, CD, CA, CB: calc-alkaline rhyolite, dacite, andesite, basalt; TR, TD, TA: tholeiitic series.

Sample 362659 (Analysis 10, Table 2; mg′ 0.64) is from the next component sill up-sequence from that overlying 'Anderson's Prospect'; poikilitic pyroxene (now pseudomorphed by amphibole) suggests an original cumulate texture.

Samples 362697 to 362700 (Analyses 6–9, Table 2) and samples 362682, 362687 and 362689 (Analyses 12

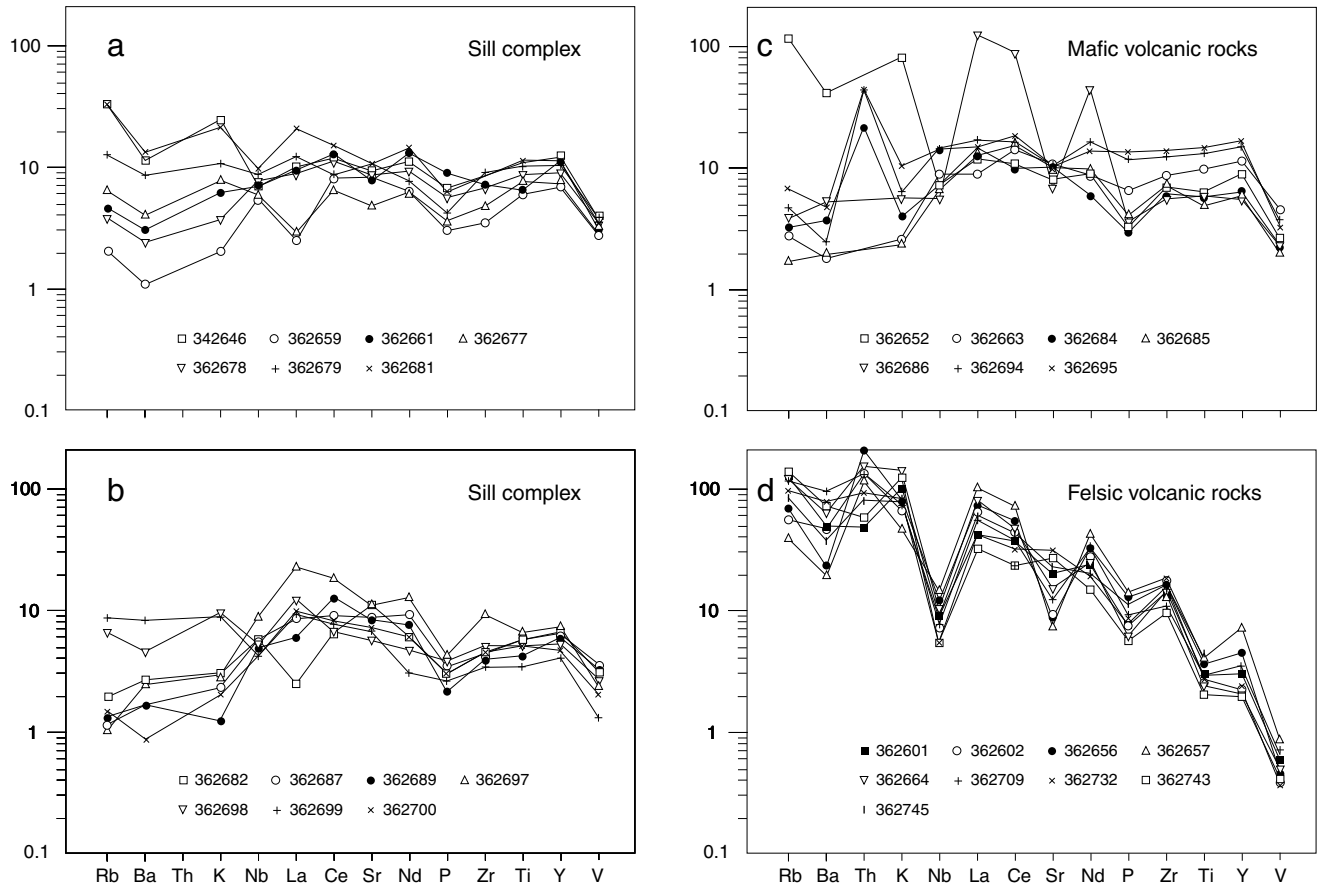

Fig. 4. Chondrite-normalised multi-element spider diagrams for: **a** and **b**: Sill complex samples. **c**: Mafic volcanic samples. **d**: Felsic volcanic samples. Normalised after Thompson *et al.* (1984).

–14, Table 2) are respectively from the basal and upper parts of a component sill underlying and to the southwest of 'Anderson's Prospect'. Sample 362697 (mg′ 0.69) is from the chilled base, and samples 362698, 362699 and 362700 (with mg′ values of 0.73, 0.75 and 0.72) were collected 1 m, 15 m and 50 m above the contact; sample 362700 has a relict cumulate texture, whereas the others are entirely metamorphic. Samples 362682, 362687 and 362689 (with mg′ values of 0.64, 0.65 and 0.69) have metamorphic textures and were collected from 10 m to 40 m below the upper contact of the component sill.

Sample 362661 (Analysis 11, Table 2; mg′ 0.60) is from the lowermost component sill exposed within the sill complex and has a metamorphic texture.

All seven of the mafic volcanic rocks analysed have metamorphic textures. Samples 362694, 362695 and 362663 (Analyses 15, 16 and 17, Table 2; mg′ values 0.52, 0.48 and 0.48) are respectively pillowed greenstone, massive greenstone and mafic tuff from unit C (Fig. 2), whereas 362684, 362685 and 362686 (Analyses 19, 20 and 21, Table 2; mg′ values 0.67, 0.67 and 0.61) are mafic tuff and hyaloclastite (362686, Analysis 21) within the main metasedimentary layer associated with 'Anderson's Prospect' in unit D (Fig. 2). The remaining sample (362652, Analysis 18, Table 2) also comes from unit D and is an altered mafic tuff (Figs 4c, 5c).

The analysed felsic volcanic rocks lack foliation and retain much of their primary texture. This is because many of the felsic layers, although having foliated marginal zones, possess relatively massive median zones. Samples 362656 and 362657 (Analyses 25 and 24, Table 2) are massive rhyolite and rhyodacitic tuff interlayered with the metasedimentary horizon at the boundary of units D and E (Fig. 2). Samples 362602, 362664 and 362709 (Analyses 23, 26 and 27, Table 2) are rhyolitic porphyries, the first two occurring at the base of the lowermost component sill in unit C (Fig. 2), and the last (362709, Analysis 27) lying along strike but being interlayered with pillowed greenstone. Of the remaining samples, 362601, 362732 and 362743

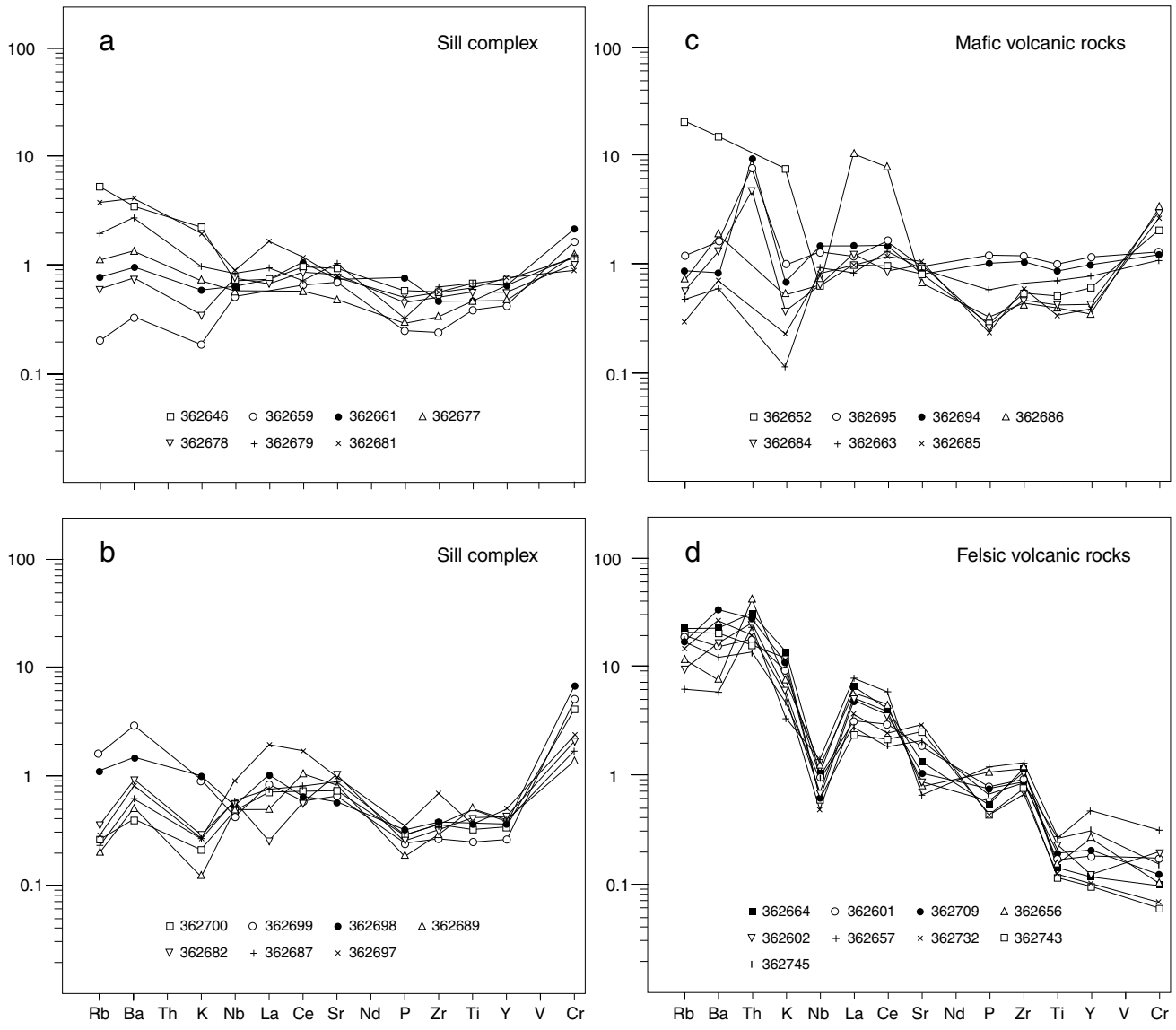

Fig. 5. MORB-normalised multi-element spider diagrams. **a** and **b**: Sill complex samples. **c**: Mafic volcanic samples. **d**: Felsic volcanic samples. Normalised after Pearce (1983).

(Analyses 22, 28 and 29, Table 2) are from rhyolitic porphyries in unit B (Fig. 2), and 362745 (Analysis 30, Table 2) is a rhyodacitic tuff from unit A (Fig. 2).

Alteration. The intensity of regional metamorphism precludes detailed evaluation of early alteration effects in any of the rock types, even though some degree of alteration should be anticipated. For example: (1) the peperitic contacts of the sill complex and the indications of soft-sediment deformation in the adjacent host rocks (above), are consistent with emplacement into water-charged rocks and associated hydrothermal circulation; (2) the high volatile contents of many of the analyses (Table 2) imply metasomatic alteration; and (3) pillow basalts and hyaloclastites commonly undergo alteration because of their mode of formation (e.g. Cas 1992). Despite this, the analyses in Table 2 for specific rock types are reasonably consistent and plot systematically on many of the petrological diagrams (below), irrespective of whether mobile or immobile and major or trace elements are employed. This consistency for samples from widely distributed sites suggests that neither pre-metamorphic alteration nor regional metamorphism has greatly distorted the chemical data, even though some redistribution of alkalies (Na, K, Rb and Ba) is probable (below).

Initial magma composition. A guide to the range of

initial compositions of magma pulses comprising the sill complex is provided by the chilled and finer-grained marginal phases within one or two metres from the contact. Samples 362697 (Analysis 6) and 362698 (7), and 362681 (2) and 362679 (3) (Table 2) are pairs of samples from two different contact zones. The high Na_2O contents of the contact samples, 362697 and 362681, imply a metasomatic contribution from the metasedimentary rocks across the contact, but this does not change the fact that the two pairs have widely differing mean mg′ values (approximately 0.71 and 0.56) and mean Ni contents (approximately 436 and 137 ppm). The data pairs respectively imply equilibrium with typical upper mantle mineralogies and some degree of fractional crystallisation of olivine, although interpretation can be complex (e.g. Wilson 1989); they are consistent with those from basaltic komatiites (Boryta & Condie 1990) and magnesian tholeiites (Cattell & Taylor 1990). In essence, provided that the two pairs represent liquid compositions, the component sills making up the sill complex represent magmatic pulses of significantly different gross composition.

Analysis of chemical data. On a Harker variation diagram of wt% $Na_2O + K_2O$ versus wt% SiO_2 (e.g. Wilson 1989, fig. 1.2), the mafic rocks (both from the sill complex and the lavas and tuffs) plot as sub-alkalic gabbros and basalts, and the felsic volcanic rocks as sub-alkalic rhyolites and dacites. The identifications are largely confirmed using the wt% SiO_2 versus log (Zr/TiO_2) plot of Winchester & Floyd (1977, fig. 2), although a few of the basaltic and sill complex samples lie in the alkali-basalt field. On diagrams of wt% K_2O and wt% Na_2O versus wt% silica (Middlemost 1975), these few samples are transitional in that they are alkalic with respect to Na_2O and sub-alkalic for K_2O. For all such cases, the samples are either from the contact zone of the sill, or from mafic hyaloclastite, and have most probably undergone Na enrichment (e.g. samples 362697 and 362698, Table 2). In essence, the only rocks that are not sub-alkalic are those affected by alteration.

The sill complex and mafic volcanic samples mainly plot as low-potassium tholeiites (fields A and B) on the Ti-Zr diagram of Pearce & Cann (1973, fig. 2). This most probably reflects the primary composition of the samples because their K_2O data are consistently low (Table 2). The dominantly tholeiitic character of the sill complex and mafic-volcanic samples is also clear on the Na_2O+K_2O – FeO* – MgO diagram (Fig. 3a), which conversely demonstrates the calc-alkaline affinity of the felsic rocks. These affinities are further shown on the Jensen diagram (Fig. 3b; Jensen 1976), where the majority of the sill complex and basaltic rocks plot as high-magnesium tholeiites (although three fall in the basaltic komatiite field), and the felsic rocks are calc-alkaline rhyolites and dacites (Fig. 3b).

Chondrite- and MORB-normalised multi-element spider diagrams (Thompson *et al.* 1984) for the various rock types are shown in Figs 4 and 5. The most obvious feature of both sets of spider diagrams is the similarity of the basaltic volcanic rocks to those of the sill complex. This is consistent with the proposed subvolcanic relationship between the basaltic and sill complex rocks. A second feature of both sets of spider diagrams (Figs 4, 5) is the distinctly different pattern of the felsic rocks. The difference in pattern is consistent with the felsic and mafic rocks respectively being calc-alkaline and tholeiitic. Such arc-style volcanism has been interpreted in terms of a type of compositionally zoned magma chamber that was kept in a liquid state by repeated inputs of mantle-derived mafic liquid (Smith 1979). Mafic volcanism could tap the lower part of the magma chamber and represent an over-supply of mantle-derived magma, whereas felsic volcanism could reflect the release, from the upper part of the chamber, of magma resulting from fractionation processes and assimilation of surrounding sialic material (Thurston 1990). Of course, if the calc-alkaline chemistry is solely ascribed to high-level assimilation, it then ceases to be a valid guide to an arc tectonic setting.

The chondrite-normalised spider diagrams for the mafic rocks (Fig. 4a–c) comprise patterns that are either flat or show a shallow downward tilt to the left with respect to LILE. The tilt is somewhat MORB-like and suggests a source that was relatively depleted in Rb, Ba and K (despite some possibility of alteration-related redistribution), whereas the flatter patterns imply that the majority of the elements analysed have retained near-chondritic proportions. Primitive MORB-like patterns and near-chondritic proportions of Ti, Zr, Y and Nb are characteristic of Archaean tholeiitic rocks, although few chemical discriminants for distinguishing between typical tholeiites and basaltic komatiites are universally applicable (Cattell & Taylor 1990; Hall & Hughes 1993). In the rocks from the sill complex (Fig. 4a, b) and even in the mafic volcanic samples (Fig. 4c), there is little or no indication of an enrichment in LILE and LREE relative to Nb (the subduction zone component – SZC – of Condie 1990), although samples 362652 (18) and 362686 (21) are notable exceptions. In contrast, the spider diagram for the felsic

volcanic rocks (Fig. 4d) possesses a distinct Nb trough (Nb depletion relative to the LILE and the LREE) and shows relative depletion of Ti against Zr and Y in a majority of samples.

With the exception of sample 362697 (6) (Fig. 5b) and samples 362652 (18) and 362686 (21) (Fig. 5c), the MORB-normalised spider diagrams for the sill complex and basaltic rocks (Fig. 5a–c) show the flat MORB-like to primitive MORB patterns of Archaean tholeiite (e.g. Snyder *et al.* 1990, fig. 9.7b; Type 1), or patterns similar to crustally contaminated komatiites (e.g. Hall & Hughes 1990, fig. 5.11). The three spider diagrams (Fig. 5a–c) show little indication of subduction-related processes in that they lack Nb and Ti negative anomalies (Wilson 1989; Condie 1990; Furnes *et al.* 1992). Similarly, with the possible exception of sample 362652 (18) (which is either crustally contaminated or altered), they lack evidence for crustal contamination, because the levels of enrichment of LILE and LREE are negligible. However, this interpretation of the LILE and LREE data could be misleading, because crustally contaminated komatiites and basaltic komatiites commonly have fractionated REE patterns, yet tend to show little enrichment in Rb and K, and generally lack a negative Nb anomaly (e.g. Hall & Hughes 1990). Although the matter remains inconclusive, limited support for this alternative possibility is provided by the patterns (Fig. 5a–c) differing from the average spider diagram for late Archaean greenstone belt metavolcanic assemblages, from which data for komatiites and basaltic komatiites have been excluded (Condie 1990).

Compared with the chondrite-normalised spider diagram (Fig. 4d) for the felsic volcanic rocks, the MORB-normalised plot (Fig. 5d) similarly shows Nb depletion relative to the LILE and the LREE (La and Ce), and, in some samples, Ti depletion against Zr and Y. These aspects, combined with the enrichment character of the more incompatible elements, are consistent with the felsic volcanic rocks having a calc-alkaline character (e.g. Furnes *et al.* 1992).

Most samples from the sill complex and the basaltic rocks plot in the basic field on the TiO_2 versus Zr diagram of Pharaoh & Pearce (1984), and thereby suggest that basalt-based tectonomagmatic discrimination diagrams may be applied to the analytical data. The use of such diagrams, even in the Phanerozoic, involves much uncertainty (e.g. Cas & Wright 1987; Pearce 1987; Wang & Glover 1992); and in the Archaean they could well be invalid (e.g. Wilson 1989; Cattell & Taylor 1990; Hall & Hughes 1993). Nevertheless, it is not uncommon for Archaean basalts to be classified in terms of modern basaltic types and their tectonic settings (e.g. Condie 1990; Boryta & Condie 1990). Thus, with due reservation, this practice will be followed.

The sill complex and basaltic rocks plot as island-arc tholeiites, with some overlap into the field of calc-alkaline basalts, on the TiO_2–MnO–P_2O_5 diagram of Mullen (1983). Similarly, they occupy the fields of island-arc basalts on the diagrams of Zr/Y versus Zr (Pearce & Norry 1989) and Ti/Zr versus Zr/Y (Condie 1990). Using a diagram of Ti/Zr versus Al_2O_3/TiO_2, Cattel & Taylor (1990) attempted to discriminate between komatiitic suites and Phanerozoic basaltic sequences. On this diagram, the sill complex and basaltic rocks plot in the fields of MORB and volcanic-arc basalts. However, approximately one-third of the samples (of both intrusive and extrusive rocks) also occupy the field comprising komatiite, komatiitic basalt and Archaean tholeiite, all of which derived from magmas that were probably erupted through Archaean continental crust (e.g. Cattell & Taylor 1990).

Discussion

Emplacement process

A sill complex, as opposed to a single intrusion that differentiated *in situ*, was recognised (Marshall & Schønwandt 1990) on the basis that: (1) the thinness, continuity and largely concordant nature of metasedimentary layers between sills are consistent with the layers being classical septa (e.g. Raudsepp & Ayre 1982); (2) interfingering with the host rocks characterises the outer limits of the complex, whereas a large forcefully emplaced intrusive body typically has marginal faulting and brecciation (e.g. Habekost & Wilson 1989); (3) large mafic intrusions typically have substantial contact-metamorphic aureoles and commonly contain contact-metamorphosed metasedimentary 'rafts', whereas here both are lacking (e.g. Habekost & Wilson 1989; Sipilä 1992); (4) the sill complex does not display the systematic distribution of the principal rock types that typifies *in situ* differentiation of a major intrusive body (e.g. Hatton & Von Gruenewalt 1990); (5) compositionally similar but very much thinner sills exist in other parts of the sequence away from the contact; (6) one example was found of an earlier sill being cut by a later one, even though this is uncommon for subvolcanic sill complexes (e.g. Raudsepp & Ayres 1982) and (7), the behaviour of the complex during regional fold-

ing is more in keeping with a well-layered sequence with marked mechanical anisotropy rather than with an integrated coherent intrusive.

In addition to the largely field-based guides (above), support is also provided by the geochemical data from contact zones in different parts of the sill complex (Table 2, samples 362679 and 362697). Although clearly part of the same magmatic system (Figs 4a, b, 5a, b) the contact samples themselves have distinctive major element chemistries and, in that they are interpreted as chilled facies, most probably constitute separate magmatic pulses. We shall therefore examine emplacement processes in the context of a progressively intruded sill complex rather than a single massive intrusion.

The sill complex was progressively emplaced within the dominantly metasedimentary sequence overlying a sequence of basaltic tuffs and lavas (Fig. 2). Although some of the septa are quite thick (up to 150 m), the majority are less than 20 m. This, together with the formation of peperitic rocks and chilled contacts, is in keeping with emplacement of the component sills into wet, probably poorly lithified, sedimentary material at shallow depths below the depositional interface (cf. Carlisle 1972; Raudsepp & Ayres 1982). In such sequences, successive sills tend to be intruded at progressively higher stratigraphic levels. This is because the position of the next sill is largely controlled by the interface between the contact-metamorphosed zone of the preceding sill and the overlying less-lithified sedimentary strata (Einsele 1980; Raudsepp & Ayres 1982). Indeed, strengthening of the sequence by intrusive and contact-metamorphic rocks is a factor in whether later magma forms intrusions or is erupted as flows (Carlisle 1972).

The rise of magma and its emplacement as sills is a complex process reflecting factors such as the depth and density relationships of the magma and potential host rocks, the dimensions of the feeder channel, the relative magnitudes of the horizontal (s_x) and vertical (s_z) stress components, the magmatic pressure (P_m), and the tensile strength (T_0) of the host materials (Williams & McBirney 1979). Nevertheless, in relation to the Guaymas Basin, Einsele (1980) demonstrated that upwelling magma will generally form sills through dilation when $P_m \geq P_s + T_0$ (where P_s is the effective overburden pressure exerted by the sediment load), and the magma reaches soft-sediment strata. He suggested that an alternating sill-sediment sequence is controlled by the thickness of the contact-metamorphosed or contact-lithified zone, the interval and volume of magmatic pulses, and the sedimentation rate; sills will continue to form (other things being equal) as long as sediment accumulation at least matches the vertical build-up of the last sill and its upper contact zone. Without drawing any tectonic analogy between the Guaymas Basin and an Archaean greenstone belt, we believe that the physical principles relating to the development of sill-sediment sequences (Einsele 1980) are equally applicable elsewhere.

The boundary between the sill complex and supracrustal rocks has the appearance of a replacement relationship rather than that of a dilational mode of emplacement (Fig. 2; p. 88). Einsele (1980) examined the decrease in porosity of sediment resulting from the expulsion of water from contact zones above and below sills. He demonstrated that the total water loss, expressed in terms of the height of an equivalent column of sediment, was of similar magnitude to the thickness of the sill. He therefore concluded that a sill could effectively create space for itself when intruding wet sediment. Even though these relationships are likely to be modified by later deformation and metamorphism, we believe that the process recognised by Einsele (1980; also see Kokelaar 1982) could have a bearing on the apparent replacement boundary between the sill complex and its host rocks.

Petrogenetic and tectonic aspects

The dominantly tholeiitic nature of the sill complex and mafic volcanic rocks of Arveprinsen Ejland is typical of most Archaean greenstone belts (e.g. Condie 1990). However, in that these rocks are high-magnesium tholeiites and include some basaltic komatiites (based on Fig. 2b and on the spider diagrams – Figs 4, 5), they most probably reflect decompressive melting of mantle with a higher potential temperature (T_p) than that forming the source of typical Archaean tholeiites (e.g. Bickle 1990; Cattell & Taylor 1990). But irrespective of this, there is some agreement that komatiitic basalts, typical Archaean tholeiites and, indeed, the igneous components of most greenstone belts, all probably erupted through continental crust (e.g. Bickle 1990; Cattell & Taylor 1990; Hall & Hughes 1990). Whether this means that they formed in ensialic rifts, or in arc-related settings such as intra-arc and back-arc basins is most uncertain (e.g. Condie 1990; Hall & Hughes 1990).

Thurston (1990) has suggested that Archaean greenstones contain four distinct stratigraphic associations. Insufficient data exist on the greenstones of Arveprin-

sen Ejland to unequivocally assign them to one of these groups, but in terms of the general descriptions presented (Thurston & Chivers 1989; Thurston 1990) they would seem to best fit the arc-volcanic association. This is supported by the existence of the sill complex, and by the calc-alkaline nature and subduction zone component (SZC – Condie 1990) of the felsic volcanic rocks (Figs 3, 4, 5). It is further supported by various tectonomagmatic discrimination diagrams (above).

Megacrystic plagioclase ($An_{85\pm5}$) is a common feature of many Archaean tholeiitic flows, sills and dykes (Green 1975; Phinney *et al.* 1988); and such are present in parts of the Arveprinsen sill complex. Phinney *et al.* (1988, p. 1320) proposed a four-stage model to explain the formation of anorthositic complexes and the megacryst-bearing flow and intrusive bodies. The main points of their model involve: (1) high-pressure fractionation of olivine and pyroxene from a picritic or komatiitic mafic melt; (2) pulses of the fractionated, less-dense melt rapidly ascending to a low-pressure (1–2 kb) chamber, in which corresponding pulses of plagioclase crystallisation reflect depressurisation and undercooling; (3) the megacrysts forming cumulate layers within a melt which is fractionating along a tholeiitic trend and ultimately crystallises as an anorthosite complex; and (4) the pulsed input inducing periodic expulsion of megacryst-bearing melt to form flows, sills and dykes.

If this model (Phinney *et al.* 1988) is applied at Arveprinsen Ejland, then the megacryst bearing sills within the sill complex would equate with expulsions of melt from the low-pressure chamber. It therefore follows that, provided the other components of the sill complex were expelled from the same magma chamber (and this would seem to be supported by the chemical data), an indication exists of the dynamic complexity, in terms of degree of fractionation and residence times, that characterised both the high- and low-pressure magma chambers. Thus, as described above and similarly reported by Phinney *et al.* (1988), the component sill might, in places, contain megacryst-rich cumulate layers, whereas in others, sparse, relatively small megacrysts (1 to 3 cm), appear to have grown *in situ* in equilibrium with the melt.

A final point stemming from the model (Phinney *et al.* 1988) is that the sill complex was most probably emplaced at pressures well below 1 kb. This is consistent with Einsele (1980), who suggested that, in the Gulf of California, the upper limit of basaltic sill emplacement is in the order of 2 to 3 km below sea level and 150 to 200 m below the sea-sediment interface. It is also consistent with Kokelaar (1982, 1986), who suggested that the fluidisation of wet sediment at peperitic contacts was improbable at depths below about 3 km of seawater or 1.6 km of wet sediment. Although speculative, these data imply that the sill complex could have been progressively emplaced beneath 2 to 2.5 km of seawater and considerably less than 0.5 km of wet sediment.

Conclusions

The Archaean sill complex of north-eastern Arveprinsen Ejland constitutes a multiple, essentially concordant intrusion within a dominantly metasedimentary sequence overlying massive and pillowed lavas, and mafic tuffs. Field observations and chemical data are consistent with the component sills of the sill complex being emplaced as an upward-younging sequence into wet, poorly lithified sedimentary strata, at shallow levels below the water-sediment interface. Magma intruded to form the component sills when, for each sill, the magmatic pressure equalled or exceeded the *effective* overburden pressure plus the vertical tensile strength of the host materials at the level of intrusion (i.e. $P_m \geq P_s + T_0$). This condition was most probably induced by the sudden decrease in T_0 at the interface between contact-lithified rock and overlying poorly lithified strata. Determinants of the thickness of the sedimentary septa between component sills principally comprised the thickness of the contact-lithified zone above the previously emplaced sill, the rate of sedimentation, and the hiatus until the next magmatic pulse. The discordant, replacement-like boundary between the sill complex and supracrustals is believed to partly reflect the capacity of a sill to create space for itself (other than by dilation) when intruding wet sediment.

The sill complex and petrogenetically related mafic volcanic rocks are high-magnesium tholeiites and basaltic komatiites (on a Jensen plot; Jensen 1976) with a continental crust influence. Together with the calc-alkaline felsic volcanics, they probably comprise an ensialic arc-volcanic association. The sill complex was emplaced from a low-pressure magma chamber, in turn linked to a high-pressure chamber. Both chambers were dynamically complex in terms of the degree of fractionation and residence times of the many small pulses of magma that passed through them. Progressive emplacement of the sill complex probably happened beneath 2 to 2.5 km of seawater and substantially less than 0.5 km of wet sediment.

Acknowledgements

John Korstgård paved the way for BM to work with the Geological Survey of Greenland on Arveprinsen Ejland, as part of the Disko Bugt Project. BM appreciates the support of The University of Technology, Sydney for allowing him to spend time in Greenland and providing financial assistance. He also acknowledges the logistic and financial support of the Geology Department at Aarhus University, Denmark, where he stayed on returning from Greenland. Finally, he expresses appreciation to Heikki Papunen at Turku University, Finland, for providing space whilst this paper was being assembled, and to Franco Mancini for helping to process the chemical data and providing stimulating discussion.

References

Bickle, M.J. 1990: Mantle evolution. In: Hall, R.P. & Hughes, D.J. (eds): Early Precambrian basic magmatism, 111–135. London: Blackie.

Boryta, M. & Condie, K.C. 1990: Geochemistry and origin of the Archaean Beit Bridge complex, Limpopo Belt, South Africa. Journal of the Geological Society (London) **147**, 229–239.

Brooks, E.R., Wood, M.W. & Garbutt, P.L. 1982: Origin and metamorphism of peperite and associated rocks in the Devonian Elwell Formation, northern Sierra Nevada, California. Bulletin of the Geological Society of America **93**, 1208–1231.

Busby-Spera, C. & White, J.D.L. 1987: Variation in peperite textures associated with differing host-sediment properties. Bulletin of Volcanology **49**, 765–775.

Carlisle, D. 1972: Late Paleozoic to Mid-Triassic sedimentary-volcanic sequence on northeastern Vancouver Island. Geological Survey of Canada Paper **72-1 B**, 24–30.

Cas, R.A.F. 1992: Submarine volcanism: eruption styles, products, and relevance to understanding the host-rock successions to volcanic-hosted massive sulphide deposits. Economic Geology **87**, 511–541.

Cas, R.A.F. & Wright, J.V. 1987: Volcanic successions – modern and ancient. A geological approach to processes, products and successions. 529 pp. London: Allen & Unwin.

Cattell, A.C. & Taylor, R.N. 1990: Archaean basic magmas. In: Hall, R.P. & Hughes, D.J. (eds): Early Precambrian basic magmatism, 11–39. London: Blackie.

Condie, K.C. 1990: Geochemical characteristics of Precambrian basaltic greenstones. In: Hall, R.P. & Hughes, D.J. (eds): Early Precambrian basic magmatism, 40–55. London: Blackie.

Einsele, G. 1980: Mechanism of sill intrusion into soft sediment and expulsion of pore water. In: Curray J.R. & Moore D.G. (eds): Initial reports DSDP, **64**, 1169–1176. Washington: U.S. Government Printing Office.

Escher, A. & Burri, M. 1967: Stratigraphy and structural development of the Precambrian rocks in the area north-east of Disko Bugt, West Greenland. Rapport Grønlands Geologiske Undersøgelse **13**, 28 pp.

Furnes, H., Pedersen, R.B., Hertogen, J. & Albrektsen, B.A. 1992: Magma development of the Leka Ophiolite Complex, central Norwegian Caledonides. Lithos **27**, 259–277.

Garde, A.A. 1994: Precambrian geology between Qarajaq Isfjord and Jakobshavn Isfjord, West Greenland, 1:250 000. Copenhagen: Geological Survey of Greenland.

Green, N.L. 1975: Archaean glomeroporphyritic basalts. Canadian Journal of Earth Sciences **12**, 1770–1784.

Habekost, E.M. & Wilson, R. 1989: Raft-like metabasaltic inclusions in the Fongen–Hyllingen layered intrusive complex, Norway, and their implications for magma chamber evolution. Journal of Petrology **30**, 1415–1441.

Hall, R.P. & Hughes, D.J. 1990: Noritic magmatism. In: Hall, R.P. & Hughes, D.J. (eds): Early Precambrian basic magmatism, 833–910. London: Blackie.

Hall, R.P. & Hughes, D.J. 1993: Early Precambrian crustal development: changing styles of mafic magmatism. Journal of the Geological Society (London) **150**, 625–635.

Härme, M. 1980: Kivilajikartan selitys, with English summary. Suomen geologinen yleiskartta – The general geological map of Finland, Lehti-Sheet C1-D1. 95 pp. Helsinki: Geological Survey of Finland.

Hatton, C.J. & Von Gruenewalt, G. 1990: Early Precambrian layered intrusions. In: Hall, R.P. & Hughes, D.J. (eds): Early Precambrian basic magmatism, 56–82. London: Blackie.

Irvine, T.N. & Baragar, W.R.A. 1971: A guide to the chemical classification of the common volcanic rocks. Canadian Journal of Earth Sciences **8**, 523–548.

Jaques, A.L. 1976: An Archaean tholeiitic layered sill from Mt Kilkenny, Western Australia. Journal of the Geological Society of Australia **23**, 157–168.

Jensen, L.S. 1976: A new cation plot for classifying subalkalic volcanic rocks. Ontario Geological Survey Miscellaneous Paper **66**, 22 pp.

Kalsbeek, F., Taylor, P.N. & Pidgeon, R.T. 1988: Unreworked Archaean basement and Proterozoic supracrustal rocks from northeastern Disko Bugt, West Greenland: implications for the nature of Proterozoic mobile belts in Greenland. Canadian Journal of Earth Sciences **25**, 773–782.

Knudsen, C., Appel, P.W.U., Hageskov, B. & Skjernaa, L. 1988: Geological reconnaissance in the Precambrian basement of the Atâ area, central West Greenland. Rapport Grønlands Geologiske Undersøgelse **140**, 9–17.

Kokelaar, B.P. 1982: Fluidization of wet sediments during the emplacement and cooling of various igneous bodies. Journal of the Geological Society (London) **139**, 21–33.

Kokelaar, B.P. 1986: Magma-water interactions in subaqueous and emergent basaltic volcanism. Bulletin of Volcanology **48**, 275–289.

Marshall, B. & Schønwandt, H.K. 1990: Geological investigations of Archaean supracrustals, Arveprinsen's Ejland, Disko Bugt, central west Greenland, 41 pp. Unpublished report, Geological Survey of Greenland, Copenhagen.

Middlemost, E.A.K. 1975: The basalt clan. Earth-Science Reviews **11**, 337–364.

Mullen, E.D. 1983: A minor element discriminant for basaltic rocks of oceanic environments and its implications for petrogenesis. Earth and Planetary Science Letters **62**, 53–62.

Naldrett, A.J. & Mason, G.D. 1968: Contrasting Archaean ultramafic bodies in Dundonald and Clergue Townships, Ontario. Canadian Journal of Earth Sciences **5**, 111–143.

Pearce, J.A. 1983: Role of the sub-continental lithosphere in magma genesis at active continental margins. In: Hawkesworth C.L. & Norry M.J. (eds): Continental basalts and mantle xenoliths, 230–249. Nantwich, UK: Shiva Publishing Ltd.

Pearce, J.A. 1987: An expert system for the tectonic characterization of ancient volcanic rocks. Journal of Volcanolgy and Geothermal Research **32**, 51–65.

Pearce, J.A. & Cann, J.R. 1973: Tectonic setting of basic volcanic rocks determined using trace element analyses. Earth and Planetary Science Letters **19**, 290–300.

Pearce, J.A. & Norry, M.J. 1979: Petrogenetic implications of Ti, Zr, Y, and Nb variations in volcanic rocks. Contributions to Mineralogy and Petrology **69**, 33–47.

Pharaoh T.C. & Pearce, J.A. 1984: Geochemical evidence for the geotectonic setting of Early Proterozoic metavolcanic sequences in Lapland. Precambrian Research **10**, 283–309.

Phinney, W.C., Morrison, D. & Maczga, D.E. 1988: Anorthosites and related megacrystic units in the evolution of Archaean crust. Journal of Petrology **29**, 1283–1323.

Raudsepp, M. & Ayres, L.D. 1982: Emplacement and differentiation of an Archaean subvolcanic metapyroxenite-metagabbro sill in the Favourable Lake area, northwestern Ontario. Canadian Journal of Earth Sciences **19**, 837–858.

Sipilä, P. 1992: The Caledonian Halti–Ridnitsohkka igneous complex in Lapland. Bulletin of the Geological Survey of Finland **362**, 5–75.

Smith, R.L. 1979: Ash-flow magmatism. Geological Society of America Special Paper **180**, 5–27.

Snyder, G.L., Hall, R.P., Hughes, D.J. & Ludwig, K.R. 1990: Early Precambrian basic rocks of the USA. In: Hall, R.P. & Hughes, D.J. (eds): Early Precambrian basic magmatism, 191–220. London: Blackie.

Suominen, V. 1988: Radiometric ages on zircons from a cogenetic gabbro and plagioclase porphyrite suite in Hyvinkää, southern Finland. Bulletin of the Geological Society of Finland **60**, 135–140.

Thompson, R.N., Morrison, M.A., Hendry, G.L. & Parry, S.J. 1984: An assessment of the relative roles of crust and mantle in magma genesis. Philosophical Transactions of the Royal Society of London **A310**, 549–590.

Thurston, P.C. 1990: Early Precambrian basic rocks of the Canadian Shield. In: Hall, R.P. & Hughes, D.J. (eds): Early Precambrian basic magmatism, 221–247. London: Blackie.

Thurston, P.C. & Chivers, K.M. 1990: Secular variation in greenstone sequence development emphasizing Superior Province, Canada. In: Gaal, G. & Groves, D.I. (eds): Precambrian ore deposits related to tectonics. Precambrian Research **46**, 21–58.

Wang, P. & Glover III, L. 1992: A tectonics test of the most commonly used geochemical discriminant diagrams and patterns. Earth-Science Reviews **33**, 111–131.

Williams, H. & McBirney, A.R. 1979: Volcanology, 397 pp. San Francisco: Freeman, Cooper & Co.

Wilson, M. 1989: Igneous petrogenesis, 466 pp. London: Unwin Hyman.

Winchester, J.A. & Floyd, P.A. 1977: Geochemical discrimination of different magma series and their differentiation products using immobile elements. Chemical Geology **20**, 325–343.

The Archaean Atâ intrusive complex (Atâ tonalite), north-east Disko Bugt, West Greenland

Feiko Kalsbeek and Lilian Skjernaa

The 2800 Ma Atâ intrusive complex (elsewhere referred to as 'Atâ granite' or 'Atâ tonalite'), which occupies an area of *c.* 400 km² in the area north-east of Disko Bugt, was emplaced into grey migmatitic gneisses and supracrustal rocks. At its southern border the Atâ complex is cut by younger granites. The complex is divided by a belt of supracrustal rocks into a western, mainly tonalitic part, and an eastern part consisting mainly of granodiorite and trondhjemite. The 'eastern complex' is a classical pluton. It is little deformed in its central part, displaying well-preserved igneous layering and local orbicular textures. Near its intrusive contact with the overlying supracrustal rocks the rocks become foliated, with foliation parallel to the contact. The Atâ intrusive complex has escaped much of the later Archaean and early Proterozoic deformation and metamorphism that characterises the gneisses to the north and to the south; it belongs to the best-preserved Archaean tonalite-trondhjemite-granodiorite intrusions in Greenland.

F.K., *Geological Survey of Denmark and Greenland, Thoravej 8, DK-2400 Copenhagen NV, Denmark.* E-mail: *fk@geus.dk.*
L.S., *Geological Institute, University of Copenhagen, Øster Voldgade 10, DK-1350 Copenhagen K, Denmark.*

Keywords: Archaean, Disko Bugt, pluton, tonalite, West Greenland

The area north-east of Disko Bugt consists mainly of polyphase Archaean grey gneisses and sequences of Archaean and Proterozoic supracrustal rocks (Garde & Steenfelt 1999, this volume). An approximately 400 km² large area is occupied by relatively homogeneous granitoid rocks, tonalitic to granodioritic in composition: the 'Atâ granite' of Escher & Burri (1967; Fig. 1). On the geological maps of Garde (1994) and Escher (1995) these rocks are shown as 'Atâ Tonalite' and the 'Atâ pluton', respectively. In this report we present a general description of the rocks and a regional survey of their composition and fabric. Because most of the rocks are not granitic, and have variable compositions, we refer to them here as the 'Atâ intrusive complex', or the 'Atâ complex'. The complex consists of two main outcrop areas, separated by a north–south-running belt of mafic metavolcanic rocks (Fig. 1). We will refer to these areas as the 'western' and 'eastern' Atâ complex where appropriate, and to the metavolcanics as the 'central supracrustal belt'.

Apart from the study of the complex on foot, a collection of 100 grid samples was prepared with a 2 km grid point distance in order to obtain a statistically reliable impression of the regional variation in composition and rock fabric.

Rocks similar to Atâ granitoids occur throughout the area north-east of Disko Bugt. Some of these (see, for example, Higgins & Soper 1999, this volume) may be similar in age and origin to the Atâ intrusive complex. Because of the uncertainty of lithological correlations, however, the present study is restricted to the rocks originally mapped as Atâ granite by Escher & Burri (1967).

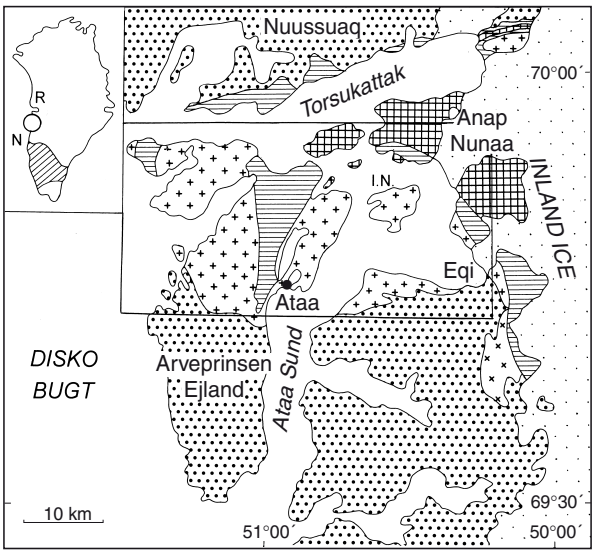

Fig. 1. Geological sketch map of the area north-east of Disko Bugt with the Atâ intrusive complex. Area covered by Figs 3 and 6 outlined. Inset shows the location of the Ataa region in Greenland (circle) between the early Proterozoic Nagssugtoqidian and Rinkian orogenic belts (N and R, respectively). I.N.: Illuluarsuit Nunataat.

Regional setting and earlier investigations

Escher & Burri (1967) were the first to map and describe the Atâ intrusive complex in some detail. The granitoid rocks of the complex separate regional gneisses (to the south) from sequences of supracrustal rocks (Fig. 1), and Escher & Burri (1967) believed that they were formed by granitisation of the gneisses and overlying supracrustals. Kalsbeek *et al.* (1988) dated samples from the eastern Atâ complex at *c.* 2800 Ma (whole-rock Rb-Sr, Pb-Pb, Sm-Nd and zircon U-Pb data), and this age has recently been confirmed by a SHRIMP U-Pb zircon date of 2803 ± 4 Ma (Nutman & Kalsbeek 1999, this volume). Gneisses to the south, believed to represent deformed Atâ granitoids, yielded a Rb-Sr whole-rock isochron age of *c.* 2670 Ma, which Kalsbeek *et al.* (1988) interpreted as dating an event of deformation and migmatisation during which Atâ granitoids were transformed into grey gneisses.

Escher & Burri (1967) described the plutonic rocks as sheared granodiorites and quartz diorites in the marginal parts of the body, grading into well-preserved granite in the central part. Samples studied by Kalsbeek *et al.* (1988) varied between tonalite-trondhjemite and granodiorite. One of the aims of the present investigation was to study the distribution of granites, granodiorites and tonalitic varieties within the Atâ complex in more detail.

At many localities, for example near the abandoned village Ataa, the rocks of the Atâ complex contain a multitude of felsic dykes, a few tens of centimetres wide, cutting each other, and running in many different directions (Kalsbeek *et al.* 1988). Often these dykes are hardly or not deformed and display well-preserved magmatic structures, even where the host rock shows a distinct planar fabric. Isotope data from these dykes fall near the *c.* 2800 Ma Rb-Sr and Pb-Pb isochrons defined by the surrounding rocks. The dykes were therefore interpreted to be of Archaean origin, and Kalsbeek *et al.* (1988) believed that the pattern of veins and dykelets was related to a system of cooling joints in the main granitoid body. Based on the state of preservation of the dykes, Kalsbeek *et al.* (1988) concluded that later Archaean and Proterozoic deformation of these rocks was insignificant.

Field investigations

The Atâ complex is well exposed, but at most inland localities the bed rock is heavily covered with lichen, and geological details can often only be studied in coastal outcrops.

The rocks are medium grained and have light- to dark-grey colours. Locally igneous layering is well preserved (Fig. 2A). At several localities felsic granitoid phases intrude darker, foliated rocks, and in coastal outcrops east of Ataa large inclusions of foliated, darker rock were observed within more felsic granitoids. Apparently the Atâ complex is polyphase, but boundaries between different phases are difficult to map inland.

Border relationships

Atâ granitoids commonly have sharp intrusive borders towards the surrounding supracrustal rocks. West of Ataa, for example, sheets of Atâ granodiorite cut into supracrustal amphibolites. Intrusive breccias have been observed at the border between the western Atâ com-

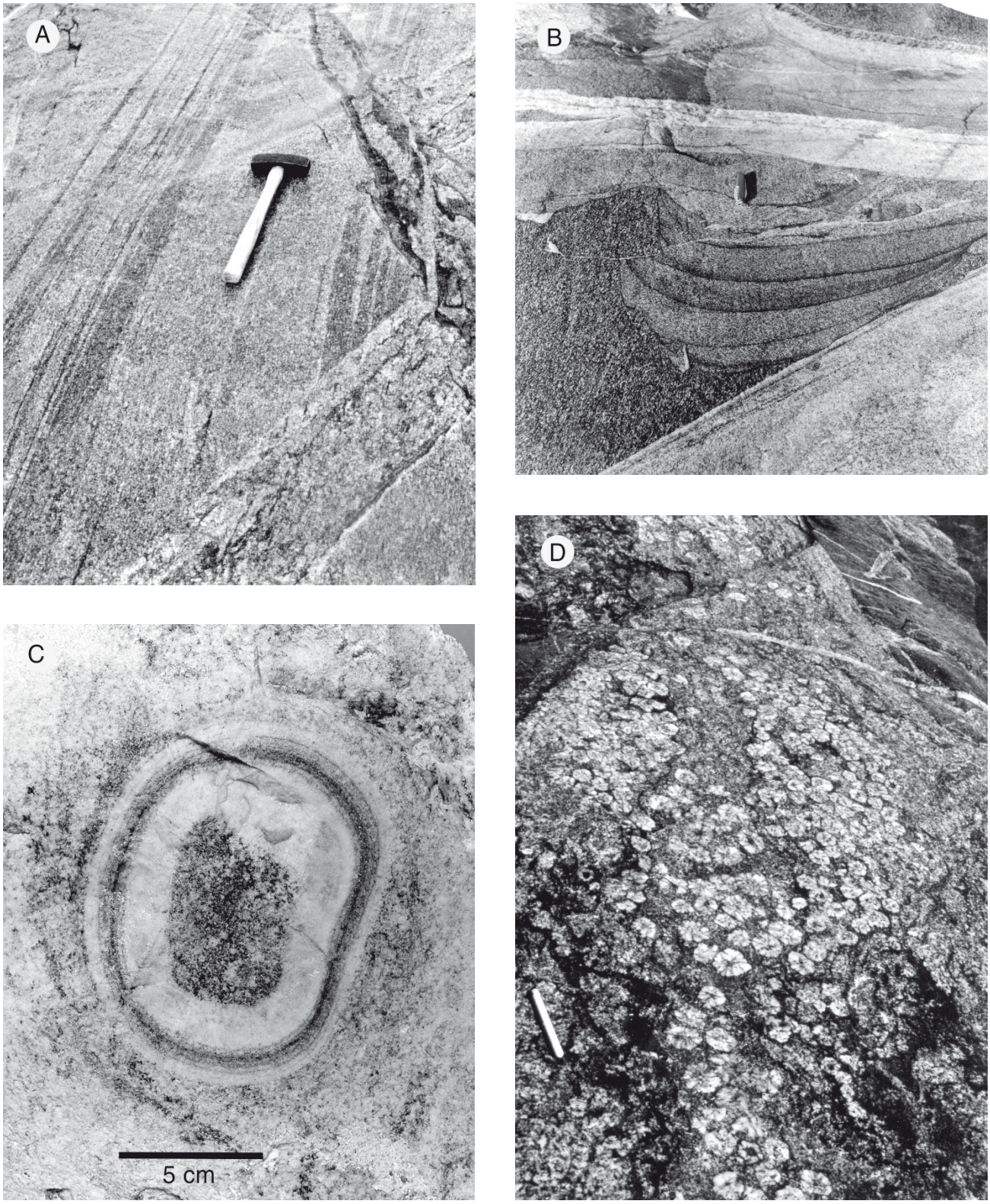

Fig. 2. **A**: Igneous layering in Atâ granitoids cut by various dykes, south-east coast of Illuluarsuit Nunataat. **B**: Trough layering in late granitoid dyke at Ataa; pocket knife for scale. **C**: Orbicule in Atâ granodiorite, south-east coast of Illuluarsuit Nunataat; largest diameter of orbicule 13 cm. **D**: Flower-like orbicular fabric in dyke within Atâ granodiorite, south-east coast of Illuluarsuit Nunataat; orbicules are up to *c*. 5 cm in diameter (pencil for scale).

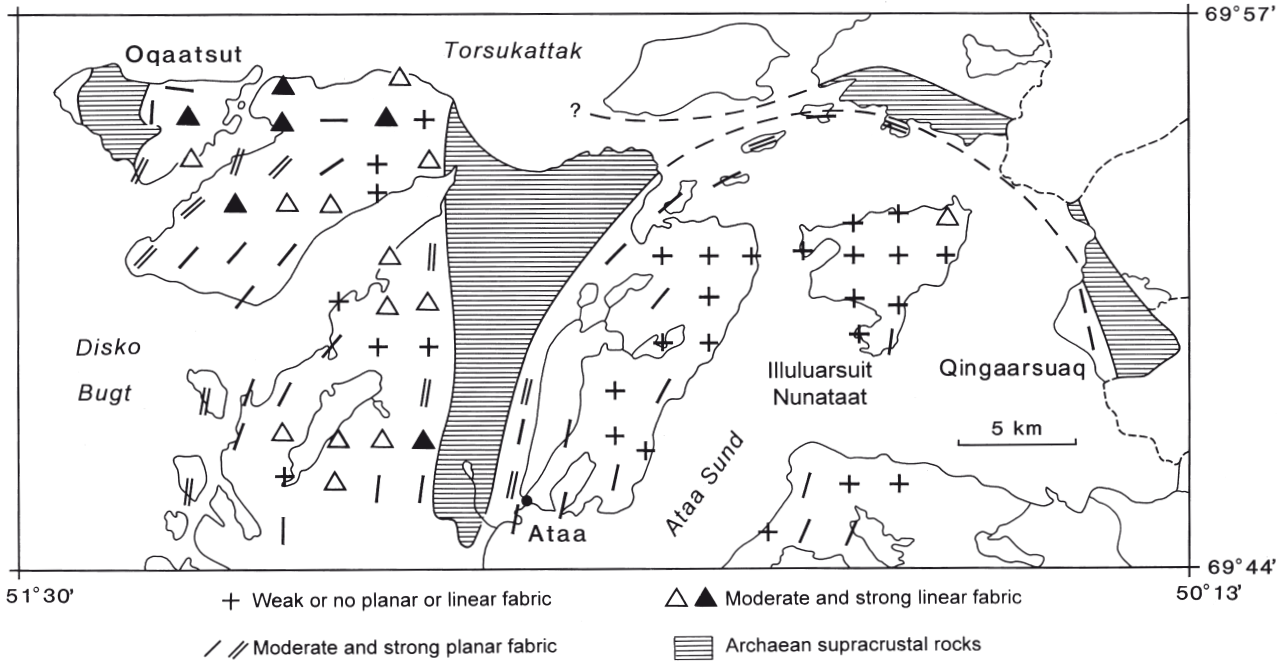

Fig. 3. Variation in intensity of rock fabrics within the Atâ intrusive complex based on the study of 100 grid samples (see text). Orientation of foliation from field observations; orientation of linear structures is not well known.

plex and the central supracrustal belt on the north coast of Arveprinsen Ejland. Over large distances, however, such features are not observed, and there is just a sharp, commonly strongly sheared border between homogeneous Atâ granitoids and homogeneous amphibolite. Rafts and inclusions of amphibolite and metagabbroic rocks in the Atâ complex occur locally, but are not common.

Towards the south the Atâ complex borders migmatitic grey gneisses, and boundary relations are here more difficult to establish. Local observations show three different relationships: (1) granitoid rocks of the eastern Atâ complex intrude into older gneisses on the mainland south of Illuluarsuit Nunataat; (2) southward on Arveprinsen Ejland and on the mainland, Atâ granitoids become increasingly folded and migmatised and lose their identity as Atâ rocks; (3) on Arveprinsen Ejland the western Atâ complex is locally intruded in the south by younger granitoid rocks, and deformed together with these. A sample of such a younger granite has yielded a SHRIMP U-Pb zircon age of 2758 ± 2 Ma (Nutman & Kalsbeek 1999, this volume). The younger granites may contain large rafts and inclusions of folded and migmatised Atâ granitoids. Because of imperfect exposure and similarity of the different rock types it is not possible to map the southern border of the Atâ complex in any detail.

Fabric

The granitoid rocks of the Atâ complex commonly exhibit a foliation or lineation of variable intensity. Mapping variations in fabric intensities was not possible in the field, partly because of heavy lichen cover. Therefore, an attempt was made to quantify fabric intensity throughout the Atâ intrusive complex with the help of the grid sample collection. Fabric intensities were graded for individual samples on a scale from 0 to 5 (0 = no visible foliation or lineation; 5 = strong planar or linear fabric). Grading was carried out independently by both authors with very similar results. Figure 3 shows the results of this approach: within the eastern Atâ complex there is a large area within which tectonic fabrics are poorly developed. Towards the supracrustal rocks this area is surrounded by increasingly gneissified granitoids. The foliation is here everywhere parallel with the border of the complex, turning from NE on Arveprinsen Ejland through E–W in the north to SE on Qingaarsuaq in the east (Fig. 3). Along the north coast of Illuluarsuit Nunataat, where only a very weak planar fabric is visible, this follows the same pattern, from ENE in the west over E–W to SE in the north-eastern corner of the island. Where igneous layering is visible, the foliation is normally parallel to it. All these features suggest that this weak

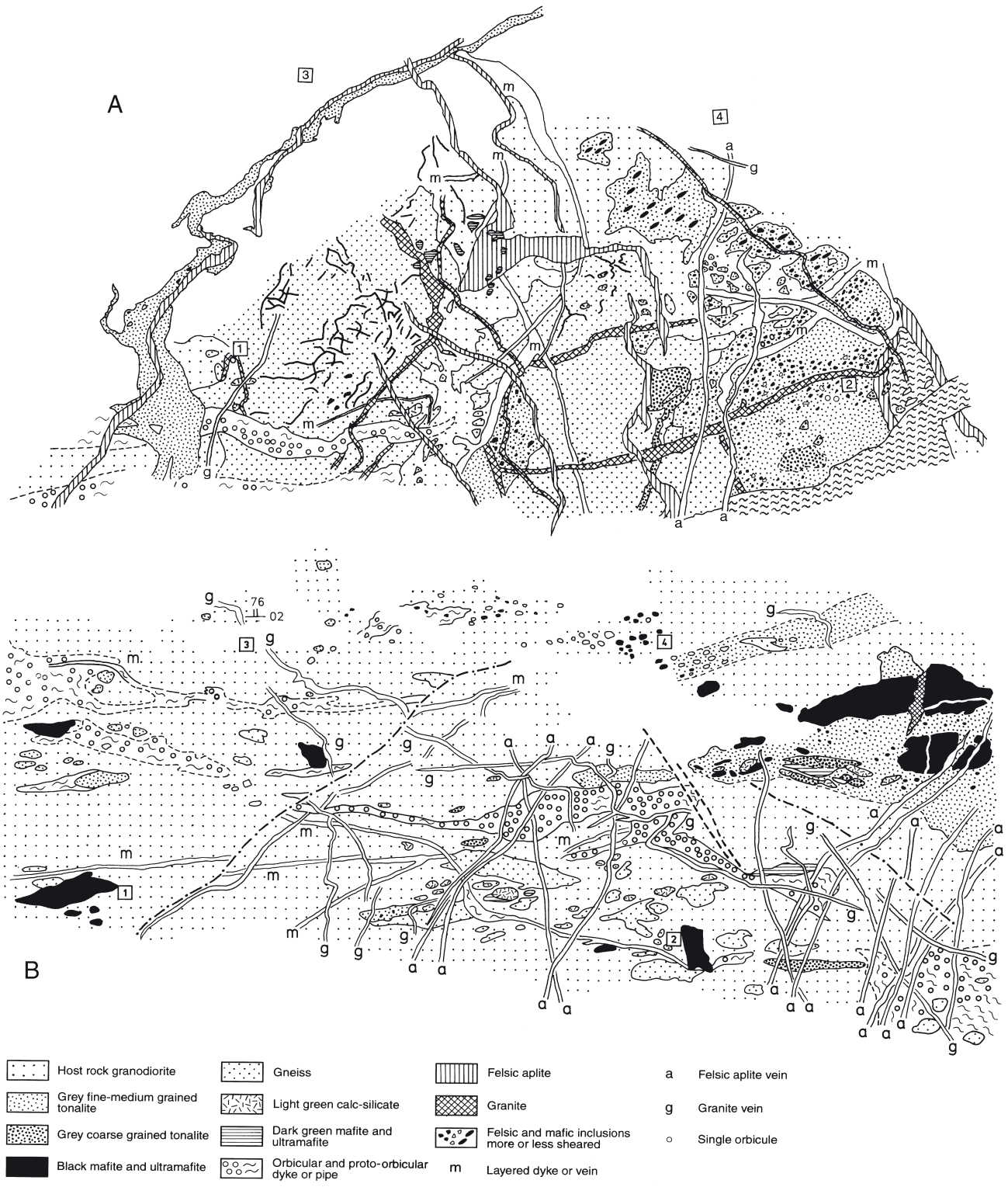

Fig. 4. **A**, **B**: Coastal outcrops on south-east Illuluarsuit Nunataat mapped in the field on photographs. Not to scale: points 1, 2, 3 and 4 mark the corners of squares with 20 m side length. Area covered by **A** is dominated by inclusions; that of **B** by Atâ granodiorite. Orbicules are rare outside the irregular dykes, but a few occur near point 2 in **A** and point 4 in **B**. Strike and dip symbol in **B** (near 3) shows the orientation of igneous layering.

fabric is due to magma flow rather than to later deformation. Petrographic observations (see p. 109) support this suggestion.

In the western complex, Atâ granitoids often exhibit a well-developed planar or linear fabric, but even in the most strongly sheared rock undeformed (Archaean) felsic dykes may be found, indicating that most of the deformation took place during or shortly after emplacement of the complex. In areas of weak deformation the rock commonly has a linear rather than a planar fabric. Due to lichen cover it is nearly impossible to measure the orientation of the lineation with any precision; in general it appears to plunge moderately to steeply east.

Felsic dykes and orbicular textures

In the southern parts of its outcrop area the rocks of the Atâ complex contain numerous felsic dykes (Fig. 4). They range up to *c.* 50 cm in width and consist of fine-grained granitoid rocks in different shades of grey, within which magmatic layering may locally be well preserved (Fig. 2B). Locally pink pegmatite dykes are also common. Some dykes exhibit beautifully preserved orbicular textures (Fig. 2D, see below).

The dykes show complex cross-cutting relationships; at some localities up to ten successive generations of veins and dykes can be distinguished. The dykes cut the foliation in the surrounding granitoid rocks, though some themselves have a planar fabric clearly discordant to that of the host rock, and often subparallel with the dyke margins. It is not uncommon to find foliated dykes cutting unfoliated ones. This suggests that the fabric is related to deformation during consolidation of the cross-cutting dyke, at a time when older dykes had already totally solidified and therefore were less susceptible to penetrative deformation. Near the southern margin of the Atâ complex the dykes are commonly folded, but folded dykes are locally cut by undeformed ones, confirming the polyphase origin of the dykes.

Felsic dykes are especially numerous around Ataa, in the southern part of Illuluarsuit Nunataat and on the mainland to the south. They become gradually less common in northward direction, and in the northern parts of the complex dykes are very rare. It is therefore possible that at least the later dykes are related to the granitoid rocks which intrude the Atâ complex at its southern margin. We do not have sufficient chronological information on the felsic dykes to substantiate this suggestion.

Granitoid rocks with spectacular orbicular textures (Fig. 2C) occur on the south-east coast of Illuluarsuit Nunataat. Orbicules and less well-developed proto-orbicules most commonly occur in irregular dykes and pipes but have also been locally observed in the granodioritic host rock (Fig. 4). The orbicules consist mainly of quartz and feldspar; commonly they show rhythmic zonation, and sometimes they have a core similar to the local Atâ granodiorite (Fig. 2C). Another kind of orbicular bodies, composed of quartz, feldspar and minor biotite, arranged into a radial pattern to form flower-like aggregates a few centimetres across (Fig. 2D), was found in a late flat-lying dyke in the same area.

The outcrops which contain orbicular dykes and pipes show extremely complex structures. Atâ granitoids here have a large variety of variably deformed supracrustal and granitoid inclusions, some of which contain second-order inclusions. A large number of veins of different compositions and generations cross-cut the Atâ granodiorite as well as the inclusions and the orbicular dykes. Only a few layered dykes or veins appear to be older than the orbicular granite.

Elliston (1984) has given convincing evidence that formation of orbicules takes place in a hydrous silica gel during alternating static and dynamic conditions, and that the occurrence of orbicules indicates crystallisation of hydrosilicates. The orbicular textures thus may suggest this locality lies near the roof of the eastern Atâ complex, where water was available to react with the granitoid magma. The presence of abundant inclusions would be consistent with this suggestion, but igneous layering here dips steeply to the east.

Petrography

Mineralogical composition

Samples of the Atâ complex consist mainly of plagioclase (oligoclase to andesine) and quartz, with variable proportions of K-feldspar, biotite and hornblende. K-feldspar in any significant proportion and hornblende do not occur together in the same sample; this is a common feature in basement gneisses in Greenland, biotite taking the place of hornblende + K-feldspar. Apatite, zircon, titanite and allanite are common accessories, and opaque minerals occur in minor proportions. In many samples the plagioclase is partly replaced by epidote and fine-grained white mica; chlorite commonly replaces biotite.

Modal compositions of samples from the complex

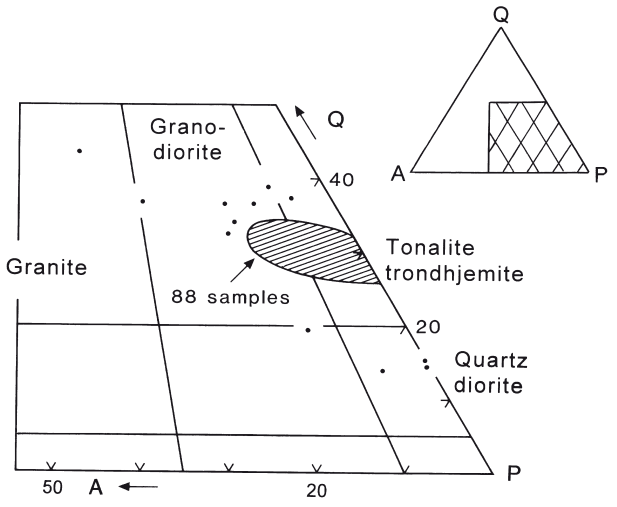

Fig. 5. Streckeisen QAP (Quartz – Alkali feldspar – Plagioclase) diagram showing the modal composition of 100 grid samples from the Atâ intrusive complex. The mode was calculated from the chemical composition of the rocks, see text.

were estimated with help of chemical analyses (see p. 110). Plotted in the Streckeisen (1976) Quartz (Q) – Alkali feldspar (A) – Plagioclase (P) diagram (Fig. 5), most samples fall in the fields of tonalite-trondhjemite and granodiorite.

Fabric

In most samples the rock is medium grained. Plagioclase commonly forms subhedral crystals a few millimetres long, with length to width ratios of the order of 1.5. Some samples have K-feldspar megacrysts up to *c.* 1 cm, with inclusions of euhedral plagioclase up to a few millimetres. Quartz is recrystallised to more fine-grained mosaics with irregular crystal boundaries.

In many samples with weak to moderately well-developed foliation, plagioclase crystals have a preferred orientation, parallel to the foliation. This fabric is often not very pronounced because of the moderate elongation of the plagioclase crystals. Biotite shows a preferred orientation parallel to that of plagioclase, but also this is not always very distinct. In many samples there is no evidence of deformation of the rock-forming minerals to explain the alignment of plagioclase and biotite crystals. This suggests that the foliation in these rocks is due to magmatic flow rather than later deformation (Paterson *et al.* 1989).

Samples with a more pronounced foliation probably underwent additional subsolidus deformation. In some cases trains of biotite crystals wrap around plagioclase, and sometimes quartz has recrystallised into ribbons parallel with the foliation. Because of sub-

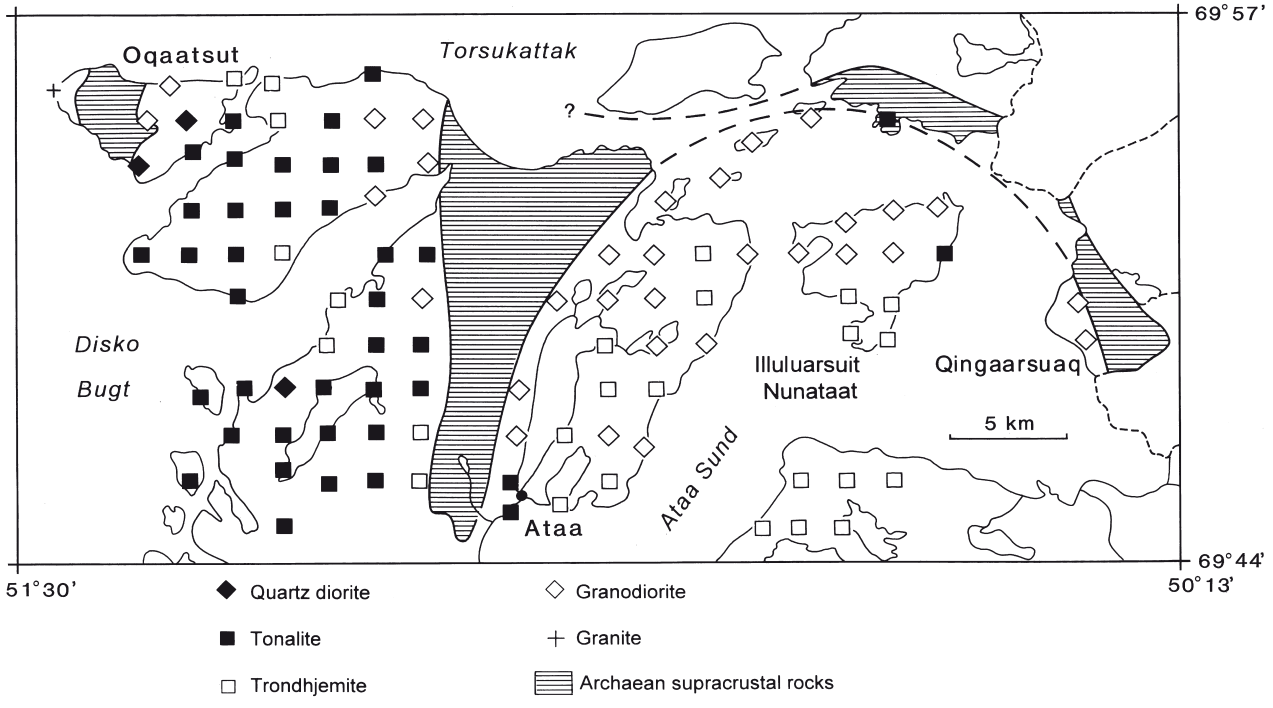

Fig. 6. Distribution of rock types within the Atâ intrusive complex. Rock classification according to Streckeisen (1976) with modal compositions calculated from the chemical compositions (see text).

Table 1. Chemical composition of selected samples from the Atâ intrusive complex

GGU no.	348655 Qd (W)	348621 To (W)	349650 To (E)	348625 Tr (E)	348697 Gd (E)
SiO_2	61.41	66.68	69.84	70.45	72.36
TiO_2	0.54	0.44	0.39	0.33	0.23
Al_2O_3	18.62	15.76	15.25	14.85	14.84
Fe_2O_3*	4.70	3.82	2.96	2.51	1.96
MnO	0.05	0.05	0.03	0.03	0.02
MgO	1.83	1.57	1.02	0.75	0.55
CaO	5.78	4.07	3.29	2.81	2.33
Na_2O	5.29	4.32	4.62	4.62	4.61
K_2O	0.66	1.38	1.36	1.86	2.36
P_2O_5	0.17	0.13	0.12	0.08	0.06
l.o.i.	0.20	0.60	0.80	0.50	0.60
Sum	99.25	98.82	99.68	98.79	99.92
Rb	16	37	38	56	57
Ba	266	402	510	562	866
Pb	7	8	9	13	9
Sr	603	460	478	407	370
La	14	21	21	20	19
Ce	36	40	42	36	33
Nd	19	17	15	16	15
Y	10	9	8	10	6
Th	3	7	7	8	6
Zr	79	121	155	133	120
Nb	2.1	3.9	3.4	4.8	3.1
Zn	62	68	65	63	54
Cu	55	10	9	14	5
Ni	16	14	5	5	4
Sc	10	6	3	3	2
V	77	54	35	28	20
Cr	26	15	8	7	8
Ga	21	19	19	19	18
Cation norm					
cor	–	0.08	0.54	0.36	0.67
qz	10.67	22.29	26.34	26.71	27.91
or	3.92	8.35	8.17	11.23	14.09
ab	47.70	39.72	42.17	42.40	41.83
an	25.22	19.81	15.80	13.72	11.29
di	1.97	–	–	–	–
hy	8.82	8.37	5.81	4.63	3.51
mt	0.59	0.49	0.37	0.32	0.25
il	0.76	0.63	0.55	0.47	0.32
ap	0.36	0.28	0.26	0.17	0.13

Major elements analysed at Activation Laboratories Ltd, Canada, by XRF on glass discs.
Fe_2O_3*: all iron reported as Fe_2O_3.
Trace elements were determined by XRF on powder tablets at the Institute of Geology, University of Copenhagen, Denmark.
Qd: quartzdiorite.
To: tonalite.
Tr: trondhjemite.
Gd: granodiorite.
The letters W and E indicate whether the samples are from the western or eastern Atâ complex.

solidus recrystallisation and alteration of the igneous minerals it is not always easy to differentiate the effects of magmatic flow and later subsolidus deformation in individual samples.

Chemical composition

To obtain statistically reliable information on the composition of the Atâ complex, aliquots of all samples from the grid collection were chemically analysed. Chemical data were acquired from Activation Laboratories Ltd., Canada; a few representative analyses are shown in Table 1.

Cation norms, with orthoclase + hypersthene recalculated into equivalent proportions of biotite + quartz (5 or + 6 hy = 8 bi + 3 qz), were used as an estimate of the modal composition of the rock. Because most samples contain only moderate amounts of mafic minerals (< 15%), this probably yields a fair approximation of the true modal composition. According to the calculations most samples classify as tonalites or trondhjemites (leuco-tonalite with < 10% mafic minerals), about one third are granodiorites, a few are quartz diorites and one is a granite (Fig. 5). There is a clear distinction between the areas west and east of the central supracrustal belt of Arveprinsen Ejland. Nearly all samples to the west are tonalites, whereas to the east trondhjemites and granodiorites are predominant (Fig. 6). This difference suggests that the eastern and western outcrop areas of Atâ granitoids may represent independent intrusions.

The only true granite in the collection is from the western tip of the island Oqaatsut north-west of Arveprinsen Ejland (Fig. 6); it is also the only muscovite-rich sample. Two other samples from Oqaatsut also have high proportions of K-feldspar relative to other Atâ granitoids. It is not clear how far these rocks relate to the Atâ complex.

Discussion, summary and conclusions

Atâ granitoids outcrop in two main areas, west and east of a belt of basic metavolcanic rocks in the northern part of Arveprinsen Ejland. The western and eastern outcrops differ in composition and may represent two independent intrusions.

The western area is dominated by tonalitic rocks, variably transformed into (hornblende-) biotite gneisses.

This body may represent a several kilometres wide sheet intruded into supracrustal rocks.

The eastern body consists mainly of trondhjemites and granodiorites, and forms a classic pluton. In its central part the rocks are often almost devoid of planar or linear fabric, and where preferred mineral orientations are visible these are probably the result of magmatic flow, parallel with the border of the pluton. Towards the margin the foliation becomes more intense. This is the result of subsolidus deformation, which probably followed soon after solidification, because many of the late granitoid veins are totally undeformed. Deformation in the marginal parts of plutons is commonly ascribed to 'ballooning' of the magmatic interior of a pluton, related to buoyancy forces or to the intrusion of new magmatic pulses (e.g. Paterson *et al.* 1989). Magmatic features such as mineral layering and orbicular fabrics are locally beautifully preserved within the eastern pluton. Altogether, this is probably one of the best preserved Archaean trondhjemite-granodiorite intrusions in Greenland, having escaped both later Archaean and early Proterozoic deformation and metamorphism. Even the Archaean K-Ar isotope systems in hornblende from metagabbroic inclusions in the Atâ complex are preserved in this area (Rasmussen & Holm 1999, this volume).

Towards the south the Atâ granitoids grade into the regional grey migmatitic gneisses. Atâ granitoids become deformed and migmatised and intruded by younger granitoid phases. Elsewhere, rocks of the Atâ complex intrude somewhat older gneisses (see Nutman & Kalsbeek 1999, this volume). Gneisses in the area south of the Atâ complex have undergone a complex history of Archaean and Proterozoic deformation (Escher *et al.* 1999; Grocott & Davies 1999, both in this volume). If rocks once belonging to the Atâ complex occur there, they cannot be recognised as such.

Archaean regions can be divided into two types: (1) granulite–gneiss terrains, consisting mainly of grey migmatitic gneisses, and (2) granite–greenstone belt terrains (e.g. Windley 1984). The area within which the Atâ complex is exposed has the characteristics of a granite–greenstone terrain: relatively low-grade basic supracrustal rocks being intruded by tonalite–granodiorite plutons. Such terrains cover large parts of Canada, South Africa and Australia (see e.g. Windley 1984) but are rare in Greenland. In north-eastern Disko Bugt there is a rapid transition between the 'granite-greenstone' terrain of northern Arveprinsen Ejland and Illuluarsuit Nunataat, and the 'grey gneiss' terrain of southern Arveprinsen Ejland and the mainland east of Ataa Sund. There is no doubt that this change in character of the rocks is due to later deformation and metamorphism in the south.

Kalsbeek *et al.* (1988) speculated that, since the Ataa region had largely escaped the early Proterozoic deformation and high-grade metamorphism that characterise the Nagssugtoqidian and Rinkian belts, to the south and to the north respectively, it did not belong to either of these belts. However, structural investigations (Escher *et al.* 1999; Garde & Steenfelt 1999; Grocott & Davies 1999, all in this volume) have shown that the area north-east of Disko Bugt, like the Rinkian belt, is characterised by large west- and north-west-directed thrust sheets. These studies suggest that the Atâ intrusive complex may lie within one of these thrust sheets, with early Proterozoic deformation concentrated along the thrust boundaries, without affecting the Atâ complex itself.

References

Elliston, J.N. 1984: Orbicules: an indication of the crystallisation of hydrosilicates, I. Earth-Science Reviews **20**, 265–344.

Escher, A. & Burri, M. 1967: Stratigraphy and structural development of the Precambrian rocks in the area north-east of Disko Bugt, West Greenland. Rapport Grønlands Geologiske Undersøgelse **13**, 28 pp.

Escher, J.C. 1995: Geological map of Greenland, 1:100 000, Ataa 69 V.3 Nord. Copenhagen: Geological Survey of Greenland.

Escher, J.C., Ryan, M.J. & Marker, M. 1999: Early Proterozoic thrust tectonics east of Ataa Sund, north-east Disko Bugt, West Greenland. In: Kalsbeek, F. (ed.): Precambrian geology of the Disko Bugt region, West Greenland. Geology of Greenland Survey Bulletin **181**, 171–179 (this volume).

Garde, A.A. 1994: Precambrian geology between Qarajaq Isfjord and Jakobshavn Isfjord, West Greenland, 1:250 000. Copenhagen: Geological Survey of Greenland.

Garde, A.A. & Steenfelt, A. 1999: Precambrian geology of Nuussuaq and the area north-east of Disko Bugt, West Greenland. In: Kalsbeek, F. (ed.): Precambrian geology of the Disko Bugt region, West Greenland. Geology of Greenland Survey Bulletin **181**, 6–40 (this volume).

Grocott, J. & Davies, S.C. 1999: Deformation at the southern boundary of the late Archaean Atâ tonalite and the extent of Proterozoic reworking of the Disko terrane, West Greenland. In: Kalsbeek, F. (ed.): Precambrian geology of the Disko Bugt region, West Greenland. Geology of Greenland Survey Bulletin **181**, 155–169 (this volume).

Higgins, A.K. & Soper, N.J. 1999: The Precambrian supracrustal rocks of Nunataq, north-east Disko Bugt, West Greenland. In: Kalsbeek, F. (ed.): Precambrian geology of the Disko

Bugt region, West Greenland. Geology of Greenland Survey Bulletin **181**, 79–86 (this volume).

Kalsbeek, F., Taylor, P.N. & Pidgeon, R.T. 1988: Unreworked Archaean basement and Proterozoic supracrustal rocks from north-eastern Disko Bugt, West Greenland: implications for the nature of Proterozoic mobile belts in Greenland. Canadian Journal of Earth Sciences **25**, 773–782.

Nutman, A.P. & Kalsbeek, F. 1999: SHRIMP U-Pb zircon ages for Archaean granitoid rocks, Ataa area, north-east Disko Bugt, West Greenland. In: Kalsbeek, F. (ed.): Precambrian geology of the Disko Bugt region, West Greenland. Geology of Greenland Survey Bulletin **181**, 49–54 (this volume).

Paterson, S.R., Vernon, R.H. & Tobisch, O.T. 1989: A review of criteria for the identification of magmatic and tectonic foliations in granitoids. Journal of Structural Geology **11**, 249–363.

Rasmussen, H. & Holm, P.M. 1999: Proterozoic thermal activity in the Archaean basement of the Disko Bugt region and eastern Nuussuaq, West Greenland: evidence from K-Ar and ^{40}Ar-^{39}Ar mineral age investigations. In: Kalsbeek, F. (ed.): Precambrian geology of the Disko Bugt region, West Greenland. Geology of Greenland Survey Bulletin **181**, 55–64 (this volume).

Streckeisen, A.L. 1976: To each plutonic rock its proper name. Earth-Science Reviews **12**, 1–33.

Windley, B.F. 1984: The evolving continents, 2nd edition, 399 pp. Chichester, UK: John Wiley & Sons.

Albitised gneisses in the area between Paakitsoq and Kangerluarsuk, north-east Disko Bugt, West Greenland

Michael J. Ryan and Jan C. Escher

Fine-grained rutile-bearing albite-rich rocks (> 95% albite) locally replace Archaean granodioritic orthogneisses in the area between Paakitsoq and Kangerluarsuk, eastern Disko Bugt. They occur as anastomosing networks within albite-rich gneiss and as replacements along linear fracture zones. Albitisation resulted from pervasive metasomatism, but the origin and nature of the albitising fluids are uncertain. A tentative comparison is made with rutile-rich albitites ('kragerøites') in southern Norway.

M.J.R., *Department of Geology, University of Portsmouth, Portsmouth PO1 3HE, UK.* E-mail: *michael.ryan@port.ac.uk.*
J.C.E., *Geological Survey of Denmark and Greenland, Thoravej 8, DK-2400 Copenhagen NV, Denmark.*

Keywords: albitisation, Archaean rocks, Disko Bugt, West Greenland

Albitised siltstones on the island Qeqertakassak, north-eastern Disko Bugt, have been described by Kalsbeek (1992). They occur within Proterozoic supracrustal rocks, the Anap nunâ Group, overlying Archaean supracrustals, granitoids and gneisses (Garde & Steenfelt 1999, this volume). Their transformation from siltstone to albitite was shown to be the result of pervasive metasomatism, possibly in two phases: one diagenetic and the other syn- or post-tectonic. Rocks comprising albite (65–75%) with quartz (10–20%) and dolomite (10–15%) were produced.

This account deals with albitised gneisses that were found during reconnaissance mapping in 1991. They occur about 45 km south of Qeqertakassak in the area between the fjords Paakitsoq and Kangerluarsuk (Fig. 1). Here distinctive, bright, white, sugary-textured, albite-rich rocks replace the pre-existing gneisses, relics of which can be seen gradually disappearing in the albitite (Fig. 2A). Rutile is a conspicuous accessory mineral in hand-samples together with apatite and zircon in thin sections.

The occurrence of albite-rich rocks was reviewed by Kalsbeek (1992) who noted that their mode of formation is not always certain. Brøgger (1935) gave the name 'kragerøite' to rocks consisting almost entirely of albite and rutile that occur in and around the town of Kragerø on the coast of southern Norway. Here upper amphibolite facies gneisses, metavolcanic rocks and metasediments of the middle Proterozoic Bamble Formation have been intruded by a suite of gabbros with associated pneumatolitic, metasomatic NaCl-scapolite bearing rocks, apatite ± rutile bearing dykes and veins, rutile-albitites and albitised breccias. Rutile segregation produced 'rutilite' bodies of up to several hundred tons that were mined commercially earlier this century.

Although the rutile-bearing albitites of eastern Disko Bugt are far more limited in size and extent, they show some similarities with the Norwegian occurrences, particularly with respect to their mineral assemblages, but not regarding the associated rock suite.

Field relations

The main area of albitised gneisses occurs along the northern shore of Paakitsoq and Paakitsup Ilorlia. Here they outcrop along a *c.* 800 m coastal section at A (Fig.

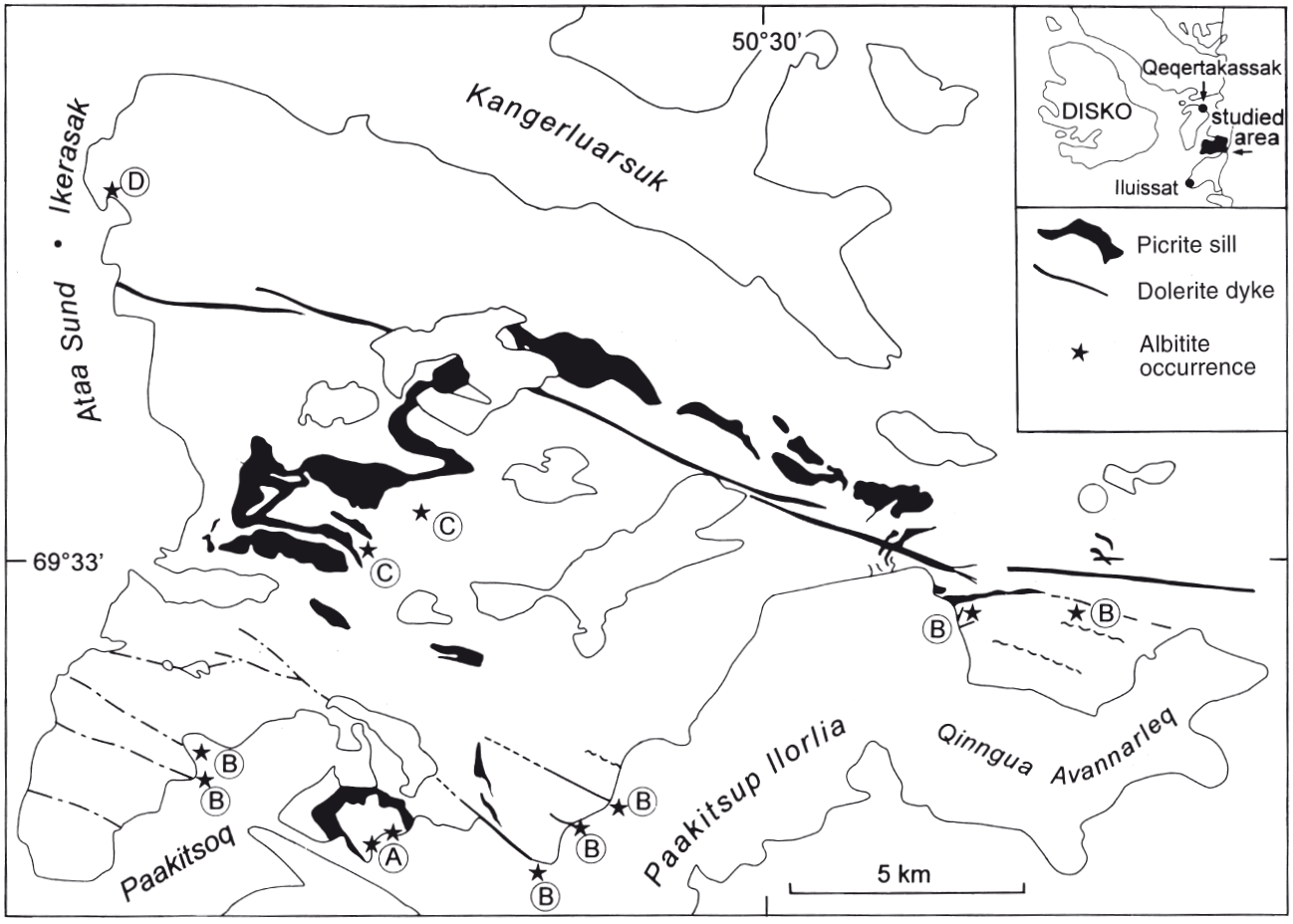

Fig. 1. Map showing localities of albitised gneisses (stars marked A–C) between Paakitsoq and Kangerluarsuk, eastern Disko Bugt. For explanation of A, B, etc. see text.

1); their inland extent is not known. To the east and west, linear fracture zones are albitised and reddened (B) and *c.* 7 km to the north of A there are two seemingly isolated areas of albitite (C), also of unknown extent. A thin albitised zone outcrops in the walls of Ataa Sund (D).

The main occurrence (A) lies close to a major zone of augen gneisses, cataclasites and mylonites that runs WNW–ESE along the narrow channel entrance to Paakitsup Ilorlia (Fig. 1). The western margin of this albitised zone is a rapid transition from unaltered gneiss through albitised gneiss with relict schlieren of gneiss (Fig. 2A) to almost pure, white albitite, over a distance of 5–10 m. At least two phases of albitisation can be recognised in the field (Fig. 2B) and at one location a small, millimetre-scale veinlet of rutile provides evidence of small-scale rutile segregation. Figure 2C shows a thin, pink albitite vein cross-cutting the gneiss foliation. The vein has a gradational contact, albeit rapid gradational over a few centimetres, and it appears to be a non-dilational vein of replacement type. To the east the albitites are in contact with an ultramafic sill which is not albitised and, therefore, could be presumed to be younger than the albitisation event. On the other hand, the fact that in most cases the albitites lie close to, and structurally above, the extensive sill complex (see Fig. 1) might indicate that they are related genetically, with the sill providing the heat for a hot brines '*per descensum*' model (see p. 117).

Of the three linear zones (B) outcropping in the north-western wall of Paakitsup Ilorlia, the western one contains both white albitite and a massive, reddened, epidotised rock. The middle zone consists of 15 m of white albitite and the eastern one has a massive, pinkish-grey, homogeneous, partly brecciated 'gneiss' adjacent to massive, white albitite, 15–20 m wide.

Fig. 2. Field occurrence of albitites. **A**: Gneiss remnants within white sugary-textured albitite. **B**: Partially albitised gneiss with an anastomosing replacement-type network of albitite, formed in two successive phases of albitisation. **C**: Albitite vein (*c.* 20 cm thick) formed by replacement along a fracture cutting the gneiss foliation.

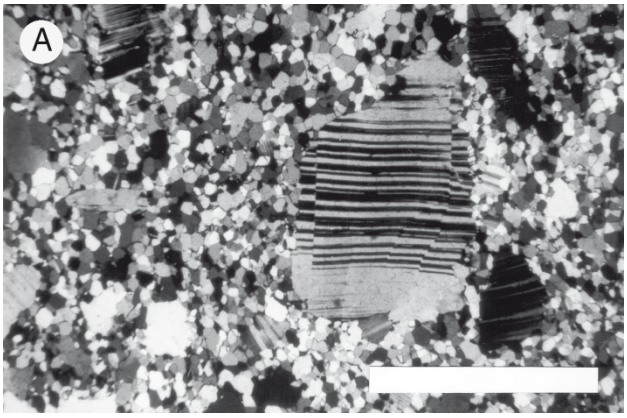

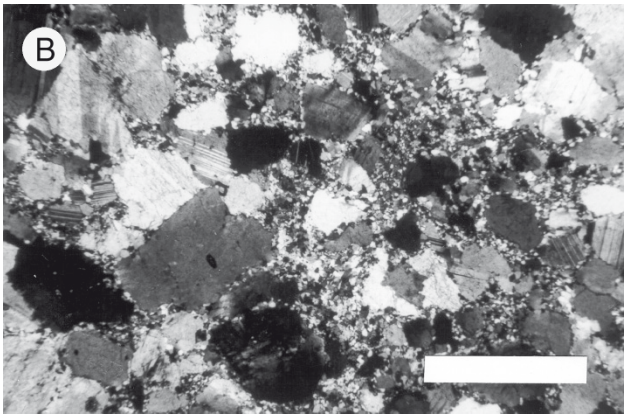

Fig. 3. Photomicrographs of albitised gneiss. **A**: Albite porphyroclast set in fine-grained anhedral albitite matrix; scale bar 5 mm. **B**: Fine-grained albitite matrix; scale bar 0.5 mm.

Petrography

The albitites consist of > 95% albite with significant rutile and apatite. Zircon is always present, quartz either absent or present in very small amounts. Carbonate is not present in the albitites and is only a very minor component in the massive, epidotised rock mentioned above.

Typically, the albitites exhibit classic mortar textures: strained, undulose, bent, microfractured albite porphyroclasts set in a mosaic of fine-grained, anhedral, polygonal, unstrained albite (Fig. 3A, B). They have a bimodal grain size: porphyroclasts are 2–4 mm, occa-

sionally 5 mm in a matrix of 0.1–0.2 mm albite grains. Rutile and apatite are often found closely associated as anhedral grains, 0.5–1.0 mm across, and in elongate clusters up to 5 mm. The rutile and apatite are neither strained nor fractured. Generally the apatite has clear cores and cloudy margins, possibly suggestive of alteration to oxy- or hydroxyl-apatite around the edges. Occasional, very minor, radiating clusters of chlorite and muscovite are found.

Samples from area C (Fig. 1) also show the typical mortar texture and contain sphene in addition to rutile. The matrix consists of albite and a little quartz with a 'dust' of tiny grains of rutile, sphene and epidote. Aggregates of chlorite with a little muscovite contain tiny rutile needles.

Reddened rocks associated with the albitites in the linear zones (B) contain abundant epidote and orange-brown biotite. The epidote is either concentrated in plagioclase cores or clustered throughout the rock, concentrated in layers and schlieren. Minor quartz, carbonate and sphene also occur.

The gneisses on either side of the main albitised zone (A) are variable quartz-dioritic to granodioritic in composition, occasionally with enough K-feldspar to be monzogranitic. They show the beginnings of a mortar texture.

Chemistry

Table 1 shows analyses of six albitites from areas A and C and one unaltered gneiss from just east of the main albitised zone at A (Fig. 1, for comparison, pure albite, $NaAlSi_3O_8$, contains 68.7% SiO_2, 19.4% Al_2O_3 and 11.8% Na_2O).

It can be seen that all six analysed albitites are very similar chemically; GGU 293844 and -863 from areas A and C respectively are almost identical. Compared with the unaltered gneiss (GGU 293845) the albitised rocks expectedly show big increases in Na_2O and Al_2O_3 and strong depletion in FeO, MgO and K_2O. TiO_2 is surprisingly low in GGU 293842, -844 and -863, and con-

Table 1. Chemical analyses of albitised gneisses

GGU no	293935	293841	293842	293844	293863	293864	293845
Locality	A	A	A	A	C	C	A
SiO_2	64.94	64.71	70.44	67.81	67.49	67.46	71.93
TiO_2	1.34	0.73	0.21	0.28	0.20	0.43	0.24
Al_2O_3	20.24	19.91	17.15	19.24	19.60	19.39	14.96
Fe_2O_3	0.41	0.30	0.40	0.09	0.10	0.12	0.55
FeO	0.18	0.17	0.17	0.32	0.21	0.19	1.36
MnO	0.00	0.01	0.00	0.01	0.01	0.01	0.03
MgO	0.24	0.36	0.24	0.07	0.07	0.08	0.69
CaO	0.90	1.81	0.55	0.43	0.44	0.52	2.78
Na_2O	10.42	10.21	9.13	11.43	11.44	11.17	4.38
K_2O	0.26	0.63	0.21	0.16	0.31	0.42	2.26
P_2O_5	0.03	0.52	0.08	0.09	0.02	0.08	0.06
Volat.	0.20	0.17	0.10	0.06	0.09	0.04	0.33
Sum	99.16	99.53	98.68	99.99	99.98	99.91	99.57
V	–	56	–	18	18	27	27
Cr	16	–	–	–	3	–	–
Ni	–	46	–	43	46	44	37
Cu	2	5	2	4	4	5	18
Zn	–	–	–	5	–	72	31
Rb	–	25	–	16	24	24	46
Sr	124	279	49	127	148	131	376
Zr	662	295	143	200	294	266	47
Ba	–	203	–	53	51	124	772

A and C denote sample localities (Fig. 1).

GGU 293845 is a non-albitised gneiss from locality A for comparison. Analyses by GGU. Most major and trace elements from XRF on glass discs; Na and Cu by AAS. Trace element data are reconnaissance values.

sidering the amount of apatite in thin sections, so is P_2O_5. Among the trace elements, high levels of Zr reflect the frequent occurrence of zircon seen in thin section. Depletion of Sr mirrors the disappearance of CaO. Na_2O/K_2O ratios range from 16 to 71 in the albitites, compared with 2 in the unaltered gneiss.

Origin of the albitites

The field evidence in the main albitite zone (A), where the transition from unaltered gneiss to pure white albitite and the replacement veins of albitite are well exposed along the coast, indicates that the albitites originated by metasomatic alteration of quartz-dioritic to granodioritic gneisses. Petrographically, the virtually monomineralic character of the albitites, > 95% albite with accessory rutile, apatite and zircon, is also consistent with a metasomatic origin.

The albitisation process apparently involved a sequence of events. Original oligoclase-andesine of the gneissic protoliths was hydrothermally altered to produce epidote and albite, with addition of OH and Na. Ferromagnesian minerals, quartz and epidote were then broken down and removed with further influx of Na and Al and removal of Fe, Mg, Ca and K. The early-formed albite porphyroblasts were then strained, bent and microfractured by a cataclasis event, followed by recrystallisation of the fine-grained, granoblastic albitic matrix to produce the mortar texture. Rutile and apatite (and possibly zircon) appear to have crystallised at this late stage, with a final segregation of rutile to produce elongate clusters and the small rutile vein.

The origin and nature of the albitising fluid are uncertain. With large-scale albitisation of siltstones on Qeqertakassak, 45 km to the north, an obvious source of fluids would be the same percolating brines proposed by Kalsbeek (1992) – the '*per descensum*' model.

The albite-rich rocks on Qeqertakassak include quartz and dolomite among their major minerals with small clusters of tiny rutile needles in all samples and hematite and biotite sometimes present. The albitites of the present study contain little or no quartz, no dolomite, large rutile crystals up to 2 mm and in clusters, apatite and zircon. Kalsbeek's analyses of dolerites and altered dolerites and dark siltstones and albite-rich rocks show the same depletion in Rb, Ba, Sr and increase in Zr in the albitised rocks as in the present study. If the same percolating brines were responsible for the albitisation in this southern area, presumably the greater depths below the Proterozoic supracrustal rocks could account for the differences in mineralogy, with higher temperatures involved. An obvious source of heat to produce hot brines is the thick, extensive picritic sills in this area. Kalsbeek (1992) also proposed a similar model for Qeqertakassak where dolerites intrude the sediments. He noted that the Anap nunâ Group sediments may have contained evaporite minerals as the source of the Na-rich brines.

Alternatively, if the rutile-bearing albitites compare with the kragerøites of southern Norway, a '*per ascensum*' origin could be invoked. However, kragerøites characteristically form part of a suite comprising gabbros, scapolitised rocks, apatite + phlogopite + enstatite mineralisation, hornblende-apatite and rutile dykes etc., which have not been found in eastern Disko Bugt.

It is well known that albitites may be the products of feldspathic fenitisation around carbonatite centres (Garson *et al.* 1984) and carbonate-lamprophyre dykes are widespread in the area around Kangerluarsuk (Escher *et al.* 1999, this volume). Thus it could be that these albitised gneisses are associated with further (earlier) carbonatitic magmatism in the area, which would make them useful guides in prospecting. In that regard, the major zone of cataclasites containing the main albitite occurrence (A) would be of interest.

References

Brögger, W.C. 1935: On several Archäan rocks from the south coast of Norway. II, The south Norwegian hyperites and their metamorphism. Skrifter utgitt av Det Norske Videnskabs-Akademi i Oslo. I. Matematisk-Naturvidenskabelige Klasse **1934**(1), 421 pp.

Escher, J.C., Ryan, M.J. & Marker, M. 1999: Early Proterozoic ductile thrusting east of Ataa Sund, north-east Disko Bugt, West Greenland. In: Kalsbeek, F. (ed.): Precambrian geology of the Disko Bugt region, West Greenland. Geology of Greenland Survey Bulletin **181**, 171–179 (this volume).

Garde A.A. & Steenfelt, A. 1999: Precambrian geology of Nuussuaq and the area north-east of Disko Bugt, West Greenland. In: Kalsbeek, F. (ed.): Precambrian geology of the Disko Bugt region, West Greenland. Geology of Greenland Survey Bulletin **181**, 6–40 (this volume).

Garson, M.S., Coats, J.S., Rock, N.M.S. & Deans, T. 1984: Fenites, breccia dykes, albitites and carbonatitic veins near the Great Glen Fault, Inverness, Scotland. Journal of the Geological Society (London) **141**, 711–732.

Kalsbeek, F. 1992: Large-scale albitisation of siltstones on Qeqertakavsak island, northeast Disko Bugt, West Greenland. Chemical Geology **95**, 213–233.

A gold-bearing volcanogenic-exhalative horizon in the Archaean(?) Saqqaq supracrustal rocks, Nuussuaq, West Greenland

Adam A. Garde, Bjørn Thomassen, Tapani Tukiainen and Agnete Steenfelt

The Saqqaq supracrustal rocks in southern Nuussuaq, West Greenland, host stratiform gold mineralisation in a 3–4 m thick impure chert horizon of volcanogenic-exhalative origin; chip samples average *c.* 0.8 ppm Au (thickness 3.3 m) over a strike length of 8 km, including 1.1 ppm Au (thickness 3.7 m) over a strike length of 1.6 km. Silicate minerals in and adjacent to the mineralised horizon include chrome-bearing tourmaline, staurolite, fuchsite, and manganiferous garnet. The Saqqaq supracrustal rocks form an almost 30 km long, NW-striking and SW-dipping sequence, which is presumed to be of Archaean age and consists of amphibolite facies mafic and ultramafic metavolcanic rocks, associated minor volcanogenic-exhalative horizons, and quartzo-feldspathic metasediments. The sequence is surrounded by Archaean(?) orthogneisses and intruded by an up to *c.* 100 m thick trondhjemitic sill, and appears to outline a large asymmetric, isoclinal fold (possibly of Archaean age) which was refolded in the lower Proterozoic.

Geological Survey of Denmark and Greenland, Thoravej 8, DK-2400, Copenhagen NV, Denmark.
E-mail: *aag@geus.dk.*

Keywords: Archaean, gold, Nuussuaq, supracrustal rocks, West Greenland

In 1986 a large unit of previously unknown supracrustal rocks was discovered in the Precambrian basement of southern Nuussuaq near the settlement of Saqqaq (Fig. 1) during helicopter reconnaissance of Tertiary basalt outliers (A.K. Pedersen, personal communication 1988). The unit was subsequently investigated during the Disko Bugt Project 1988–92 carried out by the Geological Survey of Greenland (GGU; see Kalsbeek & Christiansen 1992). Initial analyses of stream sediment and sulphide mineralised samples from the supracrustal unit showed enrichment in arsenic and traces of gold, and subsequent chip sampling revealed the existence of a several kilometres long gold-bearing horizon. In 1992 Platinova A/S investigated the supracrustal belt during two weeks of field work, which mainly comprised chip sampling of rusty horizons.

This paper presents the currently available, although somewhat sketchy knowledge of the mineralisation and its host rocks. It is based on reconnaissance geological and geochemical mapping in 1988, 1989 and 1991 (Steenfelt 1992; Garde & Steenfelt 1999, this volume) and chip sampling in 1991 (Thomassen & Tukiainen 1992), geological photogrammetry, microscope studies and whole-rock and mineral geochemistry by the authors, as well as mineralisation data obtained by Platinova A/S (Atkinson & Rutherford 1992). As will be seen below, the gold mineralisation at Saqqaq differs in many respects from the one at Eqi south-east of Nuussuaq (likewise studied during the Disko Bugt Project) which is related to carbonate alteration in Archaean acid metavolcanic rocks (Stendal *et al.* 1999, this volume).

Geology

The Saqqaq supracrustal rocks (Garde 1994) form a NW–SE-striking, *c.* 29 km long and up to *c.* 5 km wide belt (Fig. 1) which is enclosed in the Precambrian orthogneiss complex of southern Nuussuaq and locally capped by basaltic flows of Tertiary age. The supracrustal belt, which generally dips 25–40° SW, is more than 500 m thick, but its original base and top have not been recognised. The entire belt may form a recumbent isoclinal fold as suggested by large-scale, flat-lying isoclinal folds with north-west-trending axes

Fig. 1. Simplified geological map showing the Saqqaq supracrustal rocks, the auriferous metachert horizon with chip sample analyses (ppb Au and width in metres), locations of other rust zones, and the position of Fig. 3. The supracrustal sequence continues to the coast south-east of the map area.

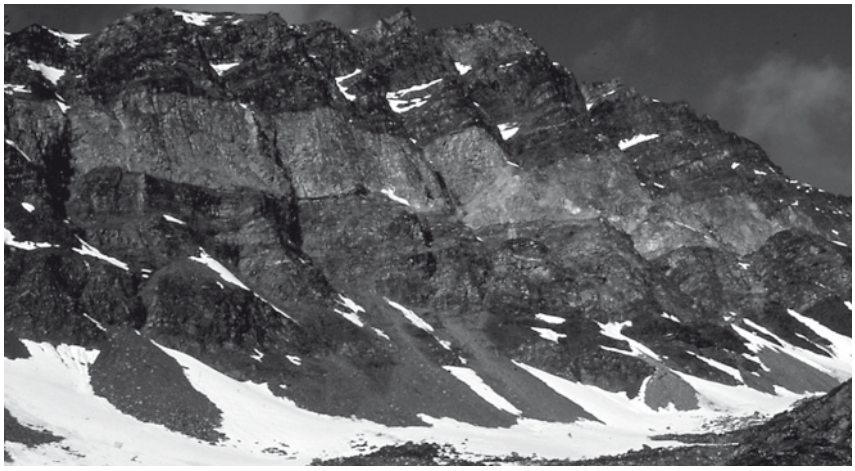

Fig. 2. Photograph of the central part of a NE-facing cliff face opposite the mountain Qaqulluit (Figs 1, 3), displaying a section through part of the Saqqaq supracrustal rocks with the rusty metachert (*c.* 30 m thick) horizon above the scree. The light grey layer in the upper part of the picture is a trondhjemitic sill; the uppermost part of the succession is not visible due to the short distance between the observer and the cliff face (compare the section made by geological photogrammetry, Fig. 3).

visible, e.g. on the cliffs north and south of the lake Iluliallip Tasia. The south-eastern end of the supracrustal belt has been folded into an upright antiform with a subhorizontal north-west-trending axis during a later phase of deformation, presumably in the Proterozoic (Garde & Steenfelt 1999, this volume). Medium- and small-scale fold structures are common in the supracrustal rocks, but their relationship with the large-scale structures is uncertain. Smaller enclaves of supracrustal rocks are common in the gneisses in the vicinity of the supracrustal belt to the north and west.

Exposures of relatively undisturbed supracrustal rocks occur in a NE-facing, up to *c.* 500 m high, steep mountain wall opposite the mountain Qaqulluit (Figs 2, 3). This slope was mapped and interpreted using multi-model geological photogrammetry (Dueholm 1992) based on photography from a helicopter (Fig. 3). The lowermost parts accessible by foot have been traversed and sampled (Fig. 4). The supracrustal sequence in the slope generally dips 30° SW. Exposures of the basement-cover contact between the supracrustal sequence and the regional orthogneiss have not

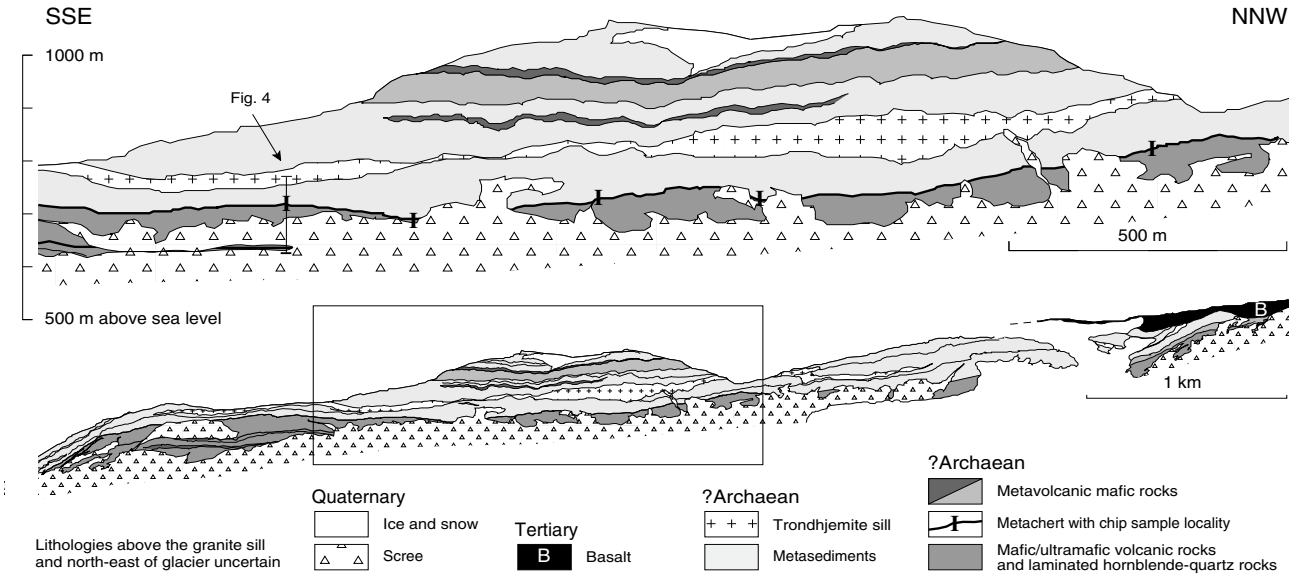

Fig. 3. Saqqaq supracrustal rocks exposed along a 6 km long NE-facing cliff face opposite the mountain Qaqulluit. Direction of view WSW (240°). See Fig. 1 for location and compare with the photograph Fig. 2. Geological interpretation and topography based on geological photogrammetry, supplemented with observations by foot from short traverses at the chip sampled localities. The lithologies indicated above the trondhjemitic sill and north-east of the glacier are uncertain.

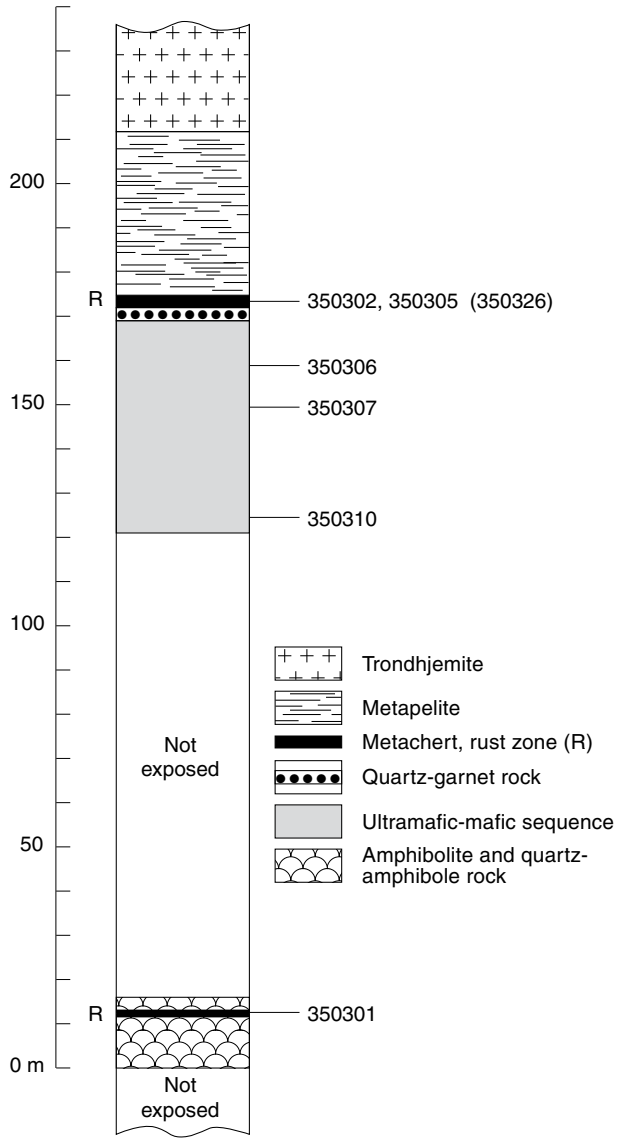

Fig. 4. Stratigraphic section of the lower part of the Saqqaq supracrustal rocks opposite the mountain Qaqulluit (Fig. 3 for location), and stratigraphic positions of samples referred to in the text and Table 1. 350301: Amphibole-quartz-garnet-tourmaline-pyrrhotite rock. 350302, 350305: Impure metachert. 350306–350307: Laminated hornblende-quartz rock. 350310: Ultrabasic metavolcanic rock. 350326: Amphibole-quartz-pyrrhotite rock (local block collected from scree immediately below the auriferous impure metachert and rusty garnet-rich horizon).

been observed by the present authors but were reported by Platinova A/S as strongly sheared and commonly mineralised with iron sulphides (see p. 125).

The lowermost outcrops, protruding between the scree fans that generally cover the lower parts of the slopes (Figs 3, 4), consist of a dark green to black, fine-grained amphibolite and very finely laminated quartz-amphibole rock. The latter rock type consists of monomineralic bands of quartz and amphibole which alternate at a scale of 0.1–0.5 mm, besides thin scattered stringers of pyrite and pyrrhotite. Within these rocks an up to 1.5 m thick, fine-grained, rusty horizon contains a number of several millimetres thick layers consisting of hornblende, plagioclase, biotite, quartz, garnet, tourmaline, pyrrhotite and ilmenite in varying proportions.

The next exposed unit consists of an ultramafic-mafic sequence with a true thickness of more than 60 m. It is composed of ultrabasic metavolcanics, which are intercalated with dark olive-green hornblendite and laminated quartz-hornblende rocks. The lowermost exposed part of this unit consists of a massive, brown-weathering, strongly carbonated ultrabasic rock. In places it displays a decimetre-sized meshwork texture that may be interpreted as partially recrystallised coarse spinifex structure; alternatively it was formed during metamorphic recrystallisation. The ultrabasic rock mostly consists of fine-grained intergrowths of chlorite, tremolite and serpentine, often with substantial amounts of dolomite and magnetite, besides sporadic pyrrhotite and pyrite. There are also local 2–4 cm thick monomineralic lenses of *c.* 0.5 cm large, equidimensional olivine grains, cut by thin serpentine veins. The olivine grains are magnesian and very homogeneous (Fo_{86}, Table 1), and the lenses are interpreted as inherited from the pre-metamorphic protolith. Upwards in the outcrop the dark green laminated hornblende-rich horizons increase in frequency and thickness (millimetres to decimetres) so that eventually they become the predominant rock type. They consist mainly of fine-grained quartz and actinolitic to ferro-tschermakitic hornblende with low but variable sodium and potasium contents (Fig. 5; Table 1).

The ultramafic-mafic sequence is overlain by two thin but conspicuous horizons of supposed volcanic-exhalative origin (see below). The lower one, a rusty weathering garnet-rich horizon with variable thickness up to 1.5 m, is greyish and conspicuously banded at a scale of millimetres to centimetres. The mineralogical composition of this rock is quartz, garnet, fuchsite, biotite, chlorite, colourless amphibole, titanite and tourmaline, along with minor ilmenite, pyrrhotite, niccolite, wolframite and scheelite. It is rich in aggregates and 1–5 cm thick monomineralic layers of up to 2 cm large euhedral garnet porphyroblasts with colours varying from dark red to almost black. The garnets contain many small pyrrhotite inclusions and are almandine-rich. The garnets also contain up to *c.* 10 wt per cent

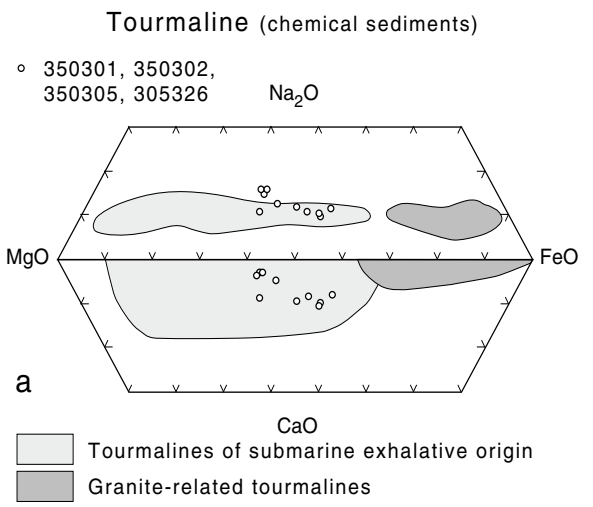

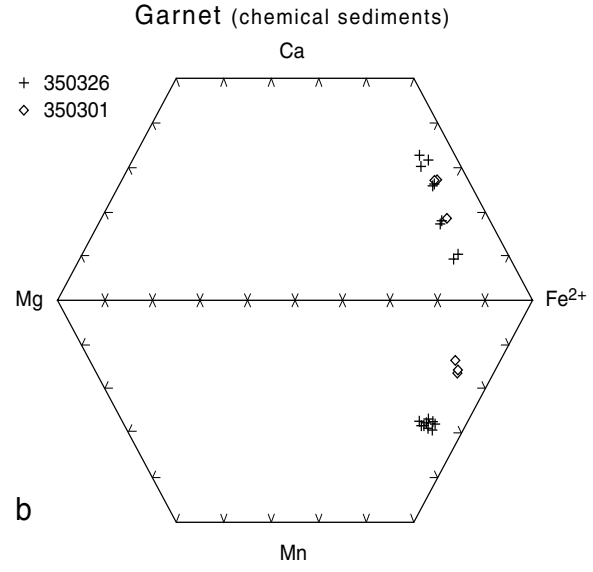

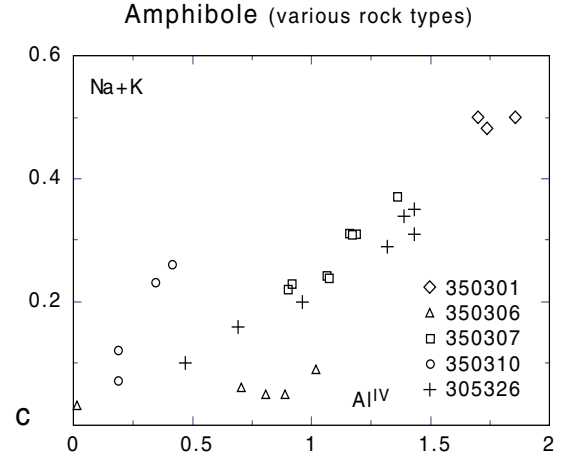

MnO (Fig. 5; Table 1); manganese-rich garnet is a characteristic component of coticule (quartz-spessartine rock) which is commonly interpreted as a volcanogenic-exhalative sea floor precipitate (Gardiner & Venugopal 1992 and references therein).

The second conspicuous horizon has a distinct lower contact to the garnet-rich horizon, is 3–4 m thick, rusty weathering, and consists of finely laminated, impure metachert with occasional small-scale folds with near-horizontal, NW-striking axes. Quartz is the predominant mineral, followed by pyrrhotite and fuchsite, and smaller amounts of one or more of the following minerals: biotite, chlorite, garnet, actinolitic hornblende, titanite, tourmaline, staurolite, tremolite, pyrite, arsenopyrite; native gold (electrum, see p. 126) has also been identified. Several of the silicate minerals (chlorite, fuchsite, staurolite, tourmaline) contain Cr_2O_3 in the range 0.5–2.0 wt per cent (Table 1), whereas chromite has not been identified. The tourmaline is intermediate in composition between dravite and schorl (Fig. 5). Like the quartz-amphibole rocks lower in the section, the metachert is mostly very fine grained and finely laminated, with widely separated trains of single grains of one or several of the above mentioned minerals. Some samples contain microfolds at a scale of centimetres, within which the fine lamination is preserved, but where pyrrhotite has been partially remobilised into thin stringers along axial surfaces. A few metachert samples have been recrystallised and appear coarser and much less distinctly banded.

The metachert horizon is succeeded upwards by *c.* 40 m of slightly migmatised, grey, fine-grained rocks consisting of quartz, plagioclase, biotite, muscovite, garnet and chlorite, and traces of pyrite. This sequence is

Fig. 5. Compositions of tourmaline, garnet and amphibole in chemical sediments, and amphibole in an ultrabasic metavolcanic rock. See Fig. 4 for sample locations and lithologies.
a: Na_2O–MgO–FeO and CaO–MgO–FeO triangular diagrams of tourmaline in chemical sediments. Comparison with compositional fields of tourmalines with known origins (from Henry & Guidotti 1985) support our interpretation that the sediments are of submarine-exhalative origin. **b**: Ca–Mg–Fe^{2+} and Mn–Mg–Fe^{2+} triangular diagrams of garnet in chemical sediments; their large iron and particularly manganese contents are reminiscent of coticule garnet. **c**: Variation diagram of amphiboles, Na + K plotted against Al in IV-coordination per unit cell. The diagram illustrates the large variation of amphibole compositions found in chemical sediments (samples 350301, 350306–07, 350326) and the low coupled substitution of Al^{IV} and Na, K for Si^{4+} in tremolite from the ultrabasic metavolcanic rock (sample 350310).

Table 1. Compositions of silicate minerals from chemical sediments and metavolcanic rocks, Saqqaq supracrustal rocks

	Garnet				Tourmaline				Amphibole								
GGU No Spot	350301 average n = 3	350326 55	350326 average n = 8	350326 s.d.	350301 average n = 2	350302 average n = 2	350305 average n = 3	350326 average n = 3	350301 average n = 2	350306 e3	350307 f59	350307 av. (g) n = 4	350307 s.d.	350310 average n = 3	350310 s.d.	350326 b30	350326 c34
SiO_2	37.55	37.43	37.15	0.15	34.96	35.24	35.11	34.68	41.84	51.22	46.14	48.87	1.40	56.02	0.97	52.57	44.47
TiO_2	0.05	0.01	0.02	0.03	1.13	0.49	0.42	1.37	0.48	0.24	0.32	0.29	0.02	0.01	0.00	0.18	0.57
Al_2O_3	21.47	20.92	21.22	0.30	31.94	32.00	31.62	31.28	15.56	6.21	10.61	8.25	1.22	1.65	0.80	3.67	12.66
Cr_2O_3	0.08	0.09	0.04	0.03	0.07	1.72	2.16	0.03	0.02	0.49	0.73	0.58	0.41	0.04	0.05	0.02	0.05
FeO^*	27.91	26.02	24.21	1.86	7.97	5.46	5.70	8.02	18.61	11.69	12.35	11.84	0.47	2.77	0.10	12.45	15.45
MgO	1.62	1.90	1.70	0.35	6.65	7.46	7.49	6.62	6.91	14.87	13.56	14.42	0.93	23.02	0.15	15.36	10.03
MnO	5.23	10.70	10.07	0.79	0.14	0.01	0.10	0.19	0.20	0.27	0.26	0.20	0.13	0.17	0.03	0.45	0.34
NiO	0.01	0.05	0.03	0.03	0.03	0.09	0.04	0.02	0.03	0.05	0.19	0.22	0.04	0.08	0.01	0.02	0.01
CaO	7.37	2.69	5.89	2.62	1.38	0.81	0.51	1.53	11.74	11.90	11.51	12.12	0.16	12.47	0.16	12.60	11.89
Na_2O	0.03	0.04	0.04	0.05	1.92	2.00	2.22	1.69	1.26	0.14	1.16	0.87	0.13	0.75	0.26	0.31	0.85
K_2O	0.04	0.01	0.02	0.02	0.01	0.07	0.03	0.08	0.67	0.11	0.28	0.07	0.04	0.03	0.03	0.07	0.58
Sum	101.37	99.87	100.39	0.58	86.18	85.34	85.41	85.49	97.30	97.18	97.12	97.72	0.79	97.01	0.39	97.69	96.90
Fe_2O_3	0.96	0.00	0.99	0.72					2.72	5.42	7.89	5.21	0.29	3.08	0.12	2.90	3.73
FeO	27.05	26.02	23.32	2.08					16.17	6.81	5.25	7.15	0.70	0.00	0.00	9.84	12.09
New sum	101.47	99.87	100.49	0.64					97.60	97.73	97.90	98.25	0.03	97.32	0.01	97.99	97.27
Cations per formula unit																	
Si	5.94	6.06	5.95	0.05	5.79	5.82	5.81	5.79	6.28	7.29	6.64	6.98	0.12	7.68	0.12	7.53	6.57
Al	4.00	3.99	4.00	0.05	6.23	6.23	6.17	6.16	2.75	1.04	1.80	1.39	0.19	0.27	0.13	0.62	2.20
Ti	0.01	0.00	0.00	0.00	0.14	0.06	0.05	0.17	0.05	0.03	0.03	0.03	0.00	0.00	0.00	0.02	0.06
Cr	0.01	0.01	0.01	0.01	0.01	0.22	0.29	0.00	0.00	0.06	0.08	0.07	0.04	0.00	0.01	0.00	0.01
Fe^{2+}	3.58	3.52	3.12	0.29	1.10	0.75	0.79	1.12	2.03	0.81	0.63	0.85	0.10	0.00	0.00	1.18	1.49
Fe^{3+}	0.11	0.00	0.12	0.08	0.00	0.00	0.00	0.00	0.31	0.58	0.85	0.56	0.03	0.32	0.01	0.31	0.41
Mn	0.70	1.47	1.37	0.11	0.00	0.00	0.00	0.00	0.03	0.03	0.03	0.02	0.02	0.02	0.00	0.05	0.04
Ni	0.00	0.01	0.00	0.01	0.00	0.00	0.00	0.00	0.00	0.01	0.02	0.03	0.01	0.01	0.00	0.00	0.00
Mg	0.38	0.46	0.41	0.09	1.64	1.84	1.85	1.65	1.55	3.16	2.91	3.07	0.16	4.70	0.02	3.28	2.21
Ca	1.25	0.47	1.01	0.45	0.25	0.14	0.09	0.28	1.89	1.81	1.77	1.85	0.01	1.83	0.02	1.93	1.88
Na	0.01	0.01	0.01	0.02	0.62	0.64	0.71	0.55	0.37	0.04	0.32	0.24	0.04	0.20	0.07	0.09	0.24
K	0.01	0.00	0.00	0.00	0.00	0.01	0.01	0.02	0.13	0.02	0.05	0.01	0.01	0.01	0.01	0.01	0.11
Total	6.00	16.00	16.00	0.00	15.77	15.72	15.77	15.73	15.38	14.87	15.15	15.11	0.04	15.04	0.07	15.03	15.23
Oxygens	24.00	24.05	24.00						23.00	23.00	23.00	23.00		22.91	0.02	23.00	23.00

Note the high chromium content in chlorite, tourmaline, staurolite and fuchsitic muscovite in several samples. The samples were collected along the profile shown in Fig. 4.

The analyses were made with the Jeol 733 Superprobe at the Geological Institute, University of Copenhagen. The electron microprobe was operated at 15 kV, 15 nA with energy dispersive data collection (major elements except Na) and crystal spectrometers (Na, Cr, Ni), and a beam diameter of 2 mm. Natural silicates and oxides of end-member compositions were used as standards.

Iron distribution of Fe_2O_3 and FeO according to isometric requirements.

interpreted as sedimentary or volcano-sedimentary in origin.

The uppermost accessible unit in the section is a prominent, *c.* 50 m thick sheet of whitish, slightly foliated trondhjemite. The rock is homogeneous and medium grained, and appears to be more leucocratic than the country rock tonalitic gneisses. Hand samples show that it has been strained during regional deformation. However, the photogrammetric interpretation (Fig. 3) clearly suggests that it is transgressive, which is supported by occasional observations of aplitic veins in the supracrustal sequence that emerge from the trondhjemite sheet. The upper, steep part of the mountain wall has not been traversed, but the supracrustal rocks appear to continue for another *c.* 200 m above the trondhjemite sill to the top of the mountain (Fig. 3).

In the north-facing cliffs south of the lake Iluliallip Tasia (Fig. 1), rock types similar to the ones at Qaqulluit were observed, and also here a gold-bearing, rusty-weathering horizon of metachert was identified and sampled in the lower part of the section. This metachert is considered to be continuous with the one at Qaqulluit, although there are structural complexities in the upper part of the section; the east–west section through the supracrustal belt suggests the presence of a large recumbent, NE-facing fold with a horizontal axis directed SE. North of the lake, the supracrustal rocks are strongly deformed by disharmonic folding, so that a clear stratigraphic section through the unit is not apparent. Ultramafic and mafic rocks predominate

Table 1 (*continued*)

	Biotite				Muscovite			Chlorite		Serpentine		Staurolite	Olivine	
GGU No	350301	350301	350307	350307	350302	350305	350305	350305	350310	350310	350310	350302	350310	350310
Spot	average n = 4	s.d.	average n = 3	s.d.	average n = 2	37	42	43	b n = 2	13	14	n = 2	average n = 3	s.d.
SiO_2	34.70	0.70	34.97	0.48	45.23	46.74	48.02	24.41	32.29	42.01	39.95	26.94	39.93	0.08
TiO_2	1.86	0.18	2.64	0.14	0.62	0.42	0.51	0.01	0.14	0.01	0.01	0.62	0.01	0.00
Al_2O_3	17.26	0.11	15.95	0.34	33.36	35.28	30.68	22.08	14.96	0.01	0.01	52.73	0.01	0.00
Cr_2O_3	0.08	0.06	0.61	0.05	0.79	0.80	0.57	0.23	0.56	0.01	0.02	1.06	0.01	0.00
FeO*	21.82	0.48	14.87	0.38	1.99	2.36	2.93	20.88	4.10	2.44	4.67	11.73	13.37	0.17
MgO	9.68	0.24	15.65	0.33	0.58	0.45	0.75	17.26	33.43	42.64	40.84	1.22	45.73	0.06
MnO	0.20	0.14	0.18	0.15	0.14	0.13	0.01	0.30	0.01	0.01	0.01	0.35	0.25	0.08
NiO	0.01	0.00	0.35	0.05	0.02	0.01	0.01	0.16	0.18	0.25	0.26	0.06	0.29	0.03
CaO	0.05	0.07	0.06	0.09	0.01	0.01	0.16	0.01	0.19	0.01	0.01	0.07	0.01	0.00
Na_2O	0.07	0.03	0.35	0.05	1.14	0.93	1.11	0.01	0.02	0.01	0.01	0.01	0.01	0.00
K_2O	8.23	0.82	7.18	0.50	8.84	7.95	8.59	0.01	0.01	0.01	0.01	0.01	0.09	0.10
Sum	93.93	1.27	92.81	0.89	92.70	95.09	93.33	85.35	85.88	87.41	85.80	94.78	99.71	0.25
Fe_2O_3					2.21	2.62	3.26	0.52	0.67					
FeO					0.00	0.00	0.00	20.42	3.49					
New sum					92.92	95.35	93.66	85.40	85.95					
Cations per formula unit														
Si	5.55	0.04	5.47	0.02	3.08	3.08	3.24	5.18	6.20	1.95	1.90	3.94	1.00	0.00
Al	3.25	0.06	2.94	0.04	2.68	2.74	2.44	5.52	3.39	0.00	0.00	9.10	0.00	0.00
Ti	0.23	0.02	0.31	0.02	0.03	0.02	0.03	0.00	0.02	0.00	0.00	0.07	0.00	0.00
Cr	0.01	0.01	0.08	0.01	0.04	0.04	0.03	0.04	0.09	0.00	0.00	0.12	0.00	0.00
Fe^{2+}	2.92	0.11	1.94	0.06	0.00	0.00	0.00	3.62	0.56	0.09	0.19	1.44	0.28	0.00
Fe^{3+}	0.00	0.00	0.00	0.00	0.11	0.13	0.17	0.08	0.10	0.00	0.00	0.00	0.00	0.00
Mn	0.03	0.02	0.02	0.02	0.01	0.01	0.00	0.05	0.00	0.00	0.00	0.04	0.01	0.00
Ni	0.00	0.00	0.04	0.01	0.00	0.00	0.00	0.03	0.03	0.01	0.01	0.01	0.01	0.00
Mg	2.31	0.07	3.65	0.11	0.06	0.04	0.08	5.46	9.57	2.95	2.90	0.27	1.71	0.00
Ca	0.01	0.02	0.01	0.02	0.00	0.00	0.01	0.00	0.04	0.00	0.00	0.01	0.00	0.00
Na	0.02	0.01	0.11	0.02	0.15	0.12	0.15	0.00	0.01	0.00	0.00	0.00	0.00	0.00
K	1.68	0.15	1.43	0.09	0.77	0.67	0.74	0.00	0.00	0.00	0.00	0.00	0.00	0.00
Total	16.00	0.00	16.00	0.00	6.82	6.71	6.70	20.00	20.00	5.00	5.00	15.00	3.00	0.00
Oxygens	45.12	0.11	45.03	0.05	11.00	11.00	11.00	28.00	28.00	6.95	6.90			

here, and the gold-bearing metachert horizon was only recognised in one small outcrop.

The lithologies and structures in the northernmost and southernmost parts of the supracrustal belt have not been studied by the authors.

Mineralisation

In the Saqqaq supracrustal rocks sulphide mineralisation occurs in four different settings: (1) in metavolcanic rocks which are almost devoid of gold, (2) in siliceous shear zones with low gold contents at contacts between the host orthogneiss and supracrustal rocks, (3) in quartz-garnet rock with an unusual sulphide paragenesis and elevated gold contents, and (4) in metachert, the main gold-bearing association.

The metavolcanic rocks contain a number of rust zones with disseminated to semi-massive pyrrhotite and pyrite and traces of chalcopyrite. Analyses of five chip samples from such mineralised zones are summarised in Table 2. It is evident that the contents of gold (average 12 ppb) and base metals are modest. Similar results were obtained by Platinova A/S: 18.5 ppb Au on average for 20 samples (Atkinson & Rutherford 1992). Analysis of a number of mineralised boulders confirms this picture of a rather pure iron sulphide mineralisation. Only one boulder of chalcopyrite-bearing ultramafic rock from the northern shore of Iluliallip Tasia with 0.3% Cu and 235 ppb Au deviates from this pattern.

Mineralisation at gneiss–supracrustal rock contacts was described by Atkinson & Rutherford (1992), according to whom this is the most common type of mineralisation and probably the most extensive. The contact zones are highly silicified (recrystallised?) and intensely banded, presumably mylonitic. Sulphide contents vary from trace to 50 per cent over 1–2 m. Pyrrhotite is dominant, but in addition pyrite, arsenopyrite, chalcopyrite, galena and sphalerite are present in trace to minor amounts. Gold contents are low, 30 ppb in average for 36 chip samples.

Table 2. Summary of mineralisation geochemistry in the Saqqaq supracrustal rocks

	Metavolcanic rocks 5 chip samples			Quartz-garnet rock 1 grab sample	Metachert 8 chip samples		
	Min.	Max.	Mean		Min.	Max.	Mean
Width m	1.0	5.0	2.1		1.5	4.5	3.3
SiO_2	48.3	55.3	50.8	51.3	66.5	87.1	78.8
TiO_2	0.4	1.3	0.7	1.7	0.2	0.5	0.3
Al_2O_3	8.3	14.3	11.1	18.6	2.8	6.8	4.1
Fe_2O_3	15.5	21.1	18.1	20.2	3.8	15.2	10.3
MnO	0.3	0.6	0.4	0.6	0.1	0.4	0.2
MgO	3.4	6.9	4.7	3.9	0.5	3.0	2.0
CaO	2.5	9.3	7.2	0.6	0.1	3.1	1.0
Na_2O	0.4	1.9	0.9	0.2	0.1	0.4	0.2
K_2O	0.1	0.6	0.4	2.2	0.1	1.7	0.6
P_2O_5	0.1	0.1	0.1	0.1	<0.1	0.1	<0.1
Au ppb	1	38	12	116	95	1831	757
Ag ppm	<5	<5	<5	<5	<5	<5	<5
As ppm	<2	190	45	1800	9	1600	404
W ppm	<4	11	6	46	<4	15	8
Ni ppm	<50	470	109	1800	<50	1500	652
Co ppm	19	70	45	150	9	110	66
Pt ppb	<5	7	5	<5	<5	6	5
Pd ppb	<2	7	3	2	3	9	5
Cr ppm	180	1000	376	240	120	2800	1403
Cu ppm	150	498	268	21	64	406	137
Zn ppm	20	104	55	27	9	42	19
Pb ppm	16	114	43	2	12	52	20
Sb ppm	<0.2	<0.2	<0.2	93.0	<0.2	29.0	9.4
Ba ppm	79	292	133	184	35	130	61

Analysis by Activation Laboratories Ltd., Ontario.
Major elements (%): fusion-inductivity coupled plasma emission spectrometry (icp).
Au, Pt, Pd: fire assay-icp.
Cu, Zn, Pb: aqua regia extraction-icp.
Ag, As, W, Ni, Co, Cr, Sb, Ba: instrumental neutron activation.

The quartz-garnet rock contains *c.* 1 vol.% of disseminated, fine-grained sulphides: niccolite, gersdorfite, pentlandite and pyrrhotite, as well as wolframite, scheelite and ilmenite. The pentlandite occurs as isolated, monomineralic grains, i.e. it is not formed by exsolution from pyrrhotite. The mineralogy is reflected by the chemical analyses (Table 2), which shows relatively high contents of nickel, arsenic and tungsten, as well as antimony and gold (116 ppb).

The auriferous metachert horizon contains a few volume per cent disseminated, fine-grained sulphides. Loose blocks indicate that semi-massive sulphide concentrations do occur, but none have been observed in outcrop. The main sulphide minerals are pyrrhotite and pyrite, accompanied by minor arsenopyrite and chalcopyrite. A tendency to lateral pyrite-pyrrhotite zonation with an increase of pyrrhotite towards NW has been observed. Grains of native gold up to 20 µm in size occur both as inclusions in arsenopyrite and as single isolated grains (Fig. 6). Energy dispersive microprobe analysis of three gold grains in arsenopyrite indicates a uniform Au/Ag ratio of 61/37, i.e. strictly speaking the mineral is electrum.

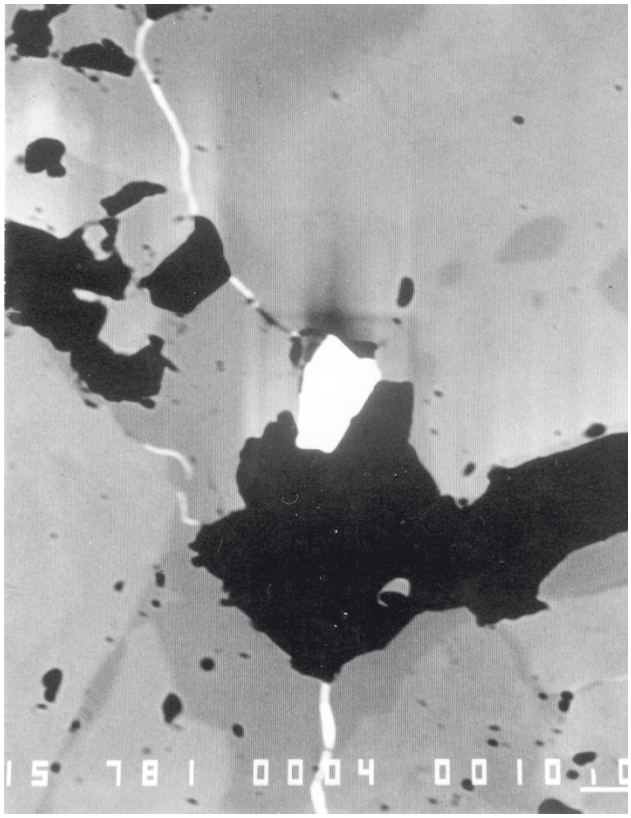

Fig. 6. Backscatter photomicrograph of gold (electrum) in the auriferous metachert, filling cracks and cavities in arsenopyrite. The gold grain in the centre (white) is *c.* 20 µm in diameter.

The metachert horizon was chip sampled (*c.* 3 kg samples) at eight localities along a lateral distance of *c.* 8.5 km (Figs 1, 3). Analyses of these samples are summarised in Table 2 (average 757 ppb Au over a width of 3.3 m) and suggest that the entire horizon is enriched in gold. The five chip samples from opposite Qaqulluit alone, collected over a strike length of 1.6 km, average 1063 ppb Au over a width of 3.7 m. Comparable values were obtained by Platinova A/S with an average of 663 ppb Au in 20 chip samples; the best result, opposite Qaqulluit, was an average of 1896 ppb Au in five samples over a lateral extent of 500 m (Atkinson & Rutherford 1992). The auriferous horizon is also enriched in arsenic (hosted in arsenopyrite),

nickel (hosted in both sulphides and silicates), chromium (apparently hosted mainly in silicates) and antimony, whereas base metal contents are rather low (Table 2).

Sphalerite and galena are only known from boulders at two localities near Iluliallip Tasia where they occur in veined rocks, perhaps originally chert, and in vein quartz respectively. The boulders contain up to 1.6 wt per cent Zn, 1.2% Pb, 0.1% Cu, 62 ppm Ag and 247 ppb Au.

Discussion

Most of the rocks studied in thin section exhibit equilibrium textures, with the exception of the ultrabasic metavolcanic rock where deformed lenses of medium-grained olivine occur in a fine-grained chlorite-tremolite-carbonate-serpentine matrix. The composition of the olivine, which appears to be very homogeneous, is shown in Table 1. The composition of the olivine (Fo_{86} and 0.29 wt% NiO) is similar to what might be expected in a fresh picritic or komatiitic lava, and together with the textures suggest to the authors that the olivines are primary and have survived later events without significant recrystallisation or chemical modification. Peak metamorphic temperature and pressure conditions of low to middle amphibolite facies are estimated from the coexisting hornblende and plagioclase (An_{38}), the common presence of biotite, almandine-rich garnet, staurolite and titanite in mafic rocks, as well as from the general composition of the calcic amphiboles which show only limited Al + Na, K substitution for Si (Fig. 5) and low TiO_2 contents. Apart from sporadic growth of late chlorite the examined rocks do not contain much evidence of recrystallisation after the peak of metamorphism.

Both the amphibole-quartz(-garnet) rocks and the metachert horizons are mostly very finely laminated, at a scale down to a fraction of a millimetre. The laminations may be rhythmic with alternating microlayers of two different mineralogical compositions (e.g. quartz-fuchsite or quartz-amphibole), but in the case of the metacherts also more complex variations may occur. For instance, several narrow zones rich in tourmaline crystals, or trains of single tourmaline or staurolite crystals may occur at variable intervals within the same thin section of metachert. The metachert often contains microfolds outlined by the lamination, and sometimes the folds are associated with recrystallisation which blurs the lamination. We therefore consider that the fine laminations in these rocks were formed by primary sedimentation and precipitation processes on the sea floor, and have survived subsequent metamorphism and deformation. This interpretation is in contrast to Atkinson & Rutherford (1992) who, from field observations, argue that the horizon represents a mylonitised shear zone analogous to the ones they observed along contacts between orthogneiss and supracrustal rocks. However, given the presence of an extensive, serpentinised and hence very ductile ultrabasic horizon close by, we consider it unlikely that the metachert should represent a siliceous mylonite zone.

The incomplete knowledge of the Saqqaq supracrustal rocks does not allow for a detailed account of their formation. A predominantly volcanic subaqueous depositional setting is indicated, which comprises a sequence of subaqueous ultramafic and mafic lavas changing upwards into pyroclastic and exhalative deposits and finally into volcaniclastic or epiclastic sediments. These rocks, probably deposited in a subsiding trough, were subsequently affected by deformation, metamorphism and metasomatism, and were intruded by a granitoid sill. Garde & Steenfelt (1999, this volume) correlate the Saqqaq supracrustal rocks with a supracrustal unit comprising similar lithologies in southern Nuussuaq 30–50 km further to the east and argue that both supracrustal units are Archaean and were formed in a back-arc or active continental margin setting.

The quartz-hornblende rocks of the metavolcanic unit, the quartz-garnet rock and the auriferous metachert most likely represent exhalative deposits formed on the sea floor by chemical precipitation from discharged metalliferous hydrothermal brines. Presumably the hydrothermal activity was contemporaneous with the ultramafic-mafic submarine volcanism. Our interpretation is supported by the composition of tourmalines from the metachert, which in a MgO–FeO–CaO–Na_2O diagram (Fig. 5) plot in the field of tourmalines supposed to have formed by chemical precipitation (Henry & Guidotti 1985). Likewise, the manganese-rich composition of garnets in the quartz-garnet rock is reminiscent of coticule of supposed volcanogenic exhalative origin (Gardiner & Venugopal 1992). Upwards in the sequence the volcanic-pyroclastic component decreases, resulting in a nearly pure exhalative deposit, the auriferous metachert horizon. The relative enrichment of the minor elements arsenic, chromium, nickel, tungsten and boron in the latter horizon is typical for gold mineralisation in Archaean greenstone belts (Hutchinson & Burlington 1984) and points towards a contribution from the ultramafic-mafic lavas.

Gold deposits hosted by chemical sediments including As-bearing sulphide-silicate iron formations are important in Archaean greenstone belts on a worldwide scale, e.g. at Lupin (Canada), Homestake (USA) (Thorpe & Franklin 1984), and in the Zimbabwe Craton (Saager *et al.* 1987). In general the gold is partly uniformly disseminated in the host units and partly located in minor quartz veins, which may be irregularly distributed or structurally controlled. Various authors (e.g. Sawkins & Rye 1974; Hutchinson & Burlington 1984) have proposed that the initial gold mineralisation is syngenetic from hydrothermal exhalations in chemical sediments on the sea floor. Subsequent folding, metamorphism and intrusion of granitoids causes remobilisation of gold into the quartz lodes so characteristic for this mineralisation, but which have not yet been discovered in the Saqqaq area. Others have stressed the epigenetic nature of most Archaean gold deposits (Groves & Foster 1991); certainly ore-grade gold mineralisation is mostly associated with quartz veins, as found for example in the Lupin district where the bulk of the gold is hosted by alteration haloes related to pervasive quartz veining (Bullis *et al.* 1994).

The auriferous metachert of the Saqqaq supracrustal rocks seems to be compatible with the syngenetic model outlined above, although a more comprehensive conclusion must await further studies. At this stage it appears that the economic potential of the Saqqaq supracrustal rocks lies in primary gold concentrations in the metachert horizon rich enough to be mineable, with additional potential for the discovery of epigenetic quartz vein gold derived from the metachert. We also emphasise that large parts of the area underlain by the Saqqaq supracrustal rocks remain untested and certainly warrant investigation.

Acknowledgements

We are grateful to J. Rønsbo, Geological Institute, University of Copenhagen, for assistance with the microprobe analysis. The Danish Natural Science Research Council funded the microprobe facilities.

References

Atkinson, J.R. & Rutherford, R. 1992: Report on 1992 field program, Saqqaq concession, West Greenland, 26 pp. Unpublished report, Platinova A/S, Toronto, Canada (in archives of Geological Survey of Denmark and Greenland).

Bullis, H.R., Hureau, R.A. & Penner, B.D. 1994: Distribution of gold and sulfides at Lupin, Northwest Territories. Economic Geology **86**, 1217–1227.

Dueholm, K.S. 1992: Geological photogrammetry using standard small-frame cameras. In: Dueholm, K.S. & Pedersen, A.K. (eds): Geological analysis and mapping using multi-model photogrammetry. Rapport Grønlands Geologiske Undersøgelse **156**, 7–18.

Garde, A.A. 1994: Precambrian geology between Qarajaq Isfjord and Jakobshavn Isfjord, West Greenland, 1:250 000. Copenhagen: Geological Survey of Greenland.

Garde, A.A. & Steenfelt, A. 1999: Precambrian geology of Nuussuaq and the area north-east of Disko Bugt, West Greenland. In: Kalsbeek, F. (ed.): Precambrian geology of the Disko Bugt region, West Greenland. Geology of Greenland Survey Bulletin **181**, 6–40 (this volume).

Gardiner, W.W. & Venugopal, D.V. 1992: Spessartine-quartz rock (coticule) occurrences in New Brunswick, Canada, and their use in exploration for massive sulphide, tin-tungsten and gold deposits. Transactions of the Institution of Mining and Metallurgy, Section B: Applied Earth Science **101**, B147–B157.

Groves, D.I. & Foster, R.P. 1991: Archaean lode gold deposits. In: Foster, R.P. (ed.): Gold metallogeny and exploration, 63–103. Glasgow & London: Blackie.

Henry, D.J. & Guidotti, C.V. 1985: Tourmaline as a petrogenetic indicator mineral: an example from the staurolite-grade metapelites from NW Maine. American Mineralogist **70**, 1–15.

Hutchinson, R.W. & Burlington, J.L. 1984: Some broad characteristics of greenstone belt gold lodes. In: Foster, R.P. (ed.): Gold, 82: the geology, geochemistry, and genesis of gold deposits, 339–371. Rotterdam: Balkema.

Kalsbeek, F. & Christiansen, F.G. 1992: Disko Bugt Project 1991, West Greenland. Rapport Grønlands Geologiske Undersøgelse **155**, 36–41.

Saager, R., Oberthür, T. & Tomschi, H.P. 1987: Geochemistry and mineralogy of banded iron-formation-hosted gold mineralization in the Gwanda greenstone belt, Zimbabwe. Economic Geology **82**, 2017–2032.

Sawkins, F.J. & Rye, D.M. 1974: Relationship of Homestake-type gold deposits to iron-rich Precambrian sedimentary rocks. Transactions of the Institute of Mining and Metallurgy **B 83**, 56–59.

Steenfelt, A. 1992: Gold, arsenic and antimony in stream sediment related to supracrustal units between Arfersiorfik and Qarajaq Isfjord (68°N to 70°30′N), West Greenland. Open File Series Grønlands Geologiske Undersøgelse **92/4**, 17 pp.

Stendal, H., Knudsen, C., Marker, M. & Thomassen, B. 1999: Gold mineralisation at Eqi, north-east Disko Bugt, West Greenland. In: Kalsbeek, F. (ed.): Precambrian geology of the Disko Bugt region, West Greenland. Geology of Greenland Survey Bulletin **181**, 129–140 (this volume).

Thomassen, B. & Tukiainen, T. 1992: Gold mineralisation in Precambrian supracrustal rocks on southern Nuussuaq, central West Greenland: 1991 results. Open File Series Grønlands Geologiske Undersøgelse **92/3**, 31 pp.

Thorpe, R.I. & Franklin, J.M. 1984: Chemical-sediment-hosted gold. In: Eckerstrand, O.R. (ed.): Canadian mineral deposit types: a geological synopsis. Geological Survey of Canada Economic Geology Report **36**, 29 only.

Gold mineralisation at Eqi, north-east Disko Bugt, West Greenland

Henrik Stendal, Christian Knudsen, Mogens Marker and Bjørn Thomassen

Gold mineralisation at Eqi, north-east Disko Bugt, West Greenland, is hosted in Archaean (*c.* 2800 Ma old) supracrustal rocks; the latter are divided by a thrust into a lower volcanic unit and an upper sedimentary and volcaniclastic unit. The lower volcanic unit comprises three parts: a basal pillowed greenstone sequence, an acid volcanic complex, and an upper mafic igneous complex.

Intensive hydrothermal activity resulted in extensive carbonatisation and sericitisation, which is most intense just above a system of acid feeder dykes within the basal greenstone sequence. Primary enrichment in gold took place during pervasive hydrothermal alteration, and the gold is mainly located in carbonate-altered rocks. Remobilisation of gold occurred during formation of later quartz veins in the altered zone; these quartz veins have gold contents of up to 60 ppm.

The geological setting, geochemistry and formation of the gold mineralisation at Eqi is similar to many Archaean gold deposits in the Abitibi belt of Canada.

H.S. & M.M.*, *Geological Institute, University of Copenhagen, Øster Voldgade 10, DK-1350 Copenhagen K, Denmark.* *Present address: *Geological Survey of Norway, Leiv Eirikssonsvei 39, N-7491 Trondheim, Norway.* E-mail: *henriks@geo.geol.ku.dk.*
C.K. & B.T., *Geological Survey of Denmark and Greenland, Thoravej 8, DK-2400 Copenhagen NV, Denmark.*

Keywords: alteration, Archaean, Disko Bugt, gold, supracrustal rocks, West Greenland

Discovery of gold anomalies by the Geological Survey of Greenland (GGU) in north-east Disko Bugt in 1988 at what later became known as the 'Eqi East Prospect', was followed by further exploration by Platinova Resources Ltd – Faxe Kalk A/S in 1989–1991 (Knudsen & Nielsen 1992) and GGU in 1991. This paper presents an overview of the current knowledge of the mineralisation, and suggests a genetic model. It is based on field work undertaken on the prospect by GGU and the Platinova – Faxe Kalk joint venture, as well as reports by Kryolitselskabet Øresund A/S on the 'Eqi West Prospect' (Gothenborg & Keto 1986).

Regional geological mapping in the north-eastern part of the Disko Bugt area was carried out by GGU in 1964 (Escher & Burri 1967) and continued in the years 1987 to 1991 (Knudsen *et al.* 1988; Kalsbeek & Christiansen 1992; Steenfelt 1992); regional mineral exploration was carried out by Kryolitselskabet Øresund A/S in 1980–82 (Gothenborg & Keto 1986), and by Platinova Resources Ltd – Rayrock-Yellowknife Resources Inc. in 1988 (Blackwell 1989).

Geology of the Eqi area

The Eqi area consists of Archaean granitoid rocks, gneisses and units of supracrustal rocks (Garde & Steenfelt 1999, this volume) which are unconformably overlain by early Proterozoic supracrustal rocks of the Anap nunâ Group. The Archaean supracrustal sequence is dated at *c.* 2800 Ma (Kalsbeek & Taylor 1999, this volume).

In the Eqi area (Fig. 1) Archaean supracrustal rocks are in tectonic contact with Archaean migmatitic

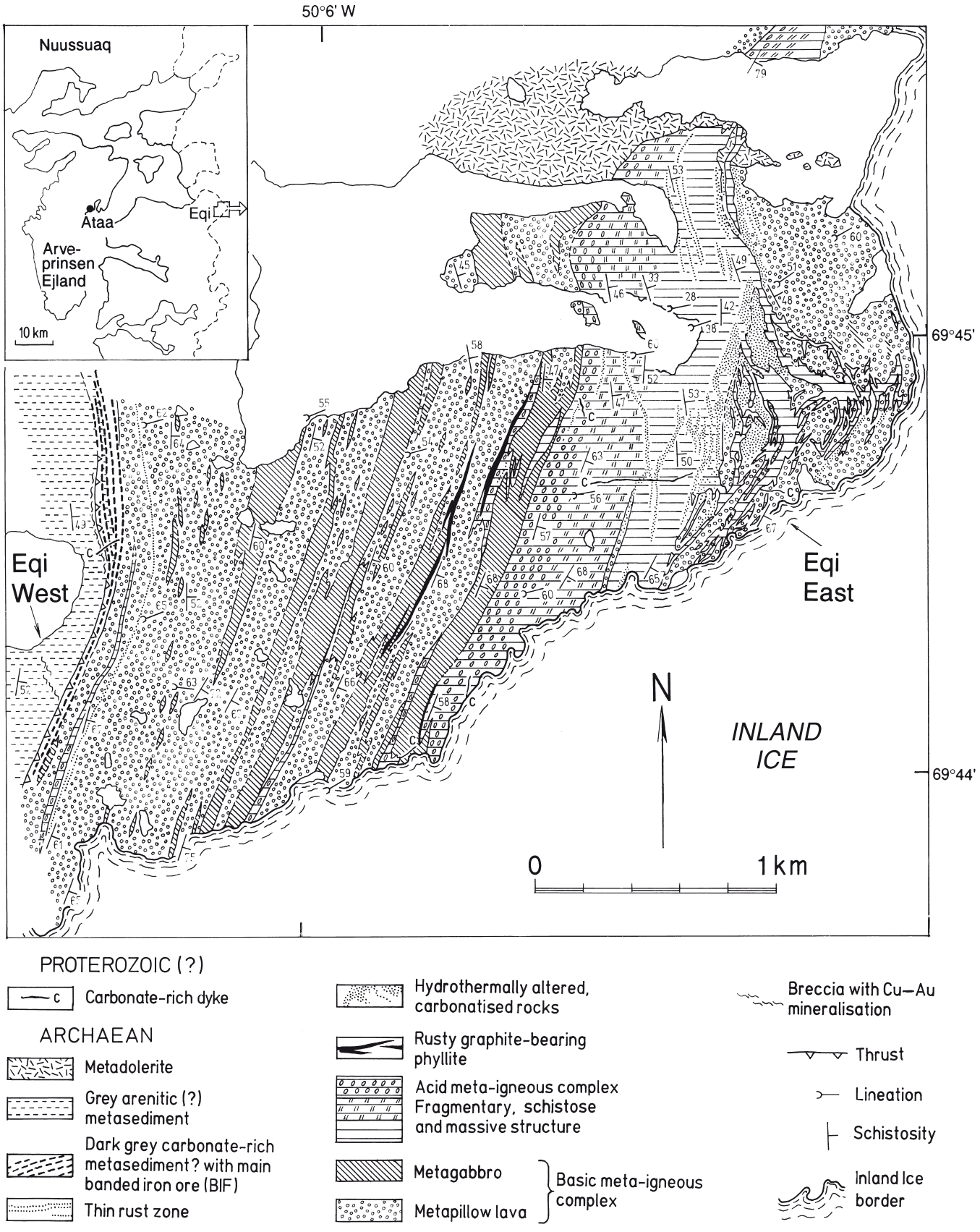

Fig. 1. Geological map of part of the Eqi area.

gneisses and variably foliated non-migmatitic granitoid rocks containing occasional layers of amphibolite. Granitoid sheets, probably related to the 2800 Ma Atâ tonalite (Garde & Steenfelt 1999; Kalsbeek & Skjernaa 1999, both in this volume) intrude the supracrustal rocks. The interleaved granitoid and supracrustal rocks are highly strained and form a conspicuous layered rock unit below an eastward-dipping thrust contact with the supracrustal sequence to the east (see geological maps of Garde 1994 accompanying this volume, and Escher 1995).

Stratigraphy

The Archaean supracrustal sequence at Eqi can be divided into an eastern succession dominated by basic meta-igneous rocks, with an important acid igneous complex in the central part of the sequence, and a western succession of metasediments and volcaniclastic rocks with subordinate intercalations of basic rocks. The eastern and western successions are separated by a thrust which dips eastwards at 50–70°, parallel to the schistosity (Fig. 1). There are also thrusts in the western succession, which converge southwards towards a boundary thrust which forms the contact with the gneisses. The thrust between the two successions coincides with a marked change in metamorphic grade, greenschist facies in the east and amphibolite facies in the west. Five kilometres to the north-west the continuation of the thrust is obscured by unconformably overlying conglomerates which form the basal part of the early Proterozoic Anap nunâ Group (Garde & Steenfelt 1999, this volume). Only the eastern Archaean succession is discussed in detail here.

Basic igneous complex. The eastern succession of supracrustal rocks is at least 3–4 km thick and consists mainly of greenschist facies pillow lavas intruded by sheets of metagabbro (Fig. 1). Primary features of the pillow lavas are often well preserved, and from the packing structure of the pillows a westward-younging direction can be determined. This suggests that the supracrustal sequence at Eqi is inverted with its lowermost part located towards the east where it is hidden beneath the Inland Ice.

Acid igneous complex. The middle part of the eastern greenstone succession contains a conspicuous unit of acid igneous rocks, interpreted as a rhyolitic dome complex. The complex is several kilometres long and up to 1 km thick (Fig. 1), and is dominated by quartz and feldspar porphyries. Its lowermost part rests on the lower pillowed greenstone succession and consists of massive rhyolitic rocks capped by a schistose sericite schist which grades upwards into an agglomerate of closely packed fragments. The schistose zone appears to have a tectonic origin since it is discordant to the bedding of the rhyolites. The agglomeratic part of the sequence consists of stretched, closely packed, rounded, elongated fragments of whitish to light grey porphyry with scattered 1–4 mm large phenocrysts of quartz and plagioclase. The matrix between the fragments also contains quartz and plagioclase. A network of rhyolitic dykes in the underlying greenstones is interpreted as a feeder dyke system to the rhyolite dome complex. The lower massive part as well as the feeder dykes consist of homogeneous light grey porphyry with scattered phenocrysts of quartz and plagioclase.

Metasedimentary rocks. At several levels within the volcanic sequence there are thin discontinuous layers of black graphite phyllites. Thin layers of banded iron formation also occur locally, the first immediately above the main acid body. The metasediments are generally overlain by greenstones. Extensive layers of banded iron formation occur in the uppermost part of the eastern greenstone-dominated succession where they are hosted in a 20–50 m thick unit which consists of layers of metasediment and acid volcanics, each up to 2–4 m thick.

Dolerite. The northern part of the acid igneous complex at Eqi is cut by a large body of black metadolerite (Fig. 1). The rock is locally deformed and strongly altered, and it is presumably of Archaean age.

Late carbonate-rich dykes. Several carbonate-rich dykes occur within the supracrustal rocks. They generally trend E–W, N–S or NE–SW (Fig. 1). They are up to 1 m thick and post-date the main deformation and shearing, but locally they are folded into open folds, possibly by passive folding during late flattening. The dykes are composed of fine-grained carbonate (75–85%), quartz (3–15%), muscovite (0–15%), chlorite (0–6%), opaque minerals (1–2%) and accessory titanite. The age of these dykes is unknown.

E–W-trending suites of ultramafic lamprophyre dykes, often with carbonate-rich centres, are widespread in the Archaean gneisses (Marker & Knudsen 1989). These dykes differ from the carbonate-rich dykes in the supracrustal sequence in that they have a differ-

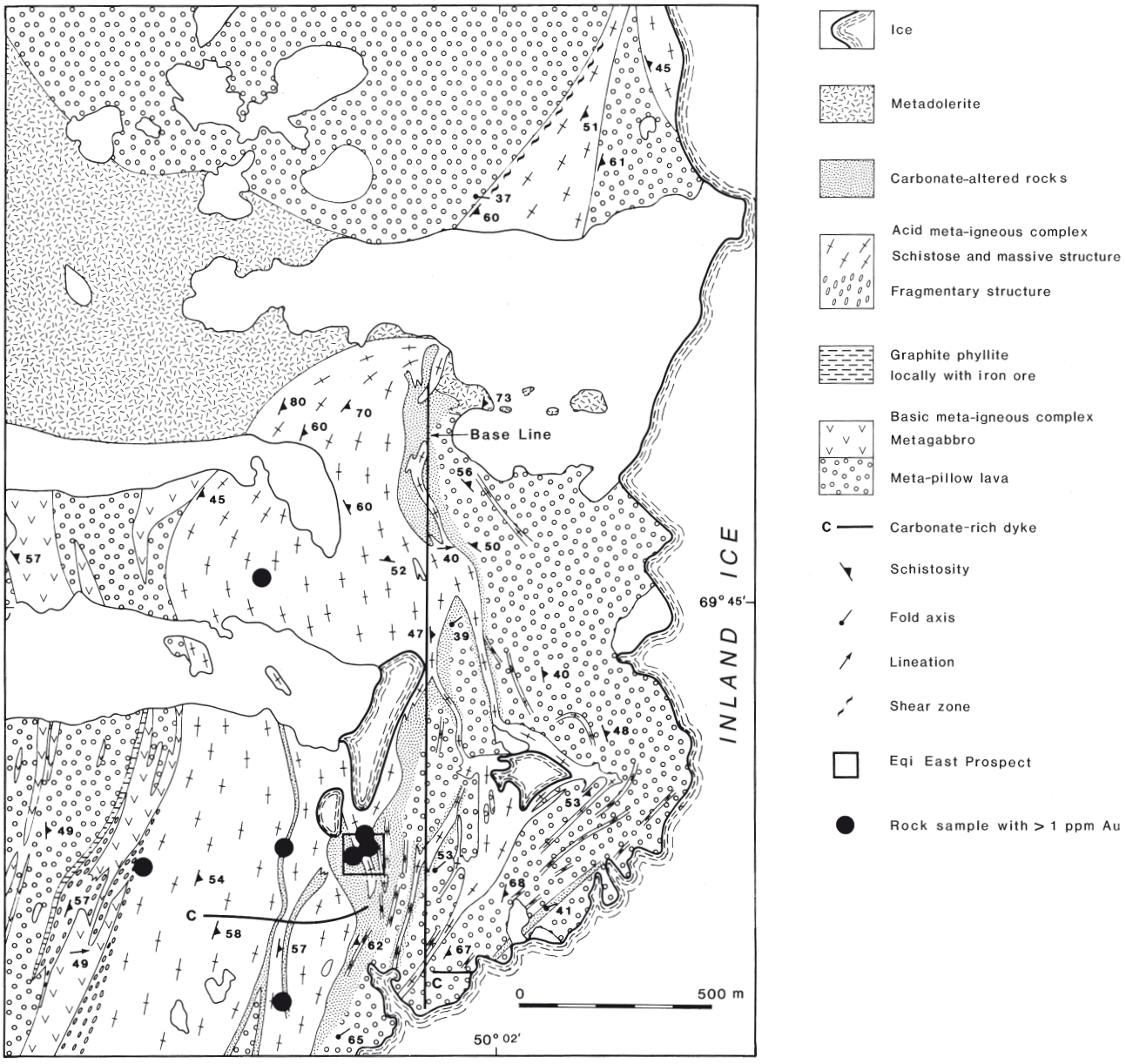

Fig. 2. Simplified geological map of the eastern Eqi area.

ent composition, commonly with igneous phlogopite preserved, and they give rise to strong contact alteration in the gneisses. The age of the lamprophyres is *c*. 1750 Ma (Larsen & Rex 1992; Rasmussen & Holm 1999, this volume).

Hydrothermal alteration

Hydrothermal alteration associated with extensive carbonatisation and local sericitisation, chloritisation and pyritisation affected the boundary area between the lower part of the acid volcanic complex and the underlying pillowed greenstones (Figs 1, 2). During hydrothermal alteration both acid and basic rocks were affected, often to such a degree that it can be difficult to determine whether the protolith was basic or acid. The acid feeder dyke system also shows evidence of an increasing degree of hydrothermal alteration towards the base of the acid volcanic sequence.

According to Knudsen *et al.* (1990) and Knudsen & Nielsen (1992) two main types of carbonate-altered rocks were formed successively: (1) massive carbonate-altered rocks with desilicification structures giving rise to thin (<5 cm) quartz veins, and (2) schistose carbonate-altered rock rich in sericite. Within both types

of carbonatised rock microjoints are filled with dark green chlorite, sericite, green mica (fuchsite?) and pyrite. A widespread product of the hydrothermal carbonate alteration is a graphitic, green mica- and chlorite-bearing ankerite rock with an irregular network of quartz veins, up to 1 m wide (Fig. 3). Tiny prisms of accessory black tourmaline are common in the altered rocks and in minor shear zones. Some tourmaline is also present in quartz ankerite veins.

Metamorphism

The rocks of the eastern supracrustal succession at Eqi are metamorphosed to the (upper) greenschist facies. The meta-pillow lavas are rich in chlorite while metagabbros are rich in pale actinolitic amphibole. Both contain subordinate epidote. The acid meta-igneous rocks are rich in sericite or fine-grained muscovite generally making up to 10–25% of the rock. Epidote, chlorite, biotite and carbonate occur in accessory amounts outside the hydrothermally altered zones. The lower schistose and massive parts of the main acid body, the feeder dyke system and particularly the hydrothermally altered rocks frequently contain chloritoid, locally making up to 10–15% of the rock, possibly reflecting iron enrichment during hydrothermal activity.

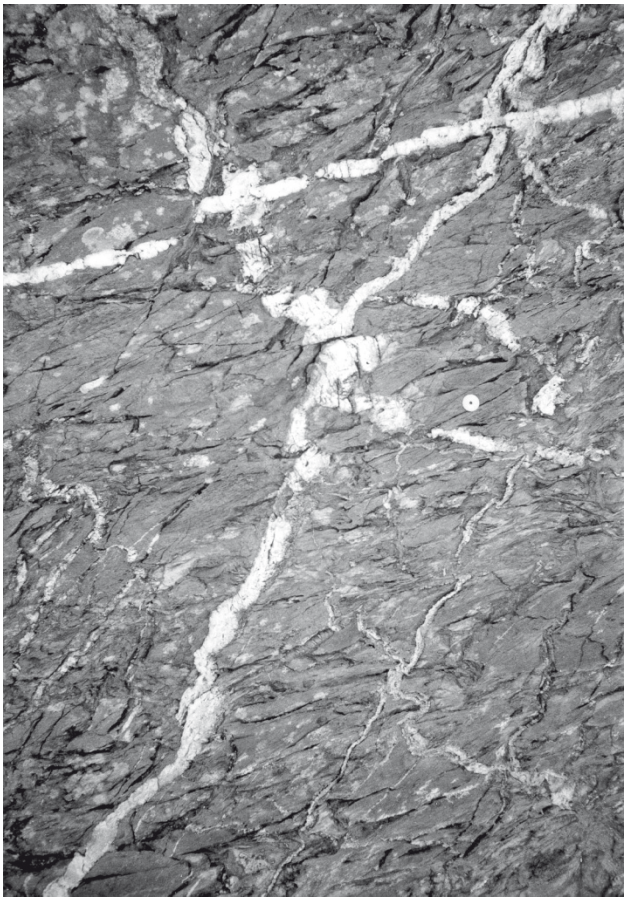

Fig. 3. Carbonate-altered rocks with quartz veins. Coin for

Structure

The supracrustal sequence at Eqi shows evidence of one episode of penetrative deformation which culminated in thrusting. The eastern succession shows only minor tight to isoclinal fold structures while the overlying western succession has a large-scale isoclinal fold. A penetrative schistosity (S_1) is related to this deformation (D_1). S_1 is parallel to axial planes in isoclinal folds formed during D_1. Fold axes plunge 45–65° NE to ENE, parallel to a pronounced penetrative stretching lineation that possibly indicates thrusting towards the SW–WSW. Fold axes may have been reorientated during the thrusting. Strain indicators, i.e. pillows and acid fragments, indicate considerable stretching, and show that the original thickness of the Eqi sequence may have been much greater than seen today. The middle zone of the rhyolite dome complex is assumed to have been sheared contemporaneously with the thrusting elsewhere in the sequence. Since the rocks in question are unconformably overlain by undeformed early Proterozoic sedimentary rocks further to the north-west, this dominant episode of deformation is inferred to be Archaean. Later deformation locally gave rise to an east–west steeply to vertically dipping fracture cleavage, locally developed as a schistosity, which may be associated with quartz filled tension gashes and small-scale open folds (amplitude <10 cm). Shear zones hosting gold-bearing quartz veins (Fig. 4) are probably related to this deformation.

Mineralisation

'Eqi West Prospect'

During the period 1980–82 Kryolitselskabet Øresund A/S carried out airborne and ground geophysical surveys, regional geological mapping, and percussion and diamond drilling on several localities with indications of copper mineralisation (Gothenborg 1983). Copper mineralisation was found along the western side of the thrust zone between the eastern and western Eqi successions. The mineralisation is hosted in concord-

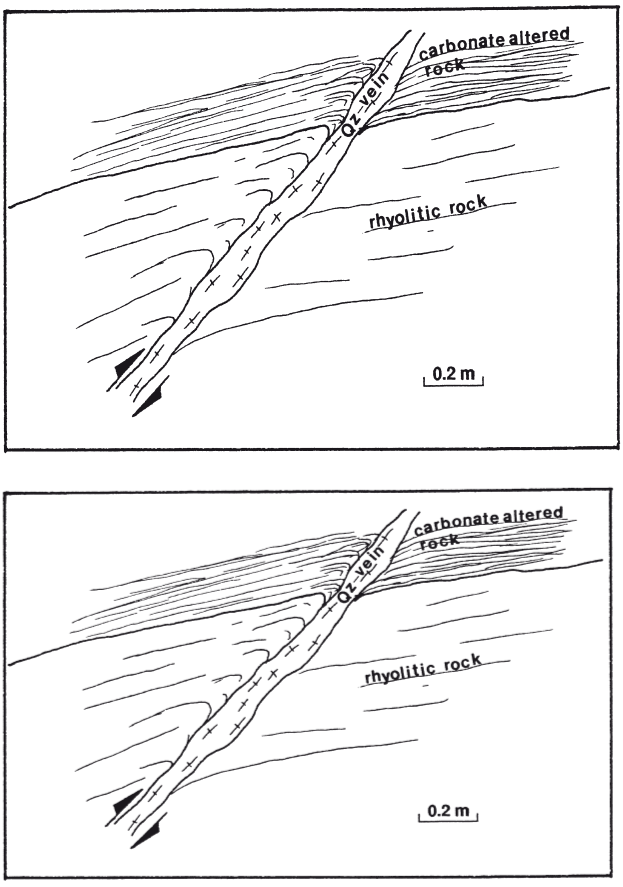

Fig. 4. Late quartz veins in small shear zones. From Knudsen & Nielsen (1992).

ant and discordant calcite, ankerite and quartz-cemented breccia zones in grey arenitic metasediments, a few tens of metres above the banded iron formation which marks the top of the metavolcanic unit. The age of the breccia zones is unknown.

The most promising occurrence, the 'Eqi West Prospect', comprises a discordant breccia zone up to 10 m wide, orientated 150°/80°NE, which outcrops over approximately 100 m. The zone consists of fragments of mica schist and phyllite cemented by calcite, ankerite, quartz, chlorite and sulphides. The predominant sulphide assemblage is pyrrhotite, chalcopyrite and pyrite with minor sphalerite, arsenopyrite, native bismuth and gold. The gold (electrum) contains 31% Ag (Sotka 1984). It occurs mainly as up to 100 µm large inclusions in chalcopyrite and occasionally in pyrrhotite. There is a strong positive correlation between the Au, Cu, Ag and Bi contents of the samples analysed. Nineteen grab samples from the prospect assayed 0.2–4.6% Cu averaging 0.84% Cu. The highest gold value obtained was 22 ppm and the best drill intersection assayed 1.3% Cu and 12 ppm Au over 3.8 m corresponding to a true thickness of *c.* 2 m (Sotka 1984).

Four grab samples collected by GGU in 1991 from this breccia zone yielded a maximum of 13.5 ppm Au and 2% Cu. Knudsen *et al.* (1988) published chemical analyses for sulphide-bearing grab samples from the area and reported up to 12.3 ppm Au in a brecciated phyllite with carbonate and chalcopyrite veins.

Eastern Eqi area

Gold mineralisation (6 ppm Au in a 1 m chip sample) was found in the eastern Eqi area by GGU in 1988. In 1989 and 1990 prospecting and mapping was carried out by the Platinova – Faxe Kalk joint venture. Subsequent analysis of sulphide-bearing rocks yielded up to 60 ppm Au in a quartz vein grab sample (Knudsen *et al.* 1990). Detailed chip sampling was carried out by GGU and Platinova – Faxe Kalk in 1991 in the 'Eqi East Prospect' (Fig. 2), the area from where the highest gold values had been obtained previously (Knudsen & Nielsen 1992).

Most of the recorded gold was found by analytical means. Locally, however, visible gold occurs in blebs up to 20 µm across in pyrite (Knudsen & Nielsen 1992) and as small grains, a few micrometres in size, associated with carbonate and goethite, the latter probably formed by alteration of pyrite.

There are several types of sulphide mineralisation in the eastern Eqi area consisting mainly of pyrite with minor chalcopyrite and pyrrhotite.

Disseminated to massive pyrite occurs as rusty zones in a 50–200 m wide transition zone between the massive rhyolites and sericite schist (Fig. 1). Pyrite mineralisation also occurs as fine-grained pyrite in centimetre to decimetre thick massive layers with quartz, and as large pyrite grains with highly strained rims in a quartzsericite matrix. In the northern part of the area the rusty pyrite-bearing zones are often sheared. This type of pyrite mineralisation is stratiform and occurs at several levels.

Disseminated pyrite in the carbonatised areas. Carbonatised rocks commonly have varying amounts of disseminated pyrite, up to 5% by volume. The pyrite is commonly recrystallised to euhedral crystals, but sometimes it exhibits cataclastic textures. Chalcopyrite is interstitial to pyrite grains and also occurs in cataclastic cracks and voids.

Table 1. Gold concentrations in different rock types of the eastern Eqi area

	N	range (ppb)	median (ppb)	No of samples with Au > 0.5 ppm
Rock samples				
acid rocks	62	5–1100	9	3
acid dykes	6	1–33	2	0
sulphide-rich rocks	8	5–172	16	0
basic rocks	11	1–126	11	0
carbonate-altered rocks	51	5–5850	22	6
quartz-veined rocks	26	5–60 000	69	8
Chip samples				
acid rocks	36	1–3000	5	3
carbonate-altered rocks	67	1–2350	5	2
quartz-veined rocks	43	1–1656	32	6

Acid rocks: rocks from the acid igneous complex as well as a variety of quartz-feldspar-sericite schists with occasional quartz and feldspar porphyroclasts. Most of these rocks have been altered by sericitisation and carbonatisation and formation of green mica. **Acid dykes**: samples belonging to the feeder dyke system associated with the acid igneous complex (Fig. 1). Pyrite occurs locally in very small amounts. **Sulphide-rich rocks**: rocks rich in fine grained primary pyrite in centimetre to decimetre thick layers or with euhedral remobilised disseminated and veinlet pyrite, which may be associated with chalcopyrite. **Basic rocks**: meta-pillow lavas altered to greenstones. Small amounts of pyrite occur disseminated within the greenstones. **Carbonate-altered rocks**: very carbonate-rich rocks with characteristic brown weathered surfaces. All samples contain varying proportions of pyrite. **Quartz veins**: quartz veins are common in carbonate-altered rocks, but also occur locally in all other rock types. Also included here are quartz-rich samples which mainly consist of vein material. Quartz veins contain variable amounts of pyrite.

Pyrite in quartz veins. Pyrite also occurs disseminated and as up to 20 mm euhedral crystals in quartz veins, locally with chalcopyrite. The quartz veins (up to several decimetres thick) are discordant to S_1 schistosity and lithological units, and occur in small shear zones in the carbonate-altered rocks and in adjacent altered acid metavolcanics indicating that the veins post-date the carbonate alteration. The strike of the shear zones is generally 140° with a dip of approximately 30° NE.

Pyrrhotite. Pyrrhotite makes up a minor proportion of the sulphides in the area, but can be found locally in abundance in breccia zones formed where discordant shear zones cut graphite-bearing layers.

Geochemistry

A total of 298 rock and chip samples from the eastern Eqi area were analysed for gold during the various investigations. Some of the samples were also analysed for 30 minor and trace elements by instrumental neutron activation analysis (INAA), and in addition all anomalous gold-bearing samples were re-analysed for Au by fire assay and atomic absorption spectrophotometry (AAS). Base metals were determined by AAS after digestion in aqua regia. Major elements were determined by X-ray fluorescence spectrometry (XRF) on glass discs. Analytical data for some of the elements are shown in Tables 1 and 2.

Two types of samples were analysed (Table 1): (1) samples of specific rock types and (2) chip samples each representing 2.5 m per sample (Fig. 5) often with mixed rock types. The latter were weighted with respect to the proportion of different rock types and classified as shown in Table 1.

General. The basic rocks are tholeiitic in composition with SiO_2 contents in the range 49–56%; ratios between K_2O and Na_2O are typical for unaltered tholeiites. Various discrimination plots of minor elements suggest that the basic lavas may have originated in an island-arc or back-arc basin setting.

The rhyolitic rocks have SiO_2 contents ranging from 72 to 87%, but K_2O and Na_2O levels fall well outside the normal igneous range, suggesting that their composition was strongly affected by alteration. Alteration increases down the sequence, with the least altered rocks in the fragmentary part of the rhyolitic dome complex and the most altered in the lower massive

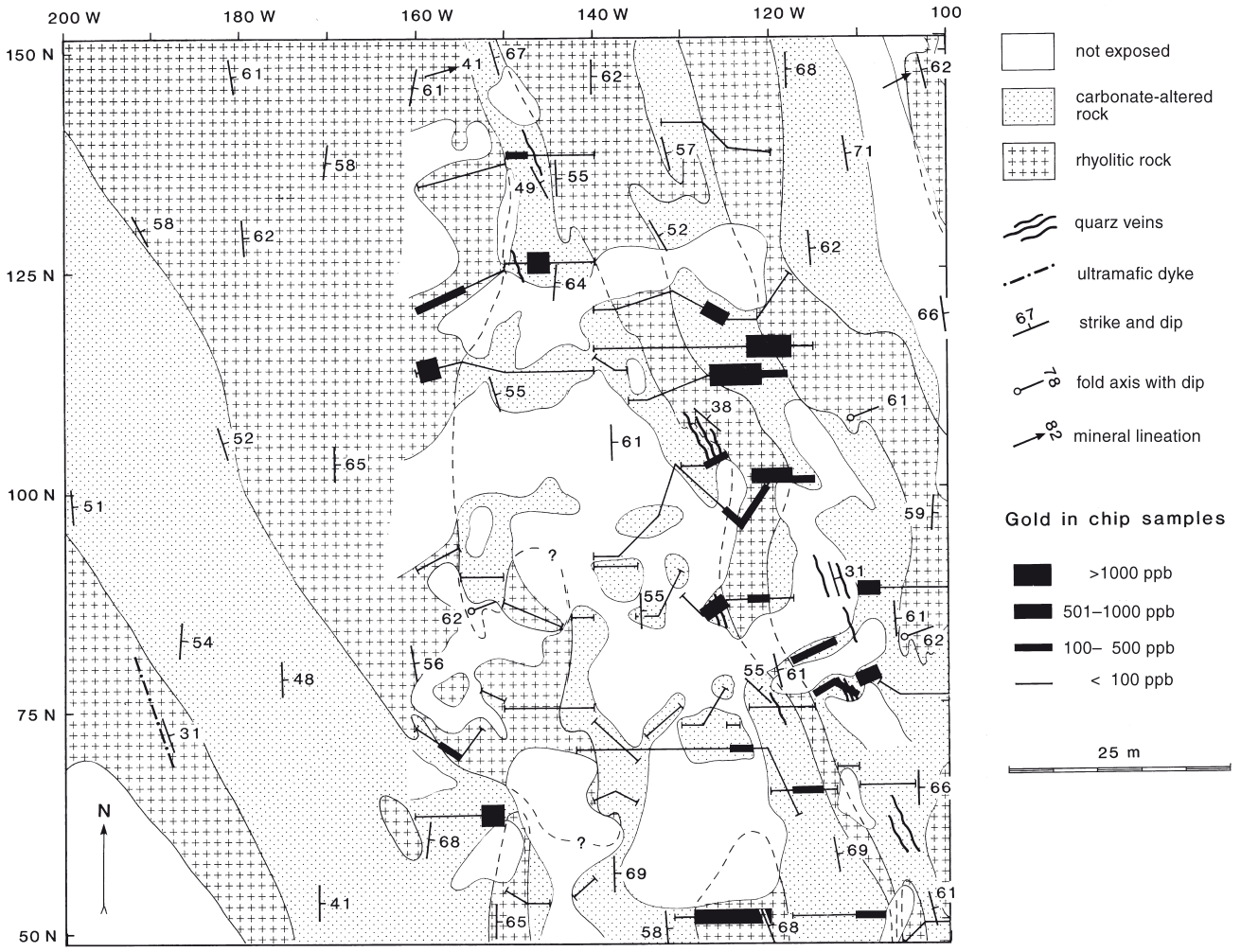

Fig. 5. 'Eqi East Prospect' with profile lines and their gold contents; for location see Fig. 2. Coordinates in metres west and north of an arbitrary point on the base line shown on Fig. 2.

part and in the feeder dyke system. SiO_2 levels increase downwards while Na_2O and K_2O levels decrease. It is suggested that this reflects circulation of fluids, generated during successive phases of intrusion, from which the upper volcanics were relatively protected and hence have their magmatic composition better preserved. Discrimination plots using Y, Nb and Rb suggest the acid igneous suite may have been emplaced in an island-arc setting.

Gold. Median gold contents of rock and chip samples are given in Table 1. Enhanced gold values occur in the sulphide-rich rocks (stratiform occurrences, 16 ppb), the carbonate-altered rocks (22 ppb) and the quartz-veined rocks (69 ppb). Median gold values for chip samples of quartz-veined rocks are also elevated (32 ppb). High Au (>0.5 ppm) is found in several rock types (Table 1). Gold in the quartz-vein-bearing rocks varies between 5 and 60 000 ppb. The highest concentration (60 ppm) is from a composite grab sample of a pyrite-bearing quartz vein in the carbonate-altered rocks.

Figure 5 shows the distribution of Au in profiles based on chip samples in the 60×100 m² 'Eqi East Prospect'. High Au values occur particularly in the east of this area where the average is 411 ppb in 27 chip samples collected over a surface area of 500 m².

Other elements. Trace element analysis has been carried out on 28 rock samples from the 'Eqi East Prospect', and selected results are given in Table 2. The acid rocks have enhanced contents of As (average 52 ppm) and Cu (320 ppm) compared to average acid volcanics (generally <5 ppm As and <40 ppm Cu, according to Wedepohl 1969–1978). This appears to

Table 2. Range and mean concentrations for selected trace elements in rocks of the Eqi area

	acid rocks		acid dykes		basic rocks		carbonate-altered rocks	
N	8		4		4		12	
element (ppm)	mean	range	mean	range	mean	range	mean	range
As	52	4–130	6	1–16	38	1–120	32	1–59
Ba	385	100–910	203	140–160	123	100–160	269	100–610
Co	34	6–110	6	1–10	111	37–280	44	12–91
Cr	265	5–1500	6	5–10	39	39–330	218	31–400
Cu	320	7–2161	40	7–118	234	94–348	89	37–212
Ni	128	50–290	<50	<50	113	50–180	134	56–200
Pb	4	2–11	5	2–10	<5	<5	<5	<5
Rb	52	5–130	33	5–47	<5	<5	25	5–56
Zn	28	3–169	18	12–30	79	23–123	69	19–121

For rock types see text and footnotes to Table 1.

reflect their strong alteration. Chromium shows extreme variation, with values up to 1500 ppm (generally <20 ppm in acid igneous rocks). On the other hand, Rb values (52 ppm) are lower than in most acid igneous rocks (commonly >100 ppm). Ba values (385 ppm) are low in comparison with other acid igneous rocks (commonly >1000 ppm) but comparison is difficult because of a wide scatter of reported Ba values. Low Rb and Ba probably correspond to the decrease in K_2O and Na_2O observed in the altered rocks. The carbonate- altered rocks show the same features as the acid rocks.

A multivariate statistical analysis was carried out on the rock samples from the eastern Eqi area using the Multivariate Statistic Package programme (Kovach 1990). The rock samples were treated as one population (N = 63) and the profile samples as another population (N = 30). 'Correponding Sample Analysis' and 'Principal Component Analysis' show the following trends: there is a general association between Au, Cu, Ag (and Cr); if the highest Cu values are omitted from the analysis, Au and Cr give a characteristic association. A second cluster is observed for As-Ba-Rb. If gold values are omitted from the statistical analysis, the elements can be grouped as follows: (1) Cr, (2) Rb-Ba, and (3) As-Co-Cu. The chip sample profiles show a strong association between SiO_2 and Au. Associations such as Au-Cu-Ag and As-Rb-Ba are characteristic of hydrothermal mineralisation, and support the contention that the concentrations of Au, As, Cu, Cr, Ba and Rb are strongly influenced by alteration.

Discussion

Geological setting

The Eqi area shows many stratigraphic and lithological similarities with the Abitibi greenstone belt in Canada (Hodgson 1986), especially at the Dome Mine, Timmins area, Ontario (Fyon & Crocket 1983; Moritz & Crocket 1991). Notable parallels in geological setting are: (1) bimodal volcanism, (2) hydrothermal alteration and (3) the relationship between the gold mineralisation and carbonatisation, and late stage quartz veining.

Geochemistry

The eastern Eqi area is characterised by primary hydrothermal alteration with enrichment in SiO_2 and Al_2O_3 in the lower part, probably caused by leaching of and deposition of Ca and other elements in the carbonate-altered zone. Element associations obtained by the multivariate statistical analysis indicate remobilisation of Au, Ag, As, Cu, and Cr during hydrothermal alteration processes. The association between Au and SiO_2 probably reflects the relation between high gold values and quartz veins. Mobilisation of hydrothermal fluids was probably related to the acid magmatic activity.

A close association of Au-Cu-Ag has also been reported from the 'Eqi West Prospect' (Sotka 1984). This mineralisation, which occurs in brittle deformed rocks, is clearly epigenetic, and could represent metals remobilised from an eastern Eqi type primary mineralisation.

Gold contents in the rocks of the 'Eqi East Prospect' are comparable to other areas with Au-bearing Archaean volcanic rocks. Rhyolitic rocks and acidic dykes at Eqi contain 9 ppb and 2 ppb Au, respectively (Table 1). Granitic plutons normally contain 1–2 ppb Au (Crocket 1991), but Boyle (1991) reports up to 50 ppb Au for quartz-feldspar porphyries in Archaean greenstone belts. The basic rocks at Eqi yield on average 11 ppb Au (Table 1) compared to 5.7 ppb Au for Precambrian tholeiitic basalts (Crocket 1991) and 3 ppb for average basalt (Boyle 1991). Anomalous Archaean greenstone belts are known from Southern Africa (Saager *et al.* 1982) and from Bogoin, Central African Republic (komatiitic and tholeiitic basalts, Dostal *et al.* 1985), which yield averages of 10.8 and 37.1 ppb Au respectively.

Alteration and formation of gold mineralisation

Hydrothermal alteration occurred initially in the form of leaching and carbonatisation of the volcanic sequence, which was most intense in and just above the feeder dyke system. It was followed by sericitisation, formation of green mica and chloritisation. This evolution of the alteration is similar to that observed in many deposits in the Timmins area, Ontario, e.g. at the Dome Mine (Fyon & Crocket 1983, Moritz & Crocket 1991).

Formation of the primary gold mineralisation at eastern Eqi is related to the pervasive carbonate alteration. Remobilisation of gold into late (post-S_1) quartz veins occurred at the 'Eqi East Prospect'. These quartz veins host the highest gold concentrations. A prominent feature seen in eastern Eqi as well as in western Eqi is that the gold-bearing sulphides often are located where post-S_1 veins or shear zones cut graphite-rich layers. This suggests that deposition or remobilisation of gold may here be controlled by strongly reducing conditions.

Eqi and Abitibi, Canada: parallels and contrasts

Hodgson *et al.* (1982) have suggested exploration criteria for gold mineralisation in greenstone belts based on Archaean gold mines in Canada. In the following some of these criteria are discussed with parallels and contrasts between gold mines in the Timmins area, Abitibi belt, and the 'Eqi East Prospect'.

1. Hodgson *et al.* (1982) noticed a very common association of gold with acidic rocks. Although the proportion of acid volcanic rocks is much smaller than that of mafic rocks, over 90% of the gold deposits are connected to intrusive or extrusive acid rocks. This is also the case at Eqi. A contrast is the large apparent stratigraphic thickness of volcanic rocks in the Abitibi greenstone belt (*c.* 40 km; Hodgson 1986) compared to one tenth of this thickness at Eqi.

2. Hodgson et al. (1982) divided the gold deposits into four main types depending on their relationships to the felsic host rock. The primary enrichment at the 'Eqi East Prospect' is comparable to the so-called 'Dome-type' which is a vein or stratiform ore zone hosted mainly by volcanic rocks with associated quartz-bearing felsic rocks.

3. Iron-rich sedimentary rocks are commonly associated with the Dome-type deposits. In the Abitibi belt occurrences magnetite exhalites are closely associated with the ore. In the eastern Eqi area these horizons (graphite-bearing phyllites with iron oxides) occur stratigraphically above the hydrothermally altered and gold mineralised area in the volcanic stratigraphy (Fig. 2). At the 'Eqi West Prospect' iron formation lies close to epigentic Cu-Au mineralisation.

4. Major carbonate alteration is common in eastern Eqi. In the Canadian gold deposits carbonate alteration is ubiquitous (e.g. in the Rundle gold deposit; Love & Roberts 1991).

5. A major change in lithology occurs in some of the Canadian deposits. In eastern Eqi the gold mineralisation is closely associated with the boundary between basic and acid igneous rocks and associated spatially with acid intrusive rocks. In western Eqi the Cu-Au mineralisation is closely associated with a thrust zone.

6. In the Canadian Shield gold is often associated with arsenopyrite, scheelite and tourmaline. This is especially characteristic for the intrusive-hosted deposits. In addition, pyrite is common, while green mica ('fuchsite') occurs only in some of the deposits. Eastern Eqi samples show enhanced As values, but As concentrations are not very high. Tourmaline is widespread at eastern Eqi and a small piece

of scheelite has been discovered under ultra-violet light in addition to an enhanced level of tungsten in heavy mineral concentrates (51–95 ppm W) compared to the regional background pattern.

7. Many of the Canadian gold mines in greenstone belts have a predominance of pyrrhotite over pyrite (Colvine 1989) whereas at eastern Eqi the rock is dominated by pyrite.

Conclusions

The gold mineralisation at the 'Eqi East Prospect' is hosted by a *c*. 2800 Ma old basic–acid succession that may have been formed in an island-arc environment. Mineralisation took place in two phases: (1) a primary, pervasive mineralisation caused by hydrothermal leaching and carbonate alteration of the rock pile related to acid igneous activity, and (2) during the formation of late quartz veins when gold was remobilised and deposited together with iron sulphides.

The 'Eqi East Prospect' has many similarities to gold mines in the Abitibi greenstone belt, especially the Timmins area, with respect to geological setting, geochemistry and mode of emplacement.

In the western Eqi area gold mineralisation is located in sulphide-bearing breccia zones close to the thrust zone which separates the eastern and western supracrustal successions.

Acknowledgement

The Carlsberg Foundation is thanked for financial support to C.K. and M.M. during their participation in the Disko Bugt Project.

References

Blackwell, J. 1989: Report of 1988 field season, Disko Bay project, 18 pp. Unpublished report, Platinova Resources Ltd. and Yellowknife Resources, Toronto, Canada (in archives of Geological Survey of Denmark and Greenland).

Boyle, R.W. 1991: Auriferous Archaean greenstone-sedimentary belts. Economic Geology Monograph **8**, 164–191.

Colvine, A.C. 1989: An empirical model for the formation of Archean gold deposits: products of final cratonization of the Superior Province, Canada. Economic Geology Monograph **6**, 37–53.

Crocket, J.H. 1991: Distribution of gold in the Earth's crust. In: Foster, R.P. (ed.): Gold metallogeny and exploration, 1–36. Glasgow and London: Blackie.

Dostal, J., Dupuy, C. & Poidevin, J.L. 1985: Geochemistry of Precambrian basaltic rocks from Central African Republic (Equatorial Africa). Canadian Journal of Earth Sciences **22**, 653–662.

Escher, A. & Burri, M. 1967: Stratigraphy and structural development of the Precambrian rocks in the area north-east of Disko Bugt, West Greenland. Rapport Grønlands Geologiske Undersøgelse **13**, 28 pp.

Escher, J.C. 1995: Geological map of Greenland, 1:100 000, Ataa 69 V.3 Nord. Copenhagen: Geological Survey of Greenland.

Fyon, J.A. & Crocket, J.H. 1983: Gold exploration in the Timmins area using field and lithogeochemical characteristics of carbonate alteration zones. Ontario Geological Survey Study **26**, 56 pp.

Garde, A.A. 1994: Precambrian geology between Qarajaq Isfjord and Jakobshavn Isfjord, West Greenland, 1:250 000. Copenhagen: Geological Survey of Greenland.

Garde, A.A. & Steenfelt, A. 1999: Precambrian geology of Nuussuaq and the area north-east of Disko Bugt, West Greenland. In: Kalsbeek, F. (ed.): Precambrian geology of the Disko Bugt region, West Greenland. Geology of Greenland Survey Bulletin **181**, 6–40 (this volume).

Gothenborg, J. 1983: Report on the ore exploration in the Atâ area, Jakobshavn, 27 pp. Unpublished report, Kryolitselskabet Øresund A/S, Copenhagen, Denmark (in archives of Geological Survey of Denmark and Greenland).

Gothenborg, J. & Keto, L. 1986: Exploration in the Atâ area, Jakobshavn, 1980–1985, 12 pp. Unpublished report, Kryolitselskabet Øresund A/S, Copenhagen, Denmark (in archives of Geological Survey of Denmark and Greenland).

Hodgson, C.J. 1986: Place of gold ore formation in the geological development of the Abitibi greenstone belt, Ontario, Canada. Transactions Institute of Mining and Metallurgy (Section B: Applied Earth Sciences) **95**, B183–B194.

Hodgson, C.J., Chapman, R.G.S. & MacGeehan, P.J. 1982: Application of exploration criteria for gold deposits in the Superior Province of the Canadian shield to gold exploration in the Cordillera. In: Levinson, A.A. (ed.): Precious metals in the northern Cordillera, 173–206. Rexdale, Ontario: Association of Exploration Geochemists.

Kalsbeek, F. & Christiansen, F. G. 1992: Disko Bugt Project 1991, West Greenland. Rapport Grønlands Geologiske Undersøgelse **155**, 36–41.

Kalsbeek, F. & Skjernaa, L. 1999: The Archaean Atâ intrusive complex (Atâ tonalite), north-eastern Disko Bugt, West Greenland. In: Kalsbeek, F. (ed.): Precambrian geology of the Disko Bugt region, West Greenland. Geology of Greenland Survey Bulletin **181**, 103–112 (this volume).

Kalsbeek, F. & Taylor, P.N. 1999: Review of isotope data for Precambrian rocks from the Disko Bugt region, West Greenland. In: Kalsbeek, F. (ed.): Precambrian geology of the Disko Bugt region, West Greenland. Geology of Greenland Survey Bulletin **181**, 41–47 (this volume).

Knudsen, C. & Nielsen, J.P. 1992: Final report on detailed gold exploration in the Eqe East Gold Prospect, NE Disko Bay,

August 1991, 10 pp. Unpublished report, Platinova Resources Ltd. and Faxe Kalk A/S, Toronto, Canada, and Copenhagen, Denmark (in archives of Geological Survey of Denmark and Greenland).

Knudsen, C., Appel, P.W.U., Hageskov, B. & Skjernaa, L. 1988: Geological reconnaissance in the Precambrian basement of the Atâ area, central West Greenland. Rapport Grønlands Geologiske Undersøgelse **140**, 9–17.

Knudsen, C., Atkinson, J. & Gothenborg, J. 1990: Evaluation of the gold potential of Archaean rocks from an area in the Disko Bay region of Greenland, 15 pp. Unpublished report, Platinova Resources Ltd. and Faxe Kalk A/S, Toronto, Canada, and Copenhagen, Denmark (in archives of Geological Survey of Denmark and Greenland).

Kovach, W.L. 1990: M.V.S.P. Shareware. A multivariate statistics package for the IBM PC and compatibles, version **2**, 21 pp. Aberystwyth: Institute of Earth Studies, University College of Wales.

Larsen, L.M. & Rex, D.C. 1992: A review of the 2500 Ma span of alkaline-ultramafic, potassic and carbonatitic magmatism in West Greenland. Lithos **28**, 367–402.

Love, D.A. & Roberts, R.G. 1991: The geology and geochemistry of gold mineralization and associated alteration at the Rundle gold deposit, Abitibi subprovince, Ontario. Economic Geology **86**, 644–666.

Marker, M. & Knudsen, C. 1989: Middle Proterozoic ultramafic lamprophyre dykes in the Archaean of the Atâ area, central West Greenland. Rapport Grønlands Geologiske Undersøgelse **145**, 23–28.

Moritz, R.P. & Crocket, J.H. 1991: Hydrothermal wall-rock alteration and formation of the gold-bearing quartz-fuchsite vein at the Dome mine, Timmins area, Ontario, Canada. Economic Geology **86**, 620–643.

Rasmussen, H. & Holm, P.M. 1999: Proterozoic thermal activity in the Archaean basement of the Disko Bugt region and eastern Nuussuaq, West Greenland: evidence from K-Ar and ^{40}Ar-^{39}Ar mineral age determinations. In: Kalsbeek, F. (ed.): Precambrian geology of the Disko Bugt region, West Greenland. Geology of Greenland Survey Bulletin **181**, 55–64 (this volume).

Saager, R., Meyer, M. & Muff, R. 1982: Gold distribution in supracrustal rocks from Archaean greenstone belts of southern Africa and from Palaeozoic ultramafic complexes of the European Alps: metallogenic and geochemical implications. Economic Geology **77**, 1–24.

Sotka, P. 1984: Report on samples from drilling profiles in the Eqip Kugssua area, West Greenland, 6 pp. Unpublished report, Kryolitselskabet Øresund A/S, Copenhagen, Denmark (in archives of Geological Survey of Denmark and Greenland).

Steenfelt, A. 1992: Gold, arsenic and antimony in stream sediment related to supracrustal units between Arfersiorfik and Qarajaq Isfjord (68°N to 70°30′N), West Greenland. Open File Series Grønlands Geologiske Undersøgelse **92/4**, 11 pp.

Wedepohl, K.H. (ed.): 1969–1978: Handbook of geochemistry, 2 vols. Berlin: Springer-Verlag.

Proterozoic tectonic overprinting of Archaean gneisses in Nuussuaq, West Greenland

Adam A. Garde and Agnete Steenfelt

Archaean orthogneisses and supracrustal rocks in eastern Nuussuaq in the southern part of the Rinkian orogen preserve much indirect evidence of Proterozoic reworking. In northern Nuussuaq, a marble occurrence which can be correlated with the Proterozoic Mârmorilik Formation of the Uummannaq district, is interleaved and intensely folded with Archaean orthogneisses. Dykes and sills of presumed Proterozoic age in southern Nuussuaq pre-date two major shear zones. Furthermore, published K-Ar and ^{40}Ar-^{39}Ar hornblende ages indicate that metamorphic temperatures of at least *c.* 550°C were reached in large parts of Nuussuaq during the Proterozoic.

Although available data are not sufficient to firmly establish the tectonic evolution of Nuussuaq, it can be shown that development of a regional flat-lying structure was succeeded first by upright folding and development of a major NW–SE-trending shear zone during crustal shortening, and subsequently by formation of an ENE–WSW-trending shear zone during crustal extension. A Rinkian detachment zone across Nuussuaq, similar to those known in the Uummannaq district, may link Proterozoic marble occurrences south of the peninsula with the marbles known in northern Nuussuaq and in the Uummannaq district.

Observations suggest that geological structures and lithologies can be traced from north to south across the fjord Torsukattak, into the Ataa area which is hardly affected by Proterozoic deformation. This is used to infer that a major crustal boundary structure along the fjord (previously assumed to form the northern boundary of the Burwell terrane in West Greenland) does not exist.

Geological Survey of Denmark and Greenland, Thoravej 8, DK-2400 Copenhagen NV, Denmark.
E-mail: *aag@geus.dk.*

Keywords: Archaean, Burwell terrane, Disko terrane, Proterozoic structures, Rinkian orogen, West Greenland

The eastern, Precambrian part of Nuussuaq is conventionally considered to belong to the southernmost part of the Proterozoic Rinkian orogen (originally established by Escher & Pulvertaft 1976), just north of the region affected by contemporaneous tectonothermal activity in the Nagssugtoqidian orogen. Recent investigations (e.g. Kalsbeek & Nutman 1996; van Gool *et al.* 1996; Hanmer *et al.* 1997; Grocott & Davies 1999, this volume) indicate, however, that the traditional distinction between the Rinkian and Nagssugtoqidian orogenies in West Greenland is in need of re-evaluation.

This paper describes the Archaean basement rocks in eastern Nuussuaq which preserve evidence of strong tectonic reworking. Reconnaissance field work undertaken by the Geological Survey of Greenland in 1988–1991 during the Disko Bugt Project suggests that the reworking is early Proterozoic in age and broadly comparable in style with contemporaneous reworking of the adjacent southernmost part of the Uummannaq district (Grocott 1984; Grocott & Pulvertaft 1990). Evidence for a local NW–SE-trending Rinkian detachment zone through Nuussuaq is presented. However, it can be shown that no major crustal boundary structure occurs along the south coast of Nuussuaq – with the

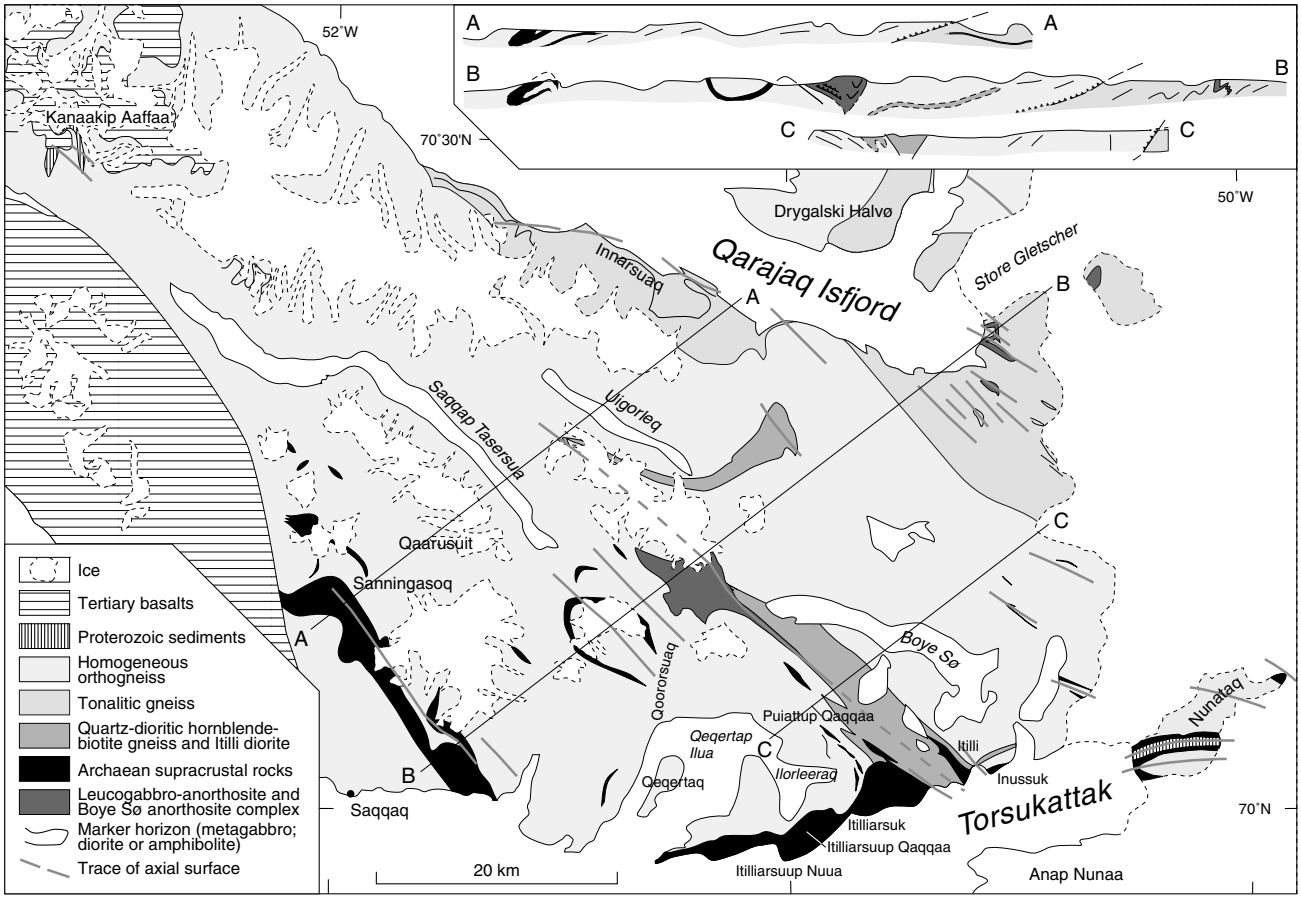

Fig. 1. Simplified geological map of eastern Nuussuaq and Nunataq (the Nuussuaq domain). Sections A–A, B–B and C–C are viewed towards NW; horizontal and vertical scales as on map. See Fig. 2 for location.

implication that the assumed Burwell terrane boundary (e.g. Hoffman 1989; van Kranendonk *et al.* 1993) cannot be substantiated in this region.

Geological investigations of eastern Nuussuaq

Prior to the Disko Bugt Project eastern Nuussuaq was poorly known, especially in its interior parts (see map by Escher 1971). The first modern investigations in the region by Escher & Burri (1967) included a survey of the south-eastern coast, where metamorphosed supracrustal rocks around Itilliarsuk were described (Fig. 1). These supracrustal rocks were at first believed to be part of the Proterozoic Anap nunâ Group which is exposed south of Torsukattak, but are now considered to be part of the Archaean basement. A prominent marble exposure at Kanaakip Aaffaa in northern Nuussuaq (see Fig. 1 and p. 145) was also shown on Escher's (1971) map, but no description was published at the time. In 1965 and 1980–1981 T.C.R. Pulvertaft (personal communication 1993) surveyed the north coast of Nuussuaq in connection with mapping and structural studies in the adjacent Uummannaq district (Grocott 1984; Pulvertaft 1986; Henderson & Pulvertaft 1987; Schiøtte 1988; Grocott & Pulvertaft 1990). In addition, the mining company Kryolitselskabet Øresund A/S investigated supracrustal rocks in southern Nuussuaq in the early 1980s.

The new field work carried out on Nuussuaq during the Disko Bugt Project was not comprehensive. Only a few areas in north-eastern and southern Nuussuaq, and on Nunataq, were visited on foot, whereas most of the region was surveyed by helicopter reconnaissance. Garde & Steenfelt (1999, this volume) present an overview of the Precambrian geology of the Disko Bugt region between Qarajaq Isfjord and Jakobshavn Isfjord with a description of the geological map at scale 1:250 000 (Garde 1994). They divide the region into four structural domains; the two northernmost of these, the Nuussuaq and Ataa domains, have their common

boundary in Torsukattak (Fig. 1; Garde & Steenfelt 1999, this volume, fig. 1). Garde & Steenfelt (1989) reported the discovery of an anorthosite complex west of Boye Sø, and Garde (1992, 1994) presented a 56 km long structural profile along the north coast of Nuussuaq. The geology of Nunataq, at the head of Torsukattak in the transitional area between the Nuussuaq and Ataa domains, is described by Higgins & Soper (1999, this volume). Rasmussen & Pedersen (1999, this volume) and Garde *et al.* (1999, this volume) describe respectively the supracrustal rocks west of Itilliarsuk, and metavolcanic rocks with gold mineralisation near Saqqaq. A study of K-Ar and ^{40}Ar-^{39}Ar mineral ages in the Disko Bugt region, including data from Nuussuaq, is presented by Rasmussen & Holm (1999, this volume). Pulvertaft (1989) has described the boundary fault system in central Nuussuaq, which separates the Precambrian basement terrain from the Cretaceous–Tertiary volcano-sedimentary basin to the west.

Lithological units and their contact relationships

The Precambrian basement of Nuussuaq comprises almost exclusively rocks of presumed Archaean age: the Nuussuaq gneisses, the Saqqaq and Itilliarsuk supracrustal rocks of southern Nuussuaq, and the Boye Sø anorthosite complex (Figs 1, 2; Garde 1994; Garde & Steenfelt 1999, this volume). Only a few mafic dykes and sills and the marble occurrence in central Nuussuaq are known, or presumed, to be of Proterozoic age.

There is evidence locally that the supracrustal rocks rest unconformably on the gneisses, although the con-

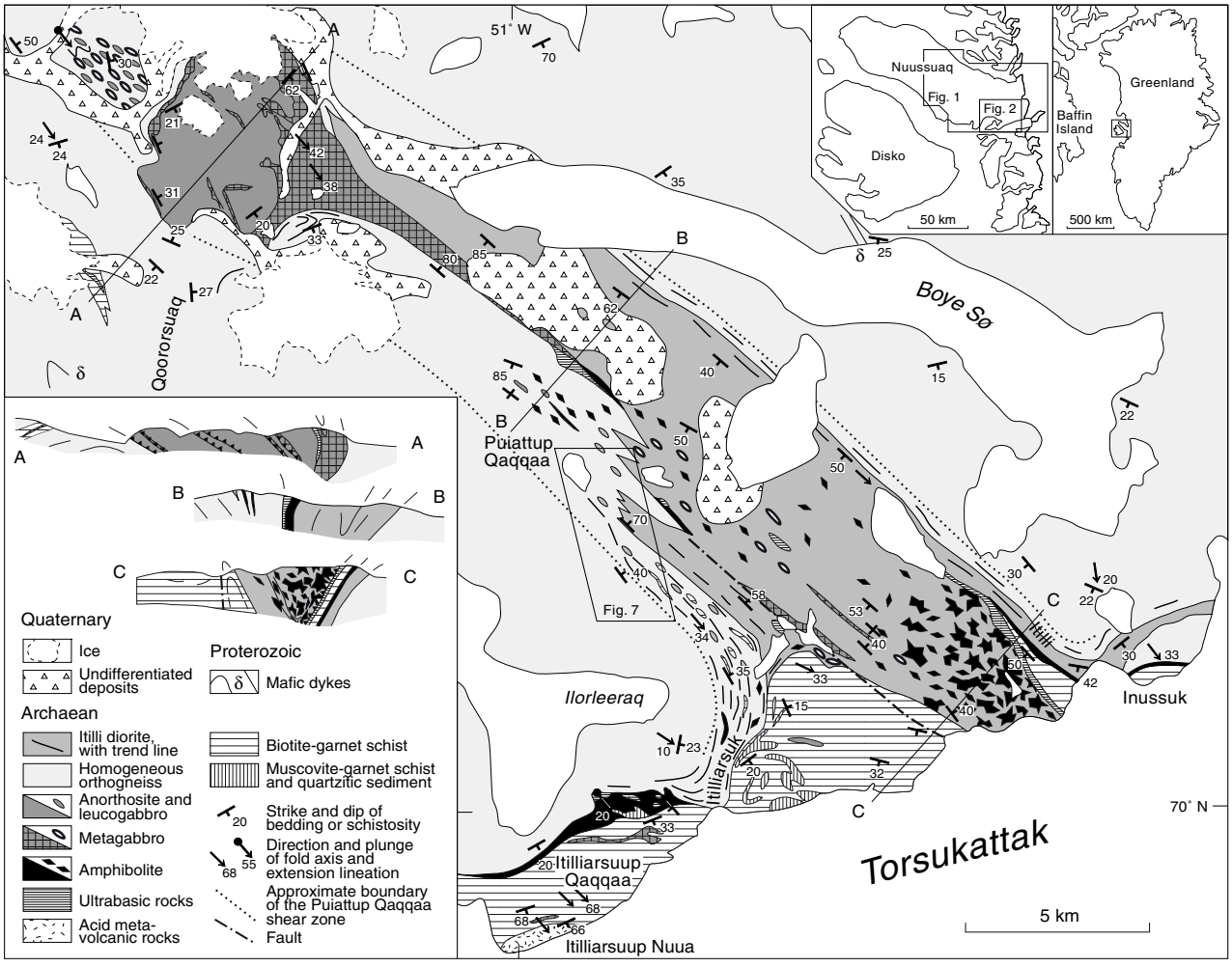

Fig. 2. Geological map of south-eastern Nuussuaq. Sections A–A, B–B and C–C are viewed towards the north-west; horizontal and vertical scales as on map.

tacts between the Itilliarsuk supracrustal rocks and Nuussuaq gneisses are too tectonised to allow a conclusion; a polymict conglomerate close to the base of the Itilliarsuk supracrustal succession contains clasts of granitoid rocks which were most likely derived from undeformed precursors of nearby orthogneisses. The contacts between the Boye Sø anorthosite complex and the Nuussuaq gneisses are also tectonic, and no primary relationships have been observed between the Saqqaq supracrustal rocks and Nuussuaq gneisses.

The Nuussuaq gneisses consist of two major lithological and tectonic units (Fig. 1; Garde & Steenfelt 1999, this volume): a predominant pale, uniform, leucocratic orthogneiss (homogeneous orthogneiss), and a darker grey, more mafic orthogneiss found in north-eastern Nuussuaq (tonalitic gneiss; commonly with layers and lenses of anorthosite, leucogabbro and gabbro). In addition, a mafic tonalitic to quartz-dioritic hornblende-biotite gneiss forms a 20 km long sheet at Uigorleq in north-eastern Nuussuaq (Fig. 1), and augen gneiss occurs in southern Nuussuaq close to Saqqaq (Garde 1994). The Itilli diorite, which extends from the Boye Sø anorthosite complex to the south coast of Nuussuaq (Fig. 2), appears to be younger than the supracrustal rocks and most of the Nuussuaq gneisses.

On Nunataq at the head of Torsukattak fjord two superimposed successions of Archaean and Proterozoic supracrustal rocks outline overturned tight to isoclinal folds (Fig. 1; Higgins & Soper 1999, this volume). The Archaean succession consists of amphibolite and garnet-mica schist. The Proterozoic succession comprises a basal quartzitic sandstone, a few metres thick marble horizon and a sequence of fine-grained semipelitic rocks; this succession is an attenuated lateral continuation of the lowermost part of the Anap nunâ Group, which is more widely exposed on Anap Nunaa south of Nunataq (Fig. 1).

Structural elements in the Nuussuaq domain

Field observations by the authors in the Nuussuaq domain suggest, as noted above, that its present structure was largely developed during Palaeoproterozoic reworking of Archaean basement rocks during the Rinkian orogeny; this view is supported by new K-Ar hornblende ages in the range of *c.* 1770–1880 Ma from various parts of the Nuussuaq domain (Rasmussen & Holm 1999, this volume). Resetting of hornblende K-Ar isotope systematics shows that a minimum temperature of *c.* 550°C was reached in the Nuussuaq domain during Rinkian metamorphism, sufficient to allow regional ductile deformation. In the Ataa domain south of Torsukattak, however, only limited resetting of Archaean mineral ages has occurred, and the metamorphic grade of Proterozoic metasediments at the present level of exposure is lower greenschist facies.

Large parts of eastern Nuussuaq are characterised by an overall flat-lying structure, which is deformed by a series of NW–SE-trending, mostly upright to overturned folds, and in the north-west recumbent isoclinal folds; interference patterns between two sets of coaxial folds with ESE–WNW-trending axes are common at the head of Qarajaq Isfjord. Asymmetric shear fabrics observed in southern Nuussuaq suggest later hanging-wall displacements in a northerly direction. A major NW–SE-trending, steeply dipping, 7 km wide shear zone, the Puiattup Qaqqaa shear zone, occurs in southern Nuussuaq near Boye Sø. Another shear zone, trending E–W, is inferred to occur along Torsukattak (Figs 2, 10) associated with strong schistosity and extension lineation fabrics which are preserved in the coastal areas on the north side of Torsukattak. The different structural elements are described below, and a tentative chronological scheme is given in Table 1.

Flat-lying structure

Large areas in the interior of Nuussuaq are covered by boulder fields and local ice caps, but a general flat-lying structure can be discerned from exposures along the north coast and at the lakes Saqqap Tasersua and Uigorleq (Fig. 1). On the north coast the flat-lying structure is marked by layers of anorthosite, leucogabbro and gabbro intercalated with tonalitic gneiss, and by a subhorizontal to shallow south-dipping tectonic boundary between homogeneous orthogneiss in the hanging wall and tonalitic gneiss in the footwall (see long profile in Garde 1992 and Garde 1994). North of Qarajaq Isfjord, Grocott (1984) and Pulvertaft (1986) reported flat-lying to south-dipping tectonic boundaries on Drygalski Halvø (shown on Fig. 1) and on Ikerasak (not shown) west of Drygalski Halvø, between grey gneiss in the hanging wall (equivalent to tonalitic gneiss on Nuussuaq) and a homogeneous, more leucocratic biotite gneiss in the footwall. These observations collectively indicate that the tonalitic gneiss makes up a major subhorizontal sheet tectonically intercalated between layers of homogeneous orthogneiss.

Almost horizontal layers of amphibolite or dioritic

Table 1. Tentative chronology of Proterozoic tectonic events and structural elements in Nuussuaq

Phase A. Tectonic intercalation of major rock units	Intercalation of tonalitic gneiss and homogeneous orthogneiss
	Intercalation of orthogneisses with anorthosite-leucogabbro-gabbro
	Intercalation of homogeneous amphibolite with Itilliarsuk supracrustal rocks?
	Intercalation of Proterozoic marble with Archaean basement
	Emplacement of Ilorleeraq dykes?
Phase B. N–S or NE–SW shortening	Formation of NW–SE trending folds and Puiattup Qaqqaa shear zone
	SE-plunging lineation
	Northerly hanging-wall movement in southern Nuussuaq
	Rotation of Ilorleeraq dykes (escape structure?)
Phase C. NNW–SSE extension	Formation of Torsukattak shear zone
	Steep SE-plunging lineation and flattening along Torsukattak

gneiss are exposed over long distances at the tops of south-facing cliffs along Saqqap Tasersua and Uigorleq. Viewed from a helicopter these mafic marker horizons appear to have a very strong schistosity which suggests that intense ductile deformation has been focused along the mafic layers. In the lower parts of the same cliffs occurs a distinct subhorizontal, few metres thick pyrite and quartz-rich horizon, which may have been deposited from fluids migrating along a shear zone.

NW–SE-trending recumbent isoclinal folds in northern Nuussuaq

Recumbent isoclinal folds have been observed both in northern Nuussuaq and locally in southern Nuussuaq. Mafic marker horizons similar to those occurring along Saqqap Tasersua and Uigorleq crop out in several places north-west of these lakes, where they outline recumbent isoclinal fold closures. The most prominent isoclinal fold is located at the mountain Kanaakip Aaffaa in northern Nuussuaq (Fig. 1; Garde & Steenfelt 1999, this volume, fig. 26) and is outlined by an up to *c.* 500 m thick sheet of cream-coloured marble with zinc mineralisation (King 1983; Garde & Thomassen 1990; Della Valle & Denton 1991), intercalated with Archaean orthogneiss. The orientations of minor fold axes and associated extension lineations are south-easterly with subhorizontal to moderate plunges (Garde & Thomassen 1990), suggesting extension in a NW–SE direction. The marble can be correlated with the lower Proterozoic Mârmorilik Formation of the adjacent Uummannaq district described by Garde (1978) and Pulvertaft (1986), which also hosts zinc mineralisation; the isoclinal folding demonstrates that intense Proterozoic deformation has occurred in northern Nuussuaq.

A number of thin, flat-lying marble horizons also occur in the orthogneisses west and north of the main marble outcrop (Fig. 3; see also Rosenkrantz *et al.* 1974; Pulvertaft 1987; Garde & Thomassen 1990). They are interpreted as tectonic remnants of the same marble

Fig. 3. Sheets of light coloured lower Proterozoic marble (near and middle distance) with shallow northerly dips, intercalated with Archaean orthogneiss. Northern Nuussuaq, looking north towards Qarajaq Isfjord and Uummannaq. Marble layer is 10–50 m thick.

unit, repeated by (Proterozoic) isoclinal folding or thrust stacking.

NW–SE-trending upright to overturned folds

Open to tight, generally NW–SE-trending folds with amplitudes from a few hundred metres to *c.* 2–3 km disturb the general flat-lying structure of central and northern Nuussuaq, and some can be traced for up to 20 km. In northern Nuussuaq the fold axes have subhorizontal plunges. One such fold occurs in steep cliffs north-west of Innarsuaq on the north coast of Nuussuaq (Garde 1992, fig. 3); it has a subhorizontal, WNW–ESE-trending fold axis and is overturned towards the south-south-west. Farther towards the south-east the plunge of the fold axes increases, and steepens to about 70° near Torsukattak (probably due to reorientation by the Torsukattak shear zone, see p. 150).

Refolded folds

Refolded folds, some of which may be of Archaean age, have been recognised in several parts of Nuussuaq. South of Store Gletscher at the head of Qarajaq Isfjord (Fig. 1), a tightly folded anorthosite layer is refolded by small-scale inclined folds. In this area outcrops displaying two superimposed sets of folds are common; the folds are approximately coaxial, with subhorizontal ESE–WNW-trending axes. Superimposed folding on a scale of 1–5 km was inferred from structural trends visible on aerial photographs of this area, an interpretation supported by structural readings obtained during helicopter reconnaissance.

Observations north-east of Saqqaq suggest the presence of one (or several) early (Archaean?) recumbent folds within the Saqqaq supracrustal rocks, refolded by upright to overturned NW–SE-trending folds with subhorizontal to SE-plunging axes.

Subhorizontal ductile shear fabrics

Shear fabrics which appear to be younger than the latest phase of folding have been observed in central and, notably, south-western Nuussuaq, for example in the area south of Qaarusuit and within the Puiattup Qaqqaa shear zone (see below). South of Qaarusuit, thin subhorizontal to south-dipping zones of intense foliation with a spacing of 10–20 cm transect minor

Fig. 4. δ-shaped porphyroclast in orthogneiss, viewed south-westwards on a steep SE–NW-striking surface, suggesting north-west-directed displacement of the hanging wall. Locality 5 km south-south-west of southern end of Saqqap Tasersua.

folds, or may be axial planar to such folds; south-east-plunging mineral lineations are common within the zones of intense foliation. Feldspar porphyroclasts of centimetre size, presumably relicts of earlier migmatite veins, locally display σ- and δ-porphyroclast structures which consistently indicate northwards or north-westwards hanging-wall movement (Fig. 4). Asymmetric boudins of amphibolite or anorthosite-leucogabbro have been observed in the orthogneiss in several parts of southern Nuussuaq, and provide further evidence of northward hanging-wall displacement.

South-east-plunging extension lineations in central and southern Nuussuaq

A late south-east-plunging extension lineation is prominent in southern Nuussuaq in the vicinity of Itilliarsuk and Itilli. The lineation steepens and becomes more intense towards the coast, where it totally overprints earlier fabrics and is accompanied by strong flattening. These observations are part of the evidence for the presence of the Torsukattak shear zone (see p. 150).

The Puiattup Qaqqaa shear zone and structure of the Boye Sø anorthosite complex

The Puiattup Qaqqaa shear zone is a prominent NW–SE-trending, synformal zone of strongly deformed rocks up to *c.* 7 km wide that extends from the south coast of Nuussuaq west of Itilli, through the Boye Sø anor-

thosite complex in central Nuussuaq. The structure may continue north-westwards to Saqqap Tasersua and beyond (Figs 1, 2). The Puiattup Qaqqaa shear zone comprises a tectonic mélange of Archaean supracrustal and infracrustal rocks which appear to have been interleaved during N–S or NE–SW compression and NW–SE extension; it may also incorporate Proterozoic sediments. The system of NW–SE-trending folds on both sides of the shear zone may have formed in response to the same phase of deformation; evidence for this is presented below.

Along the length of the shear zone both its internal structure and lithologies show considerable variation. In the north-western part, the Boye Sø anorthosite complex forms an elongate, *c.* 5 km wide lens of imbricated and locally folded tectonic slices of anorthosite and related rocks (Fig. 2, section A–A; Garde & Steenfelt 1999, this volume, fig. 15). Although the bulk of the anorthosite complex is almost undeformed, a number of thin ductile shear zones display very high strain (as is common in very competent rocks, e.g. Myers 1978). Most of these high strain zones are localised along partially disrupted layers of metagabbro (Garde & Steenfelt 1999, this volume, fig. 15). The thrust slices which make up the south-western and central portions of the complex dip north-eastwards, whereas the much thinner north-eastern part dips steeply towards the south-west. The two parts of the complex thus form the limbs of a major, highly asymmetric synformal fold, which appears to post-date the tectonic interleaving and thrusting. The hinge zone is outlined by a tight south-east-plunging fold closure in metagabbroic and ultrabasic rocks in the northern part of the complex (Fig. 2, section A–A). Towards the north-west the Boye Sø anorthosite complex breaks up into a *c.* 4 km long tail of jumbled, commonly folded enclaves of anorthosite, leucogabbro and gabbro in a matrix of orthogneiss. Farther north-west a *c.* 100 m thick composite layer of schistose and strongly folded biotite-garnet schist and amphibolite suggests that the Puiattup Qaqqaa shear zone may continue in this direction (Fig. 1).

The south-eastern part of the Puiattup Qaqqaa shear zone is developed in granitic, tonalitic and dioritic orthogneiss, metavolcanic and metasedimentary supracrustal rocks, ultrabasic rocks, and a large area of Itilli diorite and homogeneous amphibolite. Near the south-western margin of the shear zone these lithologies are tectonically interleaved, strongly foliated, and locally tightly folded. Thin lenses of supracrustal rocks and lensoid fragments of mafic dykes occur along second-order shear zones in the orthogneisses, and towards the south-western margin of the main shear zone the polyphase gneisses themselves have a very distinct small-scale layered to lensoid tectonic fabric (Fig. 5). Rootless isoclinal folds are common, and migmatitic neosome veins in the orthogneisses are deformed into thin streaks which wrap around K-feldspar porphyroclasts.

Fig. 5. Strongly deformed orthogneiss with tectonic layers and lenses of supracrustal rocks and (?)mafic dykes. Near the south-western margin of the Puiattup Qaqqaa shear zone, *c.* 4 km north of the coast of Torsukattak. Hammer shaft is 45 cm in length.

Several tectonic lenses of anorthosite-leucogabbro occur in the south-eastern part of the shear zone, ranging from a few metres to *c.* 1 km in length, and mostly located within larger enclaves of supracrustal rocks. The largest lens occurs at a minor summit 480 m high, 3 km east of Itilliarsuk (Fig. 2) and exhibits an isoclinal

Fig. 6. Upper margin of a 1 km long anorthosite lens at the 480 m top 3 km east of Itilliarsuk. The anorthosite (left), which is little deformed internally, has a thin envelope of intensely sheared leucogabbro and gabbro (right). Width of outcrop in foreground is *c.* 5 m.

fold. It comprises a core of closely packed, up to football-sized aggregates of calcic plagioclase, and a thin envelope of intensely sheared metagabbro (Fig. 6) in tectonic contact with schistose, micaceous metasediment. The disrupted anorthosite-leucogabbro lenses imply considerable lateral movement along the shear zone, although the sense of displacement is not known. These lenses may once have been contiguous with the Boye Sø anorthosite complex and transported to the south-east, or related to a body of anorthosite south of Nuussuaq (small occurrences of anorthosite-leucogabbro are known on Arveprinsen Ejland; Knudsen *et al.* 1988; Garde & Steenfelt 1999, this volume) and thus transported in a northerly direction.

At the south coast of Nuussuaq the two margins of the Puiattup Qaqqaa shear zone diverge in opposite directions, respectively towards Itilliarsuk and Inussuk until they have a common ENE–WSW trend along Torsukattak (Fig. 2). This peculiar geometry is interpreted as a result of intersection between the Puiattup Qaqqaa shear zone and a second, largely unexposed, ENE–WSW-trending shear zone along Torsukattak with downthrow of the southern side towards the south-east (see p. 150 and Fig. 10).

There are further structural complications in the south-eastern part of the Puiattup Qaqqaa shear zone. The supracrustal rocks at Itilli consists of an extensive unit of homogeneous amphibolite which has agmatitic relationships with the Itilli diorite (Fig. 2). To the north-east this amphibolite is bounded by an intensely deformed ultrabasic horizon near the north-eastern boundary of the shear zone (Fig. 2, sections B–B and C–C). To the south-west at the opposite margin of the shear zone the homogeneous amphibolite is bounded by a screen of mixed, intensely foliated metasediments and metavolcanic rocks, in which a tight, *c.* 500 m wide south-east-plunging antiform occurs (Fig. 2, section C–C); a vertical fault is located along the south-western flank of this antiform. No lithologies elsewhere within the Itilliarsuk supracrustal sequence resemble the homogeneous amphibolite at Itilli. However, it might be equivalent to the massive greenstones in the northern part of Arveprinsen Ejland opposite Torsukattak (Marshall & Schønwandt 1999, this volume). We therefore tentatively interpret the homogeneous amphibolite as a lithological and structural element which was not originally a member of the Itilliarsuk supracrustal sequence, and which became juxtaposed against the local metasediments and metavolcanic rocks as a consequence of thrusting along the underlying ultrabasic layer. The juxtaposition may have been contemporaneous with the development of the flat-lying structure elsewhere in Nuussuaq, and must have taken place prior to intrusion of the Itilli diorite and the subsequent intense deformation along the north-eastern margin of the Puiattup Qaqqaa shear zone, and before the latter acquired its present geometry.

Folds in southern Nuussuaq

Tight to isoclinal, NW–SE-trending recumbent folds of possible Proterozoic age occur in the Itilliarsuk supracrustal rocks, in the vicinity of and possibly related to the Puiattup Qaqqaa shear zone. Intense minor folding on a scale of decimetres to metres was observed during short helicopter landings in orthogneisses on the island Qeqertaq and along the coast of Qeqertap Ilua. These folds are generally tight with upright, E–W- to NNE–SSW-trending axial surfaces; hinge lines with NW–SE trends and south-east plunges are most common. Local undeformed pegmatites (up to *c.* 10 cm thick) cut the folds. The folding in this area clearly post-dates a regional, possibly Archaean, migmatisation event in the orthogneiss and may also be related to development of the Puiattup Qaqqaa shear zone.

Ilorleeraq dykes and their relationships with the Puiattup Qaqqaa shear zone

The Ilorleeraq dykes (Garde & Steenfelt 1999, this volume) are a group of mostly 2–5 m thick mafic dykes which occur in south-eastern Nuussuaq. These dykes are considered to be of early Proterozoic age, and the observation that some are affected by the Puiattup Qaqqaa shear zone or folded by the NW–SE-trending fold system implies that these structures are Proterozoic.

Two vertical, 5–10 m thick mafic dykes with 150° trend occur in an area of homogeneous orthogneiss with uniform easterly structural grain north of Boye Sø (Fig. 2). These dykes appear to be unaffected by deformation or metamorphism. No dykes have been observed along the north-eastern flank of the Puiattup Qaqqaa shear zone, but several occur in the central part. The latter dykes are also vertical, but trend at 135° parallel to the shear zone, and are variably recrystallised. Additional dykes occur north of the embayment Ilorleeraq, north of the area where the west flank of the Puiattup Qaqqaa shear zone swings into parallelism with Torsukattak. From north-east to

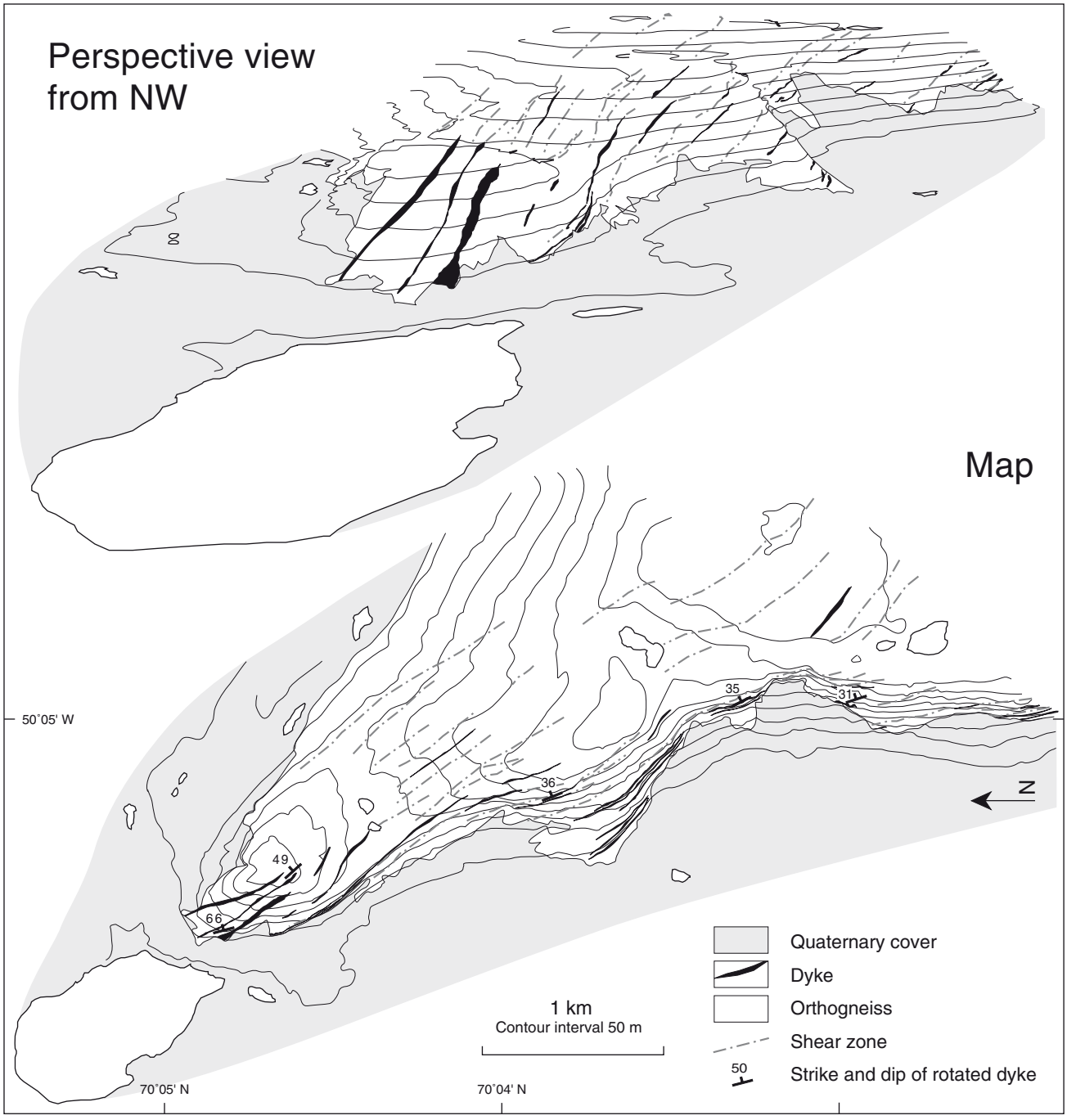

Fig. 7. Map and perspective view of Ilorleeraq dykes in the south-western part of the Puiattup Qaqqaa shear zone (location see Fig. 2), rotated from steep to flat-lying ENE-dipping orientations. The figure was constructed from seven 35-mm colour slides taken from a helicopter, using multi-model photogrammetry (Dueholm 1992; Dueholm *et al.* 1993). Modified from Dueholm *et al.* (1993, fig. 1).

south-west these dykes become progressively more intensely foliated and recrystallised as they are gradually rotated from nearly vertical to shallow NE-dipping orientations (Fig. 7). Close to Ilorleeraq the dykes have been transformed into flat-lying, discontinuous, 10–50 cm thick (rarely up to 10 m thick) layers conformable with their strongly foliated hosts (Fig. 8), and are completely recrystallised with new metamorphic hornblende.

The rotated dykes demonstrate that the north-easterly dip of the shear zone margin in this area was acquired by rotation from an earlier vertical, not flat-

Fig. 8. Intensely sheared subhorizontal Ilorleeraq dykes and dyke fragments in orthogneiss 2.5 km north-east of Ilorleeraq. The cliff face behind the lake is *c.* 100 m high.

lying orientation (see Fig. 2, section B–B), and implies that the upper part of the margin was transported towards the south-west. This observation appears to be in conflict with evidence from elsewhere in southern Nuussuaq of late hanging-wall movement in a northerly direction. However, it may be explained as a localised escape structure, which was formed in response to NE–SW compression during evolution of the Puiattup Qaqqaa shear zone.

A thin recrystallised dyke occurs *c.* 15 km north-west of Ilorleeraq in a side branch of the valley Qoororsuaq (Fig. 2). This dyke is folded in the hinge zone of a tight NW–SE-trending synformal fold which is part of the regional suite of NW–SE-trending folds (see Fig. 1). If this dyke is an Ilorleeraq dyke, and if these dykes are indeed Proterozoic, it follows that the synform (and probably also other NW–SE-trending folds elsewhere in Nuussuaq) is Proterozoic and possibly contemporaneous with the Puiattup Qaqqaa shear zone.

Fig. 9. Mafic sill (*c.* 25 m thick) of presumed Proterozoic age, apparently displaying an isoclinal fold, in orthogneiss with light snow cover. Southern Nuussuaq 20 km north-north-east of Saqqaq.

Other deformed dykes and sills

Other mafic dykes and sills occur along the south coast of Qarajaq Isfjord and south of Saqqap Tasersua. Some of the sills are differentiated, with olivine-rich cumulate bases (Garde & Steenfelt 1999, this volume); no direct relationship with the Ilorleeraq dykes has so far been established. A thick flat-lying differentiated sill visited at Sanningasoq, south of Saqqap Tasersua, is strongly sheared along its base, whereas its centre is almost undisturbed. Other intrusions exposed on steep cliff faces have irregular shapes which could be due to folding (Fig. 9; Garde 1992, fig. 3), but these observations could not be confirmed due to inaccessibility. Differentiated mafic sills of probable Proterozoic age have also been described from the Rodebay structural domain south of Torsukattak (Escher *et al.* 1999; Garde & Steenfelt 1999, both in this volume) and from the Uummannaq district (Schiøtte 1988).

Interpretation of structures along Torsukattak and on Nunataq: the Torsukattak shear zone

The apparent lack of direct lithological and structural correlation across Torsukattak, between the Nuussuaq domain and Ataa domain, suggests that the fjord hides an ENE–WSW-trending structural discontinuity. Small-scale structures at Oqaatsut, Arveprinsen Ejland and Anap Nunaa in the northernmost part of the Ataa domain (Garde & Steenfelt 1999, this volume, fig. 1) indicate that this structure is probably a major shear zone, here termed the Torsukattak shear zone. Observations by the authors and Higgins & Soper (1999, this volume) indicate that the shear zone is closely related to the isoclinal E–W-trending folds at Nunataq, and furthermore demonstrate that it is not a major crustal boundary.

On Oqaatsut west of Arveprinsen Ejland (Pedersen 1995; Garde & Steenfelt 1999, this volume, fig. 1; Rasmussen & Pedersen 1999, this volume), minor folds with E–W-trending axes plunging *c.* 30° eastwards have been observed in the northernmost part of the Atâ tonalite close to Torsukattak (H. Rasmussen, personal communication 1992). At the north coast of Arveprinsen Ejland the general N–S-trending Archaean structural grain of the supracrustal rocks is overprinted by a younger E–W-trending steep foliation and minor shear zones (M. Marker, personal communication 1991). Fur-

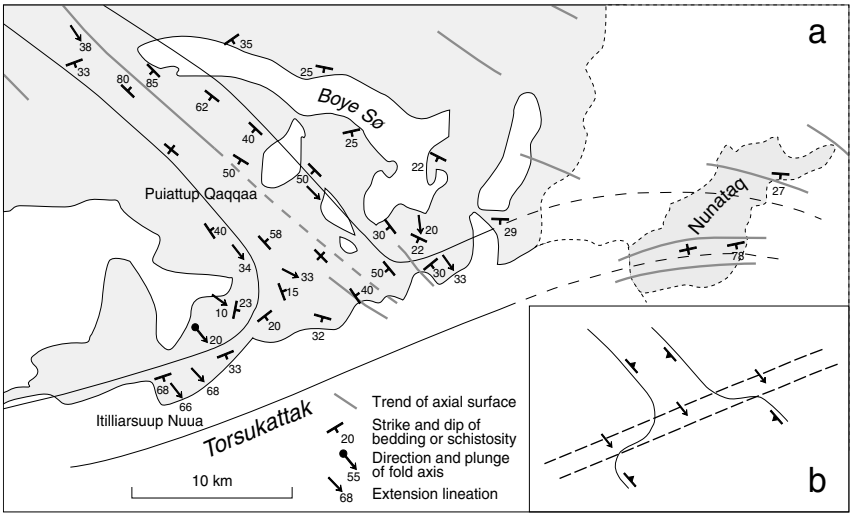

Fig. 10. **a**: Measured fabrics and extension lineations between Nunataq and Itilliarsuup Nuua, south-east Nuussuaq, where the Puiattup Qaqqaa and Torsukattak shear zones intersect.
b: Diagram showing how a SSE-dipping shear zone with downthrow to the south-east would affect the flanks of a NW–SE-trending synform fold. The peculiar geometry at the south-eastern end of the Puiattup Qaqqaa shear zone can be explained by intersection with the northern part of the Torsukattak shear zone.

thermore, the Proterozoic sediments on the island Qeqertakassak in Torsukattak and on Anap Nunaa display an east–west structural grain (Andersen 1991; Kalsbeek 1992; Escher 1995), and extensive albitisation in these areas (Kalsbeek 1992) might possibly be related to major shearing. In addition, N.J. Soper and A.K. Higgins (personal communication 1991) demonstrated that along the north coast of Anap Nunaa the intensity of Proterozoic deformation increases northwards. On the large isolated peninsula of Nunataq, at the head of Torsukattak, an overturned anticline in southern Nunataq is bordered northwards by an isoclinal syncline, which incorporates both Archaean and Proterozoic supracrustal rocks described above; the folds are therefore Proterozoic (Fig. 1; Higgins & Soper 1999, this volume).

Archaean supracrustal rocks lithologically similar to those at Nunataq reappear at Inussuk on the south coast of Nuussuaq (Figs 1, 2), on strike with the northern flank of the isoclinal syncline on Nunataq; it is therefore conceivable that the northern flank of the Proterozoic isoclinal syncline at Nunataq continues westwards along Torsukattak and gradually develops into the ENE–WSW-trending Torsukattak ductile shear zone. Farther west, at Itilli, the strike of the supracrustal rocks changes along the Puiattup Qaqqaa shear zone. To the south-west at Itilliarsuup Qaqqaa the supracrustal rocks are strongly flattened with a prominent south-east-plunging extension lineation (described above), which overprints earlier structures and becomes further intensified towards Itilliarsuup Nuua. We assume that this lineation post-dates the shallow SE-plunging lineations found to the north-east and that it reflects intense deformation in the interior part of the Torsukattak shear zone, with a large oblique shear component parallel to the lineation.

Interpretation of the Torsukattak shear zone

Both the intensification and steepening of fabric elements in the southernmost part of Nuussuaq and the geometry of the south-eastern end of the Puiattup Qaqqaa shear zone, where the two synform flanks swing in opposite directions, can be interpreted in terms of late deformation along the Torsukattak shear zone. Figure 10a shows measured fabric elements at the south coast of Nuussuaq between Nunataq and Itilliarsuup Nuua, and the common boundaries of the Puiattup Qaqqaa and Torsukattak shear zones. The diagram in Fig. 10b shows schematically how a narrow shear zone with the orientation of the Torsukattak shear zone would widen a synformal structure with the orientation of the Puiattup Qaqqaa shear zone and reorientate its margins, assuming that the main sense of displacement was parallel to the extension lineation with oblique south-east downthrow of the southern side. The resulting geometry along the schematic shear zone (Fig. 10b) matches the observed structures along the north coast of Torsukattak (Fig. 10a) and may also match the wide overall syncline outlined by the Proterozoic sediments on Anap Nunaa south of the fjord (Andersen 1991; Garde 1994). An oblique downthrow of the Ataa domain on the southern side of Torsukattak could also account for the previously discussed contrast in metamorphic grade across the fjord.

The model implies crustal extension across Torsu-

kattak late in the Proterozoic structural evolution. It follows that the tight to isoclinal folds on Nunataq, and the Puiattup Qaqqaa shear zone (and also adjacent upright NW–SE-trending folds) must be assumed to have developed during one or several earlier compressive phases during the Proterozoic (see Table 1).

Discussion

Proterozoic reworking of Nuussuaq and relative timing of tectonic events

Substantial indirect evidence suggests that eastern Nuussuaq and Nunataq have been affected by major Proterozoic structural and metamorphic reworking, although the data available and reported here are not sufficient to establish a comprehensive Archaean and Proterozoic tectonic history of the region. The evidence for Proterozoic reworking can be summarised in three points. First, the Lower Proterozoic marbles and associated rocks are interleaved and folded with Archaean orthogneisses in both northern Nuussuaq and Nunataq. Secondly, Ilorleeraq dykes and differentiated olivine-bearing sills, both of presumed Proterozoic age, pre-date the development of the Puiattup Qaqqaa shear zone and probably also pre-date the regional system of NW–SE-trending folds in Nuussuaq. Thirdly, hornblende K-Ar age determinations (Rasmussen & Holm 1999, this volume) show that metamorphic temperatures of about 550°C were reached in the early Proterozoic over large parts of Nuussuaq.

The present structure of the Precambrian region of Nuussuaq can be presumed to reflect several successive tectonic events, but these are not fully documented or understood, and the relative chronology can only be established for some of the structural elements described above (Table 1). The intercalation of sheets and enclaves of anorthosite-leucogabbro-gabbro with the tonalitic gneiss, and the interleaving of a major sheet of tonalitic gneiss within two sheets of homogeneous orthogneiss in northern Nuussuaq, both pre-date the NW–SE-trending upright to overturned folds, but may have been contemporaneous with at least some of the isoclinal folds. The Puiattup Qaqqaa shear zone is either contemporaneous with, or post-dates, the latter folds. The Torsukattak shear zone is interpreted as post-dating the Puiattup Qaqqaa shear zone, and it is suggested that oblique slip in the Torsukattak shear zone parallel to the extension lineation resulted in major downthrow of the Ataa domain relative to the Nuussuaq domain during crustal extension. Asymmetric flat-lying shear fabrics in southern Nuussuaq which indicate northward hanging-wall movement (presumably during a period of compression) are relatively late structures which post-date the latest phase of folding, but their age relative to the Puiattup Qaqqaa and Torsukattak shear zones is uncertain.

A Rinkian detachment zone through Nuussuaq?

Several Rinkian detachment zones affect Archaean gneisses and Proterozoic metasedimentary rocks in the Uummannaq district north of Nuussuaq, and commonly exploit marble horizons of the Mârmorilik Formation (Pulvertaft 1986; Henderson & Pulvertaft 1987; Grocott & Pulvertaft 1990, and references therein). Detachment zones along Proterozoic marble units have also recently been described from the northern part of the Nagssugtoqidian orogen (Kalsbeek & Nutman 1996; van Gool *et al.* 1996). We propose that a detachment zone of similar nature transects Nuussuaq from south-east to north-west, linking the Anap nunâ Group south of Nuussuaq with the Mârmorilik Formation in the Uummannaq district, and in part hosted by the Puiattup Qaqqaa and Torsukattak shear zones. The proposed detachment zone would originate in Nunataq; as noted above, the isoclinally folded quartzite, marble and semipelite sequence on Nunataq is correlated with the lowest part of the Anap nunâ Group in southern Anap Nunaa (Higgins & Soper 1999, this volume). From the overturned isocline in Nunataq the detachment zone would continue westwards along the Torsukattak shear zone, and then swing into the Puiattup Qaqqaa shear zone and follow it north-westwards towards Saqqap Tasersua. Here the general structure is flat-lying, although structural details are poorly known. North-west of Saqqap Tasersua folded Proterozoic marble is interleaved with flat-lying Archaean gneisses. Linear structures in the marble are parallel to, and on line with the Puiattup Qaqqaa shear zone. The thin tectonic enclaves of marble in northern Nuussuaq provide a structural link further northwards to the nearest marble outcrops of the Mârmorilik Formation on Storøen and Ikerasak in the Uummannaq district (see e.g. Pulvertaft 1986, fig. 3).

Absence of a suitable boundary structure south of Nuussuaq for the previously proposed Burwell terrane

In some plate-tectonic reconstructions of the Proterozoic evolution of the North Atlantic Region (e.g. Hoffman 1989), the Burwell terrane has been extended eastwards from Baffin Island into central West Greenland, with its northern boundary inferred to lie at the south coast of Nuussuaq (i.e. along Torsukattak). As shown above, we have been unable to confirm the presence of a major crustal boundary in this area. Field observations on Nunataq and along the coasts of Torsukattak show that geological units and structures can be traced from the Ataa domain to the Nuussuaq domain, although they are partially concealed by Proterozoic isoclinal folds and the Torsukattak shear zone. Therefore, there is no evidence for the presence of the Burwell terrane in this region.

Van Kranendonk *et al.* (1993) and van Kranendonk & Wardle (1996) proposed the term Disko terrane for the unreworked Archaean rocks south of Torsukattak; the observations presented here suggest that the Ataa domain may only be a local tectonic lens more or less in its original position, which has escaped Proterozoic deformation. Discussion of the plate-tectonic implications of this conclusion in eastern Canada and on Baffin Island is beyond the scope of the present paper.

Acknowledgements

John Grocott, Kingston University, UK, and A.K. Higgins, Geological Survey of Denmark and Greenland, are sincerely thanked for discussions and constructive comments on draft versions. The paper was reviewed by Mogens Marker, at the time with the Danish Lithosphere Centre and Lilian Skjernaa, University of Copenhagen; their help is gratefully acknowledged.

References

Andersen, J. 1991: Tidlig proterozoisk rift-relateret sedimentation og post-sedimentær deformation. Anap nunâ, Diskobugten, Vestgrønland, 73 pp. Unpublished cand. scient. thesis, Københavns Universitet, Danmark.

Della Valle, G. & Denton, P. 1991: Geological report on the 1990 zinc and lead exploration programme in central Nûgssuaq peninsula, Marmorilik Formation, West Greenland, 17 pp. Unpublished report, Intergeo-Exploration (in archives of Geological Survey of Denmark and Greenland).

Dueholm, K.S. 1992: Geologic photogrammetry using standard small-frame cameras. In: Dueholm, K.S. & Pedersen, A.K. (eds): Geological analysis and mapping using multi-model photogrammetry. Rapport Grønlands Geologiske Undersøgelse **156**, 7–17.

Dueholm, K.S., Garde, A.A. & Pedersen, A.K. 1993: Preparation of accurate geological and structural maps, cross-sections or block diagrams from colour slides, using multi-model photogrammetry. Journal of Structural Geology **15**, 933–937.

Escher, A. 1971: Geological map of Greenland, 1:500 000, Søndre Strømfjord – Nûgssuaq, sheet 3. Copenhagen: Geological Survey of Greenland.

Escher, A. & Burri, M. 1967: Stratigraphy and structural development of the Precambrian rocks in the area north-east of Disko Bugt, West Greenland. Rapport Grønlands Geologiske Undersøgelse **13**, 28 pp.

Escher, A. & Pulvertaft, T.C.R. 1976: Rinkian mobile belt of West Greenland. In: Escher, A. & Watt, W.S. (eds): Geology of Greenland, 104–119. Copenhagen: Geological Survey of Greenland.

Escher, J.C. 1995: Geological map of Greenland, 1:100 000, Ataa 69 V.3 Nord. Copenhagen: Geological Survey of Greenland.

Escher, J.C., Ryan, M.J. & Marker, M. 1999: Early Proterozoic thrust tectonics east of Ataa Sund, north-east Disko Bugt, West Greenland. In: Kalsbeek, F. (ed.): Precambrian geology of the Disko Bugt region, West Greenland. Geology of Greenland Survey Bulletin **181**, 171–179 (this volume).

Garde, A.A. 1978: The Lower Proterozoic Marmorilik Formation, east of Mârmorilik, West Greenland. Meddelelser om Grønland **200**(3), 71 pp.

Garde, A.A. 1992: Interpretation of flat-lying Precambrian structure by geological photogrammetry along a 65 km coastal profile in Nuussuaq, West Greenland. In: Dueholm, K.S. & Pedersen, A.K. (eds): Geological analysis and mapping using multi-model photogrammetry. Rapport Grønlands Geologiske Undersøgelse **156**, 35–40.

Garde, A.A. 1994: Precambrian geology between Qarajaq Isfjord and Jakobshavn Isfjord, West Greenland, 1:250 000. Copenhagen: Geological Survey of Greenland.

Garde, A.A. & Steenfelt, A. 1989: A new anorthosite/gabbro complex at Nûgssuaq, central West Greenland. Rapport Grønlands Geologiske Undersøgelse **145**, 16–20.

Garde, A.A. & Steenfelt, A. 1999: Precambrian geology of Nuussuaq and the area north-east of Disko Bugt, West Greenland. In: Kalsbeek, F. (ed.): Precambrian geology of the Disko Bugt region, West Greenland. Geology of Greenland Survey Bulletin **181**, 6–40 (this volume).

Garde, A.A. & Thomassen, B. 1990: Structural and economic aspects of the Proterozoic marble on Nûgssuaq, West Greenland. Open File Series Grønlands Geologiske Undersøgelse **90/6**, 14 pp.

Garde, A.A., Thomassen, B., Tukiainen, T. & Steenfelt, A. 1999: A gold-bearing volcanogenic-exhalative horizon in the Archaean(?) Saqqaq supracrustal rocks, Nuussuaq, West Greenland. In: Kalsbeek, F. (ed.): Precambrian geology of the Disko Bugt region, West Greenland. Geology of Greenland Survey Bulletin **181**, 119–128 (this volume).

Grocott, J. 1984: Geometry of superimposed colinear deformations in the Ikerasak area, Umanak district, central West Greenland. Precambrian Research **26**, 235–263.

Grocott, J. & Davies, S.C. 1999: Deformation at the southern boundary of the late Archaean Atâ tonalite and the extent of Proterozoic reworking of the Disko terrane, West Greenland. In: Kalsbeek, F. (ed.): Precambrian geology of the Disko Bugt region, West Greenland. Geology of Greenland Survey Bulletin **181**, 155–169 (this volume).

Grocott, J. & Pulvertaft, T.C.R. 1990: The Early Proterozoic Rinkian belt of central West Greenland. In: Lewry, J.F. & Stauffer, M.R. (eds): The Early Proterozoic Trans-Hudson Orogen of North America. Geological Association of Canada Special Paper **37**, 443–463.

Hanmer, S., Mengel, F., Connelly, J. & van Gool, J. 1997: Significance of crustal-scale shear zones and synkinematic dykes in the Nagssugtoqidian orogen, SW Greenland: a reexamination. Journal of Structural Geology **19**, 59–75.

Henderson, G. & Pulvertaft, T.C.R. 1987: Lithostratigraphy and structure of a Lower Proterozoic dome and nappe complex. Geological map of Greenland, 1:100 000, Mârmorilik 71 V.2 Syd, Nûgâtsiaq 71 V.2 Nord and Pangnertôq 72 V.2 Syd. Descriptive text, 72 pp., 3 maps. Copenhagen: Geological Survey of Greenland.

Higgins, A.K. & Soper, N.J. 1999: The Precambrian supracrustal rocks of Nunataq, north-east Disko Bugt, West Greenland. In: Kalsbeek, F. (ed.): Precambrian geology of the Disko Bugt region, West Greenland. Geology of Greenland Survey Bulletin **181**, 79–86 (this volume).

Hoffman, P.F. 1989: United plates of America, the birth of a craton: Early Proterozoic assembly and growth of Laurentia. Annual Review of Earth and Planetary Sciences **16**, 543–603.

Kalsbeek, F. 1992: Large-scale albitisation of siltstones on Qeqertakavsak island, north-east Disko Bugt, West Greenland. Chemical Geology **95**, 213–233.

Kalsbeek, F. & Nutman, A. P. 1996: Anatomy of the Early Proterozoic Nagssugtoqidian orogen, West Greenland, explored by reconnaissance SHRIMP U-Pb dating. Geology **24**, 515–518.

King, A.R. 1983: Report on prospecting and correlating programme in the Maarmorilik Formation, West Greenland 1982, 21 pp. Unpublished report, Greenex A/S (in archives of Geological Survey of Denmark and Greenland).

Knudsen, C., Appel, P.W.U., Hageskov, B. & Skjernaa, L. 1988: Geological reconnaissance in the Precambrian basement of the Atâ area, central West Greenland. Rapport Grønlands Geologiske Undersøgelse **140**, 9–17.

Marshall, B. & Schønwandt, H.K. 1999: An Archaean sill complex and associated supracrustal rocks, Arveprinsen Ejland, north-east Disko Bugt, West Greenland. In: Kalsbeek, F. (ed.): Precambrian geology of the Disko Bugt region, West Greenland. Geology of Greenland Survey Bulletin **181**, 87–102 (this volume).

Myers, J. 1978: Formation of banded gneisses by deformation of igneous rocks. Precambrian Research **6**, 43–64.

Pedersen, L.F. 1995: Beskrivelse og analyse af deformationsstrukturer på Naajaat Qaqqaat og Oqaatsut, Disko Bugt, Vestgrønland. Indikationer på partitionering af paleostressfeltet i forbindelse med strike-slip bevægelser i Torsukattak fjorden, 158 pp. Unpublished cand. scient. thesis, Københavns Universitet, Danmark.

Pulvertaft, T.C.R. 1986: The development of thin thrust sheets and basement-cover sandwiches in the southern part of the Rinkian belt, Umanak district, West Greenland. In: Kalsbeek, F. & Watt, W.S. (eds): Developments in Greenland geology. Rapport Grønlands Geologiske Undersøgelse **128**, 75–87.

Pulvertaft, T.C.R. 1987: Geological map of Greenland, 1:100 000, Agpat 70 V.2 Nord. Copenhagen: Geological Survey of Greenland.

Pulvertaft, T.C.R. 1989: Reinvestigation of the Cretaceous boundary fault in Sarqaqdalen, Nûgssuaq, central West Greenland. Rapport Grønlands Geologiske Undersøgelse **145**, 28–32.

Rasmussen, H. & Holm. P.M. 1999: Proterozoic thermal activity in the Archaean basement of the Disko Bugt region and eastern Nuussuaq, West Greenland: evidence from K-Ar and $^{40}Ar/^{39}Ar$ mineral age investigations. In: Kalsbeek, F. (ed.): Precambrian geology of the Disko Bugt region, West Greenland. Geology of Greenland Survey Bulletin **181**, 55–64 (this volume).

Rasmussen, H. & Pedersen. L.F. 1999: Stratigraphy, structure and geochemistry of Archaean supracrustal rocks from Oqaatsut and Naajaat Qaqqaat, north-east Disko Bugt, West Greenland. In: Kalsbeek, F. (ed.): Precambrian geology of the Disko Bugt region, West Greenland. Geology of Greenland Survey Bulletin **181**, 65–78 (this volume).

Rosenkrantz, A., Münther, V. & Henderson, G. 1974: Geological map of Greenland, 1:100 000, Agatdal 70 V.1 Nord. Copenhagen: Geological Survey of Greenland.

Schiøtte, L. 1988: Field occurrence and petrology of deformed metabasite bodies in the Rinkian mobile belt, Umanak district, West Greenland. Rapport Grønlands Geologiske Undersøgelse **141**, 36 pp.

Van Gool, J., Marker, M., Mengel, F. & field party 1996: The Palaeoproterozoic Nagssugtoqidian orogen in West Greenland: current status of work by the Danish Lithosphere Centre. Bulletin Grønlands Geologiske Undersøgelse **172**, 88–94.

Van Kranendonk, M.J. & Wardle, R.J. 1996: Burwell domain of the Palaeoproterozoic Torngat Orogen, northeastern Canada: tilted cross-section of a magmatic arc caught between a rock and a hard place. In: Brewer, T.S. (ed.): Precambrian crustal evolution in the North Atlantic region. Geological Society Special Publication (London) **112**, 91–115.

Van Kranendonk, M.J., St.-Onge, M.R. & Henderson, J.R. 1993: Paleoproterozoic tectonic assembly of Northeast Laurentia through multiple indentations. Precambrian Research **63**, 325–347.

Deformation at the southern boundary of the late Archaean Atâ tonalite and the extent of Proterozoic reworking of the Disko terrane, West Greenland

John Grocott and Steven C. Davies

The *c.* 2800 Ma old Atâ tonalite in the area north-east of Disko Bugt, West Greenland has largely escaped both Archaean and Proterozoic regional deformation and metamorphism. At its southern margin the tonalite is in contact with migmatitic quartz-feldspar-biotite gneiss and to the south both are progressively deformed in a high-grade gneiss terrain. The main deformation in the high grade gneisses involved hanging wall north-west displacements on a system of low-angle ductile shear zones that structurally underlie the Atâ tonalite. This shear zone system is folded by a large-scale, steeply inclined and north-west-trending antiform defined by the change in dip of planar fabrics. Minor folds related to the antiform are present and there is some evidence that folding was synkinematic with emplacement of a suite of *c.* 1750 Ma old ultramafic lamprophyre dykes.

In much of the north-east Disko Bugt area it remains difficult to separate Archaean from Proterozoic structures and hence the extent of the Archaean terrane that has escaped intense Proterozoic reworking remains uncertain.

J.G. & S.C.D., *School of Geological Sciences, CEESR, Kingston University, Kingston-upon-Thames, Surrey KT1 2EE, UK.* E-mail: *j.grocott@kingston.ac.uk.*

Keywords: Archaean, deformation, Disko terrane, Proterozoic, structure, West Greenland

North-east of Disko Bugt in West Greenland, Archaean plutonic igneous rocks have escaped both Archaean and Proterozoic regional deformation and metamorphism near the abandoned settlement of Ataa on Arveprinsen Ejland (Fig. 1). The plutonic rocks have been known as the 'Atâ granite' (Escher & Burri 1967; Kalsbeek *et al.* 1988), but, because hardly any granites are present (Kalsbeek & Skjernaa 1999, this volume), the term 'Atâ tonalite' (Garde 1994) is employed in the present volume. The Atâ tonalite has an age of *c.* 2800 Ma (Kalsbeek *et al.* 1988; Nutman & Kalsbeek 1999, this volume) and is intrusive into strongly deformed, high-grade amphibolites and metasedimentary rocks of an Archaean greenstone belt (Fig. 1; Kalsbeek 1990). On Anap Nunaa, 20 km north-east of Ataa, Archaean supracrustal rocks are overlain unconformably by low-grade, and less deformed, Proterozoic sedimentary rocks (Garde & Steenfelt 1999, this volume). North of Anap Nunaa, intensity of Proterozoic deformation and grade of Proterozoic metamorphism increase across Nuussuaq (Garde & Steenfelt 1989, 1999, this volume) toward the Rinkian orogen (Fig. 2; Grocott & Pulvertaft 1990).

On Arveprinsen Ejland, south of a line between Vaskebugt and Ataa (Fig. 3), tonalitic rocks become progressively more deformed southwards, and the southern half of the island is underlain by high-grade gneisses. Escher & Pulvertaft (1976) identified a lineament which transects these gneisses along the inlet Paakitsoq (Fig. 1) as the boundary between the Proterozoic Rinkian and Nagssugtoqidian orogenic belts (Fig. 2). However, Kalsbeek *et al.* (1988) showed that the Rinkian belt and the Nagssugtoqidian orogen are not in direct contact in the area north-east of Disko Bugt, but are separated by an Archaean domain which includes the Atâ tonalite. This domain may be part of the Burwell terrane of northern Labrador and eastern Baffin Island (Grocott 1989; Hoffman 1990), although the existence of the Burwell terrane as a distinct tectono-stratigraphic entity in its type area of the north-east

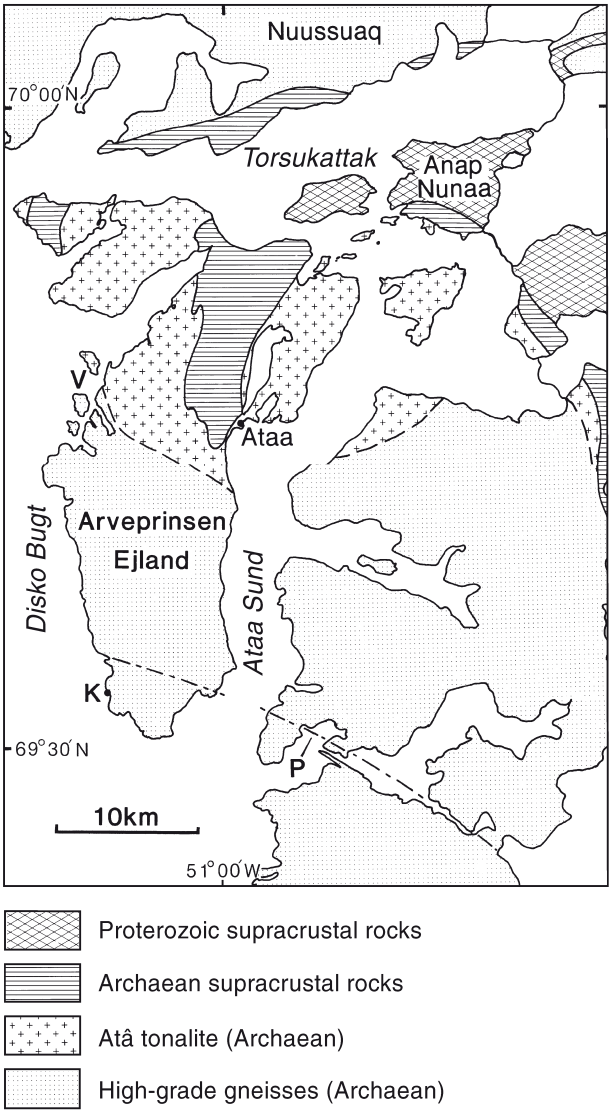

Fig. 1. Precambrian rocks of the north-east Disko Bugt region. V = Vaskebugt; K = Klokkerhuk; P = Paakitsoq lineament. From Kalsbeek (1989).

Torngat orogen in Labrador has recently been questioned (Van Kranendonk *et al.* 1993; Wardle *et al.* 1993). These authors continue to interpret Archaean rocks in the area north-east of Disko Bugt and on south-east Baffin Island as elements of a distinct tectono-stratigraphic terrane for which, in view of the demise of the Burwell terrane, they have proposed the name 'Disko terrane' after the exposures of dated Archaean crust in the Disko Bugt area (Fig. 2; Kalsbeek *et al.* 1988).

The location of orogenic sutures at the boundaries of the Disko terrane in West Greenland, and the extent of intense Proterozoic reworking within it, remain uncertain. Kalsbeek *et al.* (1987) have identified Palaeoproterozoic magmatic arc rocks in the Nagssugtoqidian orogen south of the Disko Bugt area, and infer that a cryptic suture, marking the southern boundary of the terrane, exists in the central part of the orogen (Fig. 2). However, the northern limit of reworking of the Disko terrane by deformation in the Nagssugtoqidian orogen is unknown. The high-grade gneiss terrain south of the Atâ tonalite may well be the result of intense Proterozoic reworking of Archaean rocks, but there is no geochronological evidence supporting this and, on available evidence, intense deformation at the southern margin of the Atâ tonalite could be of Archaean age or could have both Archaean and Proterozoic components. Therefore, high-grade gneisses on

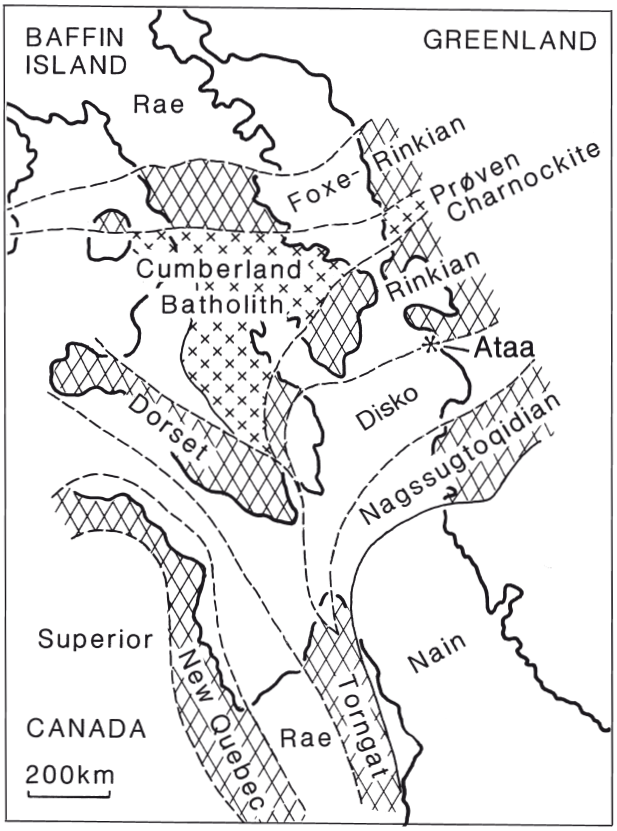

Fig. 2. Location of Ataa in relation to the Precambrian tectonic framework of NE Canada and West Greenland. Archaean terranes (Rae, Superior, Disko and Nain) largely unaffected by Proterozoic reworking are shown in white. Proterozoic belts (New Quebec, Torngat, Dorset, Nagssugtoqidian, Rinkian and Foxe–Rinkian) are shown cross-hatched. The belts include Archaean rocks reworked during the Proterozoic as well as rocks of Proterozoic age. The southward extent of unreworked Archaean rocks in the Disko terrane in West Greenland is speculative. Modified from Grocott (1989); Hoffman (1990); Van Kranendonk (1993).

Arveprinsen Ejland and the adjacent mainland together with the Atâ tonalite may both be elements of the Disko terrane in which there has been little Proterozoic deformation and metamorphism (Fig 2; Kalsbeek *et al.* 1988).

In this paper we describe the structure and the structural history of high grade gneisses in central and southern Arveprinsen Ejland and consider whether the structures described are of Archaean or Proterozoic age. Our field work involved structural mapping at 1:20 000 scale and focused on the western half of the island (Fig. 3). Reconnaissance mapping by A.A. Garde and A. Steenfelt (personal communication 1992) and our own reconnaissance mapping and aerial photograph interpretation enabled us to trace some structures eastward across the island.

The southern margin of the Atâ tonalite

Tonalites belonging to the Atâ tonalite at Vaskebugt in central Arveprinsen Ejland (Figs 1, 3) are cut by synkinematic, medium-grained granitic rocks and granite pegmatites (Fig. 4a). Primary compositional layering in the tonalites strikes north–south (Fig. 4b), parallel to the planar element of weak shape fabrics defined by recrystallised plagioclase (Fig. 4c). The planar fabrics are folded (Fig. 4c, e) and become transposed to a mylonitic foliation in NW–SE-striking and north-east-dipping ductile shear zones (Figs 3, 4d). Stretching fabric orientations (Figs 3, 5a), asymmetric porphyroclasts (Fig. 4f) and *S-C* fabrics reveal that right normal-slip displacements occurred on these shear zones. The proportion of rock affected by ductile shear zones increases south-west of Vaskebugt and domains of low fabric intensity are uncommon south-west of the Laksebugt – Kuussuup Tasia valley (Fig. 3).

Between Vaskebugt and Laksebugt, rocks belonging to the Atâ tonalite are in contact with coarse, migmatitic biotite-quartz-feldspar gneisses (Fig. 4e). Both tonalites and migmatites are cut by younger, often pegmatitic, granitoid intrusions. The relative age of the tonalites and the migmatites is difficult to interpret in the field. Folded sheets of Atâ tonalite occasionally appear to cut across banding in the migmatitic gneiss (Fig. 4e), implying that the tonalite is younger than migmatisation (see also Escher *et al.*1999, this volume). On the other hand, enclaves of tonalite are present in the migmatitic gneisses implying that the latter are younger, and this interpretation is in accord with available geochronology (Kalsbeek *et al.* 1988). South of Laksebugt, increase in the proportion of rock affected by strong ductile deformation coincides with an increase in the proportion of migmatitic biotite-quartz-feldspar gneiss which becomes the main lithology on southern Arveprinsen Ejland. However, tonalitic rocks of similar mineralogy and appearance to the main rock type in the western part of the Atâ tonalite occur in domains of low fabric intensity throughout southern Arveprinsen Ejland.

Niaqornaarsuk to Klokkerhuk

Reverse-slip ductile shear zones (D_m)

In southern Arveprinsen Ejland, anastomosing ductile shear zones are present in migmatitic biotite-quartz-feldspar gneisses with rare horizons of anorthosite, amphibolite and garnet-mica schist (Figs 3, 6). In a domain of low fabric intensity 1 km north of Niaqornaarsuk (Fig. 3), the gneisses contain an upper amphibolite facies assemblage of garnet-diopside-hornblende-biotite-quartz-feldspar. Within the shear zones the assemblage hornblende-biotite-quartz-feldspar implies that during D_m the rocks were metamorphosed at amphibolite grade.

Foliation in the shear zones strikes WSW–ENE, dips south-south-east (Fig. 5g), and the gneisses contain strong stretching lineations that plunge south-east (Fig. 5c). Kinematic indicators, viewed parallel to the kinematic *XZ* plane (perpendicular to the foliation and parallel to the stretching lineation), allow shear sense to be determined. At Niaqornaarsuaq (Fig. 3), narrow, generally concordant, amphibolite dykes show asymmetric foliation boudinage implying right reverse-slip displacement on the shear zones (Fig. 7a). This interpretation is supported by asymmetric porphyroclast systems and north-west vergence of sheath folds viewed in the kinematic *XZ* plane. Ductile shear zones are the main structural element between Niaqornaarssuk and Klokkerhuk.

Low fabric intensity domains between D_m shear zones

In domains of low fabric intensity between the shear zones, *L* or *L* > *S* tectonite fabrics are present in migmatitic biotite-quartz-feldspar gneisses. Major folds of gneissic banding are present 1 km north of Niaqor-

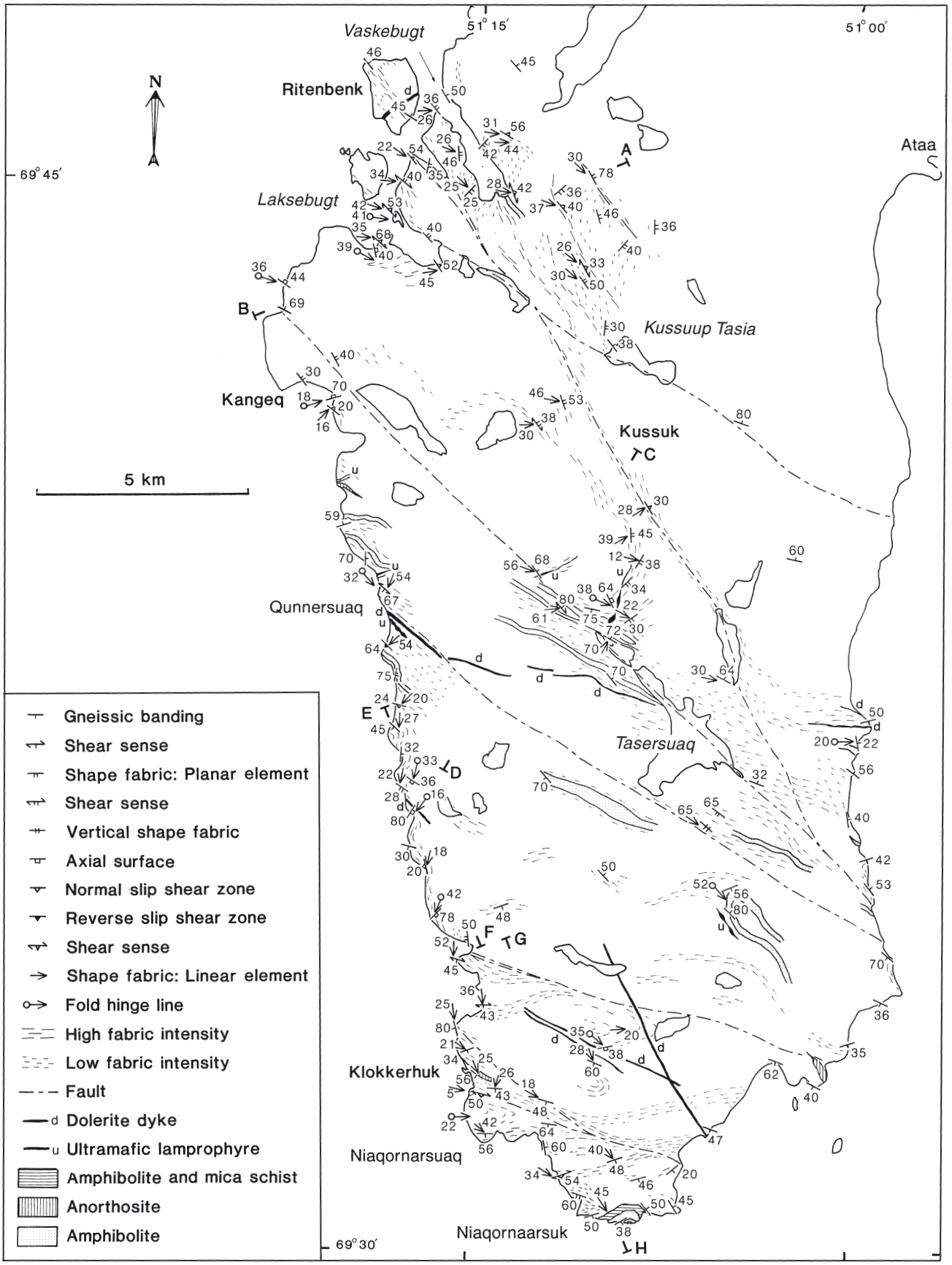

Fig. 3. Structural map of central and southern Arveprinsen Ejland, north-east Disko Bugt. South-west of a line between Vaskebugt and Kuussuup Tasia the main lithology is migmatitic biotite-quartz-feldspar gneiss. The Atâ tonalite is exposed north-east of this line. Sections A–B, C–D and E–H are given in Fig. 9.

naarsuaq and east of Klokkerhuk (Fig. 3). The axial traces of the folds are parallel to the strike of the reverse-slip shear zones implying that they are the same age (D_m) but they could equally be older structures (Garde & Steenfelt 1999, this volume).

Right strike-slip ductile shear zone ($D_{m''}$)

A 200 m wide, south-dipping ductile shear zone which post-dates the reverse-slip shear zones is exposed 500 m south of Klokkerhuk and strikes ESE–WNW (Fig. 6). The stretching lineation plunges between 5° west to 18° east. Clockwise rotation of D_m stretching lineations in the northern margin of the shear zone, immediately east of Klokkerhuk (Fig. 3), implies that shear sense is right-lateral and this is confirmed by asymmetric porphyroclast systems (Fig. 7b) and *S-C* fabrics. Grain size reduction is extreme in some narrow zones in the shear zone which contain ultramylonitic rocks. The mineral assemblage biotite-hornblende-quartz-feldspar indicates that metamorphic grade was amphibolite facies during deformation.

Post-shear zone folds (D_p)

Some poles to foliation for the Klokkerhuk area scatter along a π-girdle when plotted stereographically and define a moderately east-south-east-plunging fold axis (Fig. 5g). The poles which plot on the girdle were measured from south-vergent minor folds exposed 2 km east of Niaqornaarsuaq. The folds have axial surfaces inclined to the north.

Klokkerhuk to Qunnersuaq

Folding of D_m ductile shear zones (D_n and D_p folds)

Steeply-inclined and moderately-plunging open folds (F_n), with a wavelength of about 1 km, deform the ductile shear zones between Klokkerhuk and Qunnersuaq (Figs 3, 6). The folds have NE–SW-striking, steeply-inclined axial surfaces and plunge gently to moderately south-west (Fig. 8a). The fold envelope trends NNW–SSE parallel to the coast (Fig. 3), and defines the limb of a major, open D_n fold between Qunnersuaq and Klokkerhuk. This fold is responsible for the change in the plunge direction of the D_m linear fabric from south-east to south-west between Niaqornaarsuk and Qunnersuaq (Fig. 5c). D_n folding is not, in general, associated with overprinting of D_m fabrics, although crenulations, new planar fabrics and intersection lineations are present locally, particularly in hinge zones of D_n minor folds. The NE–SW trend of the D_n fold axial surfaces is consistent with folding during displacement on the right strike-slip shear zone exposed 500 m south of Klokkerhuk.

The reorientated D_m shear zones between Qunnersuaq and Klokkerhuk contain asymmetric porphyroclast systems and *S-C* fabrics which imply that displacement was reverse-slip (Fig. 7c). These kinematic indicators and the orientation of the stretching lineation shows that, in their present orientation, displacement on the shear zones was to the north at Klokkerhuk and to the north-east at Qunnersuaq (Figs 3, 6).

A second phase of post-shear zone folds (F_p) is present between Klokkerhuk and Qunnersuaq. The folds are open to close and south to south-west vergent with a wavelength of 10 m to 25 m (Fig. 7d). They are moderately to steeply inclined to the north or north-east and most plunge gently south-east (Fig. 8b). There is no systematic change in D_p fold axial surface orientation between Niaqornaarsuk and Qunnersuaq from which we infer that the folds are later than the D_n deformation.

The Paakitsoq lineament

The Paakitsoq lineament trends ESE–WSW across southern Arveprinsen Ejland and intersects the coast 3 km north of Klokkerhuk (Fig. 1). It is one of a set of similarly orientated lineaments in central and southern Arveprinsen Ejland (Fig. 3). The lineament was chosen by Escher & Pulvertaft (1976) as the boundary between the Rinkian and the Nagssugtoqidian orogenic belts because it separated a terrain having north-east-striking steep belts (Nagssugtoqidian) from a terrain to the north with dome-and-basin or flat-lying structure (Rinkian).

In western Arveprinsen Ejland the Paakitsoq lineament is a fault marked by a 10 m thick crush breccia and epidote-quartz mineralisation. The fault has a left-slip separation of about 300 m. We have no slickenline orientation data or shear sense data from the crush breccia, but similarity of structural style, structural history and metamorphic grade on each side of the fault zone mitigate against there being large vertical displacements across it.

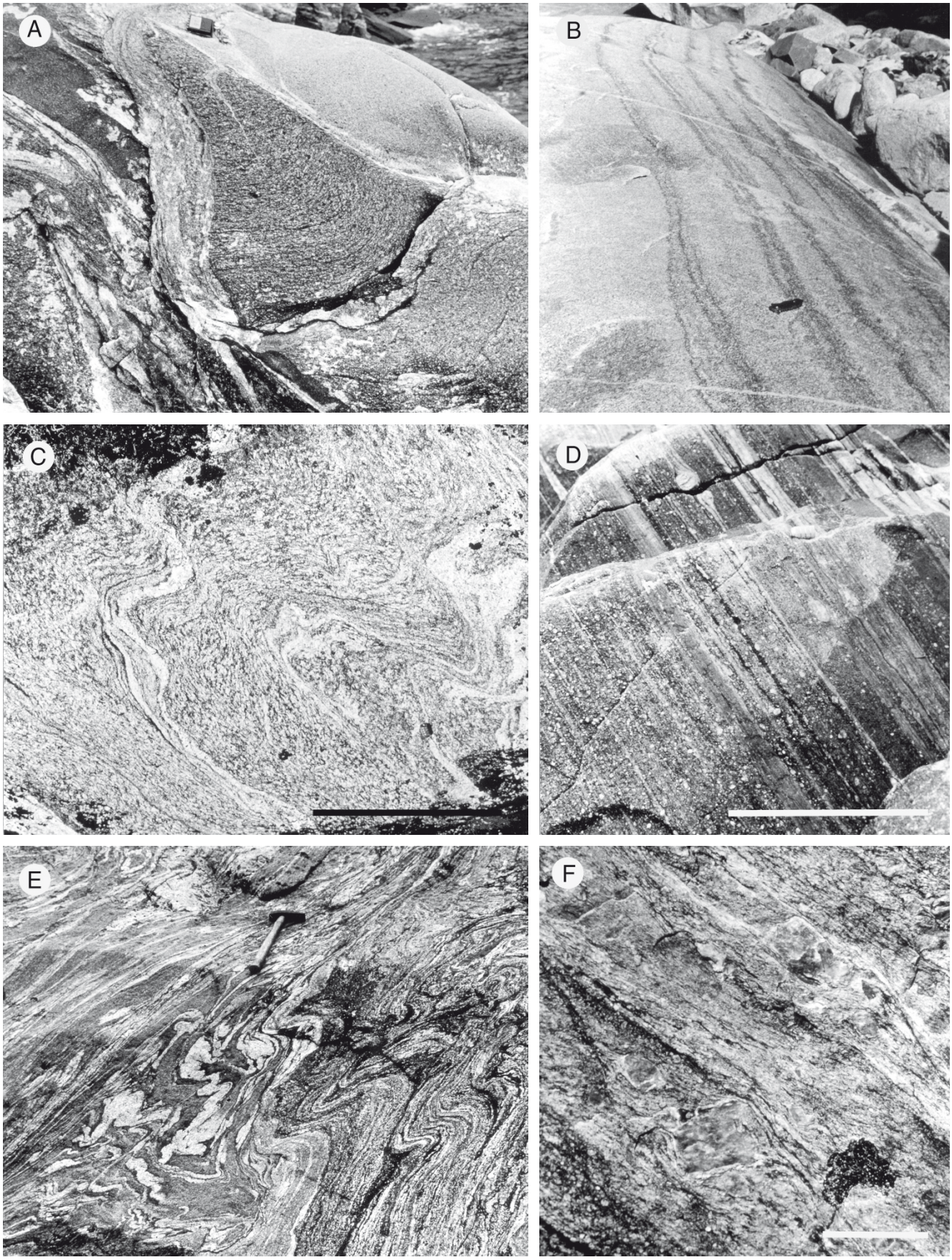
A
B
C
D
E
F

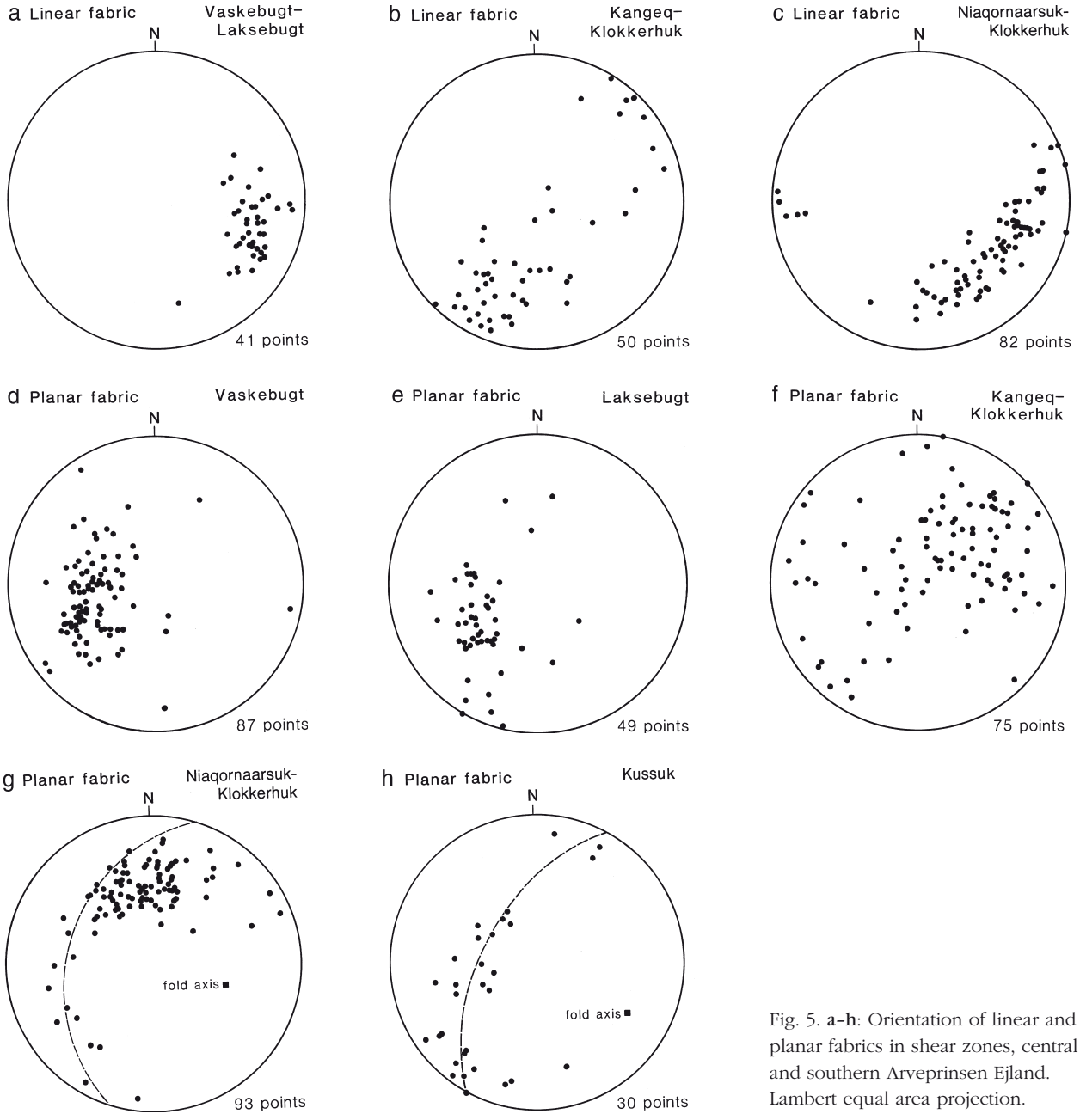

Fig. 5. **a–h**: Orientation of linear and planar fabrics in shear zones, central and southern Arveprinsen Ejland. Lambert equal area projection.

Fig. 4. Fabrics at the southern margin of the Atâ tonalite between Vaskebugt and Laksebugt. **A**: Weakly foliated tonalite cut by a medium-grained granite sheet, south side of Vaskebugt. Compass clinometer (top centre) is 12 cm long. **B**: Primary compositional layering in tonalite, south side of Vaskebugt. Pocket knife (centre) is 12 cm long. **C**: folded shape fabrics in tonalite, north side of Vaskebugt. The folds are viewed to the north-west and axial surfaces dip north-eastward. Scale bar is 30 cm long. **D**: Mylonitic migmatitic biotite-quartz-feldspar gneiss in D_m + $D_{m'}$ shear zone, north side of Laksebugt. The foliation is viewed to the north-west and dips north-eastward. Scale bar is 20 cm long. **E**: Folded migmatitic biotite-quartz-feldspar gneiss (left of photograph) and tonalitic gneiss derived from Atâ tonalite (right of photograph). The folds are viewed to the south-east and axial surfaces dip north-eastward. Fabric intensity in the migmatitic gneiss increases to the left. The hammer shaft (centre) is 35 cm long. **F**: Feldspar σ-porphyroclast system showing normal-slip displacement in a D_m shear zone south of Kussuk. The porphyroclasts are shown in the kinematic *XZ* plane of the shear zone viewed to the north-west. The planar fabric dips north-eastward. The scale bar is 3 cm long.

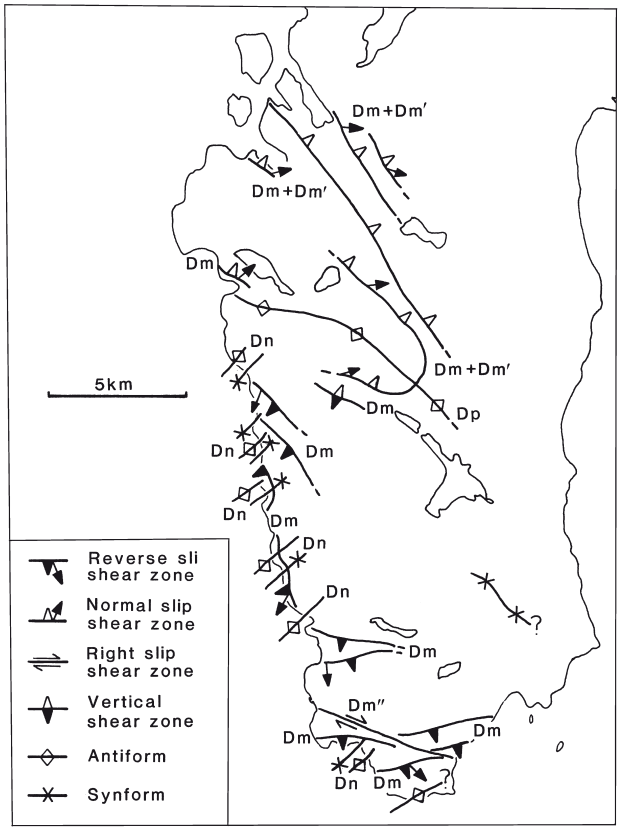

Fig. 6. Overview of major structures in the western and central part of central and southern Arveprinsen Ejland.

Qunnersuaq to Kussuk

A major south-vergent fold pair that folds the D_m shear zones is exposed between Qunnersuaq and Kussuk (Figs 3, 6, 9). The antiform is a tighter and more prominent fold than the synform (Fig. 9, section C–D). The axial surface trace of the synform is located south of Qunnersuaq where shallow-dipping planar fabrics in D_m shear zones are folded into a belt of steeply-dipping rocks in the southern limb of the antiform (Fig. 9, section C–D). A north-dipping and north-vergent, axial-plane foliation overprints the D_m planar fabric in this steep belt. The antiformal axial surface trace is exposed to the north-east, 4 km south-east of Kussuk (Fig. 3), and plunges moderately south-east (Fig. 5h). The Qunnersuaq–Kussuk folds are attributed to D_p deformation based on style and orientation (compare Figs 5h and 8b). They can be traced to the south-east as a major structure on the mainland east of Ataa Sund (Escher *et al.* 1999, this volume).

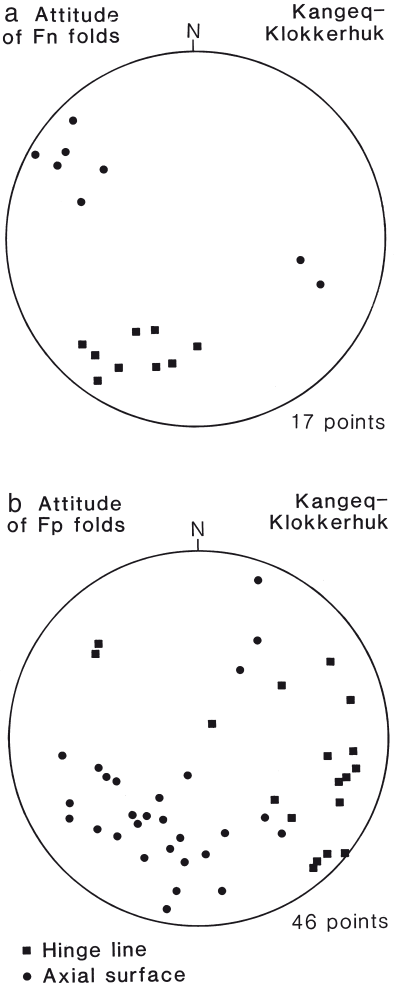

Fig. 8. **a**: Attitude of F_n folds between Kangeq and Klokkerhuk. **b**: Attitude of F_p folds between Kangeq and Klokkerhuk. Lambert equal area projection. Dots: poles to fold axial surfaces; squares: fold hinge lines.

Fig. 7. Sense of shear indicators and minor folds, Niaqornaarsuk to Kangeq, Arveprinsen Ejland. **A**: Asymmetric boudinage of amphibolite dyke at Niaqornaarsuaq. Structure is viewed to the south-west in the kinematic *XZ* plane and foliation dips south. Sense of shear is right reverse-slip. The hammer shaft (centre) is 35 cm long. **B**: Right strike-slip, σ-porphyroclast system in $D_{m''}$ shear zone south of Klokkerhuk. The scale bar is 3 cm long. **C**: σ-porphyroclast system indicating reverse-slip displacement in D_m ductile shear zone at Qunnersuaq. The porphyroclast is shown in the kinematic *XZ* plane viewed to the south-east. The foliation dips to the south-west. The coin is 2.5 cm in diameter. **D**: South-vergent D_p folds 5 km south of Qunnersuaq. The folds are viewed to the east. The hammer shaft (centre) is 35 cm long. **E**: *S-C* mylonites in a D_m shear zone, 2 km south-east of Kangeq in the northern limb of the Qunnersuaq–Kussuk antiform. The structure is viewed to the south-west in the *XZ* kinematic plane. Displacement of the hanging wall was to the north-east. **F**: South-vergent D_p fold of narrow ultramafic lamprophyre dyke exposed 2.5 km south of Qunnersuaq.

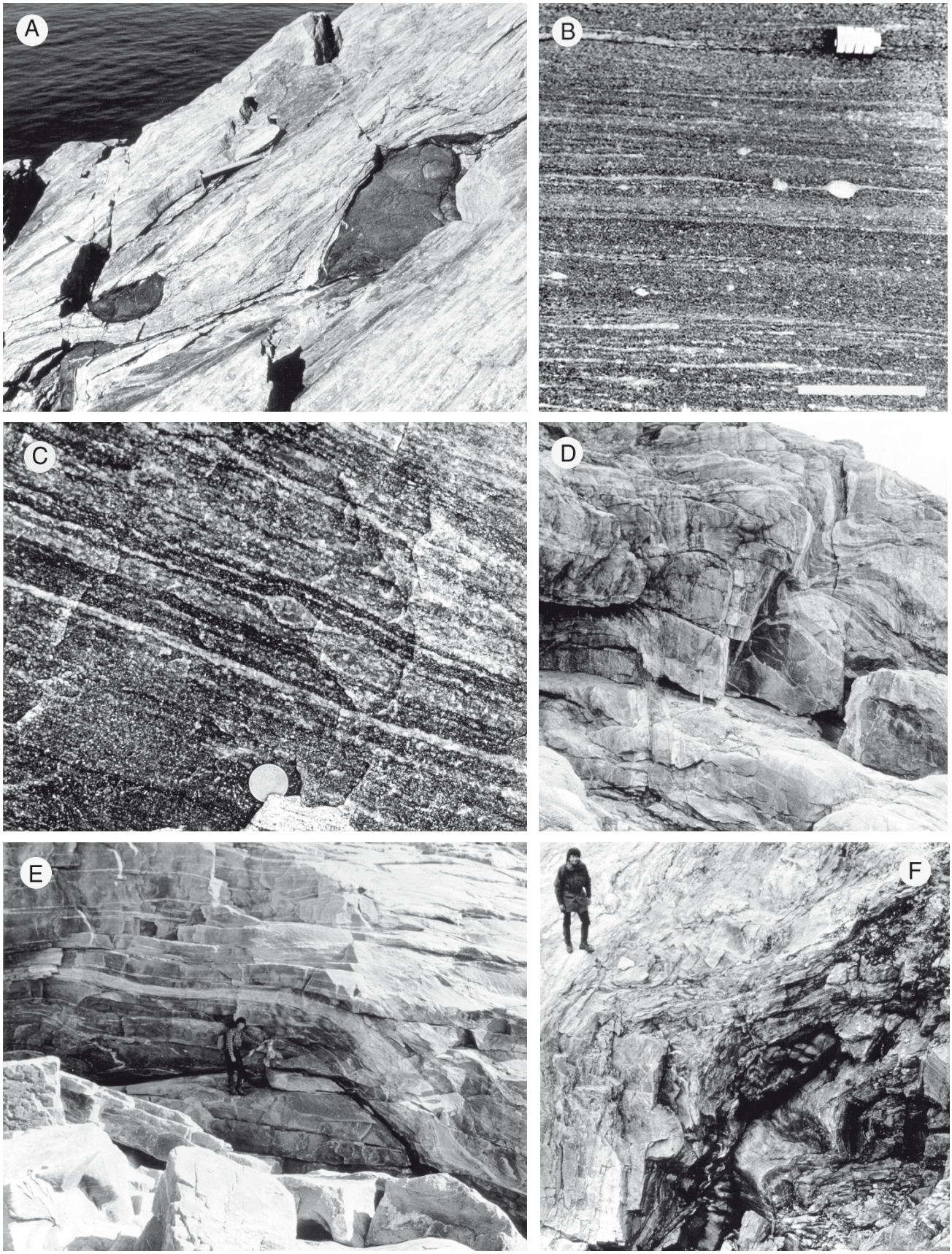
A
B
C
D
E
F

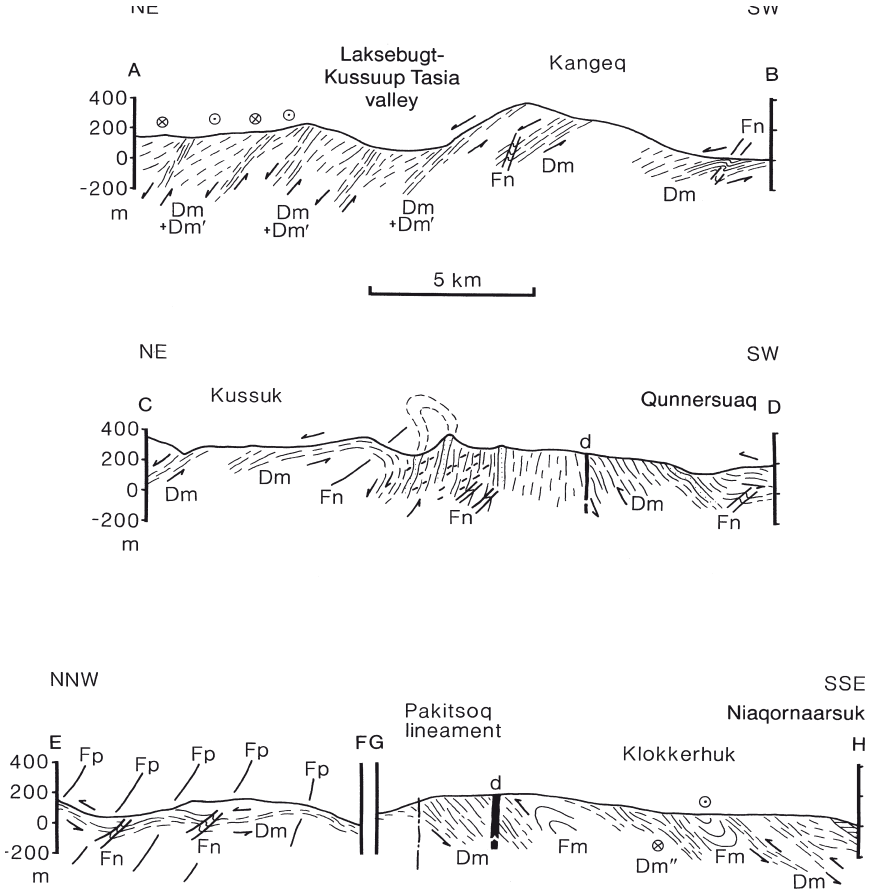

Fig. 9. Cross sections, central and southern Arveprinsen Ejland. Lines of the cross sections are shown on Fig. 3.

Kuussuup Tasia

This area is characterised by NW–SE-striking and north-east-dipping ductile shear zones on the north-east limb of the Qunnersuaq–Kussuk antiform (Figs 3, 6, 9). The width of the shear zones, and the proportion of the rocks affected by them, decreases north-east of Kuussuup Tasia toward the Atâ tonalite. The linear fabric plunges north-east at Kangeq and at Kussuk, but to the north it rotates clockwise to plunge south-east 4 km north of Kuussuup Tasia (Fig. 3). As it rotates, the pitch of the lineation in the foliation plane becomes shallower (Fig. 3).

This pattern is part of a general clockwise rotation of the linear fabric in the northern limb of the Qunnersuaq–Kussuk antiform (Figs 3, 6). Asymmetric porphyroclast systems in the shear zones imply that the sense of shear is right normal-slip, with an increasing right strike-slip component north-east of the Laksebugt – Kuussuup Tasia valley. The shear zones at Kuussuup Tasia are along strike from the right normal-slip shear zones already described in the Vaskebugt–Laksebugt area (Fig. 3).

Structural relationships

The map (Fig. 6) and cross-sections (Fig. 9) imply that Qunnersuaq–Kussuk folds are responsible for the change in dip direction of the ductile shear zone system across central Arveprinsen Ejland. Apparently, the north-east-dipping, right normal-slip shear zones north of the antiform belong to the same system as the south-west- or south-dipping, right reverse-slip shear zones at Qunnersuaq. This interpretation can be tested stereographically by simply unfolding the planar fabrics by rotation about the fold axis. As expected, this rotation brings the linear fabric in shear zones exposed in the northern limb of the Qunnersuaq–Kussuk antiform at Kangeq (Fig. 7e) to the same orientation as the lin-

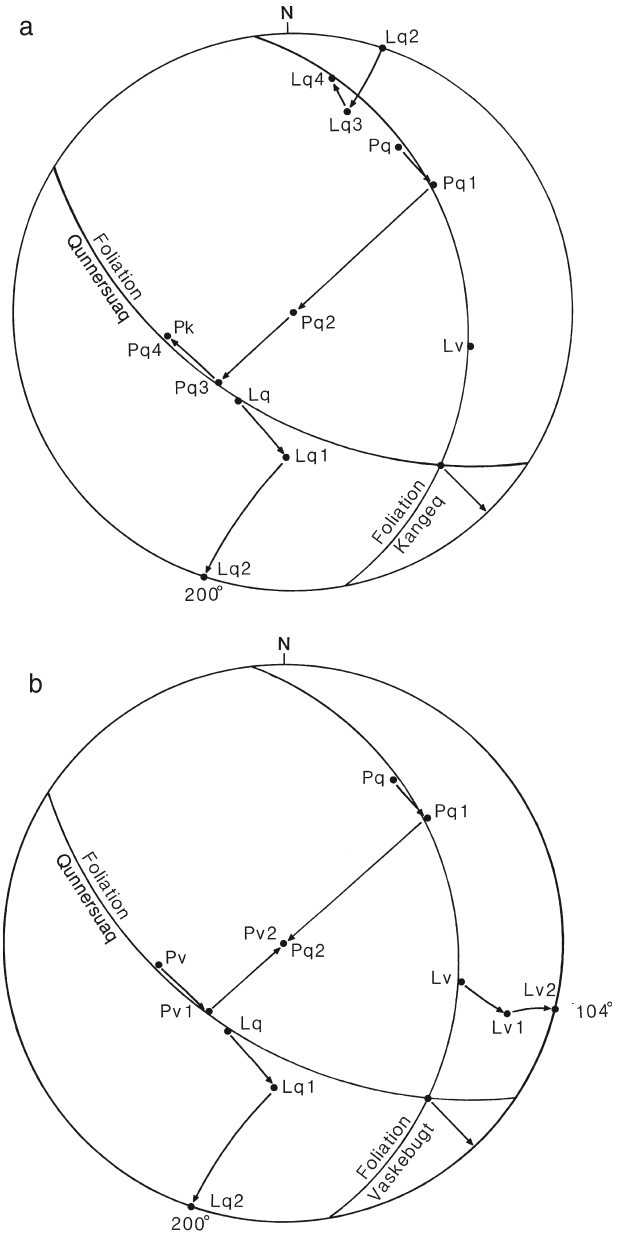

Fig. 10. Structural analysis of the Qunnersuaq–Kangeq antiform. **a**: Rotation of the foliation at Qunnersuaq (P_q) to the orientation of the foliation at Kangeq (P_k) about the hinge line of the antiform (stages P_q–P_{q1}–P_{q2}–P_{q3}–P_{q4}) causes the lineation at Qunnersuaq (L_q) to rotate to a north-east plunge direction (L_{q4}) through stages L_q–L_{q1}–L_{q2}–L_{q3}–L_{q4}. This plunge direction is the plunge direction of the stretching fabric in D_m shear zones exposed at Kangeq (see Fig. 5b). The plunge direction of the lineation at Vaskebugt (L_v) is shown for comparison. **b**: Rotation of the planar fabrics at Qunnersuaq and Vaskebugt to a common orientation about the axis of the Qunnersuaq–Kussuk antiform (paths P_q–P_{q1}–P_{q2} and P_v–P_{v1}–P_{v2} respectively). The linear fabrics in each limb do not restore to a common orientation (paths L_q–L_{q1}–L_{q2} and L_v–L_{v1}–L_{v2}).

ear fabric in the southern limb of the antiform at Qunnersuaq (Fig. 10a).

The orientation of the linear fabric cannot be accounted for so easily everywhere in the northern limb of the antiform. When the planar fabrics measured at Vaskebugt are rotated stereographically about the axis of the Qunnersuaq–Kussuk antiform so that they coincide with the orientation of the planar fabric at Qunnersuaq, the reoriented lineations do not coincide (Fig. 10b). Clearly, the orientation of the east- or south-east-plunging linear fabric typical of most of the northern limb of the Qunnersuaq–Kussuk antiform cannot be simply explained by folding.

Clockwise rotation of the linear fabric in the northern limb of the Qunnersuaq–Kussuk antiform (Fig. 6) might imply that D_m linear fabrics have been progressively deformed and reorientated during ductile shearing ($D_{m'}$) at the southern margin of the Atâ tonalite. In this view, the sense of rotation of the linear fabric is consistent with right strike-slip deformation (Fig. 11). However, we have found no overprinting relationships allowing D_m and $D_{m'}$ fabrics to be separated in the shear zones in the northern limb of the antiform, and we have observed only a single linear fabric in the shear zones interpreted as a resultant fabric (Grocott 1979). Lack of overprinting and the fact that we have not documented a strain gradient northward or southward across the northern limb of the antiform associated with the rotation of the lineation means that our conclusion that D_m is earlier than $D_{m'}$ is provisional.

Finally, it is tempting to correlate $D_{m'}$ with the deformation responsible for the right strike-slip ductile shear zone exposed south of Klokkerhuk ($D_{m''}$). This is unlikely, however, because such shear zones would show a left strike-slip displacement in map view in the northern limb of the Qunnersuaq–Kussuk antiform.

Age of the structures

Samples from the Atâ tonalite have given U-Pb zircon ages of 2794 ± 15 Ma and 2803 ± 4 Ma and it is likely that its crystallisation age is close to 2800 Ma (Kalsbeek *et al.* 1988; Nutman & Kalsbeek 1999, this volume). At Laksebugt, samples of migmatitic biotite gneiss have given a Rb-Sr whole-rock isochron age of 2672 ± 52 Ma, significantly younger than the Atâ tonalite; this is suggested as the date of the migmatisation event (Kalsbeek *et al.* 1988). The migmatitic rocks lie to the south of the Atâ tonalite and are deformed by D_m and $D_{m'}$.

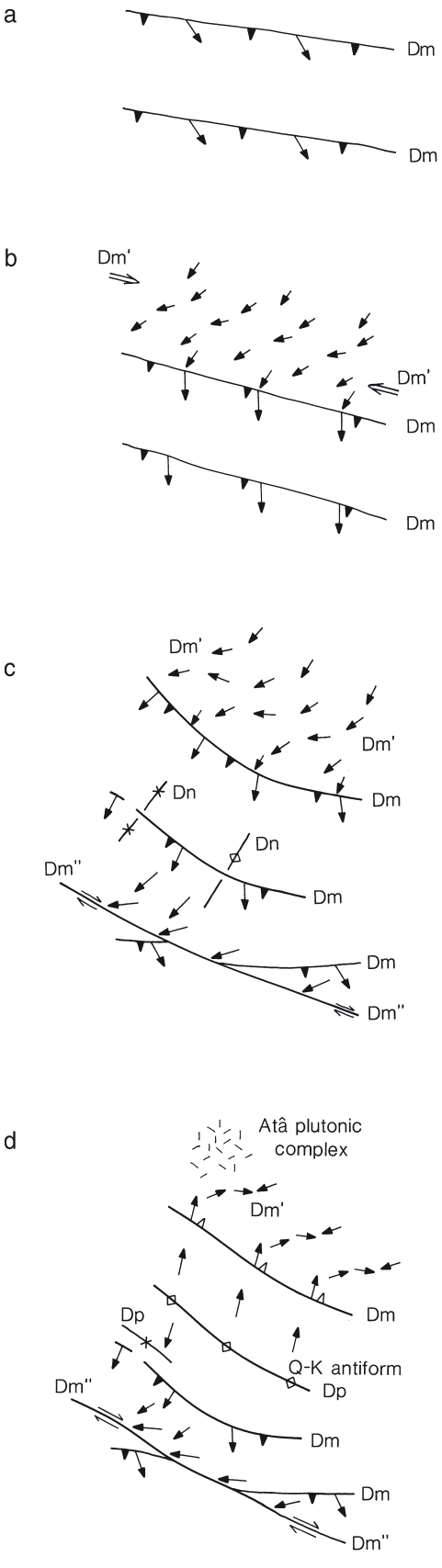

Reworking of Archaean gneisses during the Proterozoic is often reflected by disturbance of the Rb-Sr isotope system (Kalsbeek 1981; Dawes *et al.* 1988), but this is not always the case (Andersen & Pulvertaft 1985). The migmatitic biotite-quartz-feldspar gneisses at Laksebugt yield well-fitted Rb-Sr whole-rock isochrons. If these isochrons date migmatisation, then the later deformation and metamorphism have not significantly disturbed the isotope system. This could imply that the ages of both D_m and $D_{m'}$ are close to the age of migmatisation; about 2700 Ma. However, given that it is difficult to predict the resilience of the Rb-Sr system to resetting, this argument for an Archaean age for these deformations is not strong.

Shear zones of the D_m and $D_{m''}$ deformation phases are cut by strongly discordant Proterozoic ultramafic lamprophyre dykes on Arveprinsen Ejland (Larsen & Rex 1992). Several narrow dykes are exposed at the coast between Qunnersuaq and Klokkerhuk (Fig. 3) where D_n and D_p folds are common. The dykes postdate D_n folds but are deformed to varying degrees of intensity by moderately-inclined, gently south-east-plunging D_p folds (Fig. 7f). There is also a spatial relationship between D_p folds and the ultramafic lamprophyre dykes which further implies that dyke emplacement may be synkinematic with D_p. Partial or complete recrystallisation of the dykes to hornblende schist accompanied folding.

East of Ataa Sund (Fig. 1) ultramafic lamprophyres cut Palaeoproterozoic metasedimentary rocks (Marker & Knudsen 1989; Thomsen 1991). Two ultramafic lamprophyre dykes, exposed on the mainland east of Ataa, have yielded K-Ar ages of 1782 ± 70 Ma and 1743 ± 70 Ma respectively (Larsen & Rex 1992; see also Rasmussen & Holm 1999, this volume). These ages are similar to a Rb-Sr whole-rock age of 1760 ± 185 Ma for fine-grained Palaeoproterozoic sediments on Anap Nunaa (Kalsbeek *et al.* 1988) and probably reflect cooling

Fig. 11. Structural evolution of central and southern Arveprinsen Ejland. **a**: D_m shear zones developed throughout the area with displacement of the hanging wall to the north-west. **b**: A right strike-slip shear zone ($D_{m'}$) has reworked D_m shear zones at the southern margin of the Atâ tonalite. Reworking is reflected by rotation of linear fabrics. **c**: D_n folding associated with a right strike-slip shear zone ($D_{m''}$) on southern Arveprinsen Ejland. **d**: Folding (D_p) of the shear zones on central Arveprinsen Ejland by the Qunnersuaq–Kussuk antiform. D_m shear zones retain a reverse-slip shear sense in the southern limb of the fold (closed triangles) but have a normal-slip shear sense in the northern limb of the fold (open triangles).

following low-grade metamorphism in the metasedimentary rocks and in the dykes. Since ultramafic lamprophyres post-date D_m and $D_{m'}$ shear zones, these ages provide an upper age bracket for D_m and $D_{m'}$ deformations on Arveprinsen Ejland.

Proterozoic reworking of the Disko terrane

The Atâ tonalite and the greenstone belt on Arveprinsen Ejland are virtually unaffected by Proterozoic deformation over a wide area north-east of Disko Bugt (Kalsbeek *et al.* 1988). These Archaean rocks represent the type area for the Disko terrane as defined by Van Kranendonk *et al.* (1993). Migmatitic, biotite-quartz-feldspar gneisses to the south of the Atâ tonalite are also of Archaean age, but the age of intense ductile deformation and amphibolite facies metamorphism in these high grade gneisses is uncertain. More geochronology is therefore required to identify the extent of intense Archaean and Proterozoic deformation in the Disko terrane in the Disko Bugt region.

The structural style of the high-grade gneisses on central and southern Arveprinsen Ejland (low-angle ductile shear zones folded by major, upright antiformal or dome-like structures – the Qunnersuaq–Kussuk antiform) is typical of surrounding Palaeoproterozoic belts. In central Baffin Island, upright gneiss domes fold low-angle, polyphase, ductile shear zones (Henderson *et al.* 1988, 1989) and later sinistral strike-slip deformation was superposed on the structures (Henderson 1981). Farther north in West Greenland, upright folds of flat-lying structures are typical of the structural style of the Rinkian belt (Henderson & Pulvertaft 1967; Grocott & Pulvertaft 1990). Closer to north-east Disko Bugt, there are also strong similarities between the structural style on eastern Nuussuaq, where Archaean crust has been affected by strong Proterozoic deformation in the Rinkian belt, and in the domain south of the Atâ tonalite on the mainland east of Ataa Sund (Escher *et al.* 1999, this volume). In the latter area, basic and picritic sills in the vicinity of Paakitsoq thought to be of Proterozoic age are affected by west-vergent, low-angle ductile shear zones that may correlate with D_m shear zones in central and southern Arveprinsen Ejland. All these points mitigate in favour of the main shear zone deformation in central and southern Arveprinsen Ejland (D_m) being of Proterozoic rather than Archaean age.

On the other hand, Archaean supracrustal rocks south-east of Anap Nunaa contain thrusts that appear to be truncated by the unconformity at the base of Proterozoic sedimentary rocks (Garde & Steenfelt 1999, this volume). These thrusts can be traced to the south into the high-grade gneiss terrain east of Ataa Sund described by Escher *et al.* (1999, this volume) where they are presumably reworked by Proterozoic structures. This implies that strong Archaean as well as strong Proterozoic deformation, both characterised by low-angle shear zones, has affected the high-grade gneiss terrain south of the Atâ tonalite.

Conclusions

The main phase of deformation in the high-grade gneiss terrain of central and southern Arveprinsen Ejland involved displacements to the north-west on flat-lying ductile shear zones (D_m in Fig. 11a). The shear zones structurally underlie the Atâ tonalite which was consequently displaced north-west in the hanging wall of this shear zone system. The D_m shear zones were reworked by NE- to ENE-striking, right strike-slip shear zones responsible for clockwise rotation of the linear fabric near the southern margin of the Atâ tonalite ($D_{m'}$ in Fig. 11b) and an isolated right strike-slip shear zone south of Klokkerhuk ($D_{m''}$ in Fig. 11c). Locally, D_m shear zones are deformed by open to close, steeply-inclined, south-west-plunging D_n folds which have north-east-striking axial surfaces. The D_m-$D_{m'}$ shear zone system was deformed by major folds associated with the final phase of ductile deformation (D_p) between Qunnersuaq and Kussuk (Fig. 11d). Major and minor folds associated with D_p deformation have NW–SE-trending axial surfaces steeply inclined to the north-east and with gently south-east-plunging hinge lines.

The age of deformation in D_m and $D_{m'}$ ductile shear zones remains uncertain. At Laksebugt deformed rocks yielded an Rb-Sr whole rock isochron giving an age of 2672 ± 52 Ma suggested to date pre-shear zone migmatisation. This establishes the Archaean age of the rocks in the high-grade gneiss terrain on southern Arveprinsen Ejland and provides a lower limit on the age of deformation. It does not necessarily mean that the deformation was of Archaean age. Structural style in the high-grade gneiss terrain on Arveprinsen Ejland is similar to that in the Rinkian belt to the north of the Atâ tonalite where Archaean rocks have been strongly affected by Proterozoic deformation and metamorphism. Moreover, there is evidence from the mainland east of Ataa Sund that intense deformation on low-

angle shear zones, with similar displacement patterns to the D_m shear zones on Arveprinsen Ejland, is of Proterozoic age. The last phase of folding on Arveprinsen Ejland (D_p) appears to be the same age as a suite of ultrabasic lamprophyre dykes which have given K-Ar mineral ages of about 1750 Ma. This provides an upper limit on the age of the main D_m and $D_{m''}$ deformations on Arveprinsen Ejland.

Acknowledgements

We thank all our colleagues on the Survey's Disko Bugt Project for discussion on the geology of Arveprinsen Ejland. We also thank the base camp team at Ataa who provided us with excellent logistical support in the 1992 field season.

References

Andersen, M.C. & Pulvertaft, T.C.R. 1985: Rb-Sr whole rock 'ages' from reworked basement gneisses in the Umanak area, central West Greenland. Bulletin of the Geological Society of Denmark **34**, 205–212.

Dawes, P.R., Larsen, O. & Kalsbeek, F. 1988: Archean and Proterozoic crust in North-West Greenland: evidence from Rb-Sr whole-rock age determinations. Canadian Journal of Earth Sciences **25**, 1365–1373.

Escher, A. & Burri, M. 1967: Stratigraphy and structural development of the Precambrian rocks in the area north-east of Disko Bugt, West Greenland. Rapport Grønlands Geologiske Undersøgelse **13**, 28 pp.

Escher, A. & Pulvertaft, T.C.R. 1976: Rinkian mobile belt of West Greenland In: Escher, A. & Watt, W.S. (eds): Geology of Greenland, 104–119. Copenhagen: Geological Survey of Greenland.

Escher, J.C., Ryan, M.J. & Marker, M. 1999: Early Proterozoic thrust tectonics east of Ataa Sund, north-east Disko Bugt, West Greenland. In: Kalsbeek, F. (ed.): Precambrian geology of the Disko Bugt region, West Greenland. Geology of Greenland Survey Bulletin **181**, 171–179 (this volume).

Garde, A.A. 1994: Precambrian geology between Qarajaq Isfjord and Jakobshavn Isfjord, West Greenland, 1:250 000. Copenhagen, Geological Survey of Greenland.

Garde, A.A. & Steenfelt, A. 1989: A new anorthosite/gabbro complex at Nûgssuaq, central West Greenland. Rapport Grønlands Geologiske Undersøgelse **145**, 16–20.

Garde, A.A. & Steenfelt, A. 1999: Precambrian geology of Nuussuaq and the area north-east of Disko Bugt, West Greenland. In: Kalsbeek, F. (ed.): Precambrian geology of the Disko Bugt region, West Greenland. Geology of Greenland Survey Bulletin **181**, 6–40 (this volume).

Grocott, J. 1979: Shape fabrics and superimposed simple shear strain in a Precambrian shear belt, West Greenland. Journal of the Geological Society (London) **136**, 471–488.

Grocott, J. 1989: Early Proterozoic assembly of NE Laurentia: constraints from Baffin Island and West Greenland. Tectonic Studies Group Annual Meeting, Imperial College. Programme and Abstracts, 48 only.

Grocott, J. & Pulvertaft, T.C.R. 1990: The Early Proterozoic Rinkian belt of central West Greenland. In: Lewry, J.F. & Stauffer, M.R. (eds): The Early Proterozoic Trans-Hudson Orogen of North America. Geological Association of Canada Special Paper **37**, 443–463.

Henderson, G. & Pulvertaft, T.C.R. 1967: The stratigraphy and structure of the Precambrian rocks of the Umanak area, West Greenland. Meddelelser fra Dansk Geologisk Forening **17**, 1–20.

Henderson, J.R. 1981: Structural analysis of sheath folds with horizontal x-axes, northeast Canada. Journal of Structural Geology **3**, 203–210.

Henderson, J.R., Grocott, J. Henderson, M.N., Falardeau, F. & Heijke, P. 1988: Results of fieldwork in the Foxe Fold Belt near Dewar Lakes, Baffin Island, N.W.T. Geological Survey of Canada Paper **88-1C**, 101–108.

Henderson, J.R., Grocott, J., Henderson, M.N. & Perreault, S. 1989: Tectonic history of the Lower Proterozoic Foxe–Rinkian Belt in central Baffin Island, N.W.T. Geological Survey of Canada Paper **89-1C**, 185–197.

Hoffman, P.F. 1990: Dynamics of the assembly of northeast Laurentia in geon 18 (1.9-1.8 Ga). Geoscience Canada **17**(4), 222–226.

Kalsbeek, F. 1981: The northward extent of the Archaean basement of Greenland – a review of Rb-Sr whole rock ages. Precambrian Research **14**, 203–219.

Kalsbeek, F. 1989: GGU's expedition in the Disko Bugt area, 1988. Rapport Grønlands Geologiske Undersøgelse **145**, 14–16.

Kalsbeek, F. 1990: Disko Bugt Project, central West Greenland. Rapport Grønlands Geologiske Undersøgelse **148**, 21–24.

Kalsbeek, F. & Skjernaa, L. 1999: The Archaean Atâ intrusive complex (Atâ tonalite), north-east Disko Bugt, West Greenland. In: Kalsbeek, F. (ed.): Precambrian geology of the Disko Bugt region, West Greenland. Geology of Greenland Survey Bulletin **181**, 103–112 (this volume).

Kalsbeek, F., Pidgeon, R.T. & Taylor, P.N. 1987: Nagssugtoqidian mobile belt of West Greenland: a cryptic 1850 Ma suture between two Archaean continents – chemical and isotopic evidence. Earth and Planetary Science Letters **85**, 365–385.

Kalsbeek, F., Taylor, P.N. & Pidgeon, R.T. 1988: Unreworked Archaean basement and Proterozoic supracrustal rocks from north-eastern Disko Bugt, West Greenland: implications for the nature of mobile belts in Greenland. Canadian Journal of Earth Sciences **25**, 773–782.

Larsen, L.M. & Rex, D.C. 1992: A review of the 2500 Ma span of alkaline-ultramafic, potassic and carbonatitic magmatism in West Greenland. Lithos **28**, 367–402.

Marker, M. & Knudsen, C. 1989: Middle Proterozoic ultramafic lamprophyre dykes in the Archaean of the Ataa area, central West Greenland. Rapport Grønlands Geologiske Undersøgelse **145**, 23–28.

Nutman, A.P. & Kalsbeek, F. 1999: SHRIMP U-Pb zircon ages for Archaean granitoid rocks, Ataa area, north-east Disko Bugt. In: Kalsbeek, F. (ed.): Precambrian geology of the Disko Bugt region, West Greenland. Geology of Greenland Survey Bulletin **181**, 49–54 (this volume).

Rasmussen, H. & Holm, P.M. 1999: Proterozoic thermal activity in the Archaean basement of the Disko Bugt region and eastern Nuussuaq, West Greenland: evidence from K-Ar and ^{40}Ar-^{39}Ar mineral age investigations. In: Kalsbeek, F. (ed.): Precambrian geology of the Disko Bugt region, West Greenland. Geology of Greenland Survey Bulletin **181**, 55–64 (this volume).

Thomsen, H.S. 1991: Contrasting types of metasomatic alteration in the low-grade metamorphic Precambrian Anap Nunâ area, West Greenland, 99 pp. Unpublished cand. scient. thesis, University of Copenhagen, Denmark.

Van Kranendonk, M.J., St.-Onge, M.R. & Henderson, J.R. 1993: Palaeoproterozoic tectonic assembly of Northeast Laurentia through multiple indentations. Precambrian Research **63**, 325–347.

Wardle, R.J., Van Kranendonk, M.J., Mengel, F., & Scott, D. 1993: Geological mapping in the Torngat orogen, northernmost Labrador, Report 2. Newfoundland Department of Mining and Energy Report **93-1**, 77–90.

Early Proterozoic thrust tectonics east of Ataa Sund, north-east Disko Bugt, West Greenland

Jan C. Escher, Michael J. Ryan and Mogens Marker

The area east of Ataa Sund consists mainly of amphibolite facies grade Archaean gneisses, amphibolites and granites. Intense early Proterozoic deformation led to low-angle ductile imbrication of thrust sheets with movement directions to the west. Late tectonic Proterozoic basic sills with olivine-rich cumulates were intruded along the thrust sheets.

J.C.E., *Geological Survey of Denmark and Greenland, Thoravej 8, DK-2400 Copenhagen NV, Denmark.* E-mail: *jce@geus.dk.*
M.J.R., *Department of Geology, University of Portsmouth, Portsmouth PO1 3HE, UK.*
M.M., *Geological Institute, University of Copenhagen, Øster Voldgade 10, DK-1350 Copenhagen K, Denmark.* Present address: *Geological Survey of Norway, Leiv Erikssonsvei 39, N-7491 Trondheim, Norway.*

Keywords: Archaean rocks, Disko Bugt, Proterozoic, thrust tectonics, West Greenland

The Ataa area, north-east Disko Bugt, lies between the early Proterozoic Nagssugtoqidian and Rinkian orogenic belts of West Greenland (Fig. 1; Escher 1995). Escher & Pulvertaft (1967) proposed the boundary between the two belts to run along a fault zone in the Ataa Sund region, but Kalsbeek *et al*. (1988) believed that the area was hardly or not affected by early Proterozoic deformation, and thus did not belong to either of them. In the present study we describe the structural development of an area east of Ataa Sund, and show that large-scale westward-directed ductile thrusting took place during the early Proterozoic. Similar structures occur west of Ataa Sund (Grocott & Davies 1999, this volume) and on Nuussuaq (Garde & Steenfelt 1999, this volume), and correspond to a phase of early Proterozoic thrusting described by Pulvertaft (1986) in the southern part of the Rinkian belt.

During the Disko Bugt Project the coastal areas were mapped by rubber boat on 1:50 000 scale, and the inland areas by foot traverses in less detail. Five Archaean and six Proterozoic events in the development of the area have been recognised (Table 1).

Archaean rocks

Most of the area east of Ataa Sund consists of late Archaean rocks. Five units have been distinguished (Fig. 2; Table 1).

1. Amphibolites probably represent the oldest rock unit of the area, as they occur as numerous inclusions and boudinaged layers within migmatitic orthogneisses; locally, some of the inclusions show an early discordant foliation (Fig. 3). The thicker sheets often preserve compositional banding, seen as paler varieties of feldspar-hornblende gneiss next to darker, coarser grained, mafic amphibolite and hornblendite. Some of this banding may be original, but some may be due to metamorphic differentiation. The amphibolites were probably derived from basic lavas or tuffs, or differentiated basaltic intrusions. Locally, disseminated fine-grained sulphides give the rocks a rusty weathering appearance.

2. Migmatitic, banded, foliated granodioritic and tonalitic orthogneisses form the bulk of the rocks in

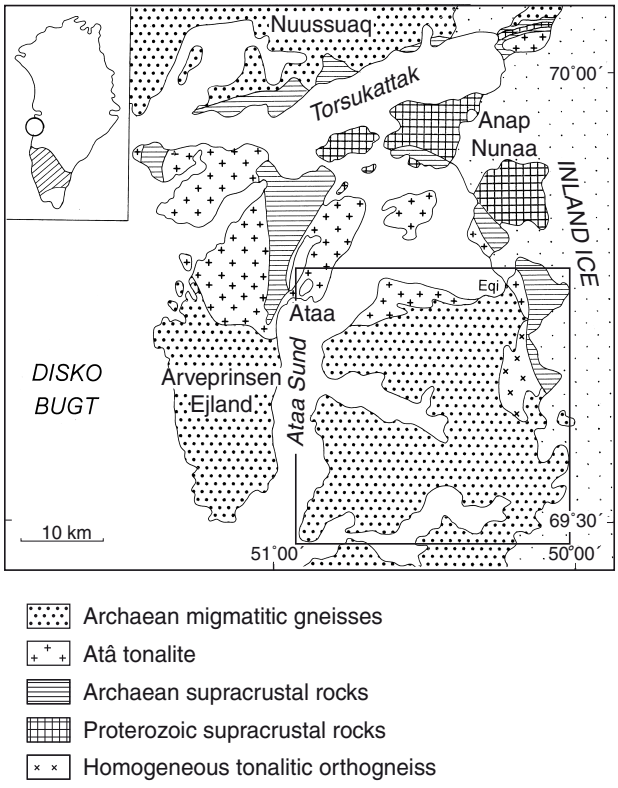

Fig. 1. Geological sketch map of the region north-east of Disko Bugt with the location of the area described in this paper.

the area. The gneisses show a polyphase intrusive origin with several generations of small-scale layering of quartzo-feldspathic and biotite (-hornblende) segregations (Fig. 4). Some of the tonalitic-dioritic layers may represent different phases of intermediate magmatic precursors of the gneisses, some may represent variable degrees of assimilation of basic enclaves, while most of the leucocratic banding seems to be a consequence of migmatitic differentiation. As noted above, the gneisses are typically rich in amphibolite inclusions. Local rusty weathering of the gneisses has been attributed to hydrothermal activity with alteration to muscovite, epidote, chlorite, hematite and occasionally carbonate and small amounts of disseminated sulphides. One sample of the migmatitic orthogneisses has yielded a SHRIMP U-Pb zircon date of 2815 ± 4 Ma (Nutman & Kalsbeek 1999, this volume).

3. Homogeneous, tonalitic orthogneisses occur in the eastern part of the area. In contrast with the migmatitic gneisses, they exhibit little migmatitic vein-

Fig. 2. Geological map of the area east of Ataa Sund, West Greenland. For location, see Fig. 1.

Table 1. Archaean and Proterozoic development of the area east of Ataa Sund; from oldest to youngest

ARCHAEAN

1. Amphibolite
2. Migmatitic orthogneiss
3. Homogeneous orthogneiss with biotite-hornblende clusters
4. Supracrustal and associated intrusive rocks (*c.* 2800 Ma)
5. Atâ tonalite (*c.* 2800 Ma)

PROTEROZOIC

6. Major folding and thrusting:
   a. W- to NW-facing recumbent folds; imbricate thrusting during ductile shear deformation with W to NW transport directions; W- to NW-trending mineral stretching lineations; penetrative mylonitic fabric
   b. Open to tight folds with steep E–W- to SE–NW-trending axial surfaces
7. Basic sills with olivine-rich cumulate
8. Minor folding:
   Open, large-scale folds and chevron-type folds; steep SE-trending axial surfaces
9. WNW- to ESE-trending faults in the Paakitsoq region
10. Dolerites and lamprophyres (*c.* 1750 Ma to *c.* 1650 Ma)
11. Albitisation of gneisses

ARCHAEAN

- Quaternary
- Atâ pluton, mainly trondhjemitic. Zircon U-Pb age 2794 Ma
- Established boundary
- Transitional boundary

PROTEROZOIC

- Granitic rocks
- Strike and dip
- Dolerites. Rb-Sr whole-rock isochron, age 1645 Ma
- Metadolerite
- Fold axis
- Ultramafic lamprophyre/lamproite dykes and diatremes. K-Ar biotite age 1750 Ma
- Supracrustal and associated intrusive rocks. Sm-Nd model age acid metavolcanic rocks: 2800 Ma
- Mineral or stretching lineation
- Basic sills with olivine-rich cumulate;
- Ultrabasic rocks
- Thrust
- Tonalitic orthogneiss with biotite-hornblende clusters
- Fault
- Migmatitic tonalitic-granodioritic orthogneiss; with albite metasomatic alteration
- Antiform
- Synform
- Amphibolite, as layers and inclusions
- Direction of younging

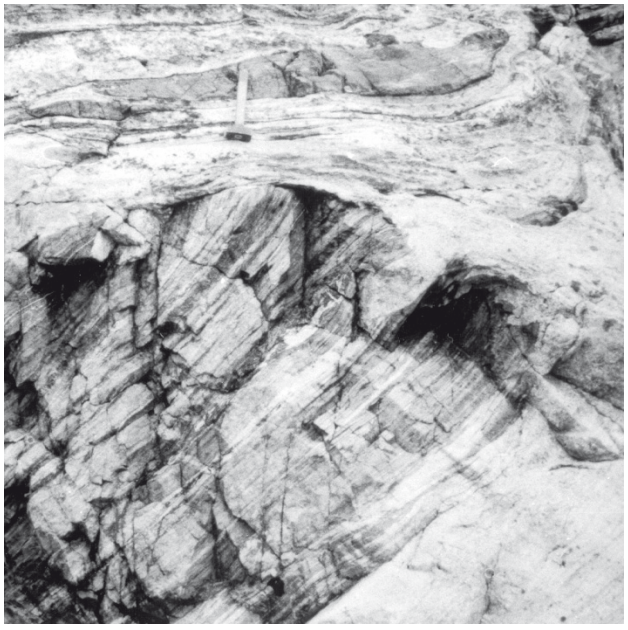

Fig. 3. Foliated amphibolite inclusion within banded migmatitic orthogneiss showing discordant relationship; innermost part of Kangerluarsuk.

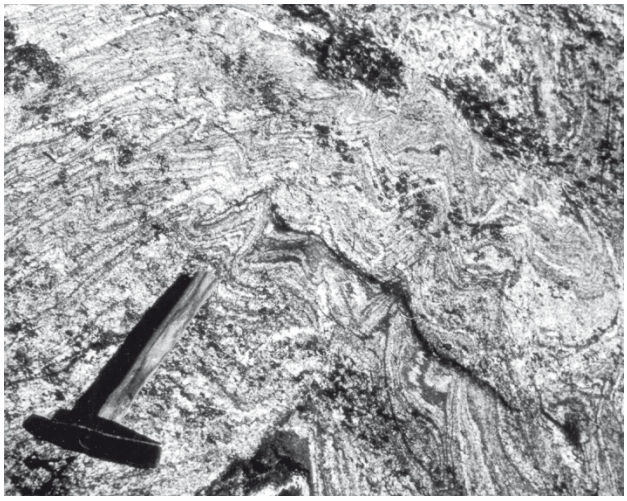

Fig. 4. Small-scale folded, migmatitic orthogneiss; Timaani Inussuit.

ing and contain few amphibolite inclusions. Small clusters of biotite and hornblende give the rock a characteristic spotted appearance. The low degree of migmatisation and the scarcity of basic inclusions may indicate that these gneisses are younger than the migmatitic gneisses. SHRIMP zircon dating (Nutman & Kalsbeek 1999, this volume) did not resolve this age difference.

4. An isolated outcrop (*c.* 1 km²) of quartzite and structurally overlying grey garnetiferous mica schists occurs along the coast at Uiartagaq (Fig. 2). These metasediments occur in the centre of a westerly-trending, synformal structure. About 35 km to the north-west of Uiartagaq, similar Archaean metasedimentary rocks with a comparable mineralogy have been mapped at Oqaatsut; 69°55′N, 51°25′W (Rasmussen & Pedersen 1999, this volume).

A belt of supracrustal rocks and associated intrusive bodies occurs along the north-eastern margin of the gneiss area in the Eqi–Maniitsoq region. (Fig. 2). The belt consists mainly of micaceous quartz-rich metasediments with a few thin layers of banded iron formation, acid and basic volcanic rocks and gabbroic rocks; they show amphibolite and greenschist facies metamorphic grade (Stendal *et al.* 1999, this volume). The dominant bedding/foliation dips to the north-east at variable angles, but well-preserved pillow structures within the primary stratification indicate a way-up direction to the south-west; the sequence is therefore overturned. Acid metavolcanic rocks in the Eqi region have yielded a Sm-Nd model age of *c.* 2800 Ma (Kalsbeek & Taylor 1999, this volume).

Fig. 5. Migmatitic orthogneiss with intrusive, polyphase, granite sheets and veins (Atâ tonalite); west of Eqi.

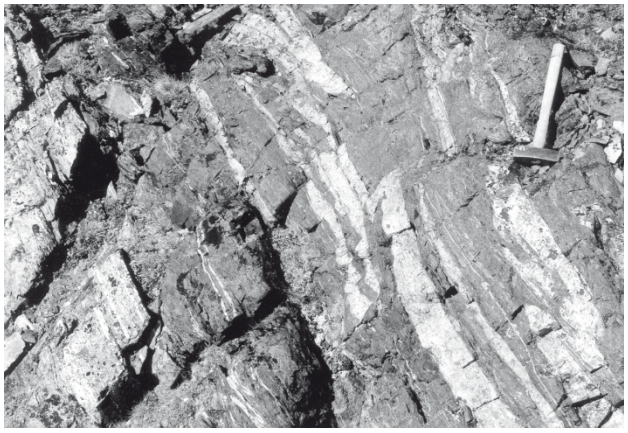

Fig. 6. Intrusive contact relationship between deformed granitoid rocks of the Atâ tonalite (lower left) and Archaean metavolcanic rocks (upper right) with veins of tonalite within amphibolite; Eqi.

5. Weakly-foliated, polyphase trondhjemitic rocks forming part of the Atâ tonalite (Atâ intrusive complex of Kalsbeek & Skjernaa 1999, this volume) occur along the northern margin of the gneiss area. The boundary between the banded migmatitic gneisses and the Atâ tonalite is transitional with a gradual, northwards increase of grey polyphase trondhjemitic veins intruding the migmatitic gneisses (Fig. 5). Although the Atâ tonalite has given about the same radiometric age as the acid volcanic rocks of Eqi, the tonalite is younger as numerous trondhjemitic veins intrude the supracrustal rocks along the contact between the two units (Fig. 6).

Proterozoic rocks

A basic sill complex with olivine cumulate layers occurs within the gneisses of the southern part of the area. Many of the sills have been emplaced within thrust faults during a late stage of the ductile regional thrusting. They show well-developed pinch and swell structure or boudinage (Fig. 7). The centres of the thicker sills show generally little deformation, while the margins have been variably altered. Most of this alteration is attributed to shear movements along the thrusts perhaps during injection of the magma. The sills show in many localities well-preserved intrusive contacts with the host gneisses and dark coloured fine-grained chilled margins; secondary chloritisation occurs along joints.

Although layering or colour banding of the sills are not apparent in the field, variations in mineral assemblages and composition are shown by thin section study and chemical analyses. These variations are either the result of *in situ* differentiation or separate injection pulses of magmas with different compositions.

Thin sections show generally a medium- to coarse-grained rock of ultramafic composition, with 1–2 mm olivine crystals enclosed by larger 5–10 mm orthopyroxene, occasionally with minor interstitial plagioclase. However, the sill situated near the narrow entrance of Paakitsoq is a micronorite, with abundant basic plagioclase and orthopyroxene, a little clinopyroxene and interstitial quartz. The lowest sill in the Kissaviap Qaqqaa region, occurring about 150 m above sea level, has a similar composition.

Some 125 km further to the north, Schiøtte (1988) has described a swarm of discordant metabasic sills within Archaean migmatitic gneisses, which show comparable composition and style of emplacement. Based on the occurrence of normal and inversed igneous layering, Schiøtte recognised inversion of the bodies relative to each other after their intrusion, and concluded that Rinkian (*c*. 1800–1900 Ma) recumbent folding postdated the intrusion of the metabasites. East of Ataa Sund, it has not been possible to establish the direction of younging of the igneous layering; however, the tectonic development of the region does not indicate any major recumbent folding of the sills. Therefore it is not clear whether the two swarms of metabasic sills can be correlated.

A few NNW-trending metadolerite dykes occur in the eastern part of the area (Fig. 2). They have been subjected to moderate deformation, shearing and boud-

Fig. 7. Boudinaged basic sill (about 20 m thick), intruded along a thrust fault; east of Kissaviap Qaqqaa.

Fig. 8. 'Falcon cliff' (view to the north) with imbricated thrust sheets of banded gneiss. Transport direction to the west. West-facing recumbent folds with related small-scale folds in upper part of cliff section near 460 m high mountain summit. Thrust planes accentuated with black lines.

inage. The foliated margins consist of amphibolite and often preserve discordant relationships with the surrounding gneisses. Cores of less-deformed dykes show relict ophitic textures or early metamorphic textures, with garnet formed by reaction between igneous pyroxene and plagioclase. One metabasic dyke, more than 10 km long, cuts through the fold interference pattern of Timaani Inussuit (described below). The age of the Timaani Inussuit structure is, however, poorly constrained, and the age of these metadolerites may be either Archaean or Proterozoic.

Main Proterozoic structural development

Proterozoic E–W compression in the Disko Bugt region led to widespread ductile deformation of the crystalline rocks. Large-scale recumbent isoclinal folds and imbricated low-angle thrust sheets, with overall westerly transport directions, have been mapped in different parts of the region. For example on northern Nuussuaq, about 65 km north of the area described here, a major recumbent west-facing fold and associated thrust sheets, formed by low-angle fault movements, deform a marble unit correlated with the early Proterozoic Mârmorilik Formation (Garde & Steenfelt 1999, this volume). Similar deformation occurred on Arveprinsen Ejland, where a series of low-angle, generally SE-dipping ductile shear zones have been described by Grocott & Davies (1999, this volume). The area east of Ataa Sund has undergone similar intense deformation during westerly-directed ductile overthrusting combined with west-verging recumbent folding. Two examples are described in detail.

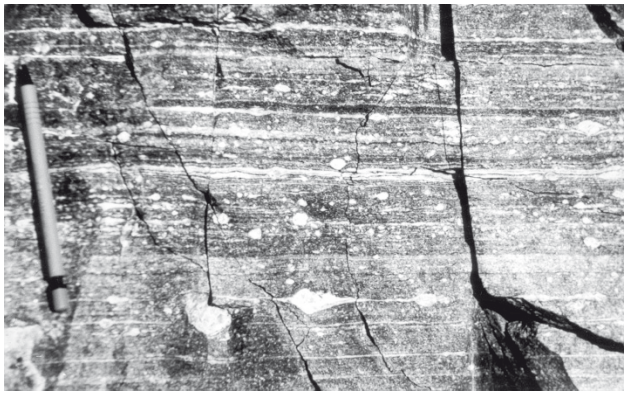

Fig. 9. Penetrative mylonitic foliation with elongated quartz and feldspar aggregates; 'Falcon cliff'.

Fig. 10. Lower part of *S*-shaped fold (view to the north) with E-dipping axial surface; 'Falcon cliff'. Person on right as scale.

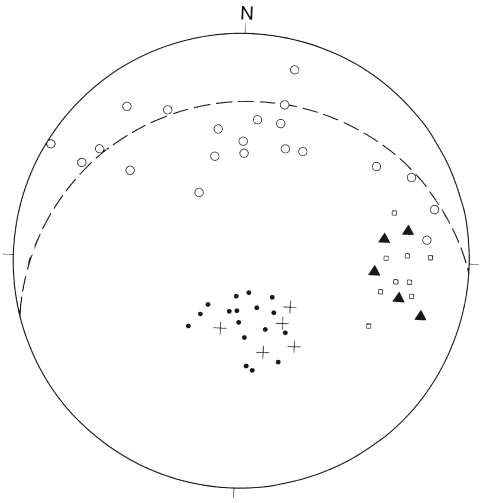

Fig. 12. Lower hemisphere Schmidt projection of measured structural data from 'Falcon cliff. (1) Event 6a (Table 1): open circles = fold axes of recumbent and related small-scale folds; dots = poles to the axial surfaces of the folds; crosses = poles to mylonitic foliation; squares = mineral stretching lineations; great circle (stippled) = 'best fit' of axial surfaces. (2) Event 6b (Table 1): filled triangles = axes of open to tight folds with steep westerly-trending axial planes.

'Falcon cliff'

About 2.5 km south of Kissaviap Qaqqaa (Fig. 2), a steep, south-facing mountain cliff, nearly 400 m high, was given the informal name of 'Falcon cliff' because of nesting Gyr falcons. The cliff represents a well-exposed, E–W cross-section through a series of imbricate thrust sheets (Fig. 8). At least eight thrust units of migmatitic gneisses have been distinguished. The upper part of the cliff section shows a number of large westerly-facing recumbent folds which are related to the thrusting. A well-developed penetrative mylonitic foliation (Fig. 9) seen within all the thrust sheets was developed during the thrust event. Quartz-feldspar-biotite stretching lineations dip to the east and south-east. The recumbent folds are associated with *S*-shaped, asymmetric, parasitic folds (Fig. 10). All folds have tight to isoclinal shapes with their axial surfaces parallel to the thrust faults. The westerly vergence of the recumbent folds and the low-angle, east-dipping imbrication are consistent with the top-to-the-west sense of movement of the thrust sheets, which is demonstrated by numerous asymmetric K-feldspar porphyroclast systems (Fig. 11). Similar shear-sense indicators within thrust structures from other localities of the mapped region also indicate a westerly sense of transport.

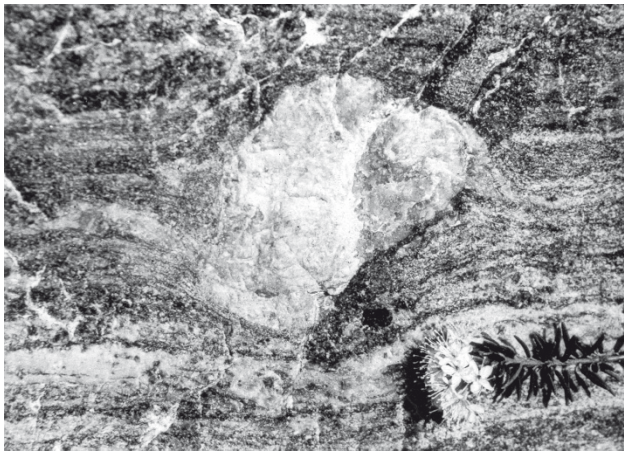

Fig. 11. Rotated, asymmetric K-feldspar porphyroclast (view to the south) indicating top to the west sense of shearing; 'Falcon cliff'. Largest diameter of porphyroclast about 8 cm.

A lower hemisphere Schmidt net projection of structural data from 'Falcon cliff' (Fig. 12) shows: (1) mineral and stretching lineations plunging about 20° to the ESE, (2) axial surfaces of parasitic folds parallel to the mylonitic foliation of the thrust sheets, both with an average dip of about 30° to the NNW (indicated as the 'best fitting' great circle) and (3) NW to NE fanning of the axes of parasitic folds.

It was not possible to recognise the basal thrust detachment zone of the imbricates, nor to appraise distances of displacement of the individual thrust sheets. The ductile folding and thrusting of the rocks and the amphibolite facies mineral assemblages indicate that deformation took place at mid-crustal depth.

Following the intense E–W regional shortening (Table 1, 6a), the region east of Ataa Sund endured a

Fig. 13. Recumbent fold refolded by vertical E–W-trending fold; 'Falcon cliff'. See text for explanation. Compass 20 cm in

period of more moderate deformation during N–S contraction (Table 1, 6b). In the 'Falcon cliff' area, a few folds related to the latter event have been recorded (Figs 12, 13).

Timaani Inussuit

A large fold structure in the Timaani Inussuit area (Fig. 2) is outlined by a string of basic inclusions and boudinaged layers of amphibolite which resemble a Ramsay type 2 mushroom-shaped interference pattern. Although no conclusive indications for the age of this structure are found, it is suggested that it was formed by interference between a major, west-facing recumbent fold (Table 1, 6a) and a few E–W-trending upright folds (Table 1, 6b); this would mean that the structure is Proterozoic in age. On the other hand, the intense isoclinal folding and refolding are reminiscent of the fold style of parts of the Archaean craton further to the south.

Later Proterozoic deformation

The youngest Proterozoic deformation recorded in the area east of Ataa Sund is of relatively weak intensity and is characterised by open, large-scale folds and smaller-scale chevron-style folds with steep NW–SE-trending axial planes and variably dipping fold axes. The chevron folds have a well-developed micaceous crenulation cleavage.

A good example of later Proterozoic large-scale folding occurs on the peninsula of Timmeernerit. In general the thrust faults of the mapped area dip eastwards. On Timmeernerit, however, a pile of thrust sheets has been folded by a large open NW–SE-trending antiform, and the thrust sheets as a consequence dip to the south. The antiform of Timmeernerit has the same trend as the Quvnerssuaq–Kugssuk antiform on Arveprinsen Ejland (Grocott & Davies 1999, this volume) and can be envisaged as a south-eastern extension of that structure.

The gneisses north and south of Paakitsoq fjord are cut by a series of parallel, sub-vertical, ESE–WNW-trending faults (Fig. 2). Some of the faults can be traced for about 42 km through the Disko Bugt region from Arveprinsen Ejland (Grocott & Davies 1999, this volume) to the Inland Ice. Although it has not been possible to measure displacement on the faults due to a lack of suitable marker horizons, the impression is that only minor displacement has occurred. The faults are characterised by 2–15 m wide brittle crush zones consisting of brecciated unfoliated epidote-quartz-feldspar rock; the breccia has locally been albitised (Ryan & Escher 1999, this volume). The brittle nature of the fault rock and the undisturbed linear shape of the faults indicate that movement took place at high crustal level during a late stage of the regional deformation.

Escher & Pulvertaft (1976) proposed that the Paakitsoq fault system formed the tectonic boundary between the Nagssugtoqidian and Rinkian mobile belts. A detailed mapping of the region south of Paakitsoq was not included in the mapping program of the Disko Bugt region, but the work on Arveprinsen Ejland by Grocott & Davies (1999, this volume) and the present authors suggests that these faults do not represent a structure of crustal dimensions.

References

Escher, A. & Burri, M. 1967: Stratigraphy and structural development of the Precambrian rocks in the area north-east of Disko Bugt, West Greenland. Rapport Grønlands Geologiske Undersøgelse **13**, 28 pp.

Escher, A. & Pulvertaft, T.C.R. 1976: Rinkian mobile belt of West Greenland. In: Escher, A. & Watt, W.S. (eds): Geology of Greenland, 104–119. Copenhagen: Geological Survey of Greenland.

Escher, J.C. 1995: Geological map of Greenland, 1:100 000, Ataa 69 V.3 Nord. Copenhagen: Geological Survey of Greenland.

Garde, A.A. & Steenfelt, A. 1999: Precambrian geology of Nuussuaq and the area north-east of Disko Bugt, West Greenland. In: Kalsbeek, F. (ed.): Precambrian geology of the Disko Bugt

region, West Greenland. Geology of Greenland Survey Bulletin **181**, 6–40 (this volume).

Grocott, J. & Davies, S.C. 1999: Deformation at the southern boundary of the late Archaean Atâ tonalite and the extent of Proterozoic reworking of the Disko terrane, West Greenland. In: Kalsbeek, F. (ed.): Precambrian geology of the Disko Bugt region, West Greenland. Geology of Greenland Survey Bulletin **181**, 155–169 (this volume).

Kalsbeek, F. & Skjernaa, L. 1999: The Archaean Atâ intrusive complex (Atâ tonalite), north-east Disko Bugt, West Greenland. In: Kalsbeek, F. (ed.): Precambrian geology of the Disko Bugt region, West Greenland. Geology of Greenland Survey Bulletin **181**, 103–112 (this volume).

Kalsbeek, F. & Taylor, P.N. 1999: Review of isotope data for Precambrian rocks from the Disko Bugt region, West Greenland. In: Kalsbeek, F. (ed.): Precambrian geology of the Disko Bugt region, West Greenland. Geology of Greenland Survey Bulletin **181**, 41–47 (this volume).

Kalsbeek, F., Taylor, P.N. & Pidgeon, R.T. 1988: Unreworked Archaean basement and Proterozoic supracrustal rocks from northeastern Disko Bugt, West Greenland: implications for the nature of Proterozoic mobile belts in Greenland. Canadian Journal of Earth Sciences **25**, 773–782.

Nutman, A.P. & Kalsbeek, F. 1999: SHRIMP U-Pb zircon ages for Archaean granitiod rocks, Ataa area, north-east Disko Bugt, West Greenland. In: Kalsbeek, F. (ed.): Precambrian geology of the Disko Bugt region, West Greenland. Geology of Greenland Survey Bulletin **181**, 49–54 (this volume).

Pulvertaft, T.C.R. 1986: The development of thin thrust sheets and basement-cover sandwiches in the southern part of the Rinkian belt, Umanak district, West Greenland. Rapport Grønlands Geologiske Undersøgelse **128**, 75–87.

Rasmussen, H. & Pedersen, L.F. 1999: Stratigraphy, structure and geochemistry of Archaean supracrustal rocks from Oqaatsut and Naajaat Qaqqaat, north-east Disko Bugt, West Greenland. In: Kalsbeek, F. (ed.): Precambrian geology of the Disko Bugt region, West Greenland. Geology of Greenland Survey Bulletin **181**, 65–78 (this volume).

Ryan, M.J. & Escher J.C. 1999: Albitised gneisses in the area between Paakitsoq and Kangerluarsuk, north-east Disko Bugt, West Greenland. In: Kalsbeek, F. (ed.): Precambrian geology of the Disko Bugt region, West Greenland. Geology of Greenland Survey Bulletin **181**, 113–117 (this volume).

Schiøtte, L. 1988: Field occurrence and petrology of deformed metabasite bodies in the Rinkian mobile belt, Umanak district, West Greenland. Rapport Grønlands Geologiske Undersøgelse **141**, 36 pp.

Stendal, H., Knudsen, C., Marker, M. & Thomassen, B. 1999: Gold mineralisation at Eqi, north-east Disko Bugt, West Greenland. In: Kalsbeek, F. (ed.): Precambrian geology of the Disko Bugt region, West Greenland. Geology of Greenland Survey Bulletin **181**, 129–140 (this volume).

Danmarks og Grønlands Geologiske Undersøgelse (GEUS)
Geological Survey of Denmark and Greenland
Thoravej 8, DK-2400 Copenhagen NV
Denmark

Bulletin Grønlands Geologiske Undersøgelse

143 Stratabound copper-lead-zinc mineralisation in the Permo-Triassic of central East Greenland. 1982. 42 pp.
By B. Thomassen, L.B. Clemmensen & H.K. Schønwandt. 90.00

144 Upper Jurassic bivalves from Milne Land, East Greenland. 1982. 126 pp.
By F.T. Fürsich. 205.00

145 Stratigraphy of the Silurian turbidite sequence of North Greenland. 1982. 121 pp.
By J.M. Hurst & F. Surlyk. 280.00

146 Paleocene gastropods from Nûgssuaq, West Greenland. 1983. 115 pp.
By H.A. Kollmann & J.S. Peel. 280.00

147 The stratigraphy of the Upper Jurassic and Lower Cretaceous sediments of Milne Land, central East Greenland. 1984. 56 pp.
By T. Birkelund, J.H. Callomon & F.T. Fürsich. 110.00

148 Upper Ordovician and Silurian carbonate shelf stratigraphy, facies and evolution, eastern North Greenland. 1984. 73 pp.
By J.M. Hurst. 125.00

149 Benthic macroinvertebrate associations from the Boreal Upper Jurassic of Milne Land, central East Greenland. 1984. 72 pp.
By F.T. Fürsich. 135.00

150 Stratigraphy and structure of the Fiskenæsset Complex, southern West Greenland. 1985. 72 pp.
By J.S. Myers. 200.00

151 The geology of the Qôrqut granite complex north of Qôrqut, Godthåbsfjord, southern West Greenland. 1985. 43 pp.
By C.R.L. Friend, M. Brown, W.T. Perkins & A.D.M. Burwell. 155.00

152 Reaction between picrite magma and continental crust: early Tertiary silicic basalts and magnesian andesites from Disko, West Greenland. 1985. 126 pp.
By A.K. Pedersen. 275.00

153 The Kimmeridgian ammonite faunas of Milne Land, central East Greeenland. 1985. 56 pp.
By T. Birkelund & J.H. Callomon. 185.00

154 The early Archaean to Proterozoic history of the Isukasia area, southern West Greenland. 1986. 80 pp.
By A.P. Nutman. 235.00

155 Topographical and geological maps of Hall Land, North Greenland. Description of a computer-supported photogrammetrical research programme for production of new maps, and the Lower Palaeozoic and surficial geology. 1987. 88 pp.
By P.R. Dawes. 425.00

156 Stratabound scheelite and stratiform tourmalinites in the Archaean Malene supracrustal rocks, southern West Greenland. 1987. 26 pp.
By P.W.U. Appel & A.A. Garde. 130.00

157 Geology and petrology of the Lower Tertiary plateau basalts of the Scoresby Sund region, East Greenland. 1989. 164 pp.
By L.M. Larsen, W.S. Watt & M. Watt. 275.00

158 Petroleum geology of North Greenland. 1989. 92 pp. (9 articles)
Edited by F.G. Christiansen. 200.00

159 Conodonts from the Upper Ordovician – Lower Silurian carbonate platform of North Greenland. 1990. 151 pp.
By H.A. Armstrong. 295.00

160 Sedimentary basins of North Greenland. 1991. 164 pp. (6 articles)
Edited by J.S. Peel & M. Sønderholm. 295.00

161 Functional morphology, evolution and systematics of Early Palaeozoic univalved molluscs. 1991. 116 pp. (2 articles)
By J.S. Peel. 210.00

162 Upper Cretaceous – Lower Tertiary decapod crustaceans from West Greenland. 1992. 46 pp.
By J.S.H. Collins & H. Wienberg Rasmussen. 85.00

163 Upper Llandovery and Wenlock *Cyrtograptus* from the Silurian Peary Land Group, North Greenland. 1992. 31 pp.
By M. Bjerreskov. 65.00

164 Acritarchs from the Lower Cambrian Buen Formation in North Greenland. 1993. 35 pp.
By G. Vidal & J.S. Peel. 75.00

165 Lithostratigraphy of the continental Devonian sediments in North-East Greenland. 1993. 108 pp.
By H. Olsen & P.-H. Larsen. 170.00

166 Dinoflagellate cyst stratigraphy of the Barremian to Albian, Lower Cretaceous, North-East Greenland. 1993. 171 pp.
By H. Nøhr-Hansen. 300.00

167 Lithostratigraphic framework of the Upper Proterozoic Eleonore Bay Supergroup of East and North-East Greenland. 1993. 38 pp.
By M. Sønderholm & H. Tirsgaard. 75.00

168 Sedimentary basin analysis of the continental Devonian basin in North-East Greenland. 1993. 80 pp.
By H. Olsen. 145.00

169 Palaeontology, stratigraphy and environmental setting of Middle Cambrian outer shelf deposits, North Greenland. 1994. 155 pp. (5 articles)
Edited by J.S. Peel. 290.00

170 Upper Cretaceous dinoflagellate cyst stratigraphy, onshore West Greenland. 1996. 104 pp.
By H. Nøhr-Hansen. 235.00

171 Research Papers. Collection of scientific articles. 1996. 90 pp. (4 articles) 110.00

172 Report of Activities, 1995. 1996. 119 pp. (20 articles) 180.00

Geology of Greenland Survey Bulletin

173 Cambrian shelf stratigraphy of North Greenland. 1997. 120 pp.
By J.R. Ineson & J.S. Peel. 250.00

174 The Proterozoic Thule Supergroup, Greenland and Canada: history, lithostratigraphy and development. 1997. 150 pp.
By P.R. Dawes. 300.00

175 Stratigraphy of the Neill Klinter Group; a Lower – lower Middle Jurassic tidal embayment succession, Jameson Land, East Greenland. 1998. 80 pp.
By G. Dam & F. Surlyk.

176 Review of Greenland Activities 1996. 1997. 112 pp. (18 articles)
Edited by A.K. Higgins & J.R. Ineson. 200.00

177 Accretion and evolution of an Archaean high-grade grey gneiss – amphibolite complex: the Fiskefjord area, southern West Greenland. 1997. 115 pp.
By A.A. Garde. 200.00

178 Lithostratigraphy, sedimentary evolution and sequence stratigraphy of the Upper Proterozoic Lyell Land Group (Eleonore Bay Supergroup) of East and North-East Greenland. 1997. 60 pp.
By H. Tirsgaard & M. Sønderholm.

179 The Citronen Fjord massive sulphide deposit, Peary Land, North Greenland: discovery, stratigraphy, mineralization and structural setting. 1998.
By F.W. van der Stijl & G.Z. Mosher. 200.00

180 Review of Greenland activities 1997. 1998. 176 pp. (26 articles)
Edited by W.S. Watt & A.K. Higgins.

181 Precambrian geology of the Disko Bugt region, West Greenland. 1999. 179 pp. (14 articles)
Edited by F. Kalsbeek. In press

Prices are in Danish kroner exclusive of local taxes, postage and handling

The series *Geology of Greenland Survey Bulletin* is a continuation of *Bulletin Grønlands Geologiske Undersøgelse* and incorporates *Rapport Grønlands Geologiske Undersøgelse*. These two series were issued by the former Grønlands Geologiske Undersøgelse (GGU) which was merged in 1995 with the former Danmarks Geologiske Undersøgelse (DGU) to form a new national geological survey: Danmarks og Grønlands Geologiske Undersøgelse (The Geological Survey of Denmark and Greenland) with the pet-name GEUS. Two other scientific series are issued by GEUS: *Geology of Denmark Survey Bulletin* and *Geology of Denmark and Greenland Map Series*.

Danmarks og Grønlands Geologiske Undersøgelse (GEUS)

Geological Survey of Denmark and Greenland
Thoravej 8, DK-2400 Copenhagen NV
Denmark

Rapport Grønlands Geologiske Undersøgelse

111	A simple model of runoff from unguaged basins in West Greenland. 1982. 26 pp. *By* R.J. Braithwaite.	40.00
112	Report on the geology of the Godthåbsfjord-Isukasia region. 1983. 127 pp. (10 articles)	125.00
113	Petrography and geochemistry of amphibolites from the Nordre Strømfjord area in the central part of the Nagssugtoqidian of West Greenland. 1983. 20 pp. *By* F.C. Mengel.	25.00
114	Processing and interpretation of aeromagnetic data in The Geological Survey of Greenland. 1982. 42 pp. *By* L. Thorning.	25.00
115	Report of Activities, 1982. 1983. 123 pp. (25 articles)	100.00
116	Tertiary volcanic rocks from Bontekoe Ø, East Greenland. 1983. 13 pp. *By* A. Noe-Nygaard & A.K. Pedersen.	25.00
117	Origin of quartzo-feldspathic supracrustal rocks from the central part of the Nagssugtoqidian Mobile Belt of West Greenland. 1984. 26 pp. *By* A. Rehkopff.	40.00
118	Greenschist facies metabasites from the Hellefiskefjord G.B. Schley Fjord area, eastern Peary Land, North Greenland. 1984. 17 pp. *By* R.E. Bevins & G. Rowbotham.	30.00
119	Precambrian gneisses and intrusive anorthosite of Smithson Bjerge, Thule district, North-West Greenland. 1984. 31 pp. *By* A.P. Nutman.	60.00
120	Report of Activities, 1983. 1984. 121 pp. (21 articles)	80.00
121	Biostratigraphic studies in western North Greenland; Operation Grant Land 1965–1966. 1984. 103 pp. (6 articles)	105.00
122	Aeromagnetic maps of parts of southern and central West Greenland: acquisition, compilation and general analysis of data. 1984. 36 pp. *By* L. Thorning.	45.00
123	The plutonic igneous and high-grade metamorphic rocks of southern Liverpool Land, central East Greenland, part of a supposed Caledonian and Precambrian complex. 1985. 39 pp. *By* R.F. Cheeney.	50.00
124	Lithostratigraphy of the Tertiary Vaigat Formation on Disko, central West Greenland. 1985. 30 pp. *By* A.K. Pedersen.	40.00
125	Report of Activities 1984. 1985. 114 pp. (26 articles)	80.00
126	Report on the 1984 geological expedition to central and western North Greenland. 1985. 128 pp. (13 articles)	100.00
127	Gardar dykes north of the Igaliko Syenite Complex, southern Greenland. 1985. 24 pp. *By* B.G.J. Upton & J.G. Fitton.	30.00
128	Developments in Greenland geology. 1986. 169 pp. (13 articles) *Edited by* F. Kalsbeek & W.S. Watt.	175.00
129	Occurrences of anorthositic rocks in the reworked Archaean basement in the Umanak area, central West Greenland. 1986. 18 pp. *By* M.C. Andersen & T.C.R. Pulvertaft.	40.00
130	Report of Activities, 1985. 1986. 129 pp. (21 articles)	85.00
131	Quaternary, pre-Holocene, marine events of western Greenland. 1986. 23 pp. *By* M. Kelly.	25.00
132	North Greenland Lower Palaeozoic palaeontology and stratigraphy: short contributions. 1986. 123 pp. (14 articles) *Edited by* J.S. Peel.	120.00
133	Report on the 1985 geological expedition to central and western North Greenland. 1987. 168 pp. (15 articles)	145.00
134	Geochronological studies in central East Greenland (four papers). 1987. 51 pp.	50.00
135	Report of Activities, 1986. 1987. 105 pp. (18 articles)	80.00

136	Early Tertiary, low-potassium tholeiites from exploration wells on the West Greenland shelf. 1987. 25 pp.	
	By N. Hald & J.G.Larsen.	25.00
137	Cambrian-Jurassic fossils, trace fossils and stratigraphy from Greenland. 1988. 159 pp. (11 articles)	
	Edited by J.S. Peel.	160.00
138	Glacier-hydrological conditions on the Inland Ice north-east of Jakobshavn/Ilulissat, West Greenland. 1988. 1 map with text.	
	By H.H. Thomsen, L. Thorning & R.J. Braithwaite.	70.00
139	Etah meta-igneous complex and the Wulff structure: Proterozoic magmatism and deformation in Inglefield Land, North-West Greenland. 1988. 24 pp.	
	By P.R. Dawes.	25.00
140	Report of Activities, 1987. 1988. 124 pp. (31 articles)	120.00
141	Field occurrence and petrology of deformed metabasite bodies in the Rinkian mobile belt, Umanak district, West Greenland. 1988. 36 pp.	
	By L. Schiøtte.	50.00
142	A pilot seismo-stratigraphic study on the West Greenland continental shelf. 1989. 16 pp.	
	By J.A. Chalmers.	50 00
143	North Greenland stratigraphy and petroleum geology. 1989. 71 pp. (3 articles)	100.00
144	Palaeozoic fossils and stratigraphy from North Greenland. 1989. 52 pp. (4 articles)	60.00
145	Report of Activities, 1988. 1989. 118 pp. (27 articles)	110.00
146	Geology of the Ammassalik region, South-East Greenland. 1989. 106 pp. (16 articles)	
	Edited by F. Kalsbeek.	130.00
147	Lower Cambrian trace fossils from Greenland. 1990. 62 pp. (2 articles)	
	Edited by J.S. Peel.	85.00
148	Current Research *including* Report of Activities, 1989. 1990. 141 pp. (28 articles)	160.00
149	Reservoir evaluation of Upper Permian buildups in the Jameson Land basin, East Greenland. 1991. 23 pp.	
	By L. Stemmerik.	60.00
150	Current Research. Short scientific papers. 1991. 43 pp. (5 articles)	50.00
151	A stratigraphic section through the Silurian turbidite sequence (Peary Land Group) in northern Nyeboe Land, North Greenland. 1991. 21 pp.	
	By P.-H. Larsen & J.C. Escher.	40.00
152	Current Research *including* Report of Activities, 1990. 1991. 111 pp. (23 articles)	150.00
153	Quaternary geology of western and central North Greenland. 1992. 34 pp.	
	By M. Kelly & O. Bennike.	100.00
154	Current Research. Short scientific papers. 1992. 59 pp. (4 articles)	70.00
155	Current Research *including* Report of Activities, 1991. 1992. 93 pp. (18 articles)	130.00
156	Geological analysis and mapping using multi-model photogrammetry. 1992. 72 pp. (8 articles)	
	Edited by K.S. Dueholm & A.K. Pedersen.	140.00
157	Lithostratigraphy and geological setting of Upper Proterozoic shoreline–shelf deposits, Hagen Fjord Group, eastern North Greenland. 1992. 27 pp.	
	By L.B. Clemmensen & H.F. Jepsen.	40.00
158	Glacier inventory and atlas of West Greenland. 1992. 194 pp.	
	By A. Weidick, C.E. Bøggild & N.T. Knudsen.	180.00
159	Current Research *including* Report of Activities, 1992. 1993. 126 pp. (24 articles)	140.00
160	Report of Activities, 1993. 1994. 92 pp. (19 articles)	120.00
161	Current Research. Short scientific papers. 1994. 79 pp. (7 articles)	130.00
162	Geology of North-East Greenland. 1994. 209 pp. (19 articles)	
	Edited by A.K. Higgins.	290.00
163	Re-interpretation of aspects of Ketilidian geology. 1994. 31 pp. (2 articles)	50.00
164	Current Research. Short scientific papers. 1994. 35 pp. (3 articles)	60.00
165	Report of Activities, 1994. 1995. 120 pp. (21 articles)	140.00

Prices are in Danish kroner exclusive of local taxes, postage and handling

This series was discontinued at the end of 1995, but most issues are still available

In pocket

1:250 000 geological map.

Precambrian geology between Qarajaq Isfjord and Jakobshavn Isfjord, West Greenland *by* A.A. Garde (1994).